Adsorption of Light Gases and Their Mixtures on SR-115 and ETS-10 Zeolites

by

Nadhir Abbas Al-Baghli

A Thesis Presented to the

FACULTY OF THE COLLEGE OF GRADUATE STUDIES

KING FAHD UNIVERSITY OF PETROLEUM & MINERALS

DHAHRAN, SAUDI ARABIA

In Partial Fulfillment of the
Requirements for the Degree of

MASTER OF SCIENCE

In

CHEMICAL ENGINEERING

June, 1994

Order Number 1359481

Adsorption of light gases and their mixtures on SR-115 and ETS-10 zeolites

Al-Baghli, Nadhir Abbas, M.S.

King Fahd University of Petroleum and Minerals (Saudi Arabia), 1994

U·M·I
300 N. Zeeb Rd.
Ann Arbor, MI 48106


بسم الله الرحمن الرحيم

Adsorption of Light Gases and Their Mixtures on SR-115 and ETS-10 Zeolites

BY

Nadhir Abbas Al-Baghli

A Thesis Presented to the

FACULTY OF THE COLLEGE OF GRADUATE STUDIES

KING FAHD UNIVERSITY OF PETROLEUM & MINERALS

DHAHRAN, SAUDI ARABIA

In Partial Fulfillment of the
Requirements for the Degree of

MASTER OF SCIENCE
In
CHEMICAL ENGINEERING

June, 1994

KING FAHD UNIVERSITY OF PETROLEUM & MINERALS
DHAHRAN, SAUDI ARABIA

This thesis, written by

NADHIR ABBAS AL-BAGHLI

under the direction of his thesis committee, and approved by all the members, has been presented and accepted by the Dean, College of Graduate Studies, in partial fulfillment of the requirements for the degree of

MASTER OF SCIENCE IN CHEMICAL ENGINEERING

Thesis Committee

Chairman (Dr. Kevin Loughlin)

Member (Dr. Habib Al-Ali)

Member (Dr. Mirza Hassan)

Dr. Dulaihan Al-Harbi
Department Chairman

Dr. Ala Al-Rabeh
Dean College of Graduate Studies

Date : 9/7/94

Dedicated to my late grandmother

ACKNOWLEDGEMENT

I am most grateful to **ALLAH** the Almighty for providing me the patience and capability to finish this work. Acknowledgement is due to King Fahd University of Petroleum & Minerals (KFUPM) for providing the facilities and financial support.

I wish to express my profound thanks and appreciation to my thesis advisor Dr. Kevin. Loughlin for his helpful comments and wise suggestions during the course of this research. He has been very cooperative with me in all the problems that I faced during my research. Acknowledgement is also due to my committee members Dr. Habib Al-Ali and Dr. Mirza Hassan for their helpful comments when reviewing this thesis.

I would like to thank the chemical engineering department, chairman, professors, staff and lab technicians for their valuable help during my study. Appreciation is also extended to all my friends and colleagues for all the assistance they provided to me to finish this thesis.

The effort of Dr. Mohammed Abdillahi and other members of the Research Institute of KFUPM, in extruding and characterizing the ETS-10 zeolite powder is deeply appreciated.

Finally, I would like to express my profound gratitude to my late grandmother, mother, father, sisters, brothers and relatives for all the affection and encouragement they surrounded me with.

Last, but not least, I am obliged to offer my indebtedness and sincere appreciation to my wife and children. Their affection and sacrifices made this work possible.

TABLE OF CONTENTS

123

LIST OF TABLES

LIST OF FIGURES

NOMENCLATURE

A	Surface area of adsorbent m^2
A_1	Virial first constant defined in equation 2.27 (kg/mol)
A_2	Virial second constant defined in equation 2.27 $(kg/mol)^2$
A_3	Virial third constant defined in equation 2.27 $(kg/mol)^3$
b	Van der Waal's volume (cc/mol)
b	Toth equilibrium parameter $(kPa)^t$
b_{MW}	Mathews-Weber equilibrium parameter $(kPa)^{-1}$
b_{RP}	Radke-Prausnitz first equilibrium parameter $(kPa)^{-1}$
B_1	Virial first constant defined in equation 2.26 (kg/mol)
B_2	Virial second constant defined in equation 2.26 $(kg/mol)^2$
B_3	Virial third constant defined in equation 2.26 $(kg/mol)^3$
c	Unilan equilibrium parameter (kPa)
c_{RP}	Radke-Prausnitz second equilibrium parameter $(kPa)^{-n_{RP}}$
k_F	Freundlich equilibrium parameter $(mol/kg/kPa^{n_F})$
k_L	Langmuier equilibrium parameter $(kPa)^{-1}$
k_{LRC}	Loading ratio equilibrium parameter $(kPa)^{-1}$
K_0	Pre exponential factor defined by equation 2.5 (mol/kg/kPa)
K_H	Henry's constant (mol/kg/kPa)
MW	Molecular weight (g/mol)
n_F	Freundlich dimensionless parameter
n_{LRC}	Loading ratio heterogeneity parameter (dimensionless)
n_{MW}	Mathews-Weber dimensionless parameter
n_{RP}	Radke-Prausnitz heterogeneity parameter (dimensionless)
P	Pressure (kPa)
P°	Pure component pressure defined by equation 2.33 (kPa)

P_c	Critical pressure (kPa)
P_s	Saturation pressure (kPa)
q	Amount adsorbed (mol/kg of adsorbent)
q_s	Saturation concentration (mol/kg of adsorbent)
R	Universal gas constant (kJ/mol/K)
s	Unilan heterogeneity parameter (dimensionless)
S	Entropy (kJ/mol/K)
ss	Sum of squares error defined in equation 4.1
t	Toth heterogeneity parameter (dimensionless)
T	Temperature (K)
T_b	Normal boiling point (K)
T_c	Critical temperature (K)
U	Internal energy (kJ/m^2/kg of adsorbent)
v_b	Molar volume at normal boiling temperature (cc/mol)
v_c	Critical volume (cc/mol)
x	Adsorbed phase mole fraction (dimensionless)
y	Gas phase mole fraction (dimensionless)
Z_c	Critical compressibility factor (dimensionless)
α	Relative adsorptivity (dimensionless)
δ	Surface area occupied by adsorbed molecule (m^2)
$-\Delta H_0$	Isosteric heat of adsorption at zero coverage (kJ/mol)
η	Parameter related to the energy distribution (kJ/mol
φ	Function defined in equation 2.38 (dimensionless)
Φ	Energy of adsorption (kJ/mol)
π	Spreading Pressure (kPa/m)
θ	Fraction of surface covered by adsorbed molecules (dimensionless)
ω	Eccentric factor (dimensionless)

THESIS ABSTRACT

NAME OF STUDENT : **NADHIR ABBAS AL-BAGHLI**

TITLE OF STUDY : **ADSORPTION OF LIGHT GASES AND THEIR MIXTURES ON SR-115 AND ETS-10 ZEOLITES**

MAJOR FIELD : **CHEMICAL ENGINEERING**

DATE OF DEGREE : **JUNE 18 1994**

Pure, binary and ternary equilibrium adsorption data of methane, ethane ethylene, nitrogen and carbon dioxide on both SR-115 and ETS-10 zeolites are reported up to 1000 kPa pressure and a temperature range of 280-425 K. Ten pure models namely Toth, Unilan, Radke-Prausnitz, Mathews-Weber, Volmer, Virial with two and three constants, Freundlich, Langmuir-Freundlich, and the Loading Ratio Correlation are successfully applied to model the pure data using unconstrained and constrained optimization techniques. Henry's constant values and limiting heat of adsorption are extracted from the Virial three constant model and are compared to the values obtained from other models.

The ideal adsorbed solution theory in conjunction with the pure isotherms of Toth, Unilan and Virial three constant is used to model the multicomponent data. The fit of this model to these data is satisfactory except for the data of the binary system nitrogen-carbon dioxide on SR-115 zeolite. The latter poor fit may be attributed to adsorption of carbon dioxide on the binder.

Values of the relative adsorptivity calculated from the data and the IAST fits of the data show that the separation of methane from ethylene is feasible on both adsorbents; but it is best on ETS-10 zeolite. Also, the separation of

methane from ethane, and ethane from ethylene is feasible on ETS-10 particularly at low temperature. The separation of ethane from ethylene is not possible on SR-115 zeolite at any conditions. However, the separation of methane from the ternary mixture methane-ethane-ethylene is possible on both types of zeolites at any conditions.

MASTER OF SCIENCE DEGREE

KING FAHD UNIVERSITY OF PETROLEUM & MINERALS

DHAHRAN, SAUDI ARABIA

JUNE 1994

خلاصة الرسالة

اسم الطالب الكامل : نظير عباس حسين البغلي .

عنوان الرسالة : امتزاز الغازات الخفيفة ومخاليطها على زيولايت SR - 115 و ETS - 10 .

التخصص : الهندسة الكيميائية .

تاريخ الشهادة : ١٩٩٤/٦/١٨م .

تم في هذا البحث قياس امتزاز مركبات نقيه ومخاليط ثنائيه وثلاثيه للميثان ، الإيثان ، الإيثين ، النيتروجين ، وثاني أكسيد الكربون على نوعين من الزيولايت : SR - 115 و ETS - 10 تحت ضغوط وصلت إلى أكثر من ١٠٠٠ كيلوباسكال ودرجات حرارة تراوحت بين ٢٨٠ إلى ٤٢٥ كيلفن . وقد تم استخدام عشرة نماذج بنجاح لتمثيل هذه المعلومات باستخدام طريقتي التقويم المشروط وغير المشروط . النماذج المستخدمة هي توث (Toth) ، يونيلان (Unilan) ، رادكي - بروزينتز (Radke - Prausnitz) ، ماثيوس - ويبر (Mathews - Weber) ، ڤولمر (Volmer) ، ڤيريال (Virial) بمعلمين وثلاثة معالم ، فريندلك (Freundlich) ، لانغمر - فريندلك (Langmuir - Freundlich) ، ونموذج العلاقة المتبادلة لنسبة التحميل . واستخلصت قيم هنري وقيم حرارة الامتزاز من نموذج ڤيريال ذي الثلاثة معالم وقورنت مع القيم المستخلصة من بقية النماذج .

استخدمت نظرية المحلول المتز المثالي مع المعالم المحصلة من التقويم المشروط لنماذج توث ، يونيلان و ڤيريال ذي المعالم الثلاثة لنمذجة المعلومات الإتزانية للمخاليط متعددة المركبات . لوحظ أن تطابق النتائج المحسوبة باستخدام هذه النظرية مع القياسات مقنع لجميع الأنظمة باستثناء النظام الثنائي للنيتروجين وثاني أكسيد الكربون على زيولايت SR - 115 . عدم تطابق النظرية مع المعلومات المحصلة لهذا النظام معزو لامتزاز ثاني أكسيد الكربون على لاصق الزيولايت .

أوضحت قيم الامتزازية النسبية المحسوبة من المعلومات الإتزانية للمخاليط الثنائية ومن تطابق نظرية المحلول المتز المثالي مع هذه المعلومات أن فصل الميثان من الإيثين ممكن على نوعي الزيولايت المستخدم ولكنه أفضل على زيولايت ETS - 10 . كما أن فصل الميثان من الإيثان والإيثان من الإيثين ممكن على زيولايت SR - 115 لاسيما عند درجات حرارة منخفضة . فصل الإيثان من الإيثين غير ممكن على زيولايت SR - 115 تحت أي ظرف ولكن فصل الميثان من المخلوط الثلاثي المكون من الميثان ، الإيثان والإيثين ممكن على نوعي الزيولايت المستخدم وتحت أي ظرف .

درجة الماجستير في العلوم

جامعة الملك فهد للبترول والمعادن

الظهران ، المملكة العربية السعودية

يونيو ١٩٩٤م

CHAPTER 1

INTRODUCTION

Adsorption is a process in which molecules of fluid are attached to the surface of some solids due to certain forces.

Two types of adsorption can be distinguished namely, physisorption and chemisorption. In physisorption, the heat evolved when a mole of gas is adsorbed is relatively small (generally less than 20 kJ); whereas, the heat evolved in chemisorption is higher than 100 kJ. This is attributed to the bond formation between the fluid and the surface. Physisorption is rapid, non activated and reversible while chemisorption is a relatively slow process, activated and irreversible. In chemisorption, the molecules of a fluid form only one layer while a multilayer is possible in physisorption. The forces involved in physisorption are relatively weak (Van der Waals forces) and are therefore possible only at relatively low temperatures (close to the boiling point of compounds). In contrast, due to the existence of bonds between the surface and the fluid, chemisorption is possible over a wide range of temperatures (9,13).

1.1 Adsorption as a Separation Tool

Almost all adsorptive separation processes depend on physical adsorption due to the reversibility of the process. Recently, adsorption has become an important separation tool because of its efficiency. For instance, it is practically impossible to achieve high purity separation for isomers using traditional techniques like distillation; the required purity can be achieved easily by adsorptive separation. Furthermore, adsorption is an energy efficient

process and with the high expense of energy, adsorption has become a suitable alternative particularly for cryogenic processes..

1.2 Adsorbents

The surface at which the fluid get attached to is called an adsorbent while the fluid is called an adsorbate. Adsorbents differ in their chemical structure, and physical properties and consequently differ in their adsorptive properties. Hence, the appropriate choice of adsorbent is one criterion in adsorptive separation processes. Various adsorbents like silica gel, activated carbon, carbon molecular sieve and zeolites are being extensively used in various practical applications.

1.2.1 Silica Gel

Silica gel is a partially dehydrated form of polymeric colloidal silicic acid having a chemical structure of $SiO_2.nH_2O$. The water content is about 5% of the weight and is present in the form of chemically bound hydroxyl groups. Silica gel is produced from the direct removal of sodium from sodium silicate solution by ion exchange (12). Silica gel is used as the adsorbent in the separation of aromatics from paraffins and naphthenes (4).

1.2.2 Activated Carbon

Activated carbon is normally produced by the thermal decomposition of carbonaceous material followed by activation with steam or carbon dioxide at high temperature to open the pores (12). Activated carbon is an organophilic, hydrophobic material, and therefore is widely used in waste water treatment. In addition, activated carbon is used in the adsorption of gasoline vapors in automobiles and in air purification (13).

1.2.3 Carbon Molecular Sieve

This adsorbent has a very narrow distribution of micropore size; therefore it acts as a molecular sieve allowing small molecules to adsorb, leaving the large molecules in the bulk phase.

Carbon molecular sieve is produced commercially from anthracite or hard coal by controlled oxidation followed by thermal treatment (10). This adsorbent is commonly used in air separation and in the production of hydrogen from gas streams containing small amounts of hydrocarbons. In the latter application however, zeolite molecular sieves are more efficient (13).

1.2.4 Zeolites

Zeolites are mainly porous crystalline aluminosilicates consisting of an assemblage of SiO_4 and AlO_4 tetrahedra joined together in various regular arrangements (1). Uniformity of the framework is the feature that distinguish zeolites from other microporous adsorbents. Each aluminum atom present in the framework introduces one negative charge which is balanced by an exchangeable cation. The ratio of Si/Al is never less than one but there is no upper limit. Depending on this ratio, the framework structure and the type of cation, various zeolites with widely different adsorptive properties have been synthesized. Zeolites are usually hydrophilic, selectively organophilic and are used mainly in the purification of organic vapors.

1.2.5 SR-115 Zeolite

SR-115 zeolite is a synthetically produced, crystalline, silicaceous material. Its structure is composed entirely of silica. The structure of SR-115 (Figure 1.1) contains a large fraction of five member rings of silicon oxygen tetrahedra. The channel system of SR-115 zeolite is composed entirely of

near circular zig-zag channels of free cross section of 5.4 A° cross-linked by elliptical straight chain channels with a free cross section of 5.75 to 5.15 A°. At ambient temperature SR-115 zeolite can adsorb molecules as large as benzene (kinetic diameter 5.85 A°). This adsorbent is stable in air to over 1000 °C and only slowly converts to an amorphous glass at 1300°C (2,5). The properties of SR-115 are presented in Table 1.1.

1.2.6 ETS-10 Zeolite

ETS-10, an experimental titanium silicate was first synthesized in 1989 (6,7,8). It is a microporous crystalline solid consisting mainly of an assemblage of titanium oxide (TiO_2) and silicate (SiO_2). The pore sizes in ETS-10 are uniform and similar in dimension to large pored classical zeolites. Titanium is octahedrally coordinated in the framework which requires two counterbalancing cations per titanium. The structure of ETS-10 is somewhat different from classical aluminosilicate zeolites. This material is composed of chains of octahedrally coordinated zeolites type rings. The effective pore size of ETS-10 is about 8 A° and it is thermally stable in air up to 600 °C. The structure and the properties of ETS-10 are given in Figure 1.2 and Table 1.2 respectively.

1.3 Adsorption Isotherms

An adsorption isotherm is a relation between the amount of fluid adsorbed in the adsorbed phase and the pressure or concentration of the fluid in the bulk phase at constant temperature.

Brunauer and coworkers (3) divided isotherms into five classes as illustrated in Figure 1.3. The system where the pore size of the adsorbent is not much greater than the adsorbate molecule categorize class I isotherms.

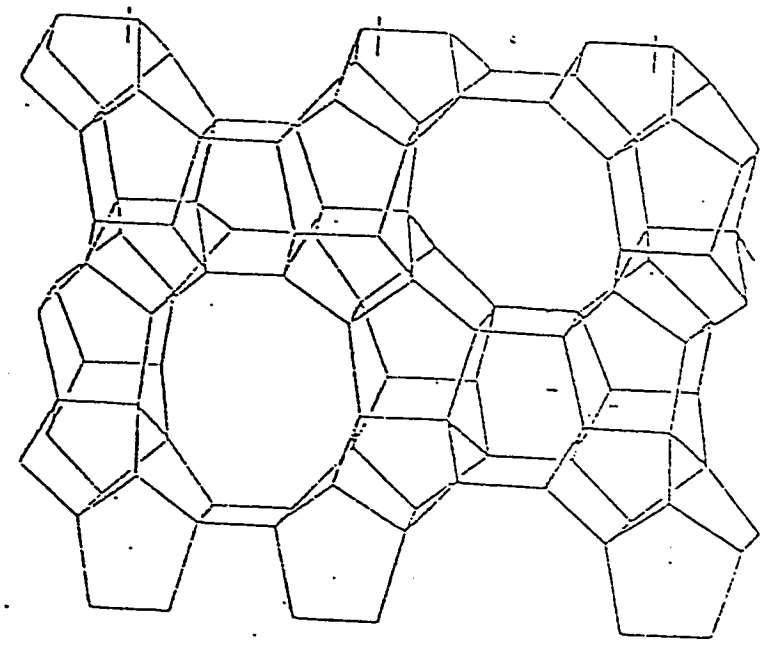

Figure 1.1 Structure of SR-115 Zeolite (2, 5)

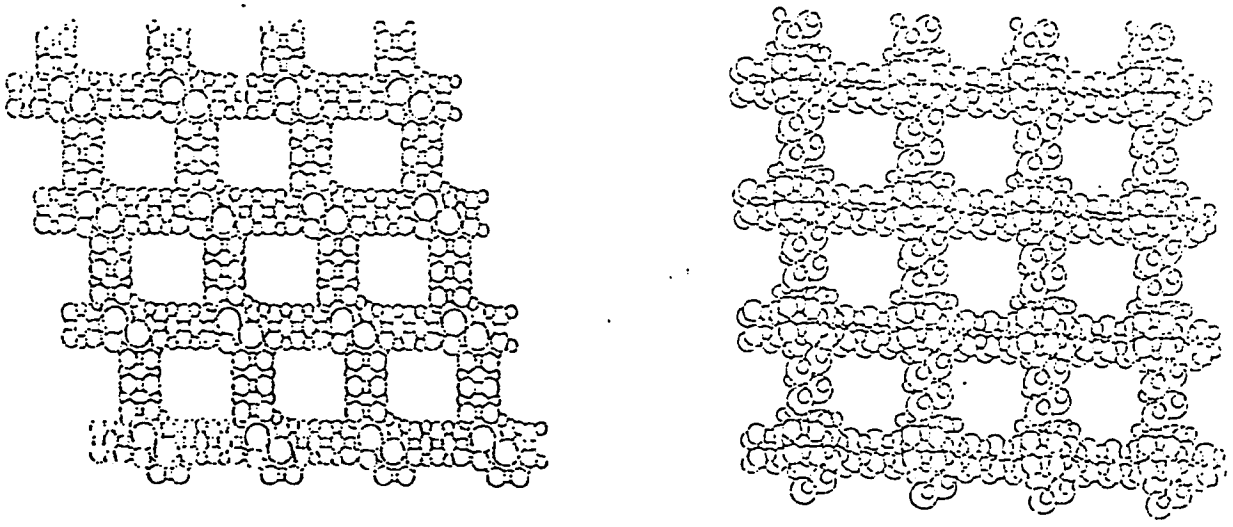

Fig 1.2 Structure of ETS-10 Zeolite (8)

For these systems, there is a saturation limit corresponding to complete filling of the pores. Isotherms of class II and III are generally observed in adsorbents which have a wide range of pore sizes. A type IV isotherm is a characteristic of the systems where the pore size of adsorbents is very much larger than the size of the adsorbate molecule. For these systems, two surface layers either on a plane surface or on the wall of a pore are formed. Class V isotherms are usually observed in systems where the intermolecular attraction is large.

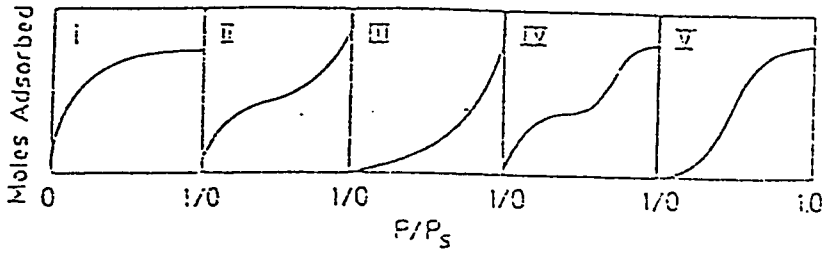

Figure 1.3 Brunauer Classification of Isotherms (3, 13)

1.4 Relevant Properties of Gases Used

Table 1.3 lists some properties of the gases used to calculate some theoretical constants required in later chapters. These properties include the critical constants of the gases, the molar volumes at saturation, the van der Waal b constants and the normal vapor pressures. The latter properties are calculated from Antoine's equation (11,14), while the saturated volume is calculated from the critical properties of the gases using Rackett's equation (14).

1.5 Scope and Objectives of This Study

In thermal power plants, the result of combustion is a gas stream rich in nitrogen and carbon dioxide. It is useful to separate this stream into two streams, nitrogen rich and carbon dioxide rich streams. The separation is economically possible using adsorption. Furthermore, it is practically important to purify natural gas which is mainly methane from other light hydrocarbons such as ethane and ethylene. The purification is both efficient and economical using adsorption. For instance, a 99.99% methane rich stream is quite feasible using adsorptive separation.

The design of adsorption processes requires both kinetic and thermodynamic equilibrium data. The equilibrium data is affected by the pressure and the temperature of the system as well as the type of adsorbent used.

In this study, equilibrium data for the adsorption of pure nitrogen, carbon dioxide and ethylene on SR-115 zeolites have been experimentally measured at various temperature. The adsorption equilibrium data of the binary systems of nitrogen and carbon dioxide on SR-115 zeolite are also collected at various temperatures and pressures. In addition, equilibrium data for the binary systems of methane-ethylene, ethane-ethylene, and the ternary system of methane-ethane-ethylene on SR-115 zeolites have been gathered at selective pressures and temperatures.

The performance of ETS-10 zeolite as a separation tool is also examined. Equilibrium data for the adsorption of pure methane, ethane and ethylene at various temperatures and binary and ternary mixtures of these gases at the same conditions used in SR-115 in addition to the binary system of methane-ethane are also collected. The measured pure component data are modeled using Toth, Unilan, Radke-Prausnitz, Mathews-Weber, Volmer, Freundlich,

Langmuir-Freundlich, Loading Ratio Correlation and Virial with two and three constants models. The multicomponent data are modeled using the Ideal Adsorbed Solution Theory (IAST) in conjunction with the pure component models of Toth, Unilan and Virial with three constants.

1.6 Literature Cited

1) Barrer, R.M., Zeolites and Clay Minerals, Academic Press Inc., New York, 1978.

2) Bin Abdul Rehman, H., Equilibrium Adsorption of Light Alkanes and Their Mixtures on 5A, 13X and S-115. MS. Thesis KFUPM, Dhahran, 1988.

3) Brunauer, S., Deming, L.S., Deming, W.E., and Teller, E.J., J. Am. Chem. Soc., 62, P. 1723, 1940.

4) Davis, W.H., Harper, J.I., and Weatherly, E.R., Pet. Ref., 31, P. 109, 1952.

5) Flanigen, E.M., Bennet, J.M., Grose, R.W., Cohen, J.P., Patton, R.L., and Kirchner, R.M., Nature, 271, P. 512, 1978.

6) Kuznicki, S.M., " Large-Pore Crystalline Titanium Molecular Sieve Zeolites", U.S. Patent, 4, 853, 202, 1989.

7) Kuznicki, S.M., " Preparation of Small-Pore Crystalline Titanium Molecular Sieve Zeolites", U.S. Patent, 4, 938, 989, 1990.

8) Kuznicki, S.M., Thrush, K.A., Alen, F.M., Levine, S.M., Hamil, M.M., Hayhurst, D.T., and Mansour, M., " Synthesis and Adsorptive Properties of Titanium Silicate Molecular Sieves", Mol. Sieves,Vol. I, Editors: Ocelli M.L., and Robson, H. New York, 1993.

9) Laidler, K.J., and Meiser, J.H., Physical Chemistry, 1st edition, California, the Benjamin Cummins Pub. Co., 1982.

10) Patel, R.L., Nandi, S.P., and Walker, P.L., Fuel, 51, P. 47, 1972.

11) Perry, R.H. and Green, D., Perry's Chemical Engineer's Handbook, 5th. ed., Mc Graw Hill., Singapore, 1985.

12) Ponec, V., Knor, Z., and Cerny, S., Adsorption on Solids, Butterworth and Co., London, 1974.

13) Ruthven, D.M., Principles of Adsorption and Adsorptive Separation Processes, Wiley, New York, 1984.

14) Smith, J.M., and Van Ness, H.C., Introduction to Chemical Engineering Thermodynamics. 3rd. ed., Mc Graw-Hill., Singapore, 1985.

Table 1.1 Properties of Linde SR-115 Zeolite (2, 5)

Chemical Composition	
Typical unit cell content	:>99% SiO_2
Crystallographic Data	
Symmetry	: Apparently orthorhombic
Dehydrated density	: 1.76 g/cc
Unit cell constants	: a = 20.06 A^o
	: b = 19.80 A^o
	: c = 13.36 A^o
Structural Properties	
Cage Type	: Chains
Framework	: Topological type of tetrahedral channels linked by D5R units.
Channel System	: Three dimensional zig-zag and straight.
Free Aperture	: Circular 5.4 A^o Elliptical 5. 75A^ox 5. 15A^o
Pore Volume	: 0.190 cc/g
Kinetic Diameter	: 6.0 A^o
Effect of Dehydration	: Stable in air up to 1000 ^oC
Micropore Size	: 5.4 A^o
Binder (wt %) for Linde type	: 20

123

Table 1.2 Properties of ETS-10 Zeolites (8)

Chemical Composition	66.1 % SiO_2 17.4 % TiO_2 10.0 % Na_2O 4.8 % K_2O 1.7 % others
Ion Exchange Capacity	≈ 4.0 meq./ g (as shipped hydrous) good stability for exchange in acidic media.
Moisture Content (As Shipped)	:≈ 15 (wt %)
Surface Area	300^+ m^2/g
Kinetic Diameter	: 8 A^o
Stability	Stable in air up to 600 ^oC
Pore volume (As Synthesized)	:11.95 cc / 100 g
Structure	Three dimensional network of interconnecting channels intersecting at the center pore.

Table 1.3 Properties of The Gases Used (2, 11, 14)

Property	N_2	CO_2	CH_4	C_2H_6	C_2H_4
Molecular Weight (MW)	28.016	44.01	16.04	30.07	28.05
Critical Temperature T_c (K)	126.20	304.20	190.70	305.40	282.40
Critical Pressure P_c (kPa)	3,394	7,387	4,729	4,884	5,066
Critical Volume v_c (cc/mol)	90.10	94.00	99.30	148.00	124.00
Normal Boiling Point T_b (K)	77.30	194.70	111.70	184.60	169.50
Critical Compressibility Z_c	0.291	0.274	0.290	0.285	0.270
Ecentric Factor ω	0.040	0.420	0.013	0.105	0.073
Van der Waal's b (cc/mol)	38.64	42.80	42.71	64.99	57.93
Molar Volume at T_b v_b (cc/mol)	35.19	35.81	37.99	56.49	45.27
Vapor Pressure at 25 °C (kPa)	super-critical	6,920	super-critical	4,189	super critical

CHAPTER 2

LITERATURE REVIEW

2.1 Thermodynamic Definition of Adsorption

When the number of molecules arriving to the surface (adsorbing) is equal to the number of molecules leaving the surface (desorbing), the system is said to be at thermodynamic equilibrium. This thermodynamic description of adsorption equilibrium is analogous to any two phase equilibrium like vapor-liquid-equilibrium. The two phases which can be distinguished when a fluid is adsorbed are the bulk phase and the adsorbed phase. The surface consists of the adsorbent and the adsorbate molecules. From the thermodynamics point of view, the adsorbent is considered as inert and its effect is limited to the creation of a force field. On the other hand, the adsorbed molecules themselves are considered to form the adsorbed phase even though no distinct boundary is recognized (28).

2.2 Forces and Heat of Adsorption

The forces involved in adsorption phenomena are of two types namely, van der Waals forces arising from dispersion and repulsion and electrostatic forces comprising polarization, dipole and quadrupole interactions. The former type is always present in physical adsorption while the latter is significant only in adsorbents which have ionic structure such as zeolites. Sorbate-sorbate interaction is important at intermediate to high loading.

When considering ionic adsorbents, the overall energy of adsorption (Φ) is given by :

$$\Phi = \Phi_d + \Phi_r + \Phi_p + \Phi_\mu + \Phi_q + \Phi_s \qquad 2.1$$

where the subscripts d, r, p, μ, q and s represent the energy contribution from dispersion, repulsion, polarization, dipole, quadrupole and sorbate-sorbate interaction.

At low coverage, the heat of adsorption (ΔH_0) may be approximated as :

$$\Delta H_0 = \Phi \qquad 2.2$$

There are available expressions in the literature for each term in equation 2.1 (2,10,16). However, they fail frequently to estimate the heat of adsorption satisfactorily. The heat of adsorption may be measured by standard calorimetric techniques and can also be calculated from the measured isotherms at several temperatures using a suitable model. The heat of adsorption obtained by the latter procedure is commonly known as the isosteric heat of adsorption.

2.3 Henry's Constant and Saturation Concentration

At very low pressure, the amount adsorbed (q) is directly proportional to the pressure (P) :

$$q = K_H P \qquad 2.3$$

Equation 2.3 is Henry's isotherm which is applicable only for linear adsorption. The constant of proportionality in this equation is called Henry's constant. Thermodynamic consistency requires that any adsorption model reduce to Henry's model as the pressure approaches zero. Therefore, Henry's constant can be obtained from any thermodynamically consistent model by applying the relation :

$$K_H = \lim_{P \to 0} \frac{q}{P} \qquad 2.4$$

Henry's constant is a strong function of temperature. The temperature dependency is described by Van't Hoff's expression (3,28):

$$K_H = K_0 exp(-\Delta H_0 / RT) \qquad 2.5$$

where K_0 is a proportionality constant, $-\Delta H_0$ is the isosteric heat of adsorption, R is the universal gas constant and T is the absolute temperature.

The saturation concentration (q_s) is an important parameter which characterizes most of the adsorption models. It is defined as :

$$q_s = \lim_{P \to P_s} q \qquad 2.6$$

where P_s is the saturation pressure. Usually, isotherms are written as :

$$\frac{q}{q_s} = \theta = f(P) \qquad 2.7$$

where θ is the fraction of surface covered with adsorbed molecules. The saturation concentration can be theoretically calculated by :

$$q_s = \frac{\varepsilon}{v^*} \qquad 2.8$$

where ε is the voidage of the adsorbent namely, 152 and 119.5 cc/kg for SR-115 and ETS-10 zeolite respectively (Tables 1.2 and 1.3), and v^* is the molar volume at temperature T given by (9):

$$v^* = v_b + \left[\frac{T - T_b}{T_c - T_b}\right](b - v_b) \qquad 2.9$$

where T_c and T_b are the critical and boiling temperatures respectively, and v_b and b are respectively the molar volume at T_b and the van der Waal's volume. Above the critical temperature, v* is given by Dubinin equation as:

$$v^* = b \qquad 2.10$$

The value of the saturation concentration calculated from the above expressions is based on the assumption of complete occupancy of the free voidage and that the adsorbed state molecules behave analogous to a highly

compressed liquid state under the same conditions. However, the actual value is a little less due to steric effects.

2.4 Spreading Pressure Concept

The spreading pressure (π) corresponds to the difference in surface tension between a clean surface and a surface covered with adsorbate (8,28). Hence, it represents the change in internal energy per mass of adsorbent (U) due to the spreading of the adsorbate over the surface of the adsorbent (A) at constant adsorbed phase entropy (S_s), volume (v_s) and adsorbed quantity (n_s)

$$\pi = \left(\frac{-\partial U}{\partial A} \right)_{S_s, v_s, n_s} \qquad 2.11$$

The spreading pressure is an abstract property and can be calculated from the equilibrium adsorption data using the integrated form of Gibbs equation :

$$\frac{\pi A}{RT} = \int_0^P \frac{q}{P} dP \qquad 2.12$$

2.5 Pure Component Adsorption Models

Several models have been developed to describe the equilibrium relationship between the amount adsorbed (q) and the pressure (P) for pure components. These models are based on assumptions which are appropriate only for limited systems. The derivation of most models is based on theoretical foundations. On the other hand, some models are based on experimental data and they are therefore thermodynamically meaningless.

The simplest model was developed by Langmuir in 1916 (18). This model is based on the following assumptions (17,18):

1) Localized adsorption (adsorbed molecules can't move freely along the

surface).

2) No interaction between adsorbed molecules.

3) All sites are energetically equivalent

4) Monolayer adsorption.

Based on the above, the Langmuir model can be written as:

$$q = \frac{k_L q_s P}{1 + k_L P} \qquad 2.13$$

where k_L is an equilibrium parameter and q_s is the saturation concentration. Henry's constant can be determined from the above equation by applying equation 2.4 to obtain:

$$K_H = k_L q_s \qquad 2.14$$

The Langmuir model is very ideal and is applicable only at low pressures. However, this model has provided the basis of several other models.

Toth, has derived a model based on monolayer adsorption taking into account the heterogeneity of the adsorbent where the energy of the sites are no longer equivalent :

$$q = \frac{q_s P}{\left(b + P^t\right)^{1/t}} \qquad 2.15$$

where b is an equilibrium parameter and t is a heterogeneity parameter. This model reduces to the Langmuir model for t = 1 which refers to a homogeneous surface. Henry's constant can be obtained from Toth model by:

$$K_H = q_s b^{-1/t} \qquad 2.16$$

Honig and Reyerson (12, 33) have developed a model based on a uniform distribution of energies of adsorption. The model is a modified version of the Langmuir model :

$$q = \frac{q_s}{2s}\ln\left[\frac{c + P\exp(s)}{c + P\exp(-s)}\right] \qquad 2.17$$

where c is an equilibrium parameter and s is a constant related to the heterogeneity of the surface. Equation 2.17 is commonly known as Unilan model (Uni for uniform distribution and Lan for Langmuir isotherm). For homogeneous surface, s vanishes and the Unilan model reduces to the Langmuir model. Henry's constant can be obtained from:

$$K_H = \frac{q_s}{cs}\sinh(s) \qquad 2.18$$

Mathews and Weber (21) extended the Langmuir model by adding a dimensionless constant (n_{MW}) which corrects for deviation of the experimental data in the systems they studied:

$$q = \frac{q_s b_{MW} P}{1 + (b_{MW} P)^{n_{MW}}} \qquad 2.19$$

where the subscript MW refers to Mathews-Weber. Henry's constant can be found from:

$$K_H = q_s b_{MW} \qquad 2.20$$

Radke and Prausnitz (25) have derived a model based on the principles of dilute solution thermodynamics:

$$q = \frac{b_{RP} q_s P}{1 + b_{RP} P + \left(\frac{b_{RP} P}{c_{RP} P^{n_{RP}}}\right)} \qquad 2.21$$

where b_{RP}, c_{RP} are equilibrium parameters and n_{RP} is a dimensionless constant. This model is found to be suitable for weekly adsorbed components. This model has been derived to make the Langmuir-Freundlich model

thermodynamically consistent. The Henry's constant can be obtained from the Radke-Prausnitz model by :

$$K_H = q_s b_{RP} \qquad 2.22$$

Volmer model can be derived from the Gibbs adsorption isotherm (28), which is given by:

$$A\left(\frac{\partial \pi}{\partial P}\right)_T = \frac{qRT}{P} \qquad 2.23$$

by using an equation of state:

$$\pi(A - \delta) = qRT \qquad 2.24$$

where δ is the surface area occupied by adsorbed molecules, given by:

$$\delta = \frac{Aq}{q_s} \qquad 2.25$$

The Volmer model can be represented as an implicit relation by:

$$P = \frac{q_s}{K_H}\left(\frac{\theta}{1-\theta}\right)\exp\left(\frac{\theta}{1-\theta}\right) \qquad 2.26$$

The Langmuir model can also be derived using the same equation of state by assuming that δ is smaller than 2A. Therefore, the term δ^2 is neglected upon substituting in the Gibbs equation.

The Gibbs adsorption isotherm may also be used in conjunction with an equation of state of Virial form:

$$\frac{\pi}{qRT} = 1 + B_1 q + B_2 q^2 + \cdots \qquad 2.27$$

to obtain the Virial adsorption isotherm:

$$P = \frac{q}{K_H}\exp(A_1 q + A_2 q^2 + \cdots) \qquad 2.28$$

This isotherm does not give information about the nature of the adsorbed phase; therefore, it is considered as a correlation. However, the values of Henry's constant calculated from this model are deamed the most accurate (1).

The models based on theoretical foundation, sometimes fail to represent accurately the experimental data. Hence, several correlations with weak theoretical basis have been developed and used satisfactorily. These correlations include Freundlich model (35) :

$$q = k_F P^{n_F} \qquad 2.27$$

Langmuir-Freundlich model (35):

$$q = \frac{q_s k_{LF} P^{n_{LF}}}{1 + k_{LF} P^{n_{LF}}} \qquad 2.28$$

and the loading ratio correlation (LRC) model (35):

$$q = \frac{q_s (k_{LRC} P)^{1/n_{LRC}}}{1 + (k_{LRC} P)^{1/n_{LRC}}} \qquad 2.29$$

These three models do not reduce to the Henry's model as the pressure approaches zero which is the main disadvantage of these models. On the other hand, the fit obtained for various data using these models has been found very reasonable especially from the Langmuir-Freundlich and the LRC models.

Ruthven (27) has derived a model for zeolite using statistical thermodynamics fundamentals. The model is based on the following assumptions:

1) The adsorbed molecules are confined within particular cavities of the zeolite lattice.
2) No interaction between sorbate molecules in different cages.

3) The interaction between an adsorbed molecule and the surface is represented by Henry's constant.

The model is given as:

$$q = \frac{K_H P + (K_H P)^2 (1 - 2\beta / V)^2 + \cdots + \frac{(K_H P)^m}{(m-1)!}\left(1 - \frac{m\beta}{V}\right)}{1 + K_H P + \frac{(K_H P)^2}{2!}\left(1 - \frac{2\beta}{V}\right)^2 + \cdots + \frac{(K_H P)^m}{m!}\left(1 - \frac{m\beta}{V}\right)^m} \qquad 2.30$$

where m is the saturation limit (an integer) defined by $m \leq V/\beta$, β is the effective volume of adsorbed molecule $[(A^\circ)^3$/molecule] and V is the cavity volume $(A^\circ)^3$. The Ruthven model is applicable only for adsorbents having a unit cell structure. The model reduces to the Langmuir model when m = 1, which means that only one molecule occupies a cavity.

The models mentioned are some of the many available in the literature. All the models mentioned except the Langmuir and Ruthven models have been used to model the data collected from this work. The selection of these models is based on frequent usage and diversity. The detail computer results and analysis are given in chapters 4,5 and 6.

2.6 Multicomponent Models

Some pure component models can be extended to describe the adsorption behavior of multicomponent systems at equilibrium. For instance, the amount adsorbed for the ith component in a mixture (q_i) can be written using the Langmuir model (19) as :

$$q_i = \frac{k_{L_i} q_{s_i} P_i}{1 + \sum_{i=1}^{N} k_{L_i} P_i} \qquad 2.31$$

For the Langmuir-Freundlich model, q_i is given by (19) :

$$q_i = \frac{k_{LF_i} q_{s_i} P_i^{n_{LF_i}}}{1 + \sum_{i=1}^{N} k_{LF_i} P_i^{n_{LF_i}}} \qquad 2.32$$

where the subscript i refers to the ith component in the mixture.

The Ruthven model can also be extended to multicomponent systems. For instance, for a binary mixture consisting of gases A and B, the number of molecules of gas A adsorbed per cavity (q_A) can be written as (27):

$$q_A = \frac{K_{H_A} P_A + \sum_j \sum_i \left(K_{H_A} P_A\right)^i \left(K_{H_B} P_B\right)^j \left(1 - \frac{i\beta_A}{V} - \frac{j\beta_B}{V}\right)^{i+j} / j!(i-1!)}{1 + K_{H_A} P_A + K_{H_B} P_B + \sum_j \sum_i \left(K_{H_A} P_A\right)^i \left(K_{H_B} P_B\right)^j \left(1 - \frac{i\beta_A}{V} - \frac{j\beta_B}{V}\right)^{i+j} / j!(i-1!)} \qquad 2.33$$

The summations in the above expression are evaluated over all values of i and j such that $i + j \geq 2$ and $i\beta_A + j\beta_B \leq V$ (27).

The multicomponent equilibrium adsorption behavior can also be predicted from knowledge of the pure component equilibrium corresponding to the mixture using the ideal adsorbed solution theory (IAST). This theory (22) presents a relationship between the gas and the adsorbed phase for the

mixtures assuming ideal behavior. Thus, the relationship between the two phases can be described by an analogous form of Raoult's law :

$$Py_i = P_i^\circ x_i \qquad 2.34$$

where P is the pressure of the system, y_i, x_i are the mole fraction of component i in the gas and the adsorbed phases respectively and P_i° is the pressure of the pure component i which it would exert as a pure component at the same temperature and spreading pressure as those of the mixture. At equilibrium, the spreading pressure for each component is constant:

$$\frac{\pi A}{RT} = \varphi = \int_0^{P_1^\circ} \frac{q_1}{P_1} dP_1 = \int_0^{P_2^\circ} \frac{q_2}{P_2} dP_2 = \cdots\cdots = \int_0^{P_i^\circ} \frac{q_i}{P_i} dP_i \qquad 2.35$$

The summation of the adsorbed phase mole fraction is unity:

$$\sum_{i=1}^{N} x_i = 1 \qquad 2.36$$

Therefore, if an appropriate pure component model is used in equation 2.35, the values of P_i°'s corresponding to each component in the mixture can be calculated. The mole fraction of each component in the mixture can be calculated from:

$$x_i = \frac{Py_i}{P_i^\circ} \qquad 2.37$$

The total amount adsorbed can then be obtained from:

$$q_{tot} = \frac{1}{\sum_{i=1}^{N} \frac{x_i}{q_i^\circ}} \qquad 2.38$$

where q_i^* is the amount adsorbed for component i in the pure state at P_i^*. Valenzuela and Myers (33) present a general algorithm for solving the IAST equation.

In this research, the algorithm of Valenzuela and Myers has been used to predict the mixture behavior using the pure models of Toth, Unilan and Virial three constant models. For Toth model, an analytical expression was developed by Valenzuela and Myers for the function φ :

$$\varphi = q_s\left[\theta - \frac{\theta}{t}\ln(1-\theta) - \sum_{j=1}^{\infty}\frac{\theta^{jt+1}}{jt(jt+1)}\right] \qquad 2.39$$

For Unilan model, the function φ can be expressed as:

$$\varphi = \frac{q_s}{2s}\int_{-s}^{s}\ln\left[1+(P/c)\exp(z)\right]dz \qquad 2.40$$

The IAST model is a special case of the general non ideal solution theory (NAS) in which, the activity coefficient and the fugacity coefficient are added to equation 2.34. The calculation procedure of the NAS is discussed by Chen et al (5).

2.7 Previous Studies

There are four variables that affect the gas-solid equilibrium nature: the type of gas or gas mixture, the type of adsorbent, the equilibrium pressure (for mixtures) and the equilibrium temperature. Changing any of these variables will definitely give different equilibrium results. Several studies have been carried out and reported in the literature for different pure and multicomponent gas mixtures on different types of adsorbents at various conditions. However, there are no studies describing the adsorption behavior

of multicomponent gas system on ETS-10 zeolite. In addition, few studies have been made on SR-115 zeolite.

The following is a review of selective studies carried out over the last twenty years for multicomponent gas systems :

Ruthven (27) applied his statistical model to the binary adsorption data on 5A molecular sieve of nitrogen-carbon monoxide (145 K and 1 atm), nitrogen-oxygen (298 K and 600 torr, and 145 K and 1 atm) and oxygen-carbon monoxide (145 K and 1 atm). The fit of the model to the data was satisfactory.

Danner and Edwin (7) studied the adsorption equilibria of the binary system of ethane-ethylene on 13X zeolite at two different temperature (20 °C and 50 °C) and 20 psia pressure. The data were modeled using the IAST, the two dimensional gas model (TDG) and a statistical thermodynamic model. The three models succeed in predicting the data.

Cochran and coworkers (6) developed a model based on the vacancy solution theory (VST) in conjunction with the Flory-Huggins activity coefficient equations. The model uses the parameters obtained from pure gas data to predict the gas mixture equilibria. This model was applied to various gas systems on activated carbon, silica gel and zeolites over a wide range of conditions. Most of the results showed excellent agreement of the model with the experimental data.

Talu and Zwiebel (30) studied the adsorption behavior of binary and ternary mixtures of carbon dioxide, hydrogen sulfide and propane on H-mordenite molecular sieve zeolite at 30 °C. The experimental data collected were modeled using a spreading pressure dependent equation (SPD), the Langmuir model, the VST model and the IAST model. They found that the binary data

were in a good agreement with the SPD, IAST and the VST models; while only the SPD model was satisfactory for the ternary data.

Rota and coworkers (26) extended the generalized statistical model to non ideal multicomponent adsorption equilibria, taking into account the interaction between unlike molecules. The model was successfully applied to the highly non ideal system of benzene-p chlorotoluene on CaX zeolite at 493 K and atmospheric pressure.

Bin Abdul-Rehman (3) studied the adsorption behavior of pure, binary, ternary and quaternary mixtures of methane, ethane, propane, and n-butane on 5A, 13X, and SR-115 zeolites at elevated pressure up to 250 Psia and temperature range of 275 to 350 K. The multicomponent data were modeled using Toth and Ruthven models. The results showed reasonable agreement for both models.

Graham and coworkers (11) used the IAST model to predict the binary data of nitrogen-carbon dioxide on ZSM-5 zeolite at various conditions. The modeling results showed closed agreement with the data.

Nitta and coworkers (23), derived a model based on the scaled particle theory and a patchwise model. The model was applied to four binary systems: methane-ethane, methane-ethylene, carbon dioxide-ethylene, and carbon dioxide-ethane on KF-1500 activated carbon at 25°C and 500 kPa. The data obtained were in satisfactory agreement with the model.

Tokunaga and coworkers (31) used the IAST model in conjunction with the multisite occupancy model to interpret the data generated for the binary system methane-carbon dioxide on KF-1500 activated carbon at 530 kPa and 25 °C. Results of the fit are comparable to those obtained experimentally.

Chen and coworkers (5) presented data for the pure hydrogen, methane, carbon monoxide, and carbon dioxide and various binary mixtures of these

components at various conditions on 5A molecular sieve. The data were correlated using the spreading pressure dependent non ideal adsorbed solution theory (SPD-NAS), the extended Langmuir (EL), and the IAST models. The authors showed that the fit of the IAST and the EL models are very similar. On the other hand, the fit of the SPD-NAS model was the best for all the systems tested.

Hyun and Danner (13) collected equilibrium data on 13X zeolite for pure ethane, ethylene, isobutane and carbon dioxide and binary mixtures of these components at various conditions. The binary data were correlated using the IAST, Ruthven and the VST models. The azeotropic behavior observed for the binary system ethylene-isobutane was predicted only by the VST model.

2.8 Literature Cited

1) Barrer, R.M., and Davis, J.A., Proc. Roy. Soc., London, A320, P. 289, 1970.

2) Barrer, R.M., Zeolites and Clay Minerals, Academic Press, London, 1978.

3) Bin Abdul Rehman, H., Equilibrium Adsorption of Light Gases and Their Mixtures on 5A, 13X, and SR-115. M.S. Thesis, KFUPM, Dhahran, 1988.

4) Breck, D.W., Zeolite Molecular Sieves. Wiley-Inter Sci., New York, 1974

5) Chen, Y.D., Ritter, J.A., and Yang, R.T., Chem. Eng. Sci., 45 (9) P. 2877, 1990.

6) Cochran, T.W., Kabel, R.L., and Danner, R.P., AIChE, 31 (2), P. 268, 1985.

7) Danner, R.P., and Edwin, C.F., Ind. Eng. Chem. Fund., 17 (4), P. 248, 1978.

8) De Boer, J.H., The Dynamical Character of Adsorption, 2nd. ed., Oxford Press, London, 1968.

9) Dubinin, M.M., Chem. Rev., 60, P. 235, 1960.

10) Hirschfelder, J.O., Curtis, C.F., and Bird, R.B., Molecular Theory of Gases and Liquids, Wiley, New York, 1954.

11) Graham, T.W., Hughes, A.D., and Rees, L.V.C., Gas Sep. Purif., 3, P. 56 June 1989.

12) Honig, J.M., and Reyerson, L.H., J. Phy. Chem., 56, P. 140, 1952.

13) Hyun, S.H., and Danner, R.P., J. Chem. Eng. Data, 27, P. 196, 1982.

14) Karavias, F., and Myers, A.L., Chem. Eng. Sci., 47 (6), P. 1435, 1992.

15) Kierlik, E., Rosinberg, M., Finn, J.E., and Monson, P.A., Mol. Phys., 75 (6), P.1435, 1992.

16) Kiselev, A.V., Adv. Chem., 102, P. 37, 1971.

17) Laidler, K.J., and Meiser, J.H., Physical Chemistry, 1st edition, The Benjamin Cummins Pub. Com., California, 1982.

18) Langmuir, I., Phys. Rev., 8, P. 149, 1916.

19) Levan, M.D., and Vermeulen, T., J. Phy. Chem. 85, P. 3247, 1981.

20) Loughlin, K.F., and Roberts, G.D., Study of Mixture Equilibria of Methane and Krypton on 5A Zeolite. ACS. Symposium Series, 135, P. 55 1980.

21) Mathews, AP., and Weber, W.J., Adsorption and Ion Exchange with Synthetic Zeolite, ACS. Symposium Series, 135, P. 27, 1980.

22) Myers, A.L., and Prausnitz, J.M., AIChE, 11 (1), P.121, 1965.

23) Nitta, T., Nozawa, M., and Kida, S., J. Chem. Eng. Jpn., 25(2), P. 176, 1992.

24) Nitta, T., Yamaguchi, A., Tokunaga, N., and Katayama, T., J. Chem. Eng. Jpn., 24 (3), P. 312, 1992.

123

25) Radke, C.J., and Prausnitz, J.M., AIChE, 18, P. 761, 1972.

26) Rota, R., Gamba, G., Paludetto, R., Carra, S., and Morbidelli, M., Ind. Eng. Chem. Fund., 27 (5), P. 848, 1988.

27) Ruthven, D.M., AIChE, 22 (4), P. 753, 1976.

28) Ruthven, D.M., Principles of Adsorption and Adsorptive Separation Processes, Wiley-Inter. Sci., New York, 1984.

29) Sircar, S., Ind. Eng. Chem. Res., 31 (7), P. 1441, 1992.

30) Talu, O., and Zwiebel, I., AIChE, 32 (8), P. 1263, 1986.

31) Tokunaga, N., Mashide, A.B.E., Nitta, T., and Katayama, T., J. Chem. Eng. Jpn., 21 (3), P. 315, 1988.

32) Tokunaga, N., Masahide, A.B.E., Nitta, T., and Katayama, T., J. Chem. Eng. Jpn., 21 (4), P. 431, 1988.

33) Valenzuela, D.P. and Myers, A.L., Adsorption Equilibrium Data Handbook., Prentice-Hall, New York, 1989.

34) Vavlitis, A.P, Ruthven, D.M., and Loughlin, K.F., J. Col. Interface Sci., 84 (2) , 1981.

35) Yon C.M., and Turnock P.H.,. Adsorption Technology, AIChE. Symposium Series, Editors: Max N.Y., and Zwiebel I., 67 (117), P. 75, 1971.

CHAPTER 3

APPARATUS AND PROCEDURE

3.1 Introduction

There are three well known experimental methods to determine the fluid-solid equilibrium data namely, chromatographic, gravimetric and volumetric. The dynamic method in gas chromatography (GC) is used for measuring equilibrium data by frontal analysis. The adsorption isotherm can be obtained from the slopes of the frontal portion of the GC peak. This method is relatively very fast but interpretation of the chromatographic data is difficult and can lead to considerable error (3).

The volumetric and gravimetric apparatus are static type measurements. The adsorbate equilibrates with the adsorbent in a closed system. The difference between the two methods is that the volume of the adsorbent to the volume of the gas space is negligible in the gravimetric method and comparably large in the volumetric method. Therefore, the amount adsorbed is found by weight measurement in the gravimetric method and by pressure and temperature measurement in the volumetric method. Both methods are accurate and reliable; however, there are some disadvantages. The volumetric method is time consuming especially for mixtures. The gravimetric method is relatively faster but it is not adequate for mixtures since the composition of the adsorbed phase can not be deduced from weight measurement.

Most of the fluid-solid equilibrium data reported in the literature for mixtures are obtained by the volumetric method. In this project, the contribution to the literature is made using the volumetric method.

3.2 Apparatus

The apparatus used consists of three chambers:

1) Storage chamber (B).

2) Mixing chamber (D).

3) Adsorption chamber (E) where the adsorbent is placed.

The ancillary parts are:

1) Furnace.

2) Water bath.

3) Vacuum pump.

4) Circulating magnetic pump.

5) Thermocouple and temperature indicator.

6) Temperature controller.

7) Differential pressure gauges.

8) Electronic manometer.

9) Gas chromatograph and integrator.

Figure 3.1 illustrates the assembly of these parts.

3.3 Procedure

3.3.1 Determination of Adsorbent Dry Weight

The dry weight of the adsorbent is determined by placing wet zeolite in a 1000 ml-flask of known weight to which is attached a rubber tube for vacuum isolation. The weight of the flask and the associated tubing is recorded using an electronic balance. Some wet zeolite is placed in the flask and the total weight is recorded. The weight of the wet zeolite can be determined by subtracting the weight of the flask and the rubber tube from the total weight. The flask is then put in the furnace and linked to the vacuum pump via the

rubber tube. The temperature of the furnace is adjusted to either 350 °C for SR-115 or 250 °C for ETS-10 respectively. After 12 hours, the flask is sealed and left to cool. The weight of the assembly and the dry zeolite is recorded. The weight of the dry zeolite is determined by subtracting the new weight from the weight of the assembly. This procedure is repeated two or three times until the same weight is obtained. The zeolite is then transferred to the adsorption chamber (cell E).

3.3.2 Calibration of Cell Volumes

The volumes of the cells D and E are determined by expanding helium which is not adsorbable into the cells. The volume of cell B had been previously determined using mercury in earlier work (2). Thus by recording the pressure of the helium in chamber B at room temperature, the total number of moles can be calculated. If some of the helium from B is transferred to D which is initially at vacuum to raise the pressure to a certain value, the volume of D can be calculated using an equation of state. Similarly, the volume of cell E can be determined by expanding the helium present in cell D to cell E. The calibration procedure is done after regenerating the zeolite present in cell E. At least fifteen runs is required to make sure that the volumetric calibration data is reproducible. The volume of a cell can then be determined from the average. The calibration data obtained for both SR-115 and ETS-10 are reported in appendix A.

3.3.3 Gas Chromatograph Calibration

The GC can be used to determine the mixture composition in the gas phase. If a gas sample is injected to the GC, n peaks corresponding to n components present in the gas sample are produced in the output. The

integrator is used to determine the area of each peak. Each area is proportional to the partial pressure of the corresponding component. To determine the proportionality constant and the time of appearance of the peak, each gas is analyzed individually by the GC. The analysis is done for each gas by injecting different samples at different pressures and recording the corresponding area. The constant of proportionality can be determined from the slope of the plot of pressure versus peak area. Regardless of the pressure, the peaks corresponding to a certain gas appear at the same time. The type of the separation column used in the chromatograph, the temperature and the flow rate of the carrier gas all affect the separation. Therefore, the choice of appropriate column, the operating temperature and the flow rate of the carrier gas is essential for analyzing gas samples especially for close boiling point components. The calibration data for the gases used with the corresponding plots and operating conditions of the chromatograph are given in Appendix A.

3.3.4 Pure Isotherms Determination

In order to obtain a pure gas isotherm data, the zeolite in cell E must be dry and free of gases. Therefore, before the start of any experiment, cell E should be regenerated under full vacuum at temperature of 350°C for SR-115 or 250 °C for ETS-10. The cell is then isolated and left to cool at room temperature. Cell B is filled with the desired gas and its temperature and pressure are recorded. Cell D which is at full vacuum at the start of experiment is connected to cell E after closing the line that connects D to the vacuum. The control valve is then used to introduce gas from cell B to cells D and E until a desired pressure of E is reached. The temperature of cell E is adjusted to the desired isotherm temperature by means of a temperature controller. At the moment where the temperature and the pressure of cell E are constant

(usually after thirty minutes of the run after heat of adsorption is dissipated), the temperature and pressure of the three cells are recorded after closing the control valve. Other runs can be taken for different values of pressure. Having obtained the temperature and the pressure data for each run, the amount adsorbed at the corresponding pressure can be calculated using an equation of state.

3.3.5 Measurements of Multicomponent isotherms

The procedure stated previously for pure component can be extended to multicomponent. In multicomponent equilibrium, the gas phase composition is varied keeping both the pressure and the temperature fixed at certain values. Hence the GC is used to determine the composition of the gas phase for each run. The heaviest gas is introduced first and the lightest last. The variation of composition in the gas phase is done by discarding the gas present in cell D after isolating cell E. Cell E is then connected to cell D and the pressure is balanced to the desired value by introducing gas from cell B via the control valve. In each run, the magnetic pump circulates the gas for at least one hour to assure that equilibrium is established. A detailed procedure is provided in reference 1.

3.4 Literature Cited

1) Al.Baghli, N., Equilibrium Adsorption of Nitrogen and Carbon Dioxide on SR-115 Silicalite, Senior Project, KFUPM., Dhahran. 1990.

2) Bin Abdul Rehman, H., Equilibrium Adsorption of Light Gases and Their Mixture on 5A, 13X and S-115,. M.S. Thesis, KFUPM, Dhahran, 1988.

3) Kaul, B.K., " A Modern Version of the Volumetric Apparatus for Measuring Gas Solid Equilibrium Data", Paper presented at the AIChE. fall meeting, San Francisco, 1984.

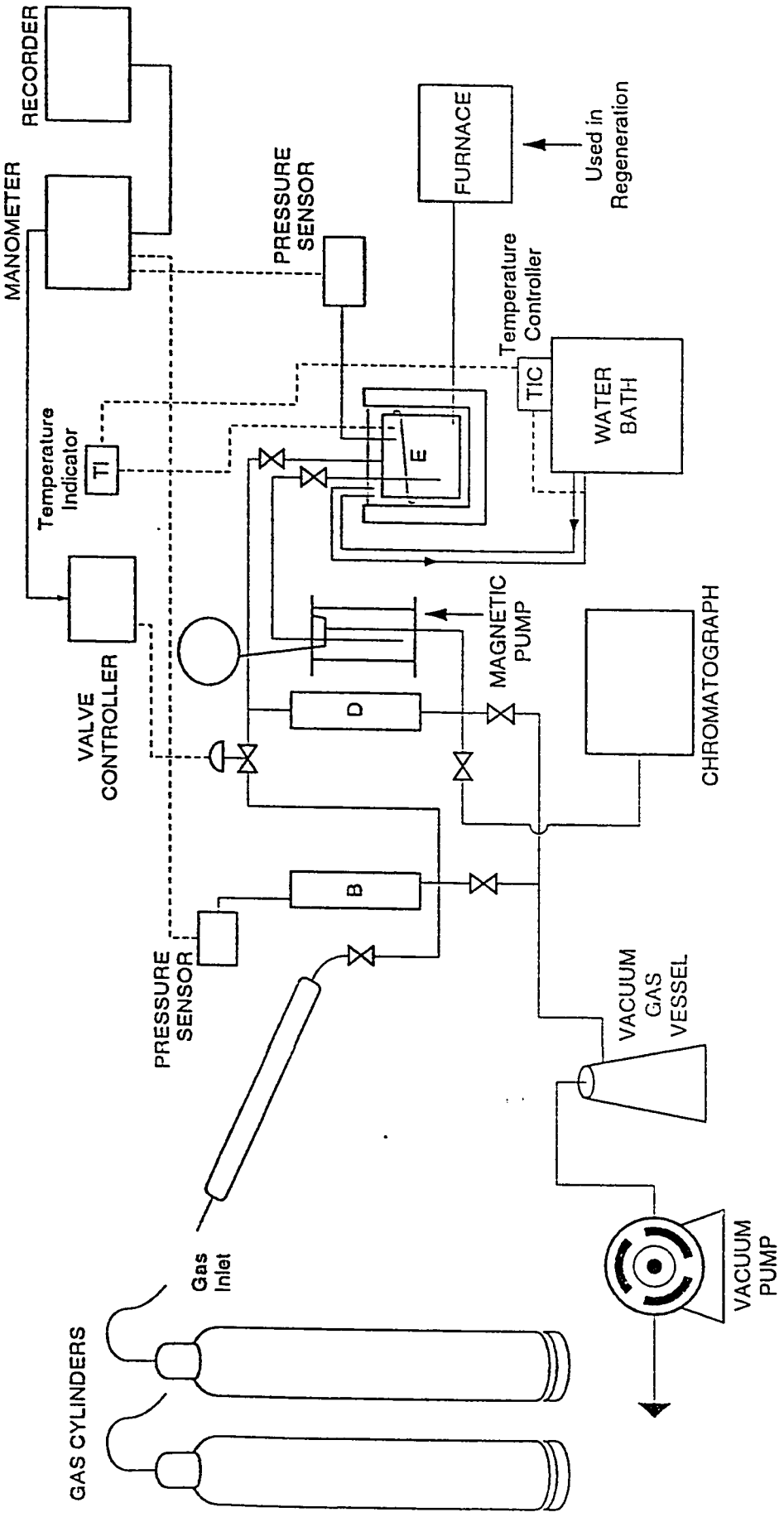

Figure 3.1 Diagram of High Pressure Multicomponent Equilibrium Adsorption Apparatus

CHAPTER 4

ADSORPTION OF NITROGEN AND CARBON DIOXIDE ON SR-115 ZEOLITE

4.1 Introduction

In this chapter, the pure and binary experimental results for the sorption of nitrogen and carbon dioxide on SR-115 zeolite are presented. The data of pure nitrogen has been obtained up to approximately 1000 kPa at three different temperatures (280, 298.2, and 300 K) and combined with the data reported by Abdullah (1) at 280, 290, 300 and 325 K. Carbon dioxide data has also been measured at five different temperatures namely, 280, 300, 315, 325 and 350 K up to approximately 1000 kPa. The measured data consist of temperature and pressure readings of the three cells (Chapter 3). The amount adsorbed per mass of adsorbent (q) at different pressure readings (P) is calculated using Soave-Redlich-Kwong equation of state to evaluate the molar values. The P-q data for nitrogen, carbon dioxide and for all the sorbate used are given in Appendix B, while the program used to calculate q is given in Appendix C.

The P-q data for nitrogen and carbon dioxide are modeled using Toth, Unilan, Radke-Prausnitz, Mathews-Weber, Volmer, Virial two constants, Virial three constants, Freundlich, Langmuir-Freundlich, and the loading ratio correlation models mentioned in chapter 2. The model parameters are evaluated by the Margules least square regression subroutine BSOLVE using the equation:

$$SS = \sum_{i=1}^{NP}\left(\frac{q_{\text{mod}}}{q_{\text{exp}}} - 1\right)^2 + \sum_{i=1}^{NP}\left(q_{\text{mod}} - q_{\text{exp}}\right)^2 \qquad 4.1$$

where ss is the sum of squares error, NP is the number of data points, and q_{mod} and q_{exp} are respectively the amount adsorbed per unit mass of adsorbent

calculated from model and experiment. A list of the units of the model parameters is given in Table 4.1.

Both constrained and unconstrained optimization have been applied for each model. In the unconstrained regression the saturation concentration parameter (q_S) is forced to be greater than the highest experimental concentration obtained at the highest pressure and lowest temperature while the remaining parameters are left to relax to their optimum values. However, in the constrained regression, the saturation concentration parameter is forced to be equal to 95% of the theoretical value calculated from equation (2.8) taking into consideration the steric effect. In addition, the parameters for each model which are found to give similar values at different temperatures, have been forced to be constant at values which minimize the total sum of squares error. In the virial model, only the virial first constant has been forced to be constant.

The binary experimental data obtained by Al-Baghli (2) at five different conditions of temperature and pressure (280 K and 350 kPa, 315 K and 350 kPa, 350 K and 350 kPa, 280 K and 700 kPa, and 315 K and 700 kPa), are modeled using the parameters obtained from the constrained regression of both nitrogen and carbon dioxide. The ideal adsorbed solution theory (IAST) is used to model the binary data using Toth, Unilan and Virial three constant isotherms. The computer programs used in modeling the multicomponent data are given in Appendix C.

4.2 Pure Component Results

The unconstrained and constrained optimization parameters for the sorption of nitrogen on the Linde SR-115 are presented in Tables 4.1 and 4.2. Each table contains ten sets representing the fit of the ten models used. The asterisked temperatures are the results obtained using Abdullah's data (1). A comparison of the results obtained from this research with those obtained from Abdullah

indicate that the results are very reproducible. This establishes the reliability of the apparatus as the data were obtained many years apart.

Comparing the total sum of squares error ($\sum SS$) obtained from each model shows that all the models except Freundlich are excellent for representing the experimental data. In the unconstrained regression, the best fit has been obtained from the loading ratio correlation model even though it has only three parameters. Volmer model gives satisfactory fit with only two parameters but the sum of squares error is rather large. Analysis of the Henry's constant values (K_H) derived from each model show little deviation from the virial model for Toth, Unilan, Radke-Prausnitz, Mathews-Webber and Volmer models.

As expected, the total sum of squares error has increased for all the models when constrained optimization is used (Table 4.3). The value of the saturation concentration of nitrogen on SR-115 has been fixed at 3.750 mol/kg of zeolite which is 95% of the theoretical value calculated by equation 2.8. In Unilan model, the heterogeneity parameter (s) decreases linearly with temperature according to (5):

$$s = \frac{\eta}{RT} \qquad 4.2$$

where η is a parameter related to the energy distribution and R is the universal gas constant. However, no dependence of s on temperature has been observed for all the systems studied in this work. Therefore, the heterogeneity parameter for Unilan has been optimized for nitrogen at 2.1 which is found to give the best fit. Due to their approximately similar values in the unconstrained regression which appeared to exhibit no trend, the values of the third constant in Toth (b), loading ratio correlation (n_{LRC}), Langmuir-Freundlich (n_{LF}), Mathews and Webber (n_{MW}) models have been optimized at 0.67, 1.15, 0.87 and 0.95 respectively. Also, the value of n_{RP} constant of Radke-Prausnitz model has been optimized at 0.71 and in the virial model the value of A_1 constant has been optimized at 0.6. These values have been found to give the best fit. In Mathews-

Weber model, the value of n_{MW} is near to unity. This indicates that this model is reducible to Langmuir model for this system. Since only one constant has been fixed in the virial models, the total sum of square error hasn't changed significantly. Therefore, the virial model is considered to be the best model in the constrained analysis. Constraining the parameters hasn't significantly affected the values of Henry's constants for all the models. The fit of Toth, Unilan and Virial models to the experimental data using the constrained parameters are presented in Figures 4.1 to 4.3.

The unconstrained and constrained regression of carbon dioxide are shown respectively in Tables 4.4 and 4.5. The regression results for the ten models used are not as good as those obtained for nitrogen or any other sorbate in this thesis. This is attributed to the constraint that forces the saturation limit to be below the theoretical value calculated from equation 2.8 namely 3.55 mol/kg of zeolite. Much better fit has been obtained when all the parameters are allowed to relax to the optimum values. However, the saturation concentration parameter exceeds the theoretical value. This suggests that carbon dioxide might be adsorbing on the binder of the zeolite. Hence, it is recommended to obtain isotherms of carbon dioxide on the pure form of SR-115 zeolite as well as on the binder. The data obtained can then be combined and compared to the results obtained in this work. In the constrained regression of carbon dioxide, values of t for Toth, s for Unilan, n_{MW} for Mathews-Webber, A_1 for virial, n_{LF} for Langmuir-Freundlich, and n_{LRC} for the L.R.C. models have been respectively optimized at 0.45, 3.45, 1.05, 1.4, 0.65, and 1.6. These values have been found to give the minimum total sum of squares error which deteriorates for all models upon constraining the parameters. Comparing the constrained regression obtained for the models, show that the L.R.C. model is the best. As for nitrogen, the fit of Mathews-Weber model appears to be similar to the fit of Langmuir model since the value of n_{MW} approaches unity. Radke-Prausnitz model hasn't worked for this system due to some computational problems.

The constrained fit of IAST model using Toth, Unilan and Virial isotherms to the experimental data is presented in Figures 4.4 to 4.6.

Table 4.6 gives a comparison between the Henry's constant values obtained from this work and the values obtained by Graham et al (4) on silicalite for both nitrogen and carbon dioxide. Before comparing the results, it is important to mention that the results of Graham et al were obtained on a pure form of silicalite with no binder. Also, the Henry's constant values used for comparison were calculated by interpolating the values obtained by Graham et al using equation 2.5. For nitrogen, the Henry's constant values of Graham et al are comparable to the values obtained from this work. However, the values obtained for carbon dioxide are ten times greater than Graham et al values. This suggests that the Henry's constant values obtained in this work for carbon dioxide have to be corrected using a model that takes into consideration the adsorption of carbon dioxide on the binder of the silicalite such as :

$$q = q_{Sil} + q_{Bin} \qquad 4.3$$

where q_{Sil} and q_{Bin} are the amount adsorbed on the silicalite and on the binder of the silicalite respectively. Much better fit and hence much better values of Henry's constants are expected to be obtained upon using this model. In fact, the test of equation 4.3 using Toth model for the silicalite and Langmuir model for the silicalite binder is being generated.

Table 4.7 gives the Vant Hoff equation parameters for both nitrogen and carbon dioxide. These values are obtained from the best fit of the semilog plot of Henry's constant values (obtained from constrained analysis) versus the reciprocal of temperature. For nitrogen, the virial three constant model is the best. Other, acceptable regression K_H values are obtained from Toth, Unilan, Radke-Prausnitz and virial two constant models. The isotherms of Volmer and Mathews-Weber are not acceptable.

For carbon dioxide, the fit of virial two constant is a little better than that of virial three constant since the values of virial second parameter when using virial

three constant model are zero which reduces this model to a three constant model.

Again, the regression K_H values obtained from Volmer and Mathews-Weber models deviate significantly from virial's and therefore are unacceptable.

The values of heat of adsorption obtained for nitrogen using virial model can be compared to the values calculated theoretically by Barrer (3) for different types of silicalite (Table 4.8). Since the structure of silicalite contains no cations, the contribution of dipole and quadrupole interactions to the heat of adsorption is negligible. Therefore, the energies of dispersion, repulsion and polarization are the main contributors to the heat of adsorption. The value of the heat of adsorption calculated experimentally in this work is of the same order of magnitude as the sum of energies of dispersion, repulsion and polarization calculated for nitrogen. The slight deviation is attributed to the fact that the cavity sizes are different and hence, molecules will reside at a different distance from SiO_2. Also, these zeolites contain AlO_2 with different composition in their structure, while silicalite is purely SiO_2. For carbon dioxide, the comparison between the theoretical and experimental value of heat of adsorption is meaningless before correcting the interpretation to the data.

4.3 Binary Results

The binary experimental results of nitrogen-carbon dioxide on the Linde SR-115 zeolite are presented on Table 4.9. The table consists of five sets. At the top of each set are the temperature and pressure at which the experiment is performed. The experimental binary results have been obtained from the temperature and pressure readings of the three cells (Chapter 3) using the Soave-Redlich-Kwong equation of state to generate the molar volumes of the sorbates. The program used to do the calculations is presented in Appendix C. Plots of the mole fraction of nitrogen in the adsorbed phase versus mole fraction of nitrogen in the gas phase are presented in Figures 4.7 to 4.11. Figures 4.12 to 4.16 present

plots of the mole fraction of nitrogen in the adsorbed phase versus amount adsorbed of nitrogen, carbon dioxide and total amount adsorbed. As shown in these plots, the results obtained are reliable, reasonable and consistent.

The quality of the adsorptive separation for any binary mixture can be determined by knowledge of the relative adsorptivity or the separation factor α_{AB} defined as :

$$\alpha_{AB} = \frac{x_A}{y_A}\frac{y_B}{x_B} \qquad 4.4$$

In terms of Henry's constant, the relative adsorptivity can be approximately expressed as a ratio of the Henry's constant values obtained for the binary components A and B (4):

$$\alpha_{AB} = \frac{K_{H_A}}{K_{H_B}} \qquad 4.5$$

The higher the value of α_{AB} is, the better the separation. It has been found that, the separation of component A from component B is economical only if α_{AB} is greater than 3 (5).

Table 4.10 lists the values of the relative adsorptivity of carbon dioxide to nitrogen. The values listed in this table have been calculated from the experimental data using equation 4.4. From this table, it is apparent that the separation of nitrogen from carbon dioxide is best at low temperature and low pressure. In addition, the separation is economically possible only for temperatures below 280 K and pressures below 700 kPa.

Concerning the data, it is suggested not to take more than ten continuous runs if small experimental error is required. If data at very high gas mole fraction of nitrogen is required, it is recommended to start with minimum of 50% nitrogen. This can be achieved by first pressurizing the adsorption cell with carbon dioxide to half the pressure required to perform the run and then expanding nitrogen until the required pressure is achieved.

The fit of IAST model using Toth, Unilan and Virial isotherms for the experimental data is not satisfactory for any of the five runs. To illustrate this, Toth model has been chosen to represent the data for the runs performed at 280 K. The x-y fits of Toth model are presented in Figures 4.7 and 4.10, while the x-q fits are presented in Figures 4.12 and 4.15. The results of the fit of the three models are given in Tables 4.11 to 4.13.

As given in Tables 4.12 and 4.13, the fits of the three models are identical. However, all the three models fail to represent the experimental data. The big deviation is attributed to the incorrect Henry's constants values obtained from pure carbon dioxide fit. Therefore, it is expected to get much better fit for the binary system if isotherms of carbon dioxide were available on pure SR-115 zeolite or after remodeling the data using equation 4.3.

4.4 Literature Cited

1) Abdullah, Equilibrium Adsorption of Nitrogen on SR-115 Zeolite, Senior Project, KFUPM, Dhahran 1989.

2) Al-Baghli, N., Equilibrium Adsorption of Nitrogen and Carbon Dioxide on SR-115 Silicalite, Senior Project, KFUPM, Dhahran 1990.

3) Barrer R.M., Zeolites and Clay Minerals, Academic Press, London, 1978.

4) Graham P., Hughes A.D., and Rees L.V.C., Gas Sep. Pur., 3, P. 56, June, 1989.

5) Myers A.L., Fundamental of Adsorption, Editors: Myers, A.L., and Belfort, G., United Engineering Trustees Inc., P. 365, 1984.

Table 4.1 Units of the Model Parameters

Model	Parameters	Units
Toth	b t	$(kPa)^t$ dimensionless
Unilan	c s	kPa dimensionless
Radke-Prausnitz	b_{RP} c_{RP} n_{RP}	1/kPa $1/(kPa)^{n_{RP}}$ dimensionless
Mathews-Weber	b_{MW} n_{MW}	1/kPa dimensionless
Virial Two Constant	A_1 A_2	kg/mol $(kg/mol)^2$
Virial Three Constant	A_1 A_2 A_3	kg/mol $(kg/mol)^2$ $(kg/mol)^3$
Freundlich	k_F n_F	$mol/kg/(kPa)^{n_F}$ dimensionless
Langmuir-Freundlich	k_{LF} n_{LF}	$(kPa)^{-n_{LF}}$ dimensionless
Loading Ratio Correlation	k_{LRC} n_{LRC}	1/kPa dimensionless

The saturation concentration Parameter (q_s) is expressed in mol/kg of zeolite. Henry's constant (K_H) is expressed in mol/kg/kPa.

Table 4.2 Unconstrained Optimization Parameters for The Sorption of Nitrogen on SR-115 Zeolite

Toth Model

Temperature (K)	ss	q_s	b	t	K_H
280	0.0034	3.402	73.71	0.682	0.00622
280*	0.0132	3.750	166.6	0.784	0.00551
290*	0.0022	3.344	167.4	0.782	0.00479
298	0.0058	2.857	317.9	0.846	0.00316
300	0.0007	2.481	497.2	0.919	0.00289
300*	0.0116	3.526	143.8	0.729	0.00389
325*	0.0080	3.750	181.7	0.720	0.00273

$\sum ss = 0.0450$

Unilan Model

Temperature (K)	ss	q_s	c	s	K_H
280	0.0100	3.750	1485	2.324	0.00550
280*	0.0157	3.740	1010	1.468	0.00518
290*	0.0026	3.392	1097	1.559	0.00451
298	0.0072	2.892	1207	1.265	0.00309
300	0.0006	2.465	961.7	0.801	0.00285
300*	0.0116	3.711	1823	1.927	0.00355
325*	0.0126	3.590	2129	1.556	0.00238

$\sum ss = 0.0604$

Radke-Prausnitz Model

Temperature (K)	ss	q_s	b_{RP}	c_{RP}	n_{RP}	K_H
280	0.0052	3.750	0.00161	0.0852	0.407	0.00603
280*	0.0104	3.750	0.00216	0.0104	0.747	0.00812
290*	0.0020	3.115	0.00205	0.0119	0.765	0.00637
298	0.0034	2.653	0.00149	0.0098	0.828	0.00396
300	0.0006	2.599	0.00111	0.6154	0.329	0.00288
300*	0.0128	3.566	0.00150	0.0119	0.669	0.00535
325*	0.0078	3.750	0.00083	0.0084	0.716	0.00311

$\sum ss = 0.0423$

Mathews-Weber Model

Temperature (K)	ss	q_s	b_{MW}	n_{MW}	K_H
280	0.0052	1.807	0.0032	0.817	0.00583
280*	0.0110	2.274	0.0026	0.789	0.00580
290*	0.0026	2.315	0.0020	0.876	0.00460
298	0.0068	2.226	0.0014	0.900	0.00311
300	0.0006	2.204	0.0013	0.949	0.00287
300*	0.0117	1.921	0.0021	0.789	0.00395
325*	0.0038	1.670	0.0018	0.621	0.00300

$\sum ss = 0.0419$

Volmer Model

Temperature (K)	ss	q_s	K_H
280	0.0171	3.750	0.00544
280*	0.1958	3.750	0.00559
290*	0.3561	3.750	0.00390
298	0.0219	3.750	0.00311
300	0.0057	3.750	0.00292
300*	0.0456	3.750	0.00394
325*	0.0290	3.750	0.00266

$\sum ss = 0.6711$

Virial Two Constant Model

Temperature (K)	ss	A_1	A_2	K_H
280	0.0079	0.657	0.0656	0.00557
280*	0.0115	0.558	0.0084	0.00553
290*	0.0026	0.485	0.0834	0.00450
298	0.0087	0.484	0.1090	0.00305
300	0.0010	0.395	0.1920	0.00279
300*	0.0115	0.628	0.0286	0.00372
325*	0.0092	0.571	0.0000	0.00245

$\sum ss = 0.0524$

123

Virial Three Constant Model

Temperature (K)	ss	A_1	A_2	A_3	K_H
280	0.0067	0.709	0.0000	0.0242	0.00563
280*	0.0118	0.536	0.0184	0.0000	0.00547
290*	0.0028	0.517	0.0237	0.0254	0.00449
298	0.0073	0.554	0.0000	0.0494	0.00308
300	0.0006	0.503	0.0361	0.0661	0.00285
300*	0.0114	0.606	0.0381	0.0000	0.00367
325*	0.0086	0.581	0.0000	0.0000	0.00248

$\Sigma ss = 0.0492$

Freundlich Model

Temperature (K)	ss	k_F	n_F
280	0.7063	0.0248	0.614
280*	0.1298	0.0268	0.623
290*	0.0646	0.0276	0.596
298	0.5620	0.0122	0.685
300	0.1390	0.0129	0.666
300*	0.1121	0.0245	0.589
325*	0.0725	0.0100	0.701

$\Sigma ss = 3.0371$

Langmuir-Freundlich Model

Temperature (K)	ss	q_s	k_{LF}	n_{LF}
280	0.0076	2.799	0.00286	0.891
280*	0.0102	3.663	0.00224	0.889
290*	0.0019	3.010	0.00204	0.920
298	0.0028	2.602	0.00139	0.957
300	0.0010	2.352	0.00128	0.984
300*	0.0134	3.196	0.00188	0.878
325*	0.0037	3.750	0.00106	0.887

$\Sigma ss = 0.0408$

Loading Ratio Correlation Model

Temperature (K)	ss	q_s	k_{LRC}	n_{LRC}
280	0.0072	2.808	0.00139	1.122
280*	0.0102	3.633	0.00106	1.122
290*	0.0019	3.015	0.00119	1.088
298	0.0028	2.603	0.00103	1.045
300	0.0010	2.356	0.00114	1.017
300*	0.0132	3.182	0.00079	1.137
325*	0.0041	3.750	0.00046	1.119

$\sum ss = 0.0404$

Units of the parameters are given in Table 4.1.

* : Data obtained from reference 1.

Table 4.3 Constrained Optimization Parameters for The Sorption of Nitrogen on SR-115 Zeolite

Toth Model

T(K)	280	280*	290*	298	300	300*	325*
ss	0.0122	0.0394	0.0054	0.0121	0.0151	0.0139	0.0155
b	74.42	67.39	77.89	105.4	112.8	93.75	118.9
K_H	0.0060	0.0070	0.0056	0.0036	0.0032	0.0043	0.0030

$\sum ss = 0.1136$

t is constrained at 0.670

Unilan Model

T(K)	280	280*	290*	298	300	300*	325*
ss	0.0580	0.0384	0.0050	0.0060	0.0017	0.0130	0.0146
c	1433	1177	1470	2257	2472	1937	2738
K_H	0.0050	0.0061	0.0049	0.0032	0.0029	0.0037	0.0026

$\sum ss = 0.1367$

s is constrained at 2.10

Radke-Prausnitz Model

T(K)	280	280*	290*	298	300	300*	325*
ss	0.0241	0.0108	0.0028	0.0097	0.0156	0.0142	0.0070
b_{RP}	0.0032	0.0019	0.0022	0.0012	0.0010	0.0018	0.0008
c_{RP}	0.0077	0.0148	0.0090	0.0076	0.0084	0.0070	0.0086
K_H	0.0119	0.0073	0.0081	0.0047	0.0037	0.0067	0.0031

$\sum ss = 0.0843$

n_{RP} is constrained at 0.710

Mathews-Weber Model

T(K)	280	280*	290*	298	300	300*	325*
ss	0.5953	0.1108	0.0976	0.2191	0.1521	0.1533	0.0707
b_{MW}	0.0010	0.0011	0.0009	0.0007	0.0006	0.0007	0.0005
K_H	0.0038	0.0042	0.0033	0.0026	0.0024	0.0025	0.0020

$\sum ss = 1.3989$

n_{MW} is constrained at 0.950

Virial Two Constant Model

T(K)	280	280*	290*	298	300	300*	325*
ss	0.0119	0.0116	0.0023	0.0053	0.0058	0.0114	0.0081
A_2	0.0904	0.0000	0.0327	0.0407	0.0837	0.0411	0.0000
K_H	0.0054	0.0057	0.0048	0.0032	0.0030	0.0037	0.0025

$\sum ss = 0.0565$

A_1 is constrained at 0.60

Virial Three Constant Model

T(K)	280	280*	290*	298	300	300*	325*
ss	0.0109	0.0116	0.0022	0.0053	0.0029	0.0114	0.0090
A_2	0.0923	0.0000	0.0000	0.0000	0.0000	0.0359	0.0000
A_3	0.0003	0.0000	0.0188	0.0304	0.0590	0.0028	0.0000
K_H	0.0055	0.0057	0.0047	0.0032	0.0029	0.0037	0.0025

$\sum ss = 0.0533$

A_1 is constrained at 0.600

Langmuir-Freundlich Model

T(K)	280	280*	290*	298	300	300*	325*
ss	0.1756	0.0119	0.0110	0.0256	0.1337	0.0315	0.0062
k_{LF}	0.0023	0.0024	0.0020	0.0014	0.0013	0.0016	0.0012

$\sum ss = 0.3949$

n_{LF} is constrained at 0.870

Loading Ratio Correlation Model

T(K)	280	280*	290*	298	300	300*	325*
ss	0.0597	0.0127	0.0064	0.0272	0.0692	0.0205	0.0059
k_{LRC}	83E-5	98E-5	78E-5	52E-5	47E-5	59E-5	43E-5

$\sum ss = 0.2016$

n_{LRC} is constrained at 1.150

Units of the parameters are given in Table 4.1.

* : Data obtained from reference 1.

All models requiring q_s have been constrained at 3.75 mol/kg of zeolite.

Volmer and Freundlich parameters have not been constrained.

Table 4.4 Unconstrained Optimization Parameters for The Sorption of Carbon Dioxide on SR-115 Zeolite

Toth Model

T(K)	280	300	315	325	350
ss	0.4218	0.1742	0.1905	0.1877	0.2438
q_s	3.550	3.550	3.550	3.550	3.550
b	2.113	5.136	2.617	3.089	4.645
t	0.543	0.589	0.441	0.444	0.448
K_H	0.900	0.220	0.402	0.279	0.244

$\sum ss = 1.2180$

Unilan Model

T(K)	280	300	315	325	350
ss	0.4469	0.1054	0.2485	0.5070	0.3957
q_s	3.550	3.550	3.540	3.550	3.550
c	21.62	49.31	84.21	134.61	326.26
s	2.713	2.623	3.444	2.976	3.993
K_H	0.454	0.188	0.191	0.087	0.074

$\sum ss = 1.7032$

Mathews-Weber Model

T(K)	280	300	315	325	350
ss	1.5357	0.8262	1.6621	1.5876	1.6655
q_s	3.550	3.550	3.550	3.550	3.550
b_{MW}	0.0480	0.0199	0.0114	0.0091	0.0049
n_{MW}	0.987	1.023	1.059	1.083	1.146
K_H	0.1703	0.0707	0.0405	0.0324	0.0175

$\sum ss = 7.2771$

Volmer Model

T(K)	280	300	315	325	350
ss	1.7118	0.9093	0.6646	0.6801	0.8913
q_s	3.550	3.550	3.550	3.550	3.550
K_H	0.8037	0.2723	0.1388	0.091	0.033

$\sum ss = 4.8569$

Virial Two Constant Model

T(K)	280	300	315	325	350
ss	0.3349	0.0934	0.1771	0.2163	0.3874
A_1	0.644	0.651	1.366	1.358	1.279
A_2	0.197	0.174	0.018	0.000	0.000
K_H	0.5055	0.1957	0.2027	0.2163	0.0580

$\Sigma ss = 1.2090$

Virial Three Constant Model

T(K)	280	300	315	325	350
ss	0.3349	0.0934	0.1771	0.2163	0.3874
A_1	1.008	0.924	1.388	1.375	1.299
A_2	0.000	0.000	0.000	0.000	0.000
A_3	0.0317	0.0321	0.0054	0.0000	0.0000
K_H	0.6113	0.2196	0.2068	0.1427	0.0601

$\Sigma ss = 1.0532$

Freundlich Model

T(K)	280	300	315	325	350
ss	2.0998	1.4048	1.3000	1.1360	0.7482
k_F	0.495	0.524	0.425	0.312	0.189
n_F	0.309	0.280	0.289	0.327	0.385

$\Sigma ss = 6.6894$

Langmuir-Freundlich Model

T(K)	280	300	315	325	350
ss	0.2202	0.0253	0.0408	0.1838	0.0736
q_s	3.550	3.550	3.550	3.550	3.550
k_{LF}	0.121	0.066	0.062	0.044	0.026
n_{LF}	0.705	0.698	0.607	0.605	0.647

$\Sigma ss = 0.5438$

Loading Ratio Correlation Model

T(K)	280	300	315	325	350
ss	0.1954	0.0514	0.0796	0.0643	0.0968
q_s	3.550	3.550	3.550	3.550	3.550
k_{LRC}	0.0560	0.0183	0.0099	0.0076	0.0035
n_{LRC}	1,431	1.449	1.593	1.555	1.529

$\Sigma ss = 0.4848$

Units of the model Parameters are given in Table 4.1.

Table 4.5 Constrained Optimization Parameters for The Sorption of Carbon Dioxide on SR-115 Zeolite

Toth Model

T(K)	280	300	315	325	350
ss	0.6949	0.4293	0.1927	0.1932	0.2425
b	1.285	2.054	2.797	3.272	4.638
K_H	2.035	0.717	0.361	0.255	0.117

$\sum ss = 1.7528$

t is constrained at 0.450

Unilan Model

T(K)	280	300	315	325	350
ss	0.2942	0.1954	0.2664	0.3134	0.4517
c	17.02	47.00	95.37	132.71	292.67
K_H	0.951	0.344	0.170	0.122	0.055

$\sum ss = 1.5212$

s is constrained at 3.450

Mathews-Weber Model

T(K)	280	300	315	325	350
ss	2.0067	0.6126	1.6717	1.7043	1.9479
b_{MW}	0.0485	0.0302	0.0125	0.0101	0.0053
K_H	0.1721	0.1072	0.0444	0.0360	0.0188

$\sum ss = 7.9432$

n_{MW} is constrained at 1.05

Virial Two Constant Model

T(K)	280	300	315	325	350
ss	0.1322	0.0716	0.1665	0.1860	0.2960
A_2	0.0436	0.0000	0.0102	0.0000	0.0000
K_H	1.1355	0.3717	0.2090	0.1492	0.0716

$\sum ss = 0.8523$

A_1 is constrained at 1.400

Virial Three Constant Model

T(K)	280	300	315	325	350
ss	0.1179	0.0791	0.1672	0.2049	0.3044
A_2	0.0000	0.0000	0.0000	0.0000	0.0000
A_3	0.0120	0.0011	0.0039	0.0000	0.0000
K_H	1.0811	0.3890	0.2084	0.1437	0.0700

$\sum ss = 0.8734$

A_1 is constrained at 1.400

Langmuir-Freundlich Model

T(K)	280	300	315	325	350
ss	0.2309	0.0493	0.1432	0.0785	0.0722
k_{LF}	0.135	0.079	0.056	0.043	0.026

$\sum ss = 0.5438$

n_{LF} is constrained at 0.650

Loading Ratio Correlation Model

T(K)	280	300	315	325	350
ss	0.2309	0.1051	0.0710	0.0350	0.0407
k_{LRC}	0.0527	0.0200	0.0099	0.0076	0.0035

$\sum ss = 0.4826$

n_{LRC} is constrained at 1.600

Units of the model Parameters are given in Table 4.1.
All models requiring q_s has been constrained at 3.55 mol/kg of zeolite.
Volmer and Freundlich parameters have not been constrained.

Table 4.6 Comparison Between Literature and Experimental Values of Henry's Constant on Silicalite

Nitrogen

Temperature (K)	Values Obtained by Graham et al (4)+ K_H (mol/kg/kPa)	Values Obtained in This Study K_H (mol/kg/kPa)
280	0.0046	0.0055
290	0.0041	0.0047*
298	0.0038	0.0032
300	0.0037	0.0030
325	0.0029	0.0025*

Carbon Dioxide

Temperature (K)	Values Obtained by Graham et al (4)+ K_H (mol/kg/kPa)	Values Obtained in This Study K_H (mol/kg/kPa)
280	0.0659	1.0811
300	0.0336	0.3890
315	0.0214	0.2084
325	0.0162	0.1437
350	0.0087	0.0700

* : Value calculated using data of reference 1.
+ : Values calculated by interpolation using equation 2.5.

Table 4.7 Vant Hoff Equation Parameters of Nitrogen and Carbon Dioxide on SR-115 Zeolite

Nitrogen

Model	$\sum ss$	$K_0 * 10^5$	$-\Delta H_0$
Toth	0.1136	1.2667	14.410
Unilan	0.1367	1.3862	13.848
Radke-Prausnitz	0.0843	0.2117	19.497
Mathews-Weber	1.3989	1.7355	12.550
Virial Two Constant	0.0565	1.0734	14.467
Virial Three Constant	0.0533	0.9935	14.644
Volmer	0.6711	2.0968	12.770

Carbon Dioxide

Model	$\sum ss$	$K_0 * 10^5$	$-\Delta H_0$
Toth	1.7528	1.1360	33.377
Unilan	1.5212	0.5483	33.326
Mathews-Weber	7.9432	1.7166	26.983
Virial Two Constant	0.8523	1.1078	31.981
Virial Three Constant	0.8734	1.0877	31.994
Volmer	4.8569	0.10564	36.874

$\sum ss$: Total sum of square error obtained from constrained regression.

K_0 : Pre exponential factor (mol/kg/kPa).

$-\Delta H_0$: Heat of adsorption (kJ/mol).

Table 4.8 Theoritical Values of Energy of Adsorption for Nitrogen and Carbon Dioxide on Different Types of Zeolites (3)

Nitrogen

Zeolite	Energy of Dispersion+ Repulsion+ Polarization (kJ/mol)	Energy Arising from Dipole and Quadrupole Interactions (kJ/mol)	Total (kJ/mol)
Chabazite	26.987	10.669	37.656
H-Mordenite	18.828	7.113	25.941
Na-Mordinite	18.828	10.460	29.288
Sieve 13 X	12.970	14.226	27.196

Carbon Dioxide

Zeolite	Energy of Dispersion+ Repulsion+ Polarization (kJ/mol)	Energy Arising from Dipole and Quadrupole Interactions (kJ/mol)	Total (kJ/mol)
H-Mordenite	28.242	18.200	46.442
Na-Mordinite	28.242	37.447	65.689
Sieve 13X	17.573	33.472	51.045
Sieve Y	20.292	14.016	34.309

Table 4.9 Experimental Results for the Sorption of Nitrogen-Carbon Dioxide Binary on SR-115 Zeolite

280 K and 350 kPa

y_{N_2}	x_{N_2}	q_{N_2}	q_{CO_2}	q_{tot}
0.000	0.000	0.000	3.402	3.402
0.149	0.041	0.135	3.168	3.303
0.267	0.071	0.229	2.970	3.199
0.363	0.102	0.315	2.791	3.106
0.440	0.131	0.396	2.629	3.025
0.501	0.161	0.474	2.479	2.953
0.550	0.189	0.548	2.343	2.890
0.591	0.217	0.613	2.214	2.828
0.625	0.245	0.679	2.095	2.774
0.655	0.272	0.740	1.984	2.724

315 K and 350 kPa

y_{N_2}	x_{N_2}	q_{N_2}	q_{CO_2}	q_{tot}
0.000	0.000	0.000	2.651	2.651
0.271	0.129	0.305	2.063	2.369
0.375	0.175	0.403	1.903	2.306
0.459	0.232	0.533	1.764	2.297
0.525	0.273	0.615	1.637	2.252
0.581	0.325	0.733	1.525	2.257
0.626	0.362	0.804	1.421	2.225
0.666	0.409	0.920	1.330	2.250
0.700	0.456	1.044	1.247	2.291
0.729	0.490	1.124	1.170	2.295

350 K and 350 kPa

y_{N_2}	x_{N_2}	q_{N_2}	q_{CO_2}	q_{tot}
0.000	0.000	0.000	1.671	1.671
0.197	0.114	0.192	1.485	1.677
0.346	0.208	0.349	1.330	1.678
0.454	0.303	0.518	1.194	1.712
0.546	0.385	0.679	1.082	1.761

123

0.613	0.458	0.830	0.982	1.813
0.670	0.514	0.949	0.898	1.846
0.715	0.573	1.104	0.823	1.926
0.755	0.620	1.238	0.759	1.997
0.786	0.661	1.366	0.701	2.067

280 K and 700 kPa

y_{N_2}	x_{N_2}	q_{N_2}	q_{CO_2}	q_{tot}
0.000	0.000	0.000	2.705	2.705
0.204	0.100	0.266	2.392	2.658
0.356	0.159	0.403	2.135	2.538
0.477	0.222	0.548	1.922	2.469
0.565	0.289	0.702	1.730	2.431
0.631	0.337	0.789	1.553	2.342
0.683	0.391	0.898	1.399	2.297
0.723	0.430	0.950	1.256	2.206
0.754	0.480	1.042	1.128	2.170
0.779	0.521	1.097	1.008	2.105

315 K and 700 kPa

y_{N_2}	x_{N_2}	q_{N_2}	q_{CO_2}	q_{tot}
0.000	0.000	0.000	2.381	2.381
0.186	0.097	0.218	2.029	2.246
0.324	0.173	0.367	1.754	2.121
0.436	0.249	0.500	1.512	2.012
0.526	0.322	0.618	1.301	1.920
0.591	0.395	0.726	1.114	1.840

x: mole fraction in the adsorbed phase.

y: mole fraction in the gas phase.

q: amount adsorbed (mol/kg of zeolite)

Table 4.10 Experimental Values of Relative Adsorptivity ($\alpha_{CO_2-N_2}$) for the Binary System N_2-CO_2 on SR-115 Zeolite

Temperature (K)	Pressure (kPa)	$\alpha_{CO_2-N_2}$
280	350	4.978
315	350	2.823
350	350	1.905
280	700	3.133
315	700	2.260

Table 4.11 x-y Fit of IAST Model Model Using Toth, Unilan and Virial Isotherms for the Binary System N_2-CO_2 on SR-115 Zeolite

280 K and 350 kPa

	Experiment	Fit of IAST Model Using Toth	Unilan	Virial
y_{N_2}	x_{N_2}	x_{N_2}	x_{N_2}	x_{N_2}
0.000	0.0000	0.0000	0.0000	0.0000
0.149	0.0410	0.0022	0.0022	0.0028
0.267	0.0710	0.0045	0.0046	0.0056
0.363	0.1020	0.0069	0.0070	0.0085
0.440	0.1310	0.0094	0.0095	0.0113
0.501	0.1610	0.0118	0.0120	0.0142
0.550	0.1890	0.0141	0.0144	0.0169
0.591	0.2170	0.0164	0.0167	0.0196
0.625	0.2450	0.0187	0.0190	0.0222
0.655	0.2720	0.0210	0.0214	0.0248
1.000	—	1.0000	1.0000	1.0000

280 K and 700 kPa

	Experiment	Fit of IAST Model Using Toth	Unilan	Virial
y_{N_2}	x_{N_2}	x_{N_2}	x_{N_2}	x_{N_2}
0.000	0.000	0.0000	0.0000	0.0000
0.204	0.100	0.0035	0.0035	0.0034
0.356	0.159	0.0074	0.0074	0.0098
0.477	0.222	0.0118	0.0118	0.0156
0.565	0.289	0.0163	0.0165	0.0206
0.631	0.337	0.0210	0.0212	0.0258
0.683	0.391	0.0258	0.0261	0.0313
0.723	0.430	0.0306	0.0310	0.0368
0.754	0.480	0.0352	0.0357	0.0421
0.779	0.521	0.0397	0.0404	0.0473
1.000	—	1.0000	1.0000	1.0000

x: mole fraction in the adsorbed phase.

y: mole fraction in the gas phase.

Table 4.12 x-q Fit of IAST Model Using Toth, Unilan and Virial Isotherms for the Binary System N_2-CO_2 at 280 K and 350 kPa

		Experiment			IAST with Toth			IAST with Unilan			IAST with Virial		
y_{N_2}	x_{N_2}	q_{N_2}	q_{CO_2}	q_{tot}	q_{N_2}	q_{CO_2}	q_{tot}	q_{N_2}	q_{CO_2}	q_{tot}	q_{N_2}	q_{CO_2}	q_{tot}
0.000	0.000	0.000	3.402	3.402	0.000	2.919	2.919	0.000	3.073	3.073	0.000	3.152	3.152
0.149	0.041	0.135	3.168	3.303	0.006	2.873	2.880	0.007	3.016	3.028	0.009	3.068	3.077
0.267	0.071	0.229	2.970	3.199	0.013	2.829	2.842	0.014	2.960	2.974	0.017	2.990	3.007
0.363	0.102	0.315	2.791	3.106	0.020	2.785	2.804	0.021	2.905	2.926	0.025	2.916	2.941
0.440	0.131	0.396	2.629	3.025	0.026	2.743	2.769	0.027	2.853	2.880	0.033	2.848	2.881
0.501	0.161	0.474	2.479	2.953	0.032	2.704	2.736	0.034	2.804	2.838	0.040	2.787	2.827
0.550	0.189	0.548	2.343	2.890	0.038	2.667	2.706	0.040	2.760	2.800	0.047	2.731	2.778
0.591	0.217	0.613	2.214	2.828	0.044	2.633	2.677	0.046	2.717	2.764	0.054	2.680	2.734
0.625	0.245	0.679	2.095	2.774	0.050	2.601	2.650	0.052	2.678	2.730	0.060	2.634	2.693
0.655	0.272	0.740	1.984	2.724	0.055	2.569	2.624	0.058	2.640	2.698	0.066	2.589	2.655
1.000	1.000	—	—	—	0.973	0.000	0.973	0.953	0.000	0.953	0.976	0.000	0.976

x: mole fraction in the adsorbed phase.

y: mole fraction in the gas phase.

q: amount adsorbed (mol/kg of zeolite)

Table 4.13 x-q Fit of IAST Model Using Toth, Unilan and Virial Isotherms for the Binary System N_2-CO_2 at 280 K and 700 kPa

		Experiment			IAST with Toth			IAST with Unilan			IAST with Virial		
y_{N_2}	x_{N_2}	q_{N_2}	q_{CO_2}	q_{tot}	q_{N_2}	q_{CO_2}	q_{tot}	q_{N_2}	q_{CO_2}	q_{tot}	q_{N_2}	q_{CO_2}	q_{tot}
0.000	0.000	0.000	2.705	2.705	0.000	3.071	3.071	0.000	3.258	3.258	0.000	3.467	3.467
0.204	0.100	0.266	2.392	2.658	0.011	3.016	3.027	0.011	3.194	3.206	0.011	3.366	3.378
0.356	0.159	0.403	2.135	2.538	0.022	2.961	2.983	0.023	3.129	3.152	0.032	3.250	3.282
0.477	0.222	0.548	1.922	2.469	0.035	2.903	2.937	0.037	3.058	3.094	0.050	3.138	3.188
0.565	0.289	0.702	1.730	2.431	0.047	2.847	2.894	0.050	2.989	3.039	0.064	3.040	3.103
0.631	0.337	0.789	1.553	2.342	0.060	2.794	2.854	0.063	2.924	3.988	0.078	2.951	3.029
0.683	0.391	0.898	1.399	2.297	0.073	2.743	2.815	0.077	2.861	2.938	0.093	2.867	2.960
0.723	0.430	0.950	1.256	2.206	0.085	2.695	2.780	0.090	2.802	2.892	0.107	2.792	2.899
0.754	0.480	1.042	1.128	2.170	0.097	2.651	2.748	0.102	2.749	2.851	0.120	2.726	2.846
0.779	0.521	1.097	1.008	2.105	0.108	2.610	2.718	0.1135	2.699	2.813	0.132	2.666	2.798
1.000	1.000	—	—	—	1.412	0.000	1.412	1.383	0.000	1.383	1.390	0.000	1.390

x: mole fraction in the adsorbed phase.
y: mole fraction in the gas phase.
q: amount adsorbed (mol/kg of zeolite)

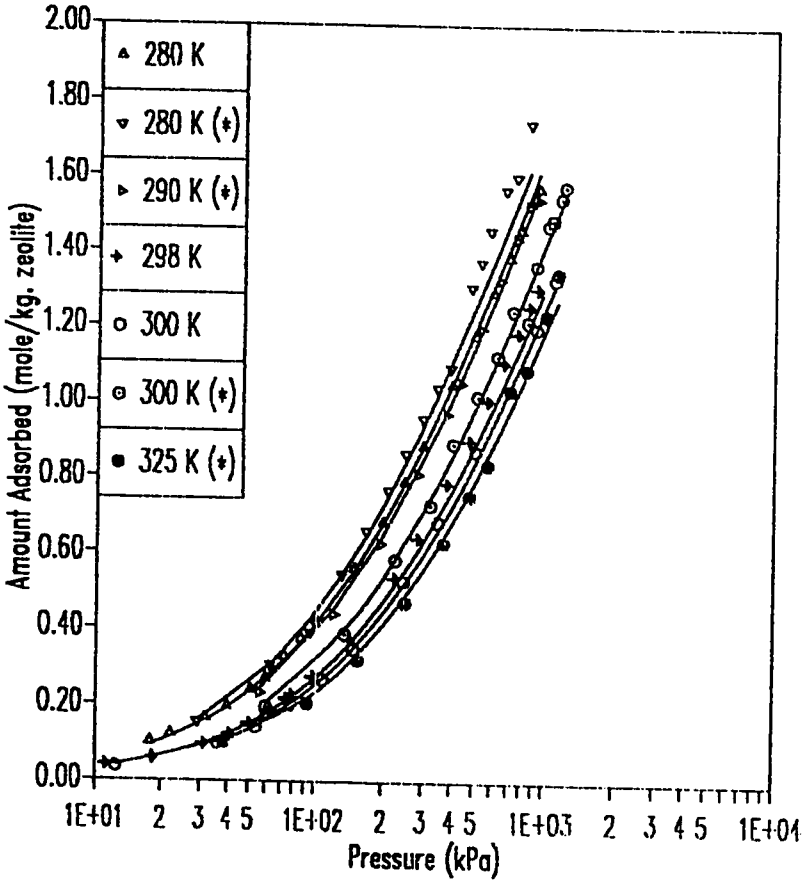

Figure 4.1 Isotherms of Nitrogen on SR-115 Zeolite:
Fit of Toth Model (—).

* : Data obtained from reference 1.

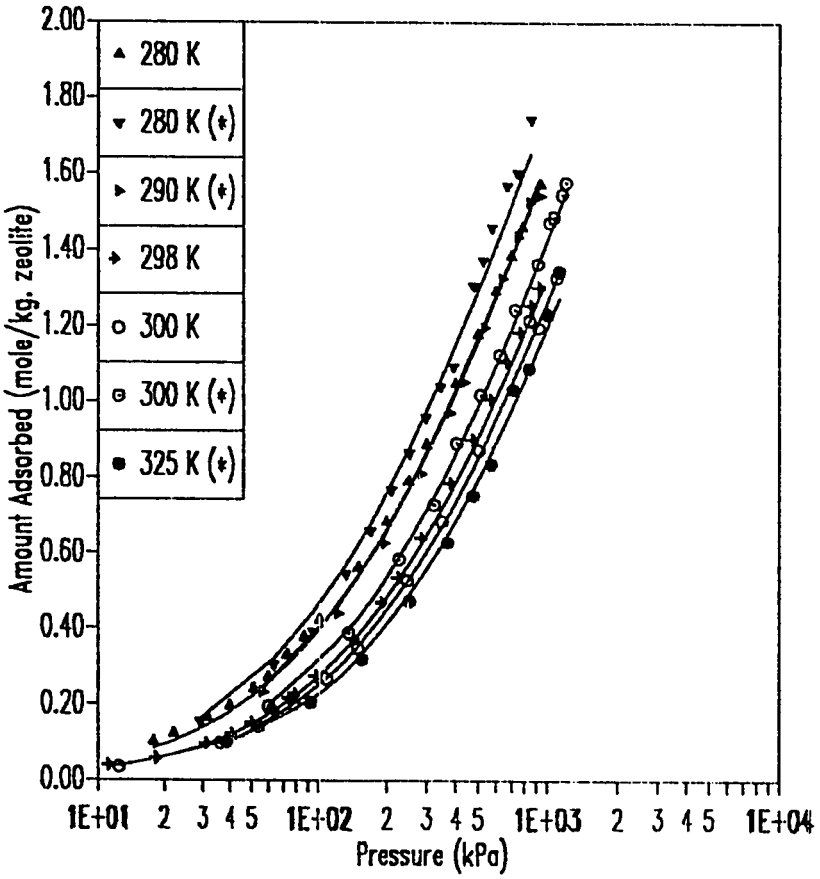

Figure 4.2 Isotherms of Nitrogen on SR-115 Zeolite:
Fit of Unilan Model (—).

* : Data obtained from reference 1.

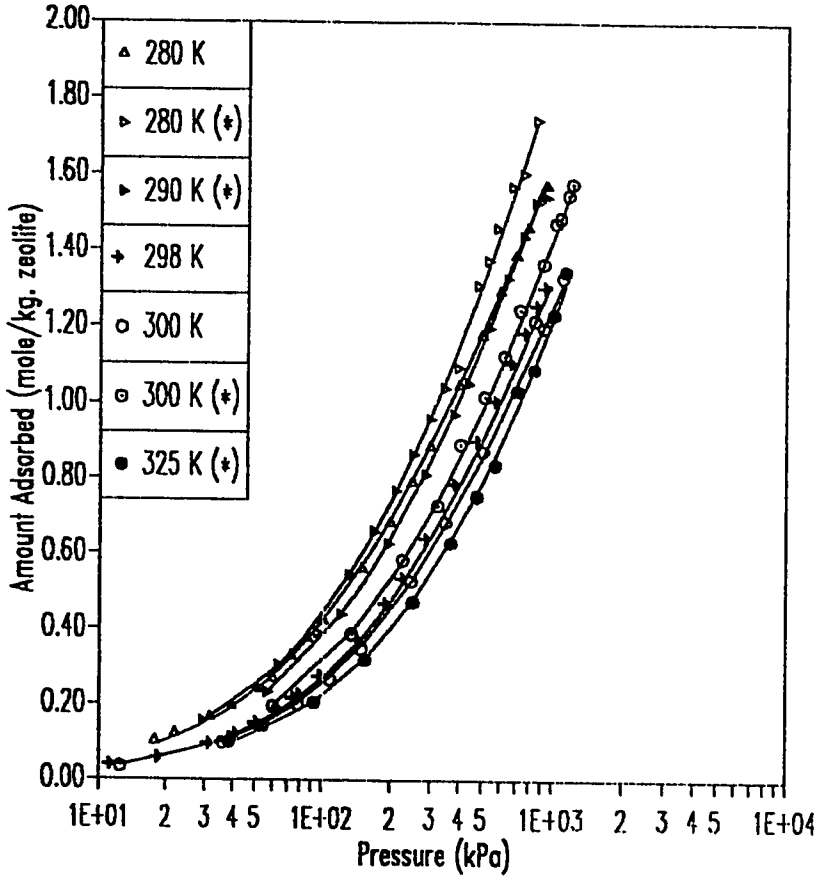

Figure 4.3 Isotherms of Nitrogen on SR-115 Zeolite:
Fit of Virial Three Constant Model (—).

* : Data obtained from reference 1.

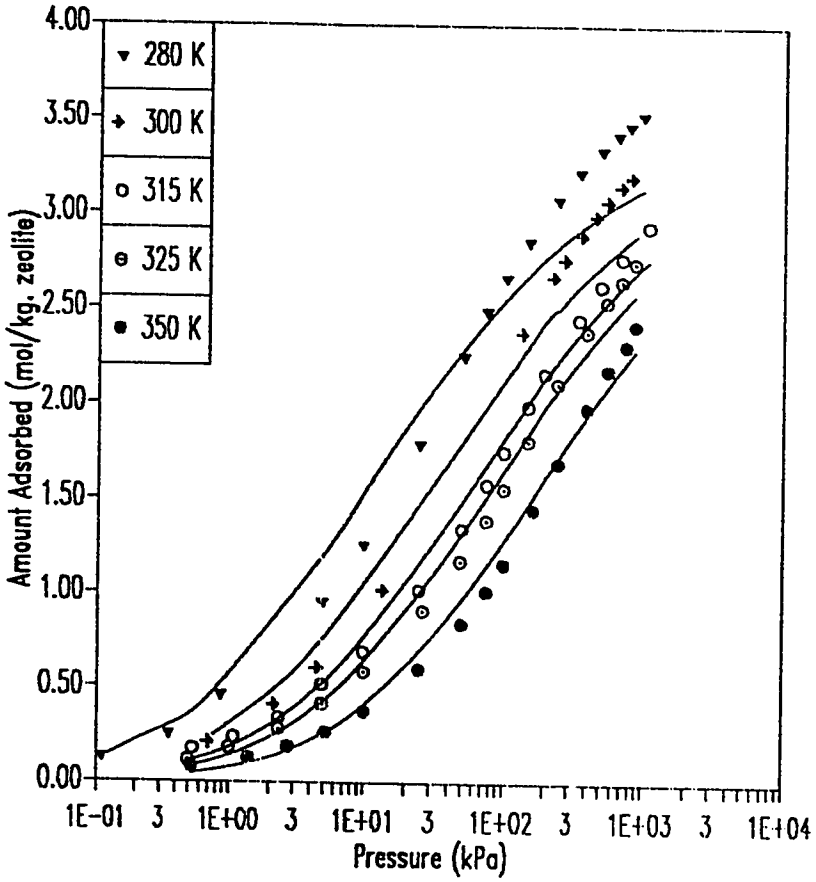

Figure 4.4 Isotherms of Carbon Dioxide on SR-115 Zeolite:
Fit of Toth Model (—).

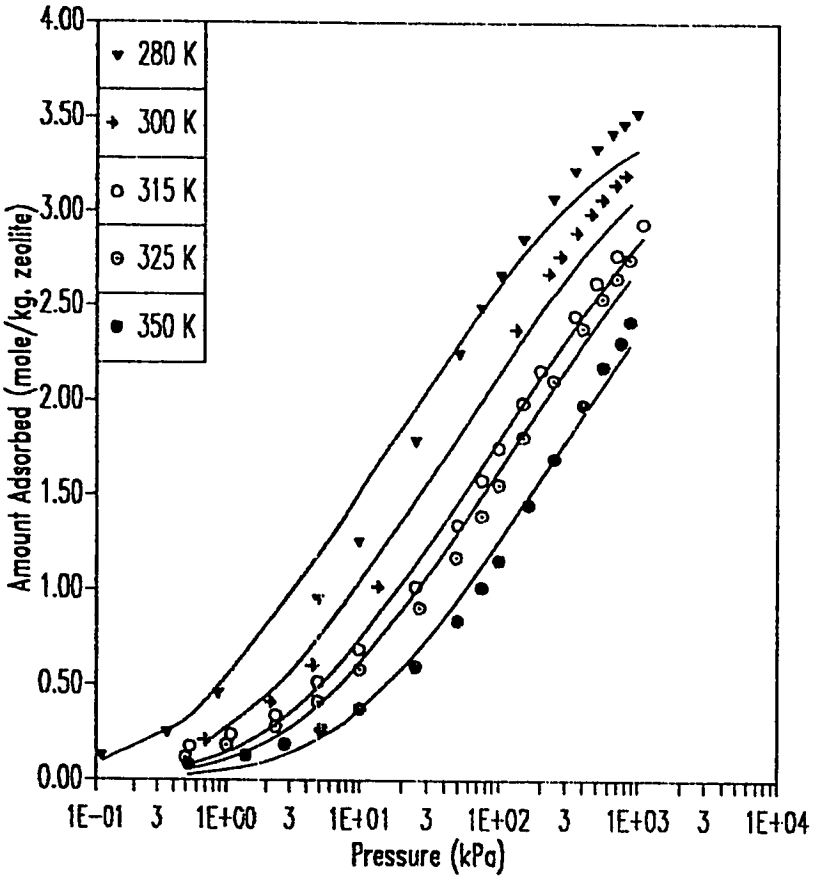

Figure 4.5 Isotherms of Carbon Dioxide on SR-115 Zeolite:
Fit of Unilan Model (—).

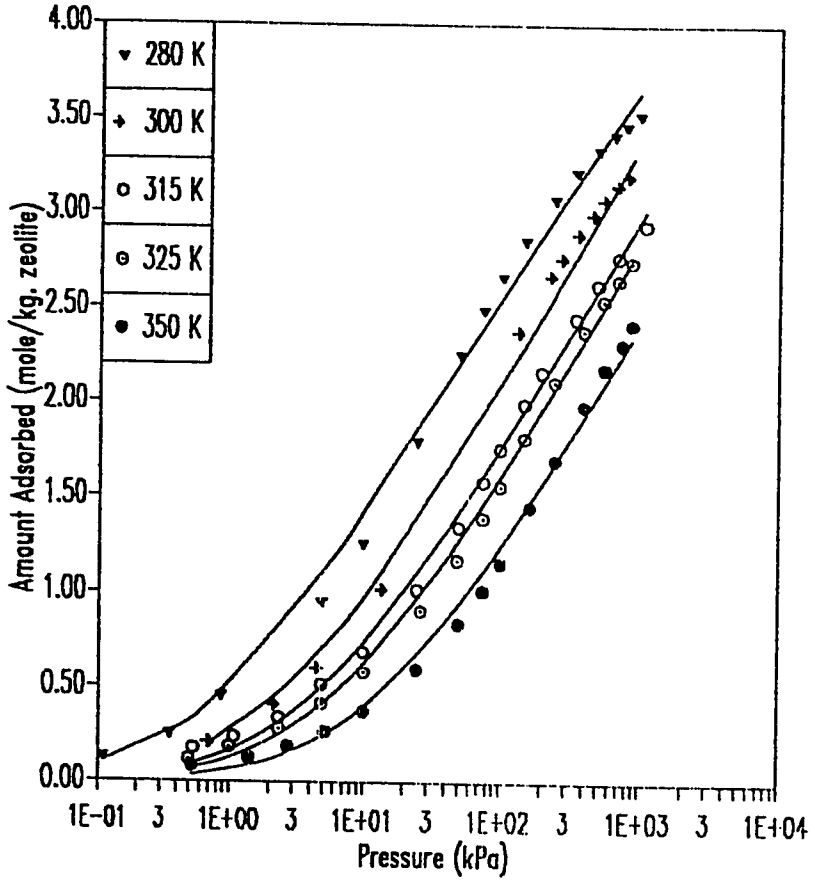

Figure 4.6 Isotherms of Carbon Dioxide on SR-115 Zeolite:
Fit of Virial Three Constant Model (—).

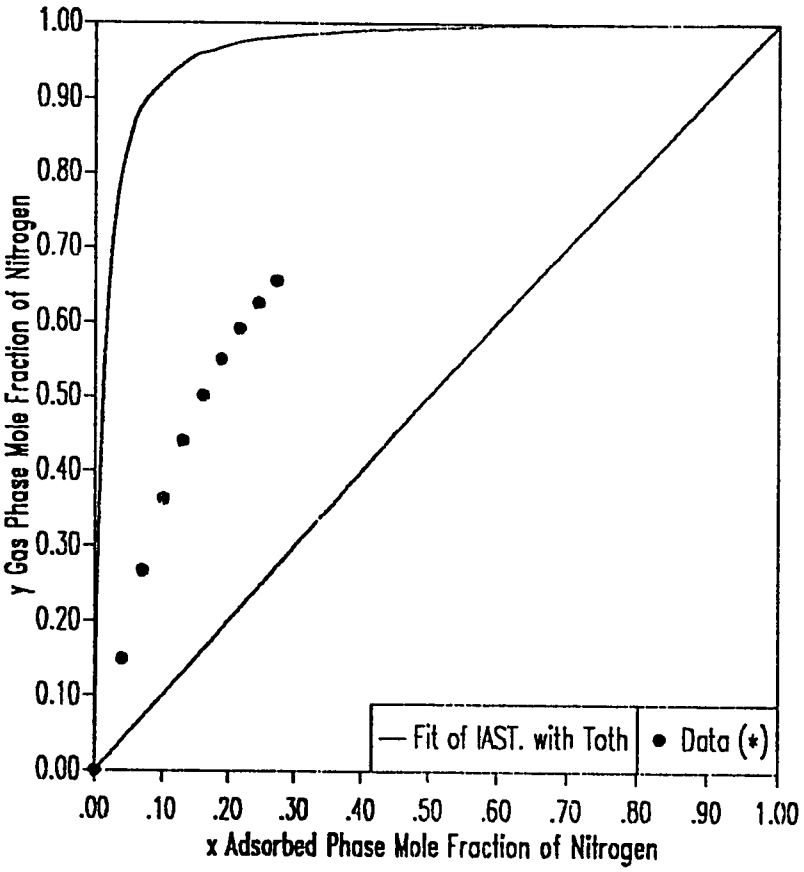

Figure 4.7 x-y Fit of IAST Model Using Toth Isotherm to the Binary System Nitrogen-Carbon Dioxide on SR-115 Zeolite at 280 K and 350 kPa.

Data obtained from reference 2.

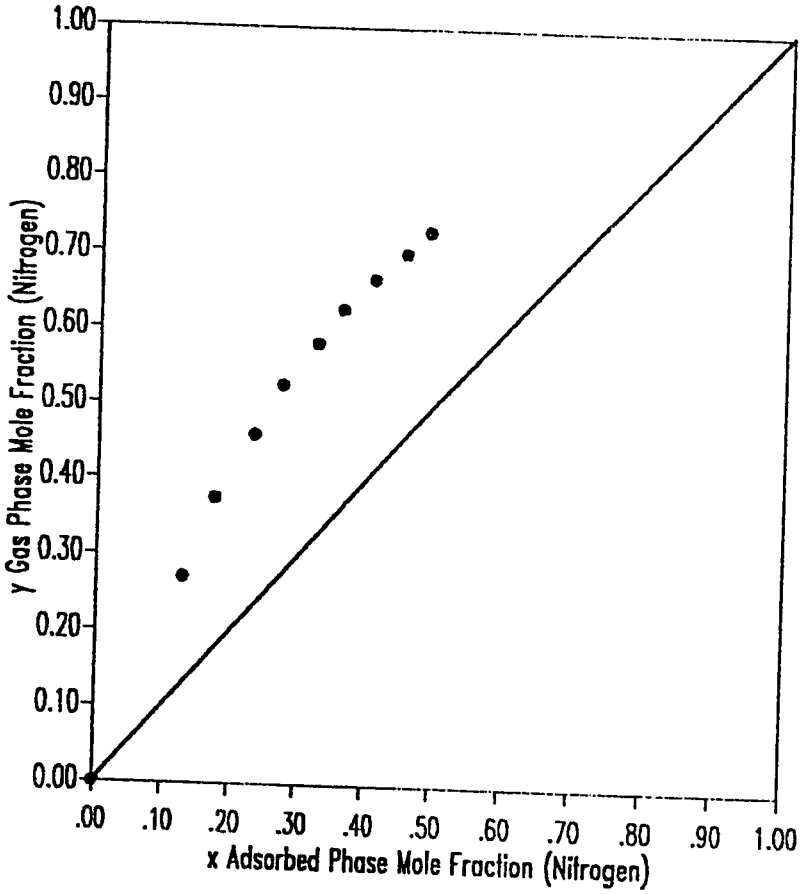

Figure 4.8 x-y Data of the Binary System Nitrogen-Carbon Dioxide on SR-115 Zeolite at 315 K and 350 kPa.

Data obtained from reference 2.

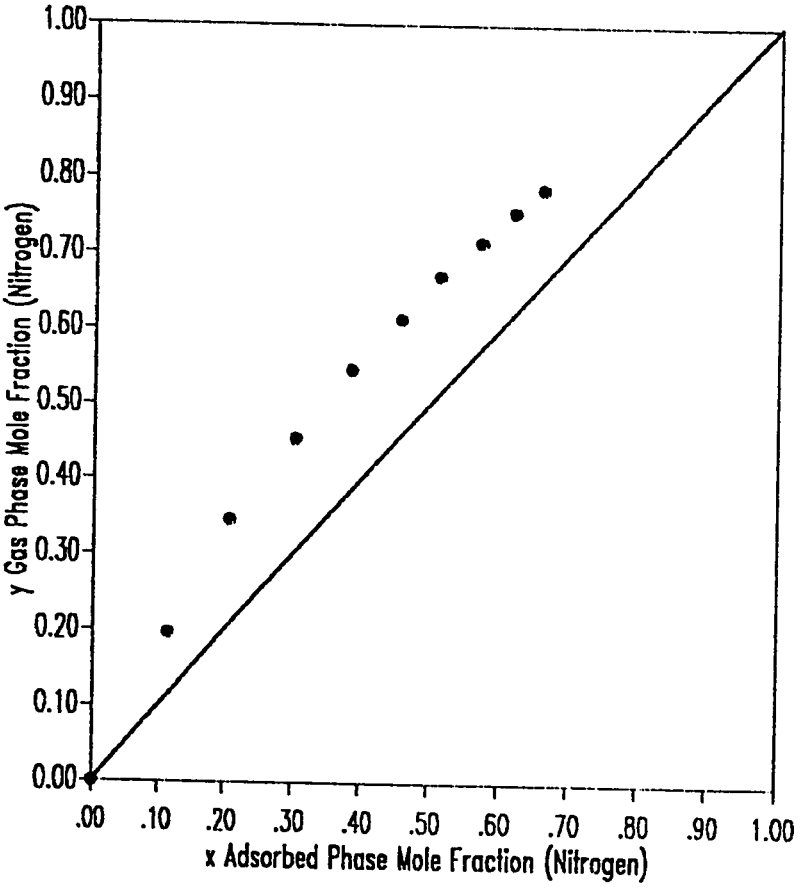

Figure 4.9 x-y Data of the Binary System Nitrogen-Carbon Dioxide on SR-115 Zeolite at 350 K and 350 kPa.

Data obtained from reference 2.

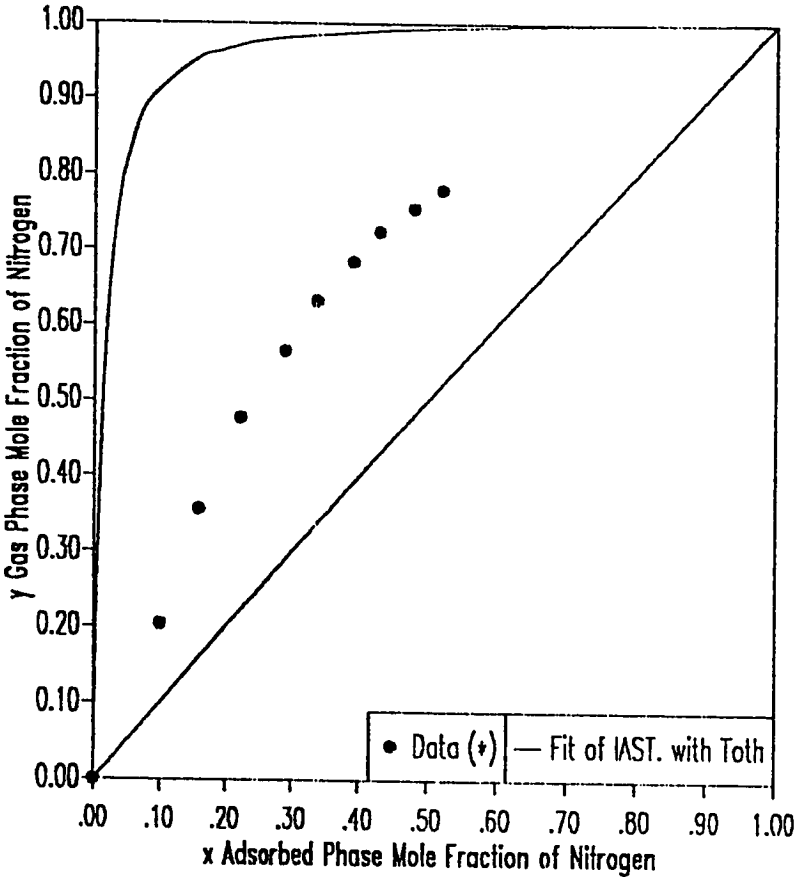

Figure 4.10 x-y Fit of IAST Model Using Toth Isotherm to the Binary System Nitrogen-Carbon Dioxide on SR-115 Zeolite at 280 K and 700 kPa.

Data obtained from reference 2.

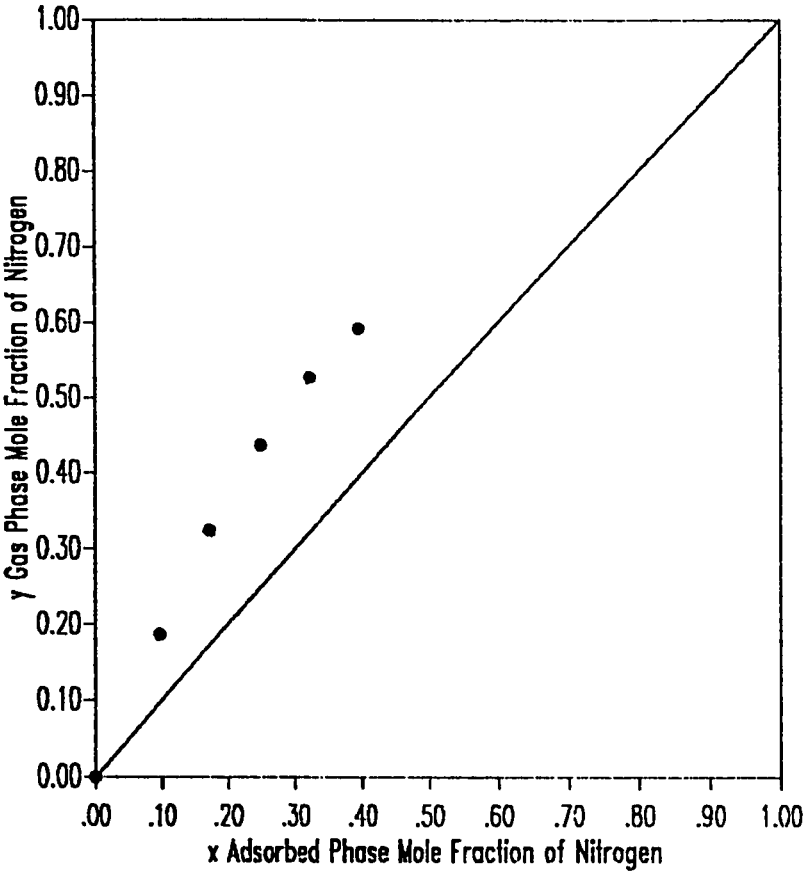

Figure 4.11 x-y Data of the Binary System Nitrogen-Carbon Dioxide on SR-115 Zeolite at 315 K and 700 kPa.

Data obtained from reference 2.

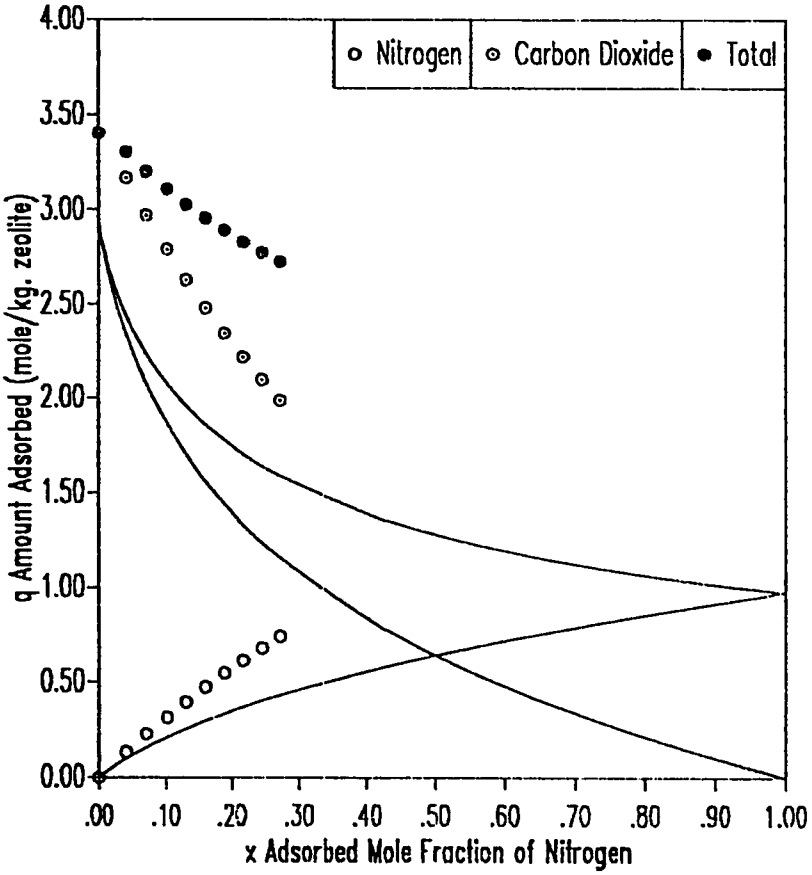

Figure 4.12 x-q Fit of IAST Model Using Toth Isotherm to the Binary System Nitrogen-Carbon Dioxide on SR-115 Zeolite at 280 K and 350 kPa.

Data obtained from reference 2.

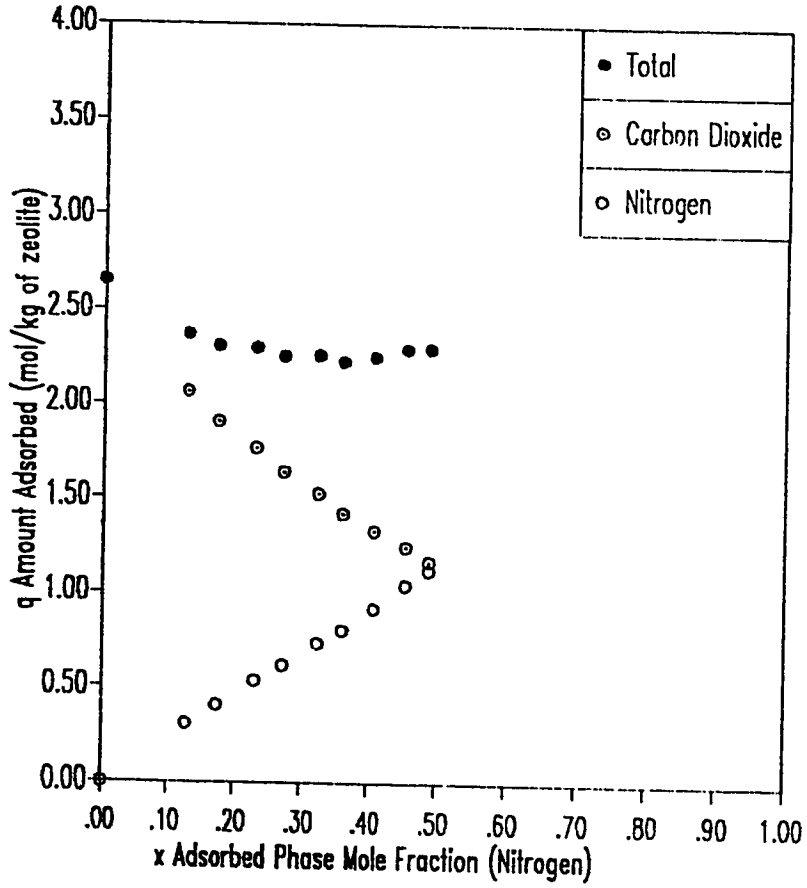

Figure 4.13 x-q Data of the Binary System Nitrogen-Carbon Dioxide on SR-115 Zeolite at 315 K and 350 kPa.

Data obtained from reference 2.

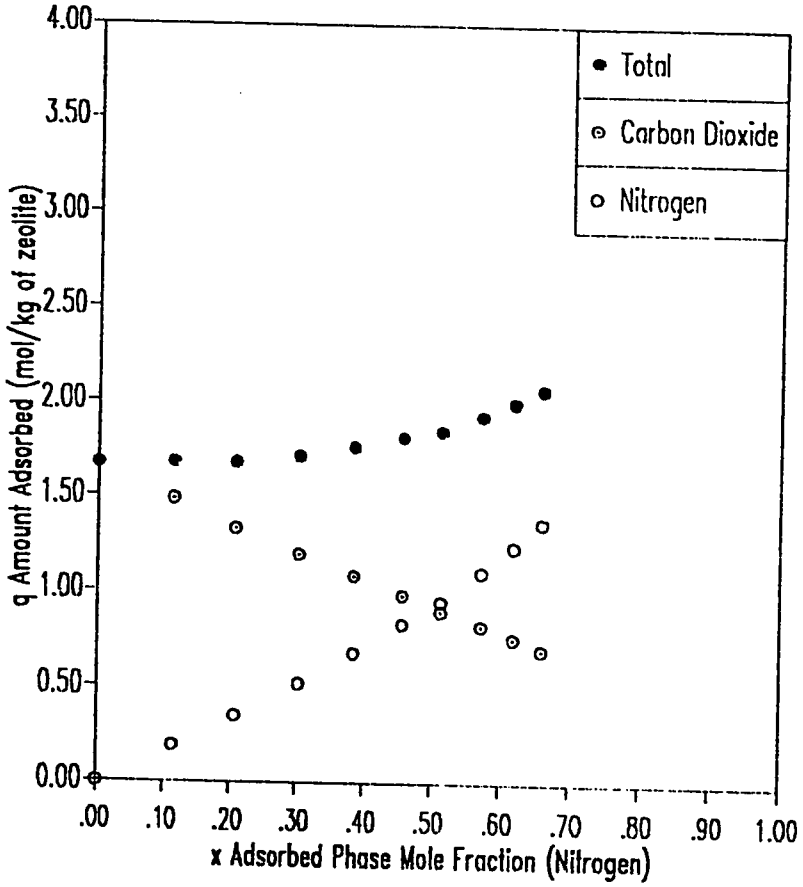

Figure 4.14 x-q Data of the Binary System Nitrogen-Carbon Dioxide on SR-115 Zeolite at 350 K and 350 kPa.

Data obtained from reference 2.

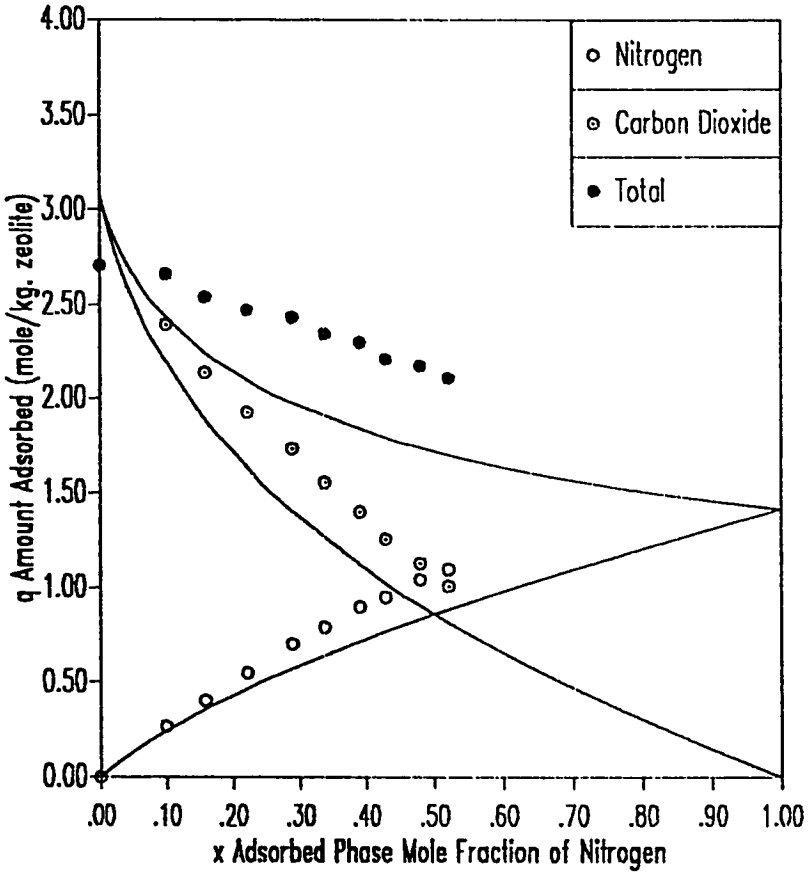

Figure 4.15 x-q Fit of IAST Model Using Toth Isotherm to The Binary System Nitrogen-Carbon Dioxide on SR-115 Zeolite at 280 K and 700 kPa.

Data obtained from reference 2.

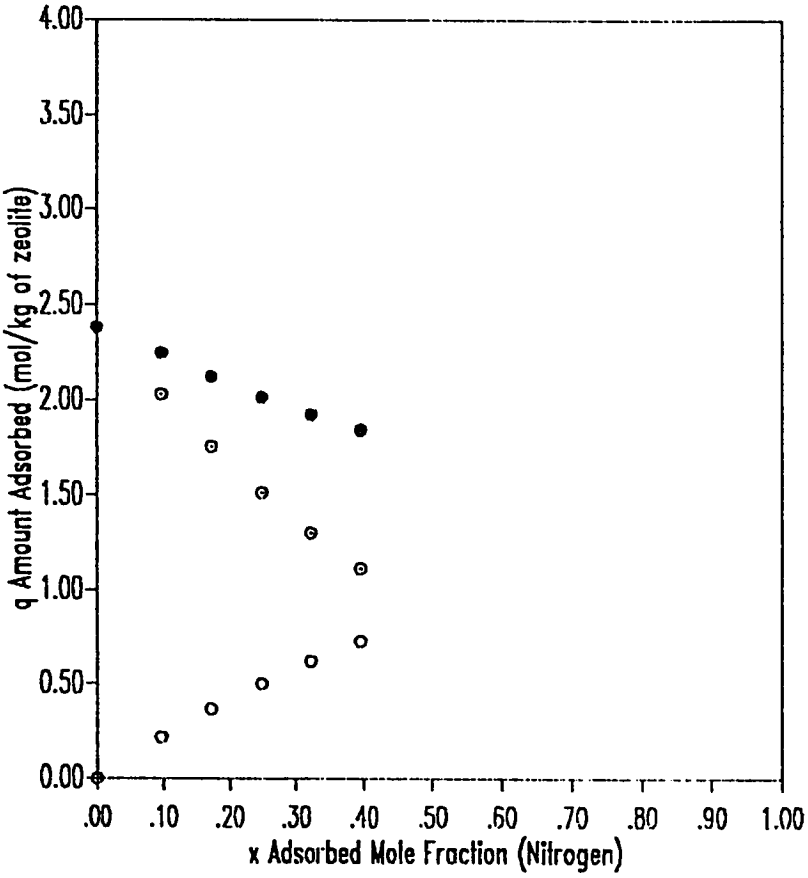

Figure 4.16 x-q Data of the Binary System Nitrogen-Carbon Dioxide on SR-115 Zeolite at 315 K and 700 kPa.

Data obtained from reference 2.

CHAPTER 5

TERNARY, BINARY AND PURE COMPONENT ADSORPTION OF METHANE, ETHANE AND ETHYLENE ON SR-115 ZEOLITE

5.1 Introduction

This chapter is devoted to the results obtained for the sorption of pure methane, ethane, and ethylene and their binary and ternary mixtures on SR-115 zeolite. Pure experimental data on methane and ethane sorption were obtained from the thesis of Bin Abdul-Rehman (2) ; while the pure data of ethylene were taken from the Senior project of Al-Saad (1). The binary and ternary equilibrium data have been measured in this work. Both constrained and unconstrained optimization has been applied to the ethylene data. On the other hand, only constrained optimization has been applied to the data of methane and ethane (the unconstrained optimization results using Toth, Mathews-Weber, L.R.C., Jaroniec and Ruthven isotherms are already given in Bin Abdul Rehman thesis (2)). The ten pure models used in chapter 4 have also been applied to the experimental data to obtain the best fit.

Binary mixture equilibrium data of methane-ethane and methane-ethylene have been gathered at 300, 325 and 350 K and pressures of 150, 200 and 250 kPa. In addition, the ternary data of methane-ethane-ethylene have been obtained at 300 and 325 K and 200 kPa with different loadings of ethane and ethylene. The data have been modeled using IAST model in conjunction with the constrained optimized parameters of Toth, Unilan and Virial three constant isotherms.

5.2 Pure Component Result

The unconstrained optimization parameters for the ethylene adsorption on SR-115 zeolite at six different temperatures are presented in Table 5.1. The fit obtained for all the models used except Freundlich and Volmer is excellent. Values of the saturation concentration parameter obtained from the fit of Toth, Unilan and Radke-Prausnitz are reasonably comparable to the value calculated theoretically by equation 2.8 namely 3.12 mole/kg of zeolite. On the other hand, the values obtained from the fit of L.R.C. and the Langmuir-Freundlich models are too low and those for the Volmer model are too high.

The values of Henry's constant calculated from Unilan , Radke-Prausnitz, Loading Ratio Correlation (L.R.C), and Virial two constant models are comparable to the values obtained from the Virial three constant model. The Henry's constant values obtained from Toth model are too high whereas those for the Volmer model are too low in comparison to the Virial three constant values.

A comparison of the total sum of squares error indicates that the Radke-Prausnitz is the best model in representing the experimental data.

In the constrained regression (Table 5.2), the saturation concentration (q_s) has been fixed at 3.12 mole per kg of SR-115 zeolite which corresponds to 95% of the theoretical value calculated from equation 2.8. The variables t in the Toth model, s in the Unilan Model, n_{RP} in Radke-Prausnitz model, n_{MW} in the Mathews-Weber model, A_1 in the Virial model n_{LF} in the Langmuir-Freundlich and n_{LRC} in the loading ratio correlation model are observed to exhibit a random variation with temperature about a mean value. Accordingly, these variables were all fixed constants in the constrained regression. The constants of these models were optimized till a minimum sum of squares was achieved. The

values of these constants together with the new minimum sum of squares are presented in Table 5.2. Note that the optimized-constrained value is not the average of the unconstrained values. For instance, consider the variable t in the Toth model: the average unconstrained value is 0.487 whereas the optimized value is 0.520. This suggests that the isotherm rotates i.e., the Vant Hoff equation parameters (K_0 and $-\Delta H_0$) values for the constrained optimization are different from the unconstrained which can be clearly observed by the difference in K_H values between the two optimizations. In fact, inspection of the K_H values indicates that the isotherm models that exhibit this rotation due to the application of the constraints are Toth, L.R.C., Radke-Prausnitz, and virial two constant. The Unilan, Mathews-Weber and Virial three constant exhibit little rotation under the constraining operation.

The unconstrained optimization for the sorption of methane and ethane on SR-115 zeolite are presented in chapter 5 of Bin Abdul Rehman's thesis. The fit of Toth, L.R.C., Mathews-Weber, Jaroniec and Ruthven models were applied successfully for both components. Values of q_s obtained by these models are all reasonable when compared to the theoretically calculated values.

The constrained optimization of methane and ethane is shown in Tables 5.3 and 5.4 respectively. The saturation concentration (q_s) has been fixed at 95% of the theoretical values obtained from equation 2.8 namely, 4.23 and 2.78 mole per kg of zeolite for methane and ethane respectively. The fit of the ten models to the pure data of methane is not as good as the fit to the pure data of ethylene. Analysis of the Henry's constant values calculated from each model indicates that the values obtained from Unilan model approach the closest to the values obtained from Virial model.

However, the experimental data is best described by Radke-Prausnitz model.

Considering the total sum of squares error calculated from the fit of the models to the pure data of ethane indicates that the regression is the worst among the data obtained for the other sorbates although only four isotherms are considered. In fact, for all the models except the L.R.C model, the fit of the isotherm at 325 K is the worst and that significantly has increased the fit error. Henry's constant values calculated from Mathews-Weber model are surprisingly very similar to those obtained from Virial model. Also, the fit of this model to the experimental data is relatively excellent. Hence, this model is the most appropriate for the ethylene adsorption data. The values of Henry's constant obtained from the Virial two constant model are also comparable to Virial three constant values. However, the values obtained from Toth, Unilan, Radke-Prausnitz, and Volmer models deviate by at least 25% from the Virial three constant values. The isotherms of methane, ethane and ethylene together with the constrained fit of Toth, Unilan and Virial three constant models are shown in Figures 5.1 to 5.9.

Recently, Hampson and Rees (4) used the Toth and the Langmuir-Freundlich model to fit the ethane equilibrium adsorption data they collected on silicalite 1. They found that the fit of Langmuir-Freundlich model to the data is much better than Toth's. The unconstrained-optimized parameters of Toth are reported at as : q_s= 1.972, b= 20.77 and t=1.220. For Langmuir-Freundlich, the parameters reported as : q_s= 2.086, k_{LF}= 0.111, n_{LF}= 1.069. These values are reported at 298 K which fortunately makes the comparison possible with the constrained parameters calculated in this work at 300 K. The values of q_s obtained by Hampson and Rees are too low when compared to the theoretical value (2.78 mole/kg). In addition, the Toth parameters calculated by them are higher than the values

calculated in this work. However, the k_{LF} parameter of Langmuir-Freundlich model obtained from both studies are comparable. Better matching is expected between the Hampson and Rees results and the results of this work if the parameters obtained by the former are constrained.

Table 5.5 gives the vant Hoff equation parameters for the sorption of methane, ethane and ethylene on SR-115 zeolite. The heat of adsorption of methane calculated by all models is similar. However, the pre exponential factor calculated using Toth and Unilan models are too high in comparison with virial three constant's. The values calculated by other models are reasonably comparable to virial three constant's value. The value of the heat of adsorption of methane calculated in this work is in excellent agreement with the value reported by Bruncker et al (7) on silicalite 1 namely 20 kJ/mole.

The heat of adsorption calculated for ethane using Toth, Mathews-Weber and virial two constant models are comparable to the value calculated using virial three constant model. The values calculated using the other models is higher. In addition, the pre exponential factor value calculated by Toth and Mathews-Weber models is closest to the value calculated by virial three constant model; the values obtained from the remaining models are all low to compensate for the high heat of adsorption.

For ethylene, the value of $-\Delta H_0$ calculated using all models except Radke-Prausnitz and Mathews-Weber models is in good agreement with the Virial three constant value. The pre exponential factor determined using Toth and Unilan models is high by a factor of 2 when compared to the value obtained using the Virial model. The vant Hoff parameters obtained using Volmer model are the best when compared to the others even though poor sum of squares error is obtained.

5.3 Binary Adsorption of Methane and Ethylene

Four experiments were carried out for the methane-ethylene binary system on the Linde SR-115 zeolite at temperatures and pressures : 300 K and 200 kPa, 350 K and 200 kPa, 325 K and 150 kPa, and 325 K and 250 kPa. The experiments were aimed at determining the effect of temperature and pressure on the adsorption behavior of this system.

The ideal adsorbed solution theory has been used in conjunction with the constrained parameters of the pure isotherms of Toth, Unilan and Virial three constant isotherms to fit the mixture data. Comparison among the experimental x-y data of this system and the x-y fit of IAST using Toth, Unilan and Virial three constant isotherms is given in Table 5.6. Figures 5.10 to 5.13 show the x-y diagram for this system at the four cases. The plots show excellent agreement between the experimental data and the corresponding values obtained from the three models. Identical fit for the three models is observed to the run at 300 K and 200 kPa while small deviation is observed in the second run at 350 K and 200 kPa. The fit of virial model at 325 K is not shown because the Virial third and fourth constants are not available for ethylene at this temperature. As a result, only Unilan and Toth fit is shown in Figures 5.12 and 5.13. In these plots, the fit of IAST combined with the Toth isotherm is a little better than that with the Unilan isotherm.

The x-y plots show that the pressure has negligible effect on the separation of methane from ethylene since the two curves for the runs carried out at the same temperature (325 K) and different pressure (150 and 250 kPa) are identical. Increasing the temperature however, has a negative effect on the separation. Hence, the separation of methane from ethylene on SR-115 zeolite is very possible at all conditions but is best at low temperature. This conclusion is also supported by the values of relative adsorptivity reported in Table 5.8. These values were calculated

using equation 4.4 at 50% gas phase mole fraction of methane. As listed in this table, the values of the relative adsorptivity calculated from data are comparable to the values calculated from the IAST fits.

The x-q fit of IAST using Toth, Unilan and Virial isotherms to the experimental data are given in Tables 5.9 to 5.12 and Figures 5.18 to 5.21. The plots show good agreement between the experimental data and the predicted model values.

5.4 Binary Adsorption of Ethane and Ethylene

The experimental runs for the binary system ethane-ethylene on SR-115 zeolite have been carried out at 300 K and 200 kPa, 350 K and 200 kPa, 325 K and 150 kPa, and 325 K and 250 kPa. The x-y diagrams for the four runs showing the fit of IAST model using Toth, Unilan and Virial isotherms are given in Figures 5.14 to 5.17. The x-q fit of the three models to the experimental data are shown in Figures 5.22 to 5.25. In the x-y diagrams, the fit of IAST using Toth, Unilan and Virial models agree satisfactorily with the experimental data of the first two runs (300 K-200 kPa and 350 K-200 kPa). In these runs the x-y data points and the three fits are found to lie on the line x=y which suggests that the separation of methane from ethylene on SR-115 zeolite is practically not possible. The experimental data obtained for the runs carried out at 325 K-150 kPa and 325 K-250 kPa still agree with this conclusion. However, the fit of both IAST using Toth and Unilan isotherms is not as good. They predict some separation which is in fact observed at the higher x values. The x-q fit for the three models is excellent especially the $x-q_{C_2H_6}$ and the $x-q_{C_2H_4}$ fit. The fit to the data of total amount adsorbed versus adsorbed phase mole fraction of ethane ($x-q_{tot}$) is not as good as the previous fits. This is expected since the total amount adsorbed is obtained by adding the amount

adsorbed of ethane and ethylene and therefore the fit error is the addition of the two fit errors.

Values of relative adsorptivity(α) calculated for this system are given in Table 5.8. These values were calculated at about 50% gas phase mole fraction of ethane using equation 4.4. The values of α listed in this table all approach unity at the first two runs which indicates no separation at these conditions. The values of α calculated from the data and the IAST fits are in close agreement except for the IAST-Toth fits at 325 K.

5.5 Adsorption of the Ternary Mixture Methane-Ethane-Ethylene

Four experimental runs for the adsorption of the ternary system methane-ethane-ethylene on SR-115 zeolite have been performed. The first and second runs have been carried out at 300 K and total pressure of 200 kPa by loading the adsorption chamber with approximately 50 kPa of ethylene in the first run and with approximately 150 kPa of ethylene in the second. The third and fourth runs are carried out at 325 K and pressure of 200 kPa; loading the adsorption chamber with 25 kPa of ethylene in the third run and with 175 kPa in the fourth. The aim of this is to have a wide spread distribution of the equilibrium data. Therefore, the first and second runs are considered as one run and so are the third and fourth runs.

The constrained optimization parameters of Toth, Unilan and Virial models obtained from the fit of the pure component isotherms are used in the IAST equations to fit the ternary data. Tables 5.17 to 5.20 give comparison between the adsorbed mole fraction of methane and ethane calculated from the experimental data to those calculated from the three models at different gas phase mole fractions. The mole fraction of ethylene in both the adsorbed and the gas phases can be obtained by subtracting the mole fraction of methane and ethane from 1.0 for the corresponding phase. The fit of the three models is satisfactory.

The x-q fit for this system using the same three models are shown in Tables 5.21 to 5.24. The prediction of the three models to the amount adsorbed on SR-115 zeolite for each component in the ternary mixture is reasonable when compared to the experimental values. The data and the IAST fits of the data show that the separation of methane from the ternary mixture methane-ethane-ethylene is quite feasible.

5.6 Literature Cited

1) Al Saad, A., Equilibrium Adsorption of Ethylene on SR-115 silicalite, Senior Project, KFUPM , Dhahran, 1991.

2) Bin Abdul Rehman, H., Equilibrium Adsorption of Light Alkanes and Their Mixtures on 5A, 13X and SR-115, M.S. Thesis, KFUPM, Dhahran 1988.

3) Bruckner, P. and Rees, L.V.C., Separation Technology, Editors: Vansant, E.F., Elsevier Science B.V., Amsterdam, P. 39, 1994.

4) Hampson, J.A. and Rees, L.V.C., Separation Technology, Editors: Vansant, E.F., Elsevier Science B.V., Amsterdam, P. 59, 1994.

5) Jianmin, L.I. and Orhan, T., Chem. Eng. Sc., 49 (2), P. 189, 1994.

6) Oho, K., Monterunil, C.N., Todor, O., McCabe, R.W., and Gandhi, H.S., Ind. Eng. Chem. Res., 30 (10) , P. 2333, 1991.

7) Rees, L.V.C., Bruckner, P. and Hampson, J.A., Gas. Sep. Pur., 5, P. 67, June, 1991.

Table 5.1 Unconstrained Optimization Parameters for The Sorption of Ethylene on SR-115 Zeolite

Toth Model

Temperature (K)	ss	q_s	b	t	K_H
300	0.0848	3.174	1.908	0.472	0.807
320	0.0169	3.759	2.250	0.407	0.513
350	0.0084	3.216	4.558	0.474	0.131
375	0.0041	3.186	10.540	0.539	0.040
400	0.0015	3.474	14.213	0.524	0.022
425	0.0294	3.576	16.451	0.506	0.014

$\sum ss = 0.1451$

Unilan Model

Temperature (K)	ss	q_s	c	s	K_H
300	0.0422	2.856	20.38	2.939	0.449
320	0.0898	3.348	69.70	3.584	0.241
350	0.0561	3.296	197.33	3.410	0.074
375	0.0305	3.423	433.35	3.151	0.029
400	0.0269	3.308	672.37	2.825	0.015
425	0.1148	3.178	928.09	2.693	0.009

$\sum ss = 0.3603$

Radke-Prausnitz Model

Temperature (K)	ss	q_s	b_{RP}	c_{RP}	n_{RP}	K_H
300	0.0554	3.234	0.184	0.260	0.446	0.594
320	0.0029	2.919	8.206	0.083	0.652	0.330
350	0.0021	2.777	0.110	0.053	0.643	0.306
375	0.0040	2.812	0.019	0.043	0.623	0.052
400	0.0049	3.090	0.009	0.031	0.593	0.027
425	0.0027	2.889	0.017	0.009	0.730	0.049

$\sum ss = 0.0721$

Mathews-Weber Model

Temperature (K)	ss	q_s	b_{MW}	n_{MW}	K_H
300	0.0983	1.556	0.223	0.887	0.346
320	0.0802	0.978	0.257	0.788	0.251
350	0.0661	1.150	0.065	0.815	0.074
375	0.0288	1.236	0.024	0.805	0.030
400	0.0044	1.134	0.015	0.766	0.017
425	0.0626	1.027	0.011	0.732	0.011

$\sum ss = 0.3404$

Volmer Model

Temperature (K)	ss	q_s	K_H
300	0.2296	3.493	0.262
320	0.3765	3.251	0.143
350	0.2469	3.254	0.049
375	0.1648	3.340	0.023
400	0.1096	3.323	0.013
425	0.2321	3.352	0.007

$\sum ss = 1.3595$

Virial Two Constant Model

Temperature (K)	ss	A_1	A_2	K_H
300	0.0631	0.597	0.394	0.377
320	0.0322	1.560	0.000	0.298
350	0.0471	1.143	0.131	0.076
375	0.0281	1.000	0.104	0.029
400	0.0067	1.084	0.020	0.016
425	0.0845	1.103	0.000	0.010

$\sum ss = 0.2618$

123

Virial Three Constant Model

Temperature (K)	ss	A_1	A_2	A_3	K_H
300	0.0489	1.111	0.000	0.087	0.451
320	0.0475	1.477	0.000	0.005	0.269
350	0.0330	1.310	0.000	0.034	0.082
375	0.0281	1.064	0.005	0.037	0.029
400	0.0050	1.116	0.000	0.004	0.016
425	0.0858	1.099	0.000	0.000	0.010

$\sum ss = 0.2483$

Freundlich Model

Temperature (K)	ss	k_F	n_F
300	7.1648	0.548	0.256
320	0.9349	0.344	0.361
350	1.7448	0.244	0.356
375	4.0384	0.122	0.410
400	1.3393	0.073	0.484
425	1.2145	0.052	0.509

$\sum ss = 16.4366$

Langmuir-Freundlich Model

Temperature (K)	ss	q_s	k_{LF}	n_{LF}
300	0.1111	2.735	0.121	0.735
320	0.0304	2.917	0.082	0.653
350	0.0051	2.677	0.039	0.702
375	0.0483	2.644	0.017	0.765
400	0.0266	2.664	0.010	0.781
425	0.0015	2.798	0.007	0.773

$\sum ss = 0.1956$

Loading Ratio Correlation Model

Temperature (K)	ss	q_s	k_{LRC}	n_{LRC}
300	0.1874	2.814	0.051	1.467
320	0.0030	2.917	0.022	1.531
350	0.0051	2.677	0.010	1.424
375	0.0483	2.646	0.005	1.307
400	0.0266	2.658	0.003	1.278
425	0.0015	2.796	0.002	1.294

$\sum ss = 0.2720$

Units of the parameters are given in Table 4.1.
Data obtained from reference 1.

Table 5.2 Constrained Optimization Parameters for The Sorption of Ethylene on SR-115 Zeolite

Toth Model

T(K)	300	320	350	375	400	425
ss	0.0707	0.0984	0.0452	0.0185	0.0320	0.0381
b	2.407	3.361	5.874	9.235	12.423	15.897
K_H	0.576	0.303	0.104	0.043	0.025	0.015

$\sum ss = 0.303$

t is constrained at 0.520

Unilan Model

T(K)	300	320	350	375	400	425
ss	0.0841	0.1126	0.0552	0.0293	0.0388	0.0922
c	28.87	54.40	158.71	359.46	668.68	1084.10
K_H	0.414	0.219	0.075	0.033	0.018	0.011

$\sum ss = 0.4122$

s is constrained at 3.200

Radke-Prausnitz Model

T(K)	300	320	350	375	400	425
ss	0.0774	0.0101	0.0032	0.0035	0.0022	0.0552
b_{RP}	0.248	0.189	0.050	0.014	0.007	0.004
c_{RP}	0.202	0.127	0.076	0.060	0.047	0.037
K_H	0.773	0.590	0.155	0.043	0.021	0.012

$\sum ss = 0.1516$

n_{RP} is constrained at 0.530

Mathews-Weber Model

T(K)	300	320	350	375	400	425
ss	12.841	2.9332	2.1549	1.3107	0.9719	0.8997
b_{MW}	0.039	0.025	0.007	0.004	0.003	0.002
K_H	0.121	0.078	0.021	0.013	0.008	0.005

$\sum ss = 21.1114$

n_{MW} is constrained at 0.860

Virial Two Constant Model

T(K)	300	320	350	375	400	425
ss	0.0803	0.0949	0.0394	0.0114	0.0050	0.0643
A_2	0.188	0.097	0.110	0.023	0.000	0.000
K_H	0.503	0.230	0.080	0.033	0.018	0.011

$\sum ss = 0.2952$

A_1 is constrained at 1.200

Virial Three Constant Model

T(K)	300	320	350	375	400	425
ss	0.0535	0.0983	0.0413	0.0116	0.0050	0.0697
A_2	0.000	0.003	0.000	0.000	0.000	0.000
A_3	0.079	0.055	0.068	0.013	0.000	0.000
K_H	0.490	0.230	0.081	0.033	0.018	0.011

$\sum ss = 0.2794$

A_1 is constrained at 1.200

Langmuir-Freundlich Model

T(K)	300	320	350	375	400	425
ss	44.940	0.4204	0.3758	0.2763	0.7442	0.3186
k_{LF}	0.805	0.495	0.023	0.014	0.010	0.006

$\sum ss = 47.074$

n_{LF} is constrained at 0.800

Loading Ratio Correlation Model

T(K)	300	320	350	375	400	425
ss	0.3162	0.1484	0.1030	0.1226	0.1444	0.0772
k_{LRC}	0.034	0.020	0.007	0.003	0.002	0.001

$\sum ss = 0.9117$

n_{LRC} is constrained at 1.400

Units of the model parameters are given in Table 4.1.
All models requiring q_s have been constrained at 3.12 mol/kg of zeolite.
Volmer and Freundlich parameters have not been constrained.
Data obtained from reference 1.

Table 5.3 Constrained Optimization Parameters for The Sorption of Methane on SR-115 Zeolite

Toth Model

T(K)	275	275	300	325	350
ss	0.2521	0.2866	0.2082	0.5815	0.0693
b	12.881	14.210	19.863	30.512	37.066
K_H	0.0406	0.0339	0.0185	0.0085	0.0059

$\sum ss = 1.3977$

t is constrained at 0.550

Unilan Model

T(K)	275	275	300	325	350
ss	0.2850	0.1961	0.1428	0.3986	0.0421
c	431.1	492.0	916.3	1821.6	2823.8
K_H	0.0287	0.0252	0.0135	0.0068	0.0044

$\sum ss = 1.0646$

s is constrained at 2.80

Radke-Prausnitz Model

T(K)	275	275	300	325	350
ss	0.0184	0.0276	0.0306	0.1076	0.0165
b_{RP}	0.0061	0.0055	0.0028	0.0012	0.0009
c_{RP}	1.412	1.303	1.155	1.174	0.900
K_H	0.0258	0.0235	0.0120	0.0051	0.0037

$\sum ss = 0.2007$

n_{RP} is constrained at 0.050

Mathews-Weber Model

T(K)	275	275	300	325	350
ss	0.4222	0.7149	1.2773	0.7521	0.4689
b_{MW}	0.0038	0.0037	0.0019	0.0008	0.0005
K_H	0.0162	0.0157	0.0082	0.0033	0.0023

$\sum ss = 3.6354$

n_{MW} is constrained at 1.20

Volmer Model

T(K)	275	275	300	325	350
ss	0.0315	0.0660	0.0510	0.2154	0.0641
K_H	0.0305	0.0262	0.0126	0.0059	0.0042

$\sum ss = 0.4280$

Virial Two Constant Model

T(K)	275	275	300	325	350
ss	0.0492	0.0417	0.0313	0.0976	0.0170
A_2	0.353	0.354	0.343	0.360	0.356
K_H	0.0267	0.0229	0.0109	0.0052	0.0032

$\sum ss = 0.2369$

A_1 is constrained at 0.030

Virial Three Constant Model

T(K)	275	275	300	325	350
ss	0.0362	0.0396	0.0248	0.0449	0.0156
A_2	0.0014	0.0020	0.0979	0.0000	0.2587
A_3	0.1093	0.1167	0.0810	0.1470	0.0245
K_H	0.0224	0.0207	0.0103	0.0047	0.0033

$\sum ss = 0.1611$

A_1 is constrained at 0.150

Langmuir-Freundlich Model

T(K)	275	275	300	325	350
ss	0.6545	0.9109	0.4748	1.1230	0.1031
k_{LF}	0.0105	0.0101	0.0064	0.0036	0.0028

$\sum ss = 3.2663$

n_{LF} is constrained at 0.750

Loading Ratio Correlation Model

T(K)	275	275	300	325	350
ss	0.7611	0.7385	0.4497	1.0413	0.0870
k_{LRC}	0.0024	0.0021	0.0011	0.0006	0.0004

$\sum ss = 3.0777$

n_{LRC} is constrained at 1.30

Units of the model parameters are given in Table 4.1.
All models requiring q_s have been constrained at 4.23 mol/kg of zeolite.
Freundlich parameters have not been constrained.
Data obtained from reference 2.

Table 5.4 Constrained Optimization Parameters for The Sorption of Ethane on SR-115 Zeolite

Toth Model

T(K)	275	300	325	350
ss	0.1251	0.1347	1.4002	0.0356
b	1.809	4.398	12.550	14.916
K_H	1.192	0.335	0.075	0.059

$\sum ss = 1.6956$

t is constrained at 0.70

Unilan Model

T(K)	275	300	325	350
ss	0.4192	0.2342	2.1780	0.0522
c	3.562	16.300	53.004	96.076
K_H	1.342	0.293	0.090	0.050

$\sum ss = 2.8835$

s is constrained at 2.78

Radke-Prausnitz Model

T(K)	275	300	325	350
ss	0.0368	0.0350	0.8880	0.0172
b_{RP}	0.4914	0.1474	0.0219	0.0224
c_{RP}	0.930	0.507	1.339	0.249
K_H	1.366	0.410	0.061	0.062

$\sum ss = 0.9770$

n_{RP} is constrained at 0.050

Mathews-Weber Model

T(K)	275	300	325	350
ss	0.3139	0.1284	0.9397	0.3177
b_{MW}	0.272	0.081	0.024	0.013
K_H	0.755	0.226	0.065	0.035

$\sum ss = 1.6998$

n_{MW} is constrained at 1.05

Volmer Model

T(K)	275	300	325	350
ss	0.5976	0.3543	1.9252	0.3050
K_H	1.529	0.456	0.078	0.064

$\sum ss = 3.1822$

Virial Two Constant Model

T(K)	275	300	325	350
ss	0.0761	0.0378	0.7780	0.0212
A_2	0.692	0.654	0.500	0.522
K_H	0.998	0.297	0.063	0.041

$\sum ss = 0.9131$

A_1 is constrained at 0.005

Virial Three Constant Model

T(K)	275	300	325	350
ss	0.0169	0.0099	0.7800	0.0537
A_2	0.002	0.126	0.089	0.228
A_3	0.267	0.210	0.213	0.137
K_H	0.743	0.224	0.065	0.037

$\sum ss = 0.8605$

A_1 is constrained at 0.005

Langmuir-Freundlich Model

T(K)	275	300	325	350
ss	0.2668	0.3577	3.9425	0.1169
k_{LF}	0.2730	0.1081	0.0348	0.0214

$\sum ss = 4.6839$

n_{LF} is constrained at 0.85

Loading Ratio Correlation Model

T(K)	275	300	325	350
ss	0.4555	0.5444	0.3072	0.3713
k_{LRC}	0.2730	0.1081	0.0348	0.0214

$\sum ss = 4.6839$

n_{LRC} is constrained at 0.85

Units of the model parameters are given in Table 4.1.
All models requiring q_s have been constrained at 3.55 mol/kg of zeolite.
Freundlich parameters have not been constrained.
Data obtained from reference 2.

Table 5.5 Vant Hoff Equation Parameters for The Sorption of Methane, Ethane and Ethylene on SR-115

Methane

Model	$\sum ss$	$K_o \cdot 10^6$	$-\Delta H_o$
Toth	1.3977	5.2735	20.250
Unilan	1.0646	5.0296	19.627
Radke-Prausnitz	0.2007	2.4079	21.099
Mathews-Weber	3.6354	1.3582	21.452
Virial Two Constant	0.2369	1.5027	22.177
Virial Three Constant	0.1611	2.4730	20.772
Volmer	0.4280	2.6932	21.118

Ethane

Model	$\sum ss$	$K_o \cdot 10^6$	$-\Delta H_o$
Toth	1.6956	3.7740	34.033
Unilan	2.8835	1.9711	35.708
Radke-Prausnitz	0.9770	1.6717	36.249
Mathews-Weber	1.6998	3.0037	33.645
Virial Two Constant	0.9131	1.5062	33.862
Virial Three Constant	0.8605	3.9544	32.956
Volmer	3.1822	1.7314	36.478

Ethylene

Model	$\sum ss$	$K_o \cdot 10^6$	$-\Delta H_o$
Toth	0.3030	1.7811	31.797
Unilan	0.4122	1.3914	31.597
Radke-Prausnitz	0.1516	0.2380	38.236
Mathews-Weber	21.111	1.7434	27.933
Virial Two Constant	0.2952	0.8999	33.041
Virial Three Constant	0.2794	0.9465	32.885
Volmer	2.3368	0.9142	31.492

$\sum ss$: Total sum of square error

K_0 : Preexponential factor (mol/kg/kPa)

$-\Delta H_0$: Heat of adsorption (kJ/mol)

Table 5.6 Fit of IAST Model Using Toth, Unilan and Virial Isotherms for the Binary System Methane-Ethylene on SR-115 Zeolite

300 K and 200 kPa

	Experiment	IAST with Toth	IAST with Unilan	IAST with Virial
y_{CH_4}	x_{CH_4}	x_{CH_4}	x_{CH_4}	x_{CH_4}
0.000	0.000	0.0000	0.0000	0.0000
0.232	0.022	0.0183	0.0189	0.0180
0.397	0.043	0.0378	0.0388	0.0374
0.499	0.061	0.0546	0.0560	0.0543
0.579	0.082	0.0723	0.0740	0.0720
0.630	0.096	0.0866	0.0885	0.0863
0.673	0.113	0.1013	0.1034	0.1010
0.708	0.130	0.1158	0.1180	0.1154
0.739	0.146	0.1311	0.1334	0.1306
0.768	0.159	0.1481	0.1506	0.1475
1.000	—	1.0000	1.0000	1.0000

350 K and 200 kPa

	Experiment	IAST with Toth	IAST with Unilan	IAST with Virial
y_{CH_4}	x_{CH_4}	x_{CH_4}	x_{CH_4}	x_{CH_4}
0.000	0.000	0.0000	0.0000	0.0000
0.228	0.026	0.0248	0.0250	0.0234
0.388	0.054	0.0506	0.0507	0.0475
0.475	0.078	0.0696	0.0695	0.0652
0.554	0.104	0.0918	0.0915	0.0856
0.623	0.129	0.1169	0.1162	0.1086
0.668	0.152	0.1375	0.1363	0.1273
0.709	0.173	0.1603	0.1586	0.1479
0.741	0.193	0.1818	0.1796	0.1671
0.768	0.211	0.2031	0.2004	0.1863
1.000	—	1.0000	1.0000	1.0000

325 K and 150 kPa

	Experiment	IAST with Toth	IAST with Unilan	IAST with Virial
y_{CH_4}	x_{CH_4}	x_{CH_4}	x_{CH_4}	x_{CH_4}
0.000	0.000	0.0000	0.0000	—
0.211	0.022	0.0156	0.0172	—
0.352	0.042	0.0305	0.0334	—
0.441	0.061	0.0429	0.0469	—
0.512	0.078	0.0554	0.0605	—
0.572	0.095	0.0686	0.0746	—
0.618	0.111	0.0809	0.0877	—
0.656	0.127	0.0931	0.1006	—
0.689	0.141	0.1056	0.1138	—
0.717	0.154	0.1179	0.1268	—
1.000	—	1.0000	1.0000	—

325 K and 250 kPa

	Experiment	IAST with Toth	IAST with Unilan	IAST with Virial
y_{CH_4}	x_{CH_4}	x_{CH_4}	x_{CH_4}	x_{CH_4}
0.000	0.000	0.0000	0.0000	—
0.260	0.027	0.0217	0.0241	—
0.416	0.054	0.0418	0.0462	—
0.524	0.079	0.0617	0.0678	—
0.604	0.103	0.0818	0.0895	—
0.659	0.128	0.0998	0.1089	—
0.705	0.153	0.1189	0.1292	—
0.741	0.171	0.1374	0.1488	—
0.772	0.189	0.1569	0.1693	—
0.796	0.207	0.1750	0.1883	—
1.000	—	1.0000	1.0000	—

Table 5.7 Fit of IAST Model Using Toth, Unilan and Virial Isotherms for the Binary System of Ethane-Ethylene on SR-115 Zeolite

300 K and 200 kPa

	Experiment	IAST with Toth	IAST with Unilan	IAST with Virial
$y_{C_2H_6}$	$x_{C_2H_6}$	$x_{C_2H_6}$	$x_{C_2H_6}$	$x_{C_2H_6}$
0.000	0.000	0.0000	0.0000	0.0000
0.077	0.087	0.0800	0.0835	0.0755
0.152	0.164	0.1575	0.1638	0.1494
0.225	0.235	0.2324	0.2409	0.2214
0.296	0.299	0.3049	0.3149	0.2917
0.365	0.358	0.3748	0.3859	0.3603
0.431	0.409	0.4414	0.4530	0.4260
0.488	0.457	0.4985	0.5103	0.4829
0.543	0.498	0.5535	0.5651	0.5379
0.592	0.535	0.6022	0.6135	0.5871
1.000	—	1.0000	1.0000	1.0000

350 K and 200 kPa

	Experiment	IAST with Toth	IAST with Unilan	IAST with Virial
$y_{C_2H_6}$	$x_{C_2H_6}$	$x_{C_2H_6}$	$x_{C_2H_6}$	$x_{C_2H_6}$
0.000	0.000	0.0000	0.0000	0.0000
0.120	0.124	0.1150	0.1111	0.1128
0.225	0.222	0.2166	0.2100	0.2129
0.322	0.309	0.3114	0.3029	0.3067
0.410	0.385	0.3981	0.3886	0.3928
0.483	0.447	0.4706	0.4606	0.4651
0.550	0.503	0.5376	0.5275	0.5321
0.606	0.551	0.5940	0.5841	0.5886
0.656	0.595	0.6446	0.6351	0.6394
0.700	0.633	0.6893	0.6804	0.6844
1.000	—	1.0000	1.0000	1.0000

325 K and 150 kPa

	Experiment	IAST with Toth	IAST with Unilan	IAST with Virial
$y_{C_2H_6}$	$x_{C_2H_6}$	$x_{C_2H_6}$	$x_{C_2H_6}$	$x_{C_2H_6}$
0.000	0.000	0.0000	0.0000	—
0.080	0.085	0.0468	0.0635	—
0.155	0.160	0.0937	0.1250	—
0.228	0.228	0.1424	0.1868	—
0.297	0.290	0.1917	0.2471	—
0.362	0.348	0.2413	0.3057	—
0.422	0.397	0.2900	0.3613	—
0.475	0.442	0.3357	0.4119	—
0.525	0.484	0.3814	0.4608	—
0.575	0.521	0.4297	0.5110	—
1.000	—	1.0000	1.0000	—

325 K and 250 kPa

	Experiment	IAST with Toth	IAST with Unilan	IAST with Virial
$y_{C_2H_6}$	$x_{C_2H_6}$	$x_{C_2H_6}$	$x_{C_2H_6}$	$x_{C_2H_6}$
0.000	0.000	0.0000	0.0000	—
0.111	0.111	0.0671	0.0915	—
0.214	0.208	0.1353	0.1800	—
0.312	0.293	0.2065	0.2674	—
0.398	0.362	0.2748	0.3471	—
0.475	0.425	0.3411	0.4209	—
0.543	0.480	0.4043	0.4881	—
0.606	0.527	0.4674	0.5522	—
0.659	0.569	0.5240	0.6076	—
0.703	0.605	0.5739	0.6546	—
1.000	—	1.0000	1.0000	—

Table 5.8 Values of the Relative Adsorptivity of the Binary Systems Ethylene-Methane and Ethylene-Ethane on SR-115 Zeolite

Ethylene-Methane

		Relative Adsorptivity			
T (K)	P (kPa)	Experiment	IAST-Toth	IAST-Unilan	IAST-Virial
300	200	15.33	17.25	16.79	17.35
350	200	10.69	12.09	12.11	12.97
325	150	12.40	17.89	16.29	—
325	250	12.83	16.74	15.14	—

Ethylene-Ethane

		Relative Adsorptivity			
T (K)	P (kPa)	Experiment	IAST-Toth	IAST-Unilan	IAST-Virial
300	200	1.13	0.96	0.91	1.02
350	200	1.16	1.05	1.09	1.07
325	150	1.18	1.79	1.29	—
325	250	1.17	1.75	1.24	—

Table 5.9 x-q Fit of IAST Model Using Toth, Unilan and Virial Isotherms for the Binary System Methane-Ethylene at 300 K and 200 kPa

	Experimental			IAST with Toth			IAST with Unilan			IAST with Virial		
x_{CH_4}	q_{CH_4}	$q_{C_2H_4}$	q_{tot}	q_{CH_4}	$q_{C_2H_4}$	q_{tot}	q_{CH_4}	$q_{C_2H_4}$	q_{tot}	q_{CH_4}	$q_{C_2H_4}$	q_{tot}
0.000	0.000	2.368	2.368	0.000	2.372	2.372	0.000	2.385	2.385	0.000	2.311	2.311
0.022	0.051	2.260	2.311	0.042	2.257	2.299	0.043	2.254	2.298	0.040	2.190	2.230
0.043	0.098	2.168	2.264	0.084	2.144	2.228	0.086	2.130	2.216	0.081	2.075	2.156
0.061	0.136	2.080	2.215	0.119	2.052	2.171	0.121	2.031	2.152	0.114	1.985	2.099
0.082	0.178	2.001	2.179	0.153	1.963	2.116	0.155	1.937	2.092	0.147	1.899	2.047
0.096	0.205	1.930	2.135	0.180	1.895	2.074	0.181	1.866	2.047	0.173	1.835	2.008
0.113	0.239	1.865	2.104	0.206	1.828	2.034	0.207	1.798	2.005	0.199	1.772	1.971
0.130	0.269	1.805	2.075	0.231	1.766	1.977	0.232	1.734	1.967	0.224	1.714	1.938
0.146	0.299	1.753	2.050	0.257	1.703	1.960	0.257	1.671	1.929	0.249	1.657	1.906
0.159	0.323	1.704	2.028	0.285	1.637	1.921	1.921	0.284	1.605	0.276	1.596	1.872
1.000	—	—	—	1.119	0.000	1.119	1.119	1.141	0.000	1.251	0.000	1.251

x: mole fraction in the adsorbed phase.
y: mole fraction in the gas phase.
q: amount adsorbed (mol/kg of zeolite)

Table 5.10 x-q Fit of IAST Model Usiing Toth, Unilan and Virial Isotherms for the Binary System Methane-Ethylene at 350 K and 200 kPa

	Experimental			IAST with Toth			IAST with Unilan			IAST with Virial		
x_{CH_4}	q_{CH_4}	$q_{C_2H_4}$	q_{tot}	q_{CH_4}	$q_{C_2H_4}$	q_{tot}	q_{CH_4}	$q_{C_2H_4}$	q_{tot}	q_{CH_4}	$q_{C_2H_4}$	q_{tot}
0.000	0.000	1.669	1.669	0.000	1.694	1.694	0.000	1.664	1.664	0.000	1.649	1.649
0.026	0.041	1.549	1.590	0.040	1.551	1.591	0.039	1.526	1.565	0.036	1.518	1.555
0.054	0.081	1.434	1.515	0.076	1.422	1.498	0.075	1.402	1.477	0.070	1.401	1.471
0.078	0.113	1.336	1.449	0.100	1.337	1.437	0.099	1.322	1.421	0.092	1.324	1.416
0.104	0.144	1.250	1.394	0.126	1.247	1.373	0.125	1.237	1.362	0.116	1.243	1.359
0.129	0.174	1.174	1.348	0.153	1.156	1.309	0.151	1.151	1.303	0.141	1.161	1.302
0.152	0.198	1.106	1.304	0.174	1.088	1.262	0.172	1.087	1.259	0.160	1.099	1.260
0.173	0.219	1.046	1.265	0.195	1.019	1.214	0.193	1.022	1.215	0.180	1.037	1.217
0.193	0.238	0.993	1.231	0.213	0.960	1.173	0.211	0.966	1.177	0.197	0.983	1.180
0.211	0.251	0.943	1.194	0.231	0.905	1.135	0.229	0.913	1.142	0.213	0.932	1.146
1.000	—	—	—	0.570	0.000	0.570	0.580	0.000	0.580	0.558	0.000	0.558

x: mole fraction in the adsorbed phase.

y: mole fraction in the gas phase.

q: amount adsorbed (mol/kg of zeolite)

Table 5.11 x-q Fit of IAST Model Using Toth, Unilan and Virial Isotherms for the Binary System Methane-Ethylene at 325 K and 150 kPa

	Experimental			IAST with Toth			IAST with Unilan			IAST with Virial		
x_{CH_4}	q_{CH_4}	$q_{C_2H_4}$	q_{tot}	q_{CH_4}	$q_{C_2H_4}$	q_{tot}	q_{CH_4}	$q_{C_2H_4}$	q_{tot}	q_{CH_4}	$q_{C_2H_4}$	q_{tot}
0.000	0.000	1.884	1.884	0.000	1.921	1.921	0.000	1.891	1.891	—	—	—
0.022	0.040	1.789	1.789	0.029	1.800	1.829	0.031	1.767	1.798	—	—	—
0.042	0.075	1.698	1.773	0.053	1.697	1.750	0.058	1.664	1.722	—	—	—
0.061	0.106	1.618	1.724	0.073	1.618	1.691	0.078	1.587	1.665	—	—	—
0.078	0.130	1.543	1.674	0.091	1.545	1.636	0.098	1.515	1.613	—	—	—
0.095	0.155	1.479	1.634	0.109	1.474	1.583	0.117	1.447	1.563	—	—	—
0.111	0.176	1.419	1.595	0.124	1.412	1.537	0.133	1.388	1.521	—	—	—
0.127	0.198	1.364	1.561	0.139	1.356	1.495	0.149	1.333	1.482	—	—	—
0.141	0.215	1.314	1.528	0.154	1.301	1.455	0.165	1.281	1.446	—	—	—
0.154	0.230	1.268	1.498	0.167	1.250	1.418	0.179	1.233	1.412	—	—	—
1.000	—	—	—	0.596	0.000	0.596	0.643	0.000	0.643	—	—	—

x: mole fraction in the adsorbed phase.
y: mole fraction in the gas phase.
q: amount adsorbed (mol/kg of zeolite)

Table 5.12x-q Fit of IAST Model Using Toth, Unilan and Virial Isotherms for the Binary System Methane-Ethylene at 325 K and 250 kPa

	Experimental			IAST with Toth			IAST with Unilan			IAST with Virial		
x_{CH_4}	q_{CH_4}	$q_{C_2H_4}$	q_{tot}	q_{CH_4}	$q_{C_2H_4}$	q_{tot}	q_{CH_4}	$q_{C_2H_4}$	q_{tot}	q_{CH_4}	$q_{C_2H_4}$	q_{tot}
0.000	0.000	2.076	2.076	0.000	2.129	2.129	0.000	2.111	2.111	—	—	—
0.027	0.054	1.956	2.010	0.044	1.981	2.025	0.048	1.952	2.001	—	—	—
0.054	0.105	1.841	1.946	0.081	1.859	1.940	0.088	1.825	1.914	—	—	—
0.079	0.149	1.739	1.888	0.115	1.749	1.864	0.125	1.714	1.839	—	—	—
0.103	0.189	1.648	1.836	0.147	1.649	1.796	0.159	1.614	1.772	—	—	—
0.128	0.229	1.564	1.793	0.174	1.566	1.740	0.187	1.532	1.719	—	—	—
0.153	0.269	1.491	1.760	0.200	1.485	1.686	0.216	1.453	1.668	—	—	—
0.171	0.294	1.426	1.720	0.225	1.413	1.638	0.242	1.382	1.623	—	—	—
0.189	0.320	1.368	1.686	0.250	1.341	1.591	0.268	1.313	1.580	—	—	—
0.207	0.343	1.313	1.656	0.471	1.279	1.551	0.291	1.253	1.544	—	—	—
1.000	—	—	—	0.821	0.000	0.821	0.886	0.000	0.886	—	—	—

x: mole fraction in the adsorbed phase.
y: mole fraction in the gas phase.
q: amount adsorbed (mol/kg of zeolite)

Table 5.13 x-q Fit of IAST Model Using Toth, Unilan and Virial Isotherms for the Binary System Ethane-Ethylene at 300 K and 200 kPa

	Experimental			IAST with Toth			IAST with Unilan			IAST with Virial		
$x_{C_2H_6}$	$q_{C_2H_6}$	$q_{C_2H_4}$	q_{tot}	$q_{C_2H_6}$	$q_{C_2H_4}$	q_{tot}	$q_{C_2H_6}$	$q_{C_2H_4}$	q_{tot}	$q_{C_2H_6}$	$q_{C_2H_4}$	q_{tot}
0.000	0.000	2.245	2.245	0.000	2.372	2.372	0.000	2.385	2.385	0.000	2.311	2.311
0.087	0.194	2.040	2.234	0.190	2.185	2.375	0.200	2.193	2.393	0.174	2.131	2.305
0.164	0.365	1.855	2.219	0.374	2.003	2.377	0.393	2.007	2.400	0.343	1.956	2.299
0.235	0.519	1.686	2.205	0.553	1.827	2.380	0.580	1.827	2.407	0.508	1.786	2.294
0.299	0.655	1.536	2.191	0.726	1.656	2.382	0.760	1.654	2.414	0.668	1.621	2.289
0.358	0.780	1.401	2.183	0.894	1.490	2.384	0.934	1.486	2.420	0.823	1.461	2.284
0.409	0.889	1.283	2.171	1.053	1.333	2.386	1.099	1.327	2.426	0.971	1.308	2.279
0.457	0.990	1.176	2.166	1.190	1.197	2.388	1.241	1.190	2.431	1.098	1.176	2.275
0.498	1.071	1.081	2.153	1.322	1.067	2.389	1.376	1.059	2.436	1.221	1.049	2.271
0.535	1.148	0.998	2.145	1.440	0.951	2.391	1.497	0.943	2.440	1.331	0.936	2.267
1.000	—	—	—	2.402	0.000	2.402	2.471	0.000	2.471	2.238	0.000	2.238

x: mole fraction in the adsorbed phase.
y: mole fraction in the gas phase.
q: amount adsorbed (mol/kg of zeolite)

Table 5.14 x-q Fit of IAST Model Using Toth, Unilan and Virial Isotherms for the Binary System Ethane-Ethylene at 350 K and 200 kPa

	Experimental			IAST with Toth			IAST with Unilan			IAST with Virial		
$x_{C_2H_6}$	$q_{C_2H_6}$	$q_{C_2H_4}$	q_{tot}	$q_{C_2H_6}$	$q_{C_2H_4}$	q_{tot}	$q_{C_2H_6}$	$q_{C_2H_4}$	q_{tot}	$q_{C_2H_6}$	$q_{C_2H_4}$	q_{tot}
0.0000	0.000	1.619	1.619	0.000	1.695	1.695	0.000	1.664	1.664	0.000	1.649	1.649
0.124	0.203	1.430	1.633	0.196	1.508	1.704	0.186	1.489	1.676	0.187	1.472	1.659
0.222	0.363	1.269	1.633	0.371	1.341	1.712	0.354	1.332	1.686	0.355	1.313	1.669
0.309	0.504	1.129	1.633	0.536	1.185	1.720	0.514	1.182	1.696	0.514	1.163	1.677
0.385	0.628	1.004	1.631	0.688	1.040	1.727	0.663	1.043	1.706	0.662	1.024	1.686
0.447	0.724	0.898	1.621	0.816	0.918	1.734	0.789	0.925	1.714	0.787	0.906	1.693
0.503	0.814	0.804	1.619	0.935	0.804	1.739	0.908	0.814	1.722	0.904	0.795	1.700
0.551	0.889	0.724	1.613	1.036	0.708	1.744	1.009	0.719	1.728	1.004	0.702	1.705
0.595	0.959	0.653	1.611	1.127	0.622	1.749	1.101	0.633	1.734	1.094	0.617	1.711
0.633	1.019	0.591	1.610	1.208	0.545	1.753	1.184	0.556	1.740	1.174	0.541	1.715
1.000	—	—	—	1.781	0.000	1.781	1.779	0.000	1.779	1.750	0.000	1.750

x: mole fraction in the adsorbed phase.
y: mole fraction in the gas phase.
q: amount adsorbed (mol/kg of zeolite)

Table 5.15 x-q Fit of IAST Model Using Toth, Unilan and Virial Isotherms for the Binary System Ethane-Ethylene at 325 K and 150 kPa

	Experimental			IAST with Toth			IAST with Unilan			IAST with Virial		
$x_{C_2H_6}$	$q_{C_2H_6}$	$q_{C_2H_4}$	q_{tot}	$q_{C_2H_6}$	$q_{C_2H_4}$	q_{tot}	$q_{C_2H_6}$	$q_{C_2H_4}$	q_{tot}	$q_{C_2H_6}$	$q_{C_2H_4}$	q_{tot}
0.000	0.000	1.844	1.844	0.000	1.921	1.921	0.000	1.891	1.891	—	—	—
0.085	0.156	1.690	1.846	0.089	1.821	1.910	0.120	1.772	1.892	—	—	—
0.160	0.295	1.549	1.844	0.178	1.722	1.900	0.237	1.657	1.893	—	—	—
0.228	0.421	1.421	1.842	0.269	1.620	1.889	0.354	1.541	1.895	—	—	—
0.290	0.534	1.306	1.840	0.360	1.519	1.879	0.469	1.428	1.897	—	—	—
0.348	0.641	1.200	1.841	0.451	1.418	1.869	0.580	1.318	1.898	—	—	—
0.397	0.729	1.108	1.837	0.539	1.321	1.860	0.687	1.214	1.900	—	—	—
0.442	0.810	1.022	1.832	0.622	1.230	1.852	0.783	1.119	1.902	—	—	—
0.484	0.885	0.945	1.830	0.703	1.141	1.844	0.877	1.027	1.904	—	—	—
0.521	0.954	0.876	1.830	0.789	1.047	1.836	0.974	0.932	1.906	—	—	—
1.000	—	—	—	1.762	0.000	1.762	1.930	0.000	1.930	—	—	—

x: mole fraction in the adsorbed phase.

y: mole fraction in the gas phase.

q: amount adsorbed (mol/kg of zeolite)

Table 5.16 x-q Fit of IAST Model Using Toth, Unilan and Virial Isotherms for the Binary System Ethane-Ethylene at 325 K and 250 kPa

	Experimental			IAST with Toth			IAST with Unilan			IAST with Virial		
$x_{C_2H_6}$	$q_{C_2H_6}$	$q_{C_2H_4}$	q_{tot}	$q_{C_2H_6}$	$q_{C_2H_4}$	q_{tot}	$q_{C_2H_6}$	$q_{C_2H_4}$	q_{tot}	$q_{C_2H_6}$	$q_{C_2H_4}$	q_{tot}
0.000	0.000	2.040	2.040	0.000	2.129	2.129	0.000	2.111	2.111	—	—	—
0.111	0.225	1.805	2.029	0.142	1.973	2.115	0.193	1.920	2.113	—	—	—
0.208	0.420	1.600	2.020	0.284	1.817	2.102	0.381	1.735	2.116	—	—	—
0.293	0.590	1.424	2.012	0.431	1.657	2.089	0.567	1.552	2.119	—	—	—
0.362	0.721	1.269	1.991	0.571	1.506	2.077	0.736	1.385	2.121	—	—	—
0.425	0.841	1.136	1.978	0.705	1.362	2.066	0.894	1.230	2.124	—	—	—
0.480	0.944	1.021	1.965	0.832	1.225	2.057	1.038	1.089	2.127	—	—	—
0.527	1.029	0.924	1.953	0.957	1.091	2.048	1.176	0.954	2.130	—	—	—
0.569	1.106	0.839	1.945	1.069.	0.971	2.040	1.296	0.837	2.133	—	—	—
0.605	1.170	0.763	1.934	1.167	0.867	2.034	1.398	0.738	2.136	—	—	—
1.000	—	—	—	1.991	0.000	1.991	2.157	0.000	2.157	—	—	—

x: mole fraction in the adsorbed phase.
y: mole fraction in the gas phase.
q: amount adsorbed (mol/kg of zeolite)

Table 5.17 x-y Fit of IAST Model Using Toth, Unilan and Virial Isotherms for the Ternary System Methane-Ethane-Ethylene on SR-115 Zeolite at 300 K and 200 kPa (High Ethane Loading)

		Experimental		IAST with Toth		IAST with Unilan		IAST with Virial	
y_{CH_4}	$y_{C_2H_6}$	x_{CH_4}	$x_{C_2H_6}$	x_{CH_4}	$x_{C_2H_6}$	x_{CH_4}	$x_{C_2H_6}$	x_{CH_4}	$x_{C_2H_6}$
0.000	0.000	—	—	0.000	0.000	0.000	0.000	0.000	0.000
0.000	0.267	0.000	0.298	0.000	0.275	0.000	0.285	0.000	0.263
0.249	0.202	0.027	0.291	0.020	0.271	0.020	0.279	0.020	0.260
0.409	0.160	0.047	0.286	0.039	0.267	0.040	0.274	0.039	0.257
0.519	0.132	0.067	0.281	0.058	0.264	0.059	0.270	0.058	0.256
0.597	0.111	0.087	0.276	0.077	0.259	0.078	0.264	0.077	0.251
0.654	0.097	0.107	0.270	0.094	0.257	0.096	0.261	0.094	0.250
0.696	0.085	0.121	0.266	0.110	0.251	0.112	0.255	0.111	0.245
0.730	0.077	0.135	0.262	0.126	0.251	0.128	0.254	0.127	0.245
0.758	0.069	0.151	0.258	0.142	0.246	0.144	0.248	0.142	0.240
0.780	0.064	0.165	0.254	0.156	0.246	0.158	0.247	0.156	0.240
1.000	0.000	—	—	1.000	0.000	1.000	0.000	1.000	0.000

Table 5.18 x-y Fit of IAST Model Using Toth, Unilan and Virial Isotherms for the Ternary System Methane-Ethane-Ethylene on SR-115 Zeolite at 300 K and 200 kPa (High Ethylene Loading)

		Experimental		IAST with Toth		IAST with Unilan		IAST with Virial	
y_{CH_4}	$y_{C_2H_6}$	x_{CH_4}	$x_{C_2H_6}$	x_{CH_4}	$x_{C_2H_6}$	x_{CH_4}	$x_{C_2H_6}$	x_{CH_4}	$x_{C_2H_6}$
0.000	0.000	—	—	0.0000	0.0000	0.0000	0.0000	0.0000	0.000
0.000	0.038	0.000	0.050	0.0000	0.0396	0.0000	0.0414	0.0000	0.0168
0.233	0.029	0.023	0.049	0.0184	0.0385	0.0189	0.0401	0.0237	0.0163
0.391	0.024	0.044	0.048	0.0369	0.0392	0.0378	0.406	0.0466	0.0153
0.499	0.020	0.065	0.047	0.0546	0.0388	0.0559	0.0400	0.0674	0.0160
0.575	0.017	0.087	0.046	0.0712	0.0381	0.0728	0.0390	0.0882	0.0145
0.633	0.015	0.107	0.045	0.0875	0.0381	0.0893	0.0389	0.1084	0.0142
0.676	0.013	0.123	0.045	0.1024	0.0366	0.1045	0.0373	0.1271	0.0156
0.711	0.012	0.139	0.044	0.1171	0.0371	0.1193	0.0377	0.1444	0.0145
0.741	0.011	0.156	0.043	0.1321	0.0372	0.1344	0.0376	0.1631	0.0157
0.765	0.010	0.172	0.043	0.1462	0.0365	0.1485	0.0369	0.1800	0.0140
1.000	0.000	—	—	1.0000	0.0000	1.0000	0.0000	1.0000	0.0000

Table 5.19 x-y Fit of IAST Model Using Toth, Unilan and Virial Isotherms for the Ternary System Methane-Ethane-Ethylene on SR-115 Zeolite at 325 K and 200 kPa (High Ethane Loading)

		Experimental		IAST with Toth		IAST with Unilan		IAST with Virial	
y_{CH_4}	$y_{C_2H_6}$	x_{CH_4}	$x_{C_2H_6}$	x_{CH_4}	$x_{C_2H_6}$	x_{CH_4}	$x_{C_2H_6}$	x_{CH_4}	$x_{C_2H_6}$
0.000	0.000	—	—	0.0000	0.0000	0.0000	0.0000	—	—
0.000	0.498	0.000	0.502	0.0000	0.3598	0.0000	0.4397	—	—
0.250	0.376	0.019	0.492	0.0247	0.3509	0.0245	0.4273	—	—
0.406	0.299	0.039	0.482	0.0483	0.3415	0.0478	0.4149	—	—
0.512	0.247	0.060	0.471	0.0711	0.3334	0.0702	0.4042	—	—
0.588	0.209	0.080	0.460	0.0931	0.3244	0.0917	0.3928	—	—
0.644	0.182	0.100	0.450	0.1141	0.3183	0.1122	0.3849	—	—
0.688	0.160	0.119	0.439	0.1346	0.3107	0.1322	0.3753	—	—
0.724	0.143	0.135	0.430	0.1553	0.3059	0.1522	0.3691	—	—
0.752	0.128	0.152	0.421	0.1740	0.2964	0.1705	0.3578	—	—
0.774	0.118	0.168	0.412	0.1917	0.2934	0.1876	0.3538	—	—
1.000	0.000	—	—	1.0000	0.0000	1.0000	0.0000	—	—

Table 5.20 x-y Fit of IAST Model Using Toth, Unilan and Virial Isotherms for the Ternary System Methane-Ethane-Ethylene on SR-115 Zeolite at 325 K and 200 kPa (High Ethylene Loading)

		Experimental		IAST with Toth		IAST with Unilan		IAST with Virial	
y_{CH_4}	$y_{C_2H_6}$	x_{CH_4}	$x_{C_2H_6}$	x_{CH_4}	$x_{C_2H_6}$	x_{CH_4}	$x_{C_2H_6}$	x_{CH_4}	$x_{C_2H_6}$
0.000	0.000	—	—	0.0000	0.0000	0.0000	0.0000	—	—
0.000	0.018	0.000	0.023	0.0000	0.0104	0.0000	0.0144	—	—
0.230	0.014	0.024	0.023	0.0182	0.0102	0.0201	0.0140	—	—
0.383	0.011	0.049	0.022	0.0360	0.0097	0.0396	0.0133	—	—
0.484	0.010	0.072	0.022	0.0524	0.0103	0.0573	0.0140	—	—
0.562	0.008	0.094	0.022	0.0690	0.0094	0.0752	0.0128	—	—
0.622	0.007	0.114	0.021	0.0855	0.0093	0.0928	0.0126	—	—
0.667	0.007	0.133	0.021	0.1010	0.0104	0.1093	0.0139	—	—
0.702	0.006	0.151	0.021	0.1154	0.0097	0.1246	0.0129	—	—
0.734	0.006	0.169	0.020	0.1314	0.0106	0.1413	0.0141	—	—
0.759	0.005	0.187	0.020	0.1459	0.0095	0.1566	0.0126	—	—
1.000	0.000	—	—	1.0000	0.0000	1.0000	0.0000	—	—

Table 5.21 x-q Fit of IAST Model Using Toth, Unilan and Virial Isotherms for the Ternary System Methane-Ethane-Ethylene on SR-115 Zeolite at 300 K and 200 kPa (High Ethane Loading)

		Experimental			IAST with Toth			IAST with Unilan			IAST with Virial		
x_{CH_4}	$x_{C_2H_6}$	q_{CH_4}	$q_{C_2H_6}$	$q_{C_2H_4}$	q_{CH_4}	$q_{C_2H_6}$	$q_{C_2H_4}$	q_{CH_4}	$q_{C_2H_6}$	$q_{C_2H_4}$	q_{CH_4}	$q_{C_2H_6}$	$q_{C_2H_4}$
0.000	0.000	—	—	—	0.000	0.000	2.372	0.000	0.000	2.385	0.000	0.000	2.311
0.000	0.298	0.000	0.651	1.533	0.000	0.656	1.726	0.000	0.687	1.725	0.000	0.602	1.688
0.027	0.291	0.059	0.625	1.462	0.046	0.626	1.635	0.047	0.649	1.628	0.044	0.576	1.591
0.047	0.286	0.099	0.600	1.398	0.088	0.597	1.554	0.090	0.615	1.542	0.084	0.552	1.508
0.067	0.281	0.138	0.578	1.340	0.127	0.575	1.477	0.129	0.588	1.461	0.122	0.553	1.431
0.087	0.276	0.175	0.556	1.288	0.163	0.550	1.412	0.165	0.558	1.395	0.157	0.512	1.368
0.107	0.270	0.212	0.538	1.241	0.195	0.535	1.346	0.197	0.540	1.329	0.189	0.500	1.306
0.121	0.266	0.236	0.520	1.198	0.224	0.511	1.299	0.226	0.515	1.281	0.217	0.480	1.262
0.135	0.262	0.260	0.504	1.158	0.252	0.501	1.243	0.253	0.502	1.225	0.244	0.472	1.211
0.151	0.258	0.286	0.490	1.121	0.278	0.481	1.200	0.279	0.481	1.183	0.270	0.455	1.172
0.165	0.254	0.309	0.476	1.089	0.301	0.474	1.153	0.302	0.473	1.137	0.293	0.450	1.129
1.000	0.000	—	—	—	0.119	0.000	0.000	1.141	0.000	0.000	1.251	0.000	0.000

123123

Table 5.22 x-q Fit of IAST Model Using Toth, Unilan and Virial Isotherms for the Ternary System Methane-Ethane-Ethylene on SR-115 Zeolite at 300 K and 200 kPa (High Ethylene Loading)

		Experimental			IAST with Toth			IAST with Unilan			IAST with Virial		
x_{CH_4}	$x_{C_2H_6}$	q_{CH_4}	$q_{C_2H_6}$	$q_{C_2H_4}$	q_{CH_4}	$q_{C_2H_6}$	$q_{C_2H_4}$	q_{CH_4}	$q_{C_2H_6}$	$q_{C_2H_4}$	q_{CH_4}	$q_{C_2H_6}$	$q_{C_2H_4}$
0.000	0.000	—	—	—	0.000	0.000	2.372	0.000	0.000	2.385	0.000	0.000	1.649
0.000	0.050	0.000	0.109	2.076	0.000	0.094	2.280	0.000	0.099	2.290	0.000	0.028	1.623
0.023	0.049	0.050	0.104	1.978	0.042	0.089	2.170	0.044	0.092	2.166	0.037	0.025	1.493
0.044	0.048	0.091	0.100	1.886	0.082	0.088	2.063	0.084	0.090	2.050	0.069	0.023	1.384
0.065	0.047	0.133	0.095	1.804	0.119	0.084	1.971	0.121	0.086	1.951	0.095	0.023	1.294
0.087	0.046	0.174	0.091	1.729	0.151	0.081	1.890	0.153	0.082	1.866	0.119	0.020	1.215
0.107	0.045	0.210	0.088	1.661	0.182	0.079	1.815	0.183	0.080	1.788	0.141	0.019	1.144
0.123	0.045	0.236	0.086	1.598	0.208	0.074	1.752	0.210	0.075	1.723	0.160	0.020	1.082
0.139	0.044	0.263	0.082	1.541	0.234	0.074	1.689	0.235	0.074	1.660	0.177	0.018	1.031
0.156	0.043	0.291	0.081	1.490	0.259	0.073	1.629	0.260	0.073	1.600	0.194	0.019	0.977
0.172	0.043	0.315	0.078	1.441	0.282	0.070	1.577	0.282	0.070	1.547	0.209	0.016	0.934
1.000	0.000	—	—	—	1.119	0.000	0.000	1.141	0.000	0.000	0.558	0.000	0.000

Table 5.23 x-q Fit of IAST Model Using Toth, Unilan and Virial Isotherms for the Ternary System Methane-Ethane-Ethylene on SR-115 Zeolite at 325 K and 200 kPa (High Ethane Loading)

		Experimental			IAST with Toth			IAST with Unilan			IAST with Virial		
x_{CH_4}	$x_{C_2H_6}$	q_{CH_4}	$q_{C_2H_6}$	$q_{C_2H_4}$	q_{CH_4}	$q_{C_2H_6}$	$q_{C_2H_4}$	q_{CH_4}	$q_{C_2H_6}$	$q_{C_2H_4}$	q_{CH_4}	$q_{C_2H_6}$	$q_{C_2H_4}$
0.000	0.000	—	—	—	0.000	0.000	2.041	0.000	0.000	2.016	—	—	—
0.000	0.502	0.000	0.955	0.946	0.000	0.710	1.263	0.000	0.893	1.138	—	—	—
0.019	0.492	0.035	0.902	0.896	0.046	0.654	1.164	0.047	0.820	1.053	—	—	—
0.039	0.482	0.069	0.854	0.849	0.086	0.606	1.082	0.087	0.759	0.983	—	—	—
0.060	0.471	0.103	0.810	0.808	0.121	0.565	1.010	0.123	0.708	0.921	—	—	—
0.080	0.460	0.138	0.770	0.769	0.152	0.528	0.949	0.155	0.662	0.869	—	—	—
0.100	0.450	0.162	0.734	0.735	0.179	0.500	0.891	0.183	0.627	0.819	—	—	—
0.119	0.439	0.190	0.701	0.705	0.204	0.472	0.842	0.209	0.592	0.777	—	—	—
0.135	0.430	0.211	0.671	0.678	0.228	0.450	0.792	0.233	0.565	0.733	—	—	—
0.152	0.421	0.232	0.644	0.652	0.249	0.424	0.757	0.255	0.534	0.704	—	—	—
0.168	0.412	0.251	0.618	0.629	0.267	0.409	0.718	0.274	0.516	0.669	—	—	—
1.000	0.000	—	—	—	0.716	0.000	0.000	0.774	0.000	0.000	—	—	—

Table 5.24 x-q Fit of IAST Model Using Toth, Unilan and Virial Isotherms for the Ternary System Methane-Ethane-Ethylene on SR-115 Zeolite at 325 K and 200 kPa (High Ethylene Loading)

		Experimental			IAST with Toth			IAST with Unilan			IAST with Virial		
x_{CH_4}	$x_{C_2H_6}$	q_{CH_4}	$q_{C_2H_6}$	$q_{C_2H_4}$	q_{CH_4}	$q_{C_2H_6}$	$q_{C_2H_4}$	q_{CH_4}	$q_{C_2H_6}$	$q_{C_2H_4}$	q_{CH_4}	$q_{C_2H_6}$	$q_{C_2H_4}$
0.000	0.000	—	—	—	0.000	0.000	2.041	0.000	0.000	2.016	—	—	—
0.000	0.023	0.000	0.044	1.865	0.000	0.021	2.018	0.000	0.029	1.987	—	—	—
0.024	0.023	0.044	0.041	1.755	0.035	0.020	1.888	0.038	0.027	1.852	—	—	—
0.049	0.022	0.088	0.040	1.652	0.067	0.018	1.774	0.073	0.024	1.737	—	—	—
0.072	0.022	0.124	0.038	1.562	0.094	0.018	1.678	0.101	0.025	1.641	—	—	—
0.094	0.022	0.158	0.036	1.481	0.119	0.016	1.591	0.128	0.022	1.555	—	—	—
0.114	0.021	0.186	0.035	1.408	0.143	0.016	1.511	0.153	0.021	1.477	—	—	—
0.133	0.021	0.210	0.034	1.344	0.164	0.017	1.440	0.175	0.022	1.408	—	—	—
0.151	0.021	0.234	0.032	1.282	0.182	0.015	1.380	0.195	0.020	1.350	—	—	—
0.169	0.020	0.256	0.031	1.229	0.201	0.016	1.316	0.216	0.022	1.289	—	—	—
0.187	0.020	0.278	0.030	1.179	0.218	0.014	1.264	0.234	0.019	1.239	—	—	—
1.000	0.000	—	—	—	0.716	0.000	0.000	0.774	0.000	0.000	—	—	—

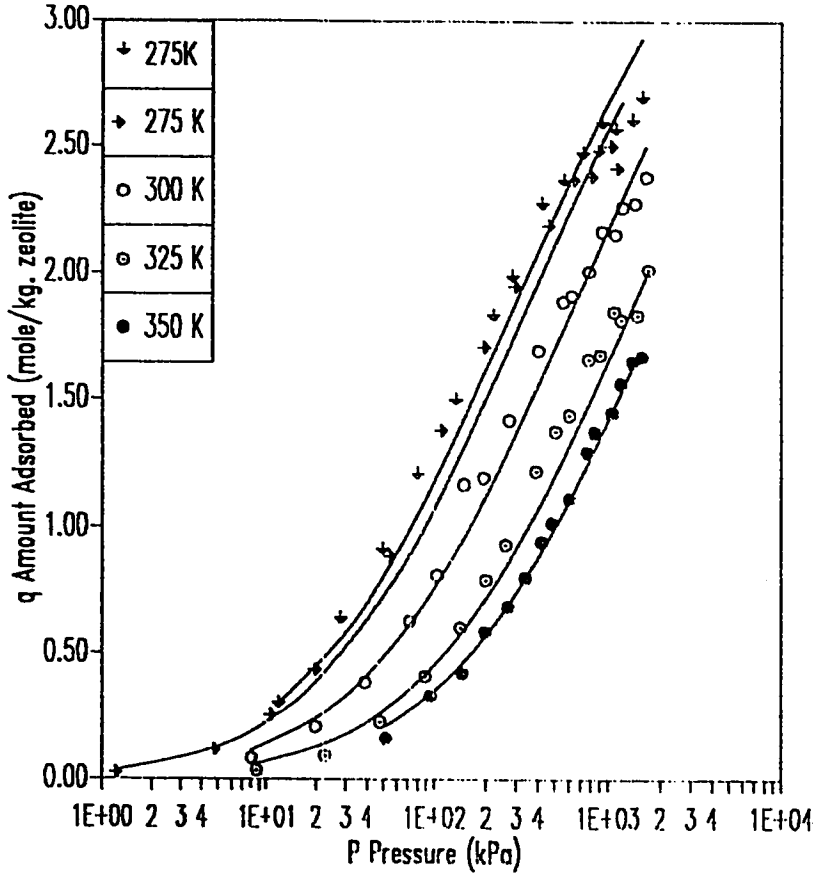

Figure 5.1 Isotherms of Methane on SR-115 Zeolite:
Fit of Toth Model (—)

Data Obtained from Reference 2.

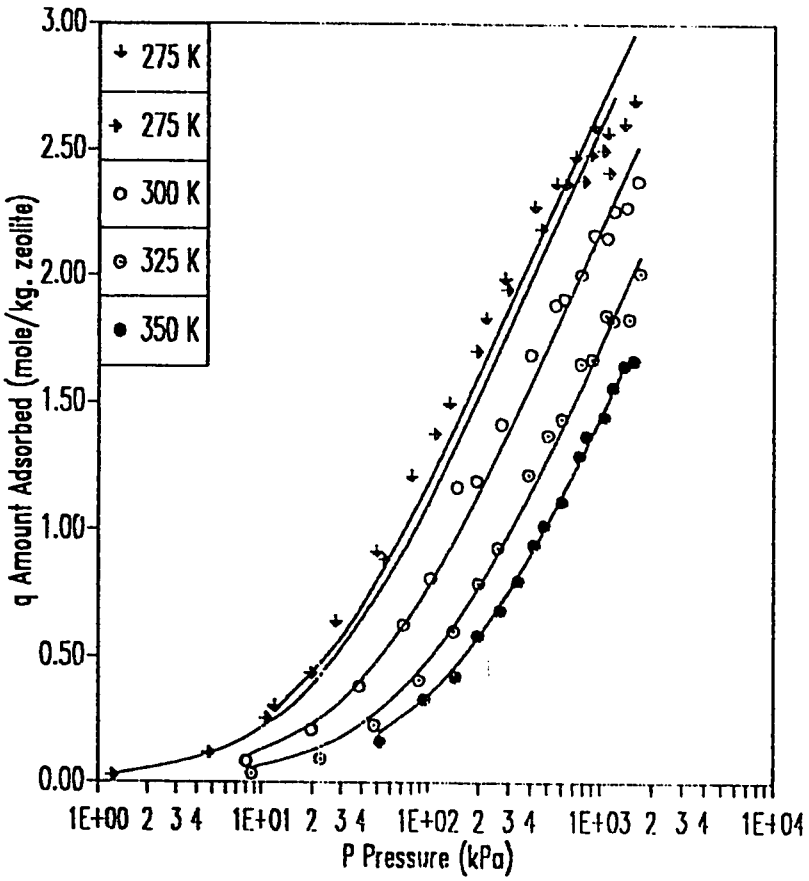

Figure 5.2 Isotherms of Methane on SR-115 Zeolite:
Fit of Unilan Model (—)

Data Obtained from Reference 2.

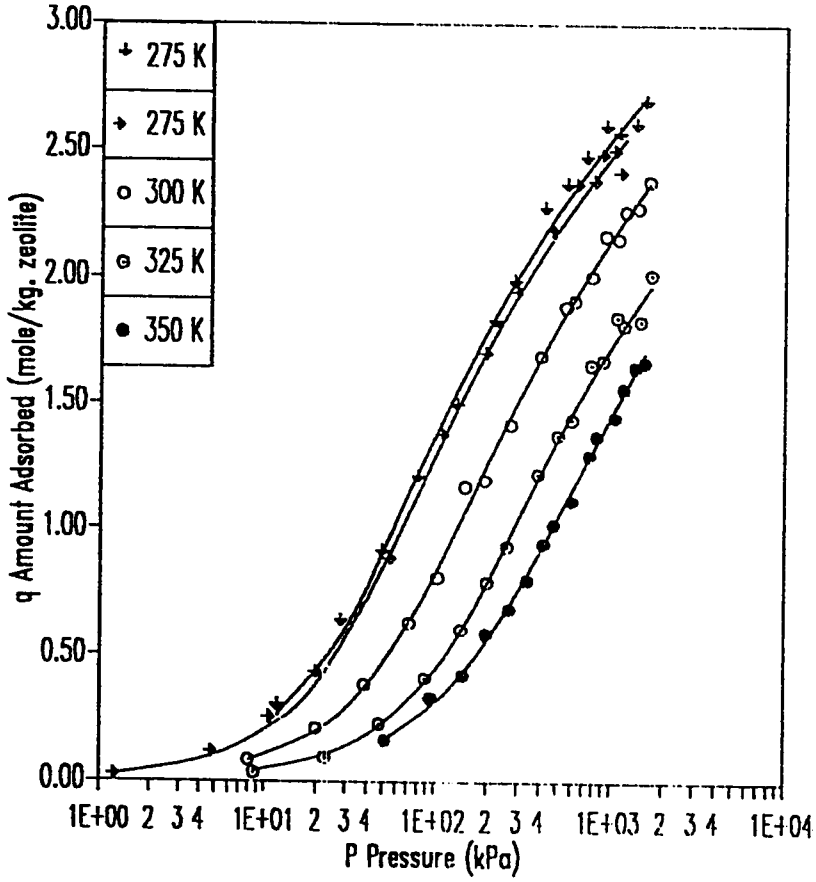

Figure 5.3 Isotherms of Methane on SR-115 Zeolite:
Fit of Virial Three Constant Model (—)

Data Obtained from Reference 2.

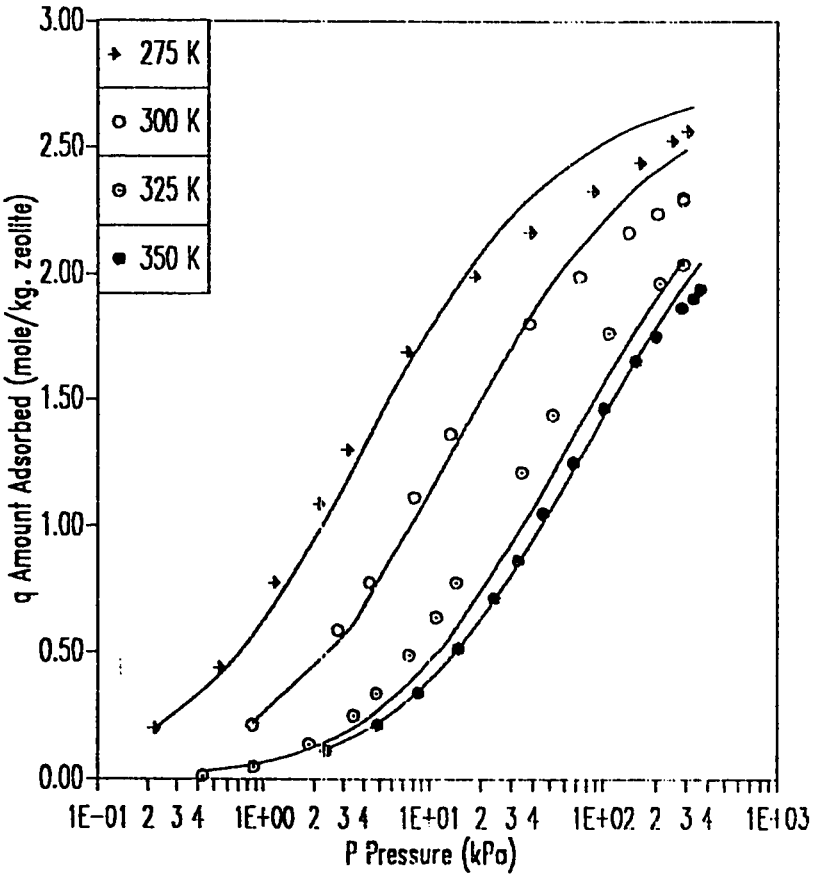

Figure 5.4 Isotherms of Ethane on SR-115 Zeolite:
Fit of Toth Model (—)

Data Obtained from Reference 2.

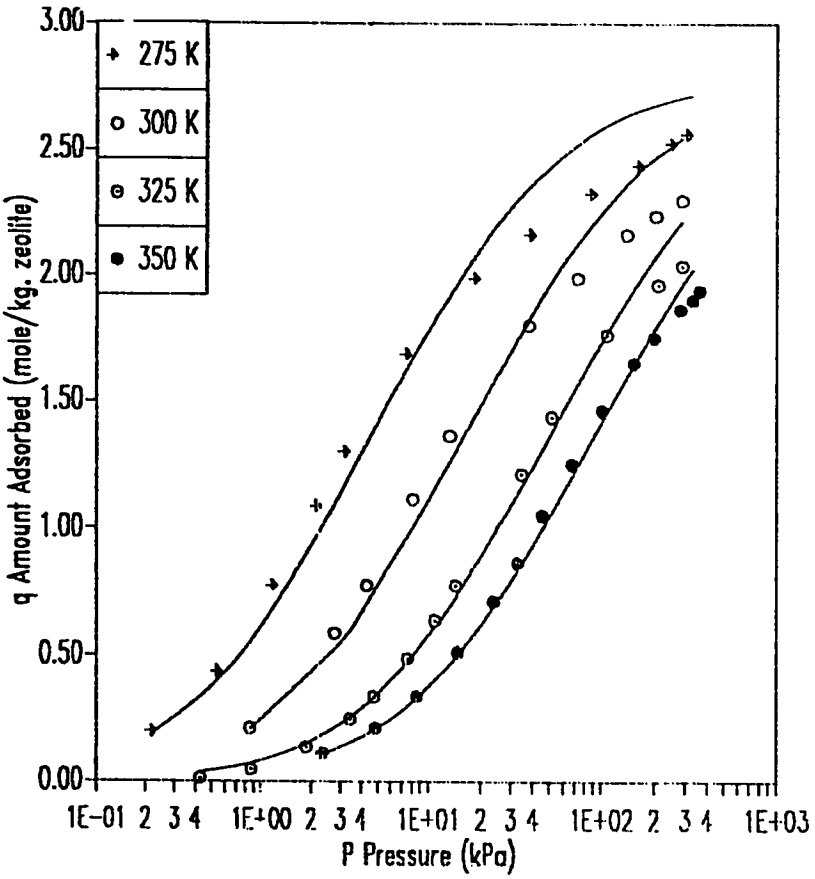

Figure 5.5 Isotherms of Ethane on SR-115 Zeolite:
Fit of Unilan Model (—)

Data Obtained from Reference 2.

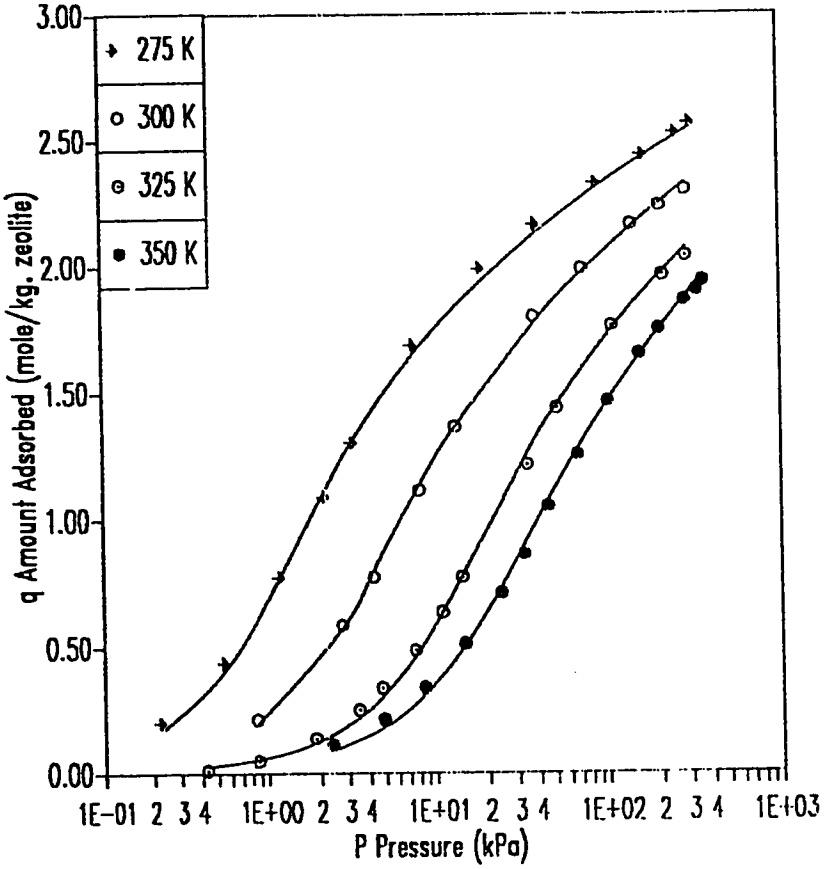

Figure 5.6 Isotherms of Ethane on SR-115 Zeolite:
Fit of Virial Three Constant Model (—)

Data Obtained from Reference 2.

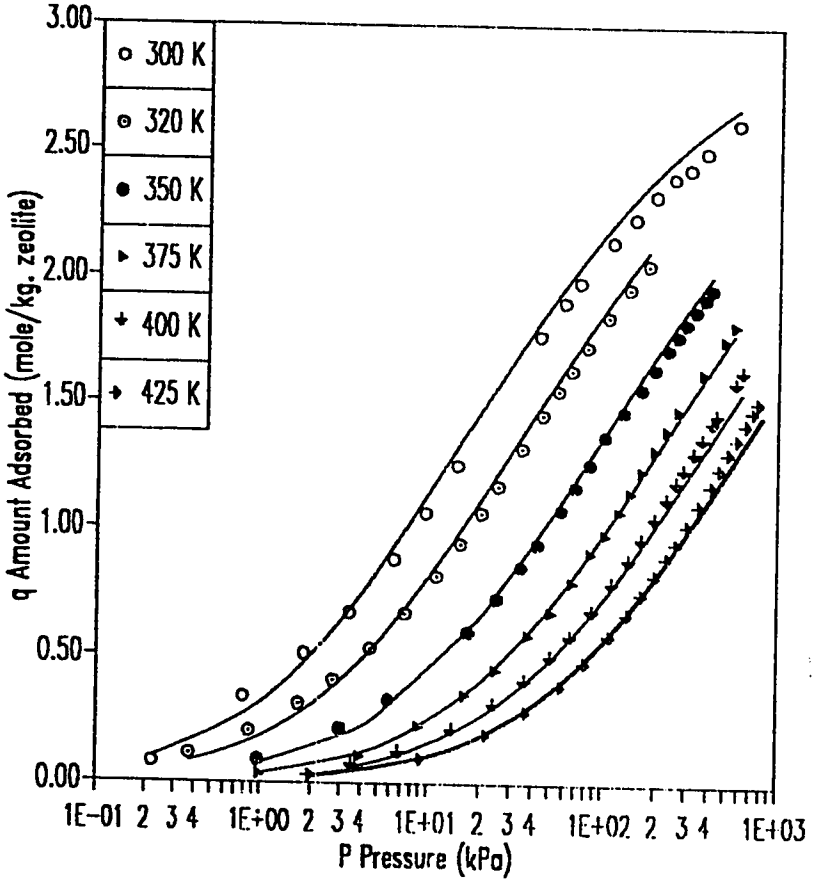

Figure 5.7 Isotherms of Ethylene on SR-115 Zeolite:
Fit of Toth Model (—)

Data Obtained from Reference 1.

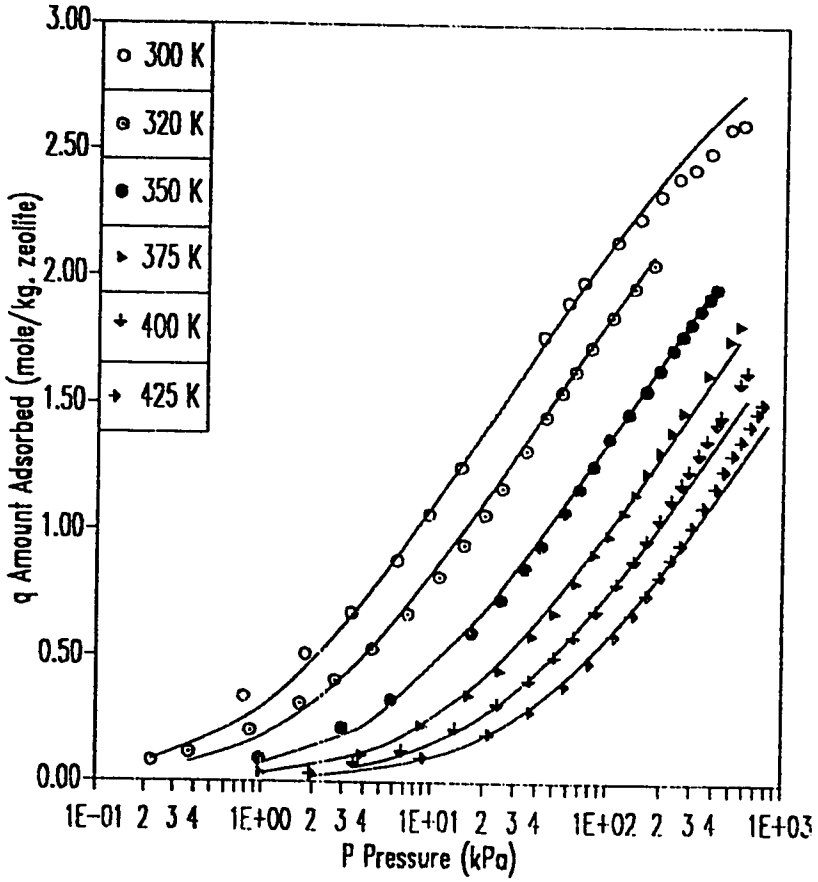

Figure 5.8 Isotherms of Ethylene on SR-115 Zeolite:
Fit of Unilan Model (—)

Data Obtained from Reference 1.

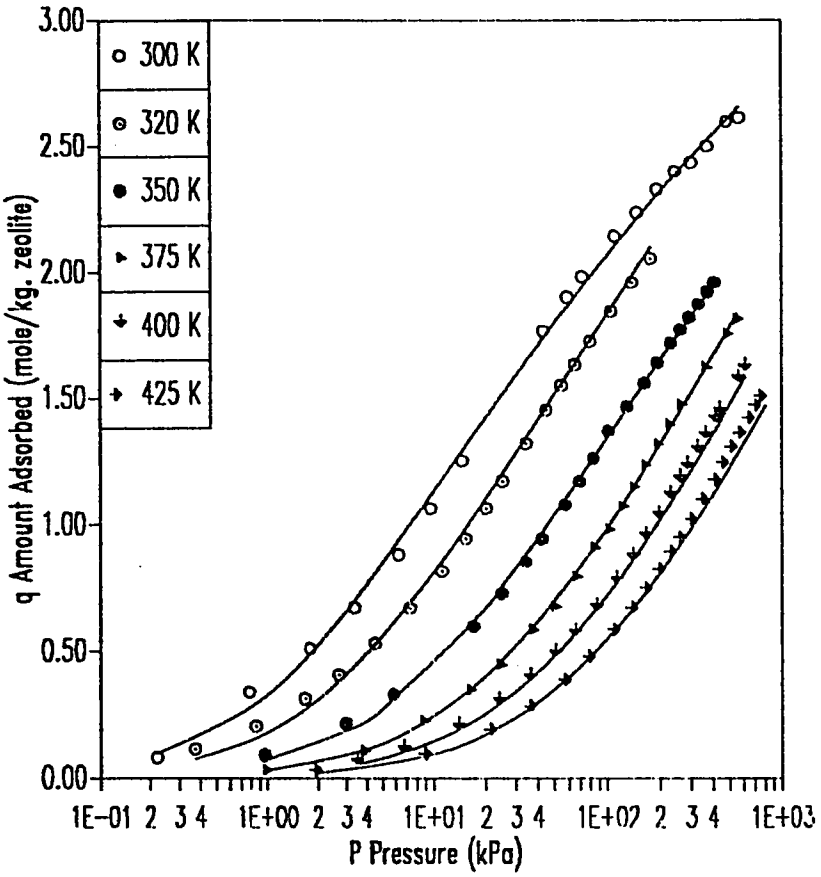

Figure 5.9 Isotherms of Ethylene on SR-115 Zeolite:
Fit of Virial Three Constant Model (—)

Data Obtained from Reference 1.

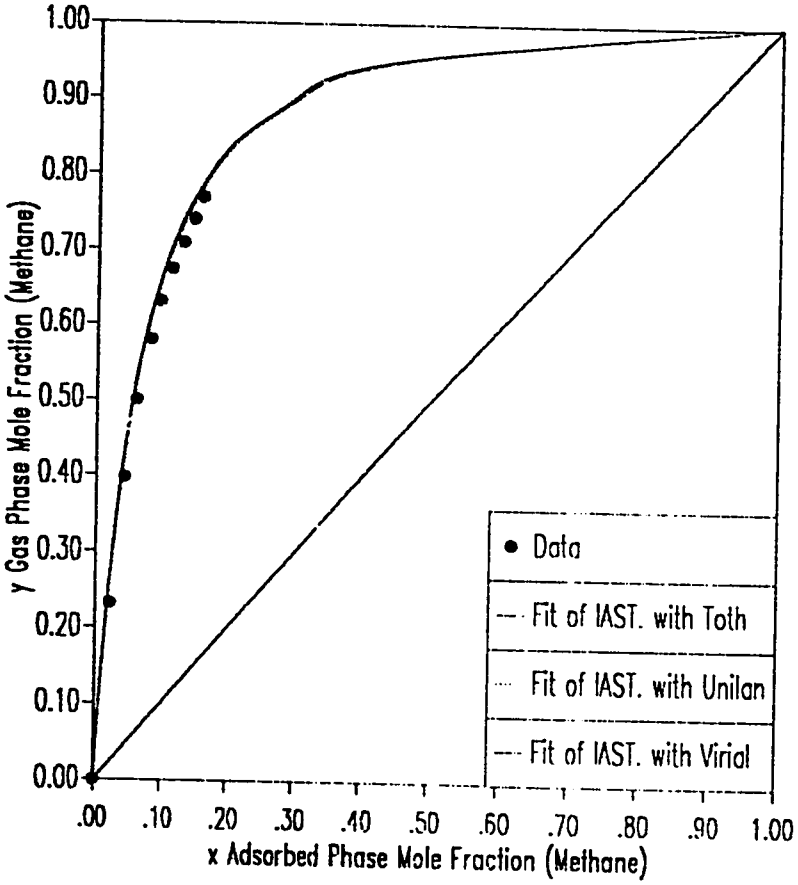

Figure 5.10 x-y Diagram for Methane-Ethylene on SR-115 Zeolite at 300 K and 200 kPa
Fit of IAST Model Using Toth, Unilan and Virial Three Constant Isotherms

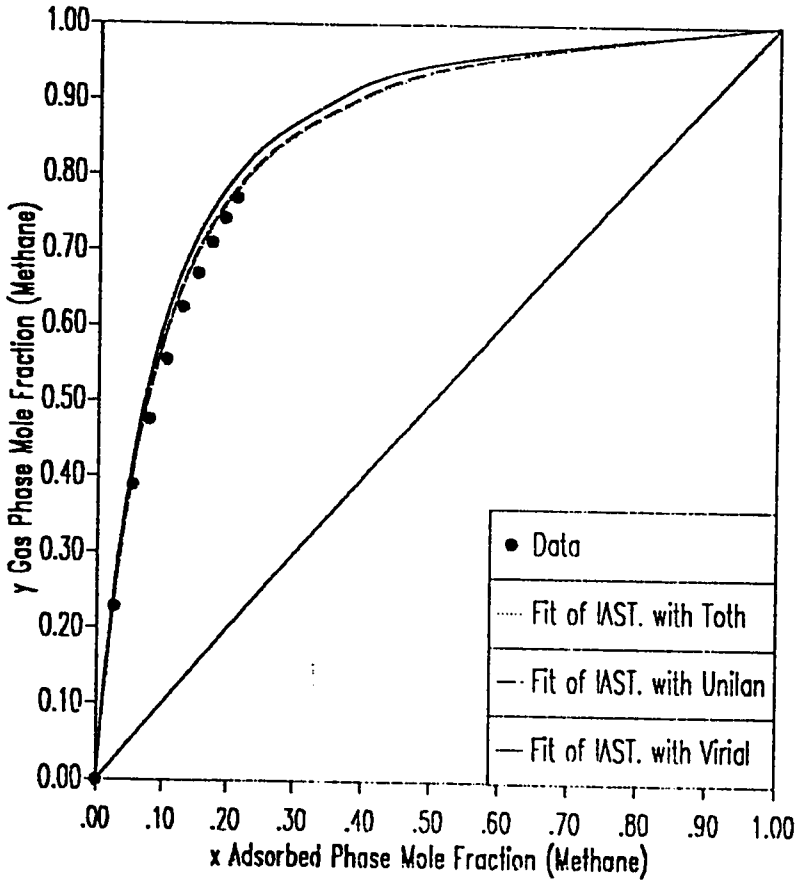

Figure 5.11 x-y Diagram for Methane-Ethylene on SR-115 Zeolite
at 350 K and 200 kPa
Fit of IAST Model Using Toth, Unilan and Virial Three Constant
Isotherms

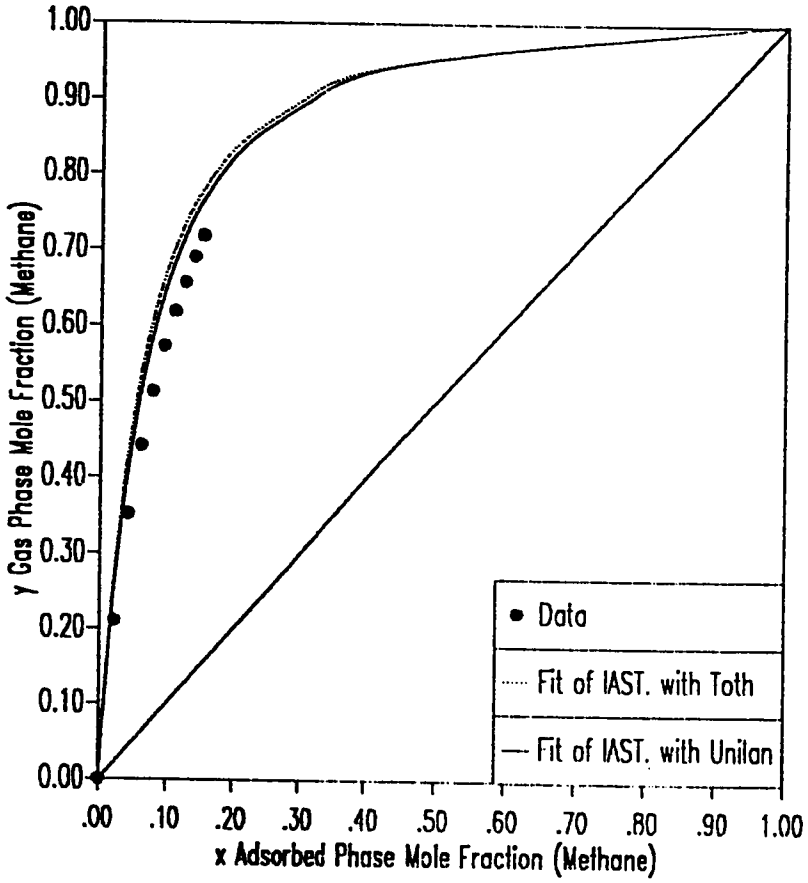

Figure 5.12 x-y Diagram for Methane-Ethylene on SR-115 Zeolite
at 325 K and 150 kPa
Fit of IAST Model Using Toth and Unilan Isotherms

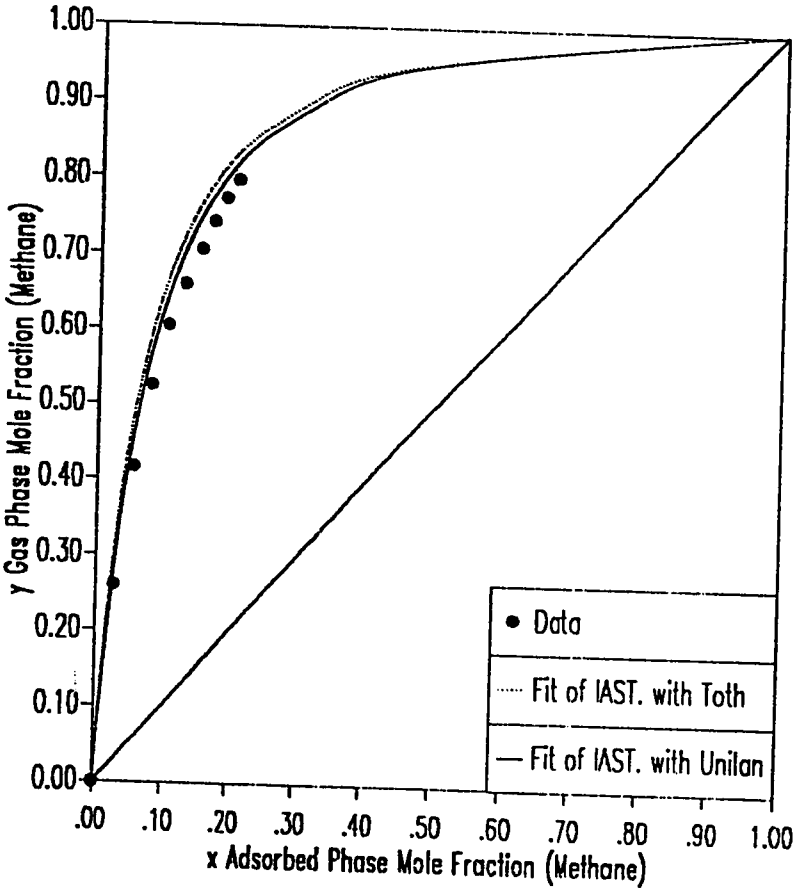

Figure 5.13 x-y Diagram for Methane-Ethylene on SR-115 Zeolite
at 325 K and 250 kPa
Fit of IAST Model Using Toth and Unilan Isotherms

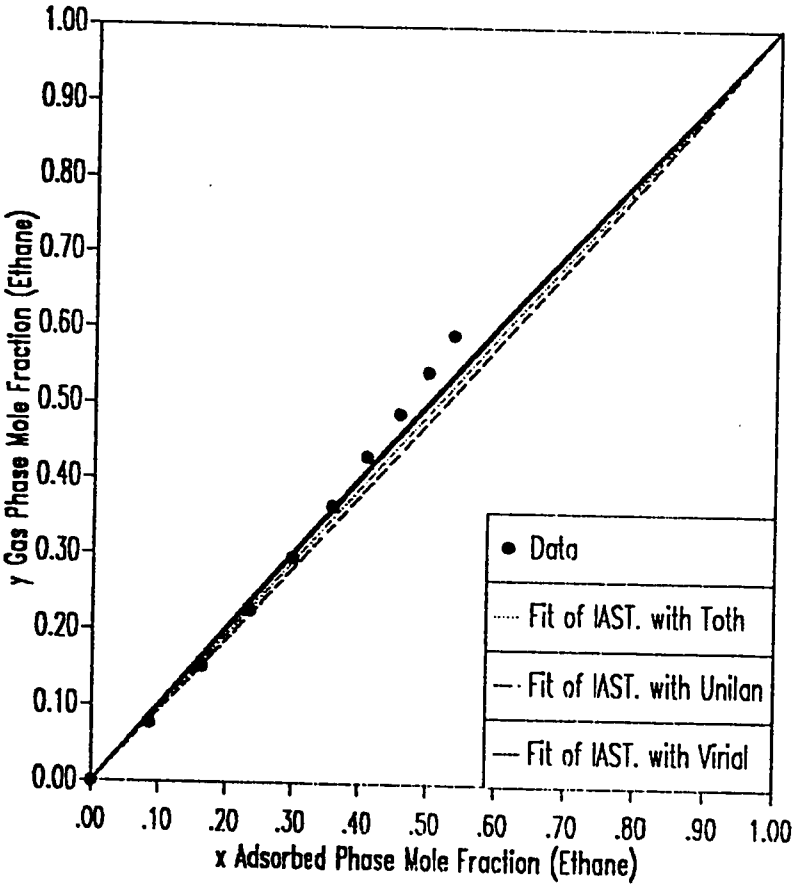

Figure 5.14 x-y Diagram for Ethane-Ethylene on SR-115 Zeolite at 300 K and 200 kPa
Fit of IAST Model Using Toth, Unilan and Virial Three Constant Isotherms

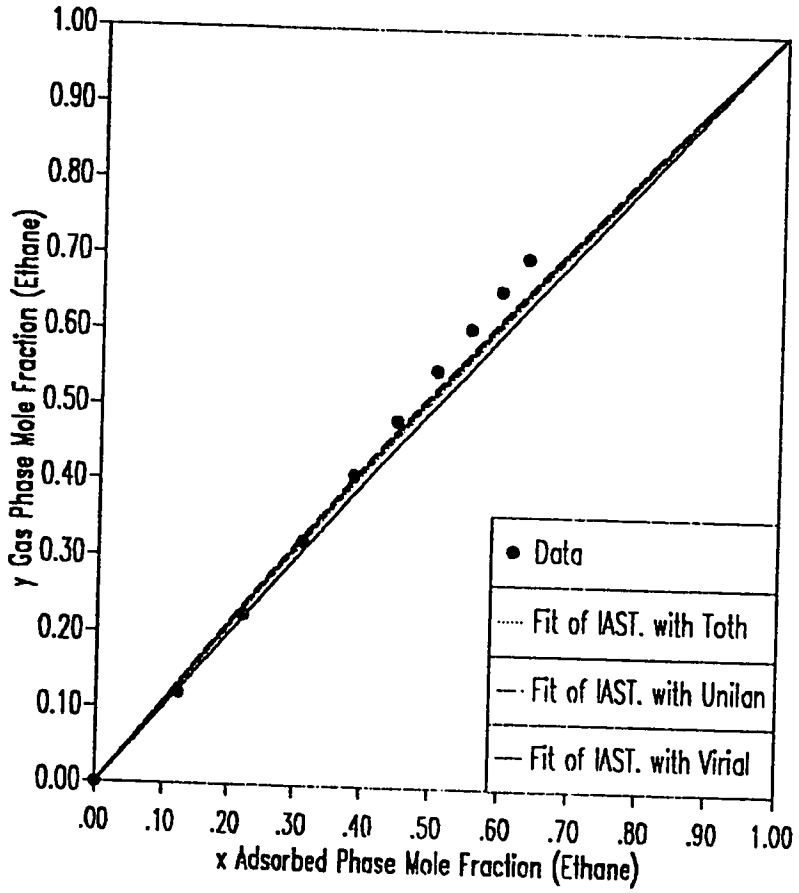

Figure 5.15 x-y Diagram for Ethane-Ethylene on SR-115 Zeolite at 350 K and 200 kPa
Fit of IAST Model Using Toth, Unilan and Virial Three Constant Isotherms

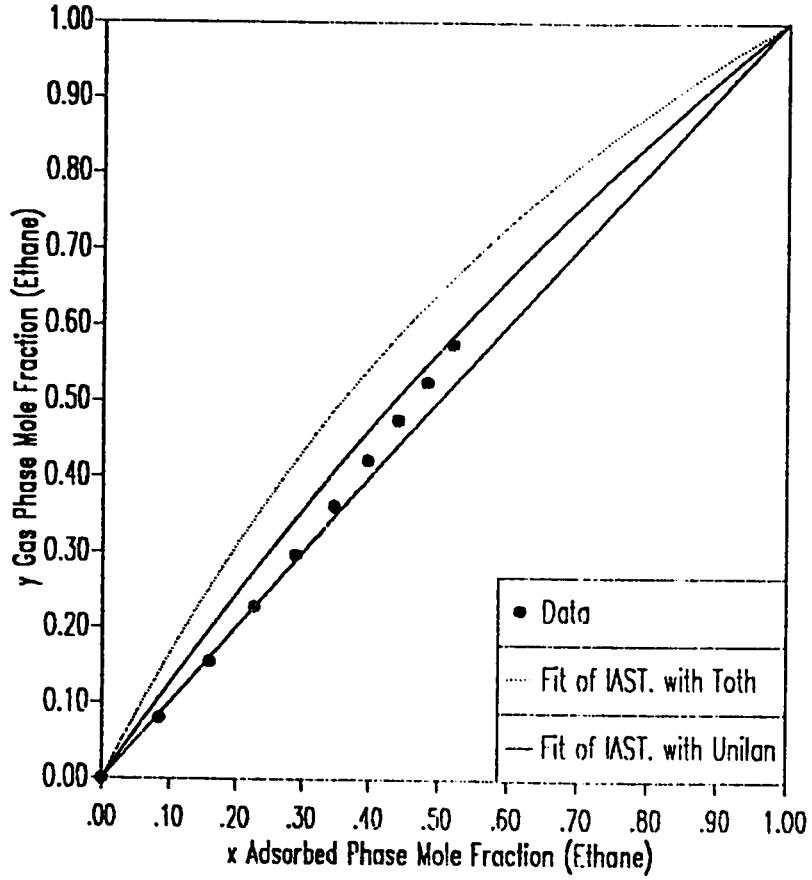

Figure 5.16 x-y Diagram for Ethane-Ethylene on SR-115 Zeolite
at 325 K and 150 kPa
Fit of IAST Model Using Toth and Unilan Isotherms

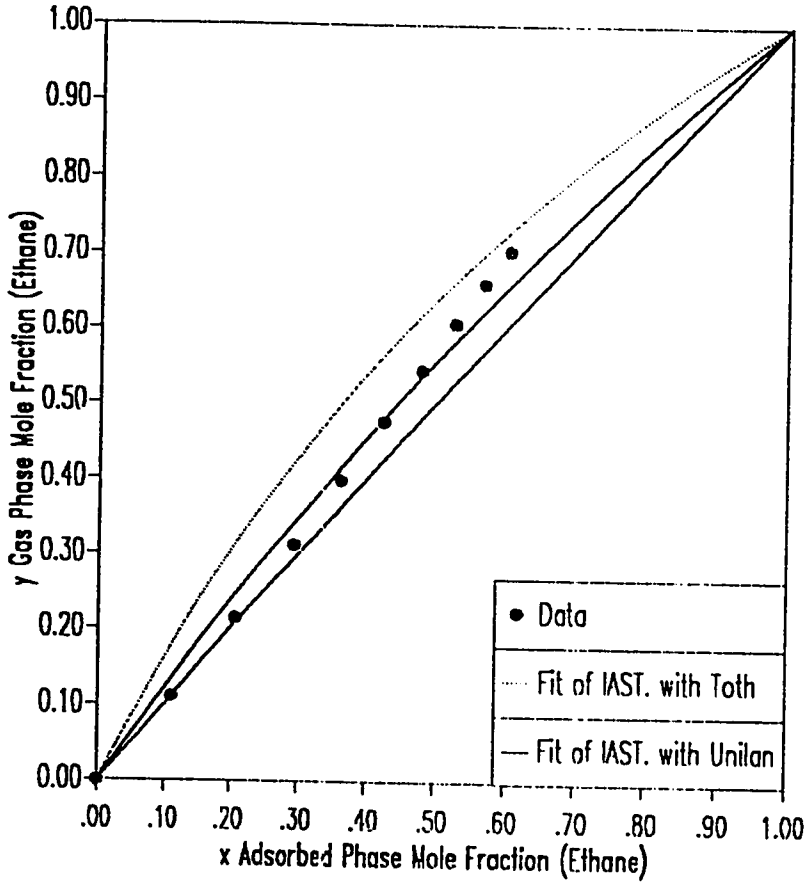

Figure 5.17 x-y Diagram for Ethane-Ethylene on SR-115 Zeolite
at 325 K and 250 kPa
Fit of IAST Model Using Toth and Unilan Isotherms

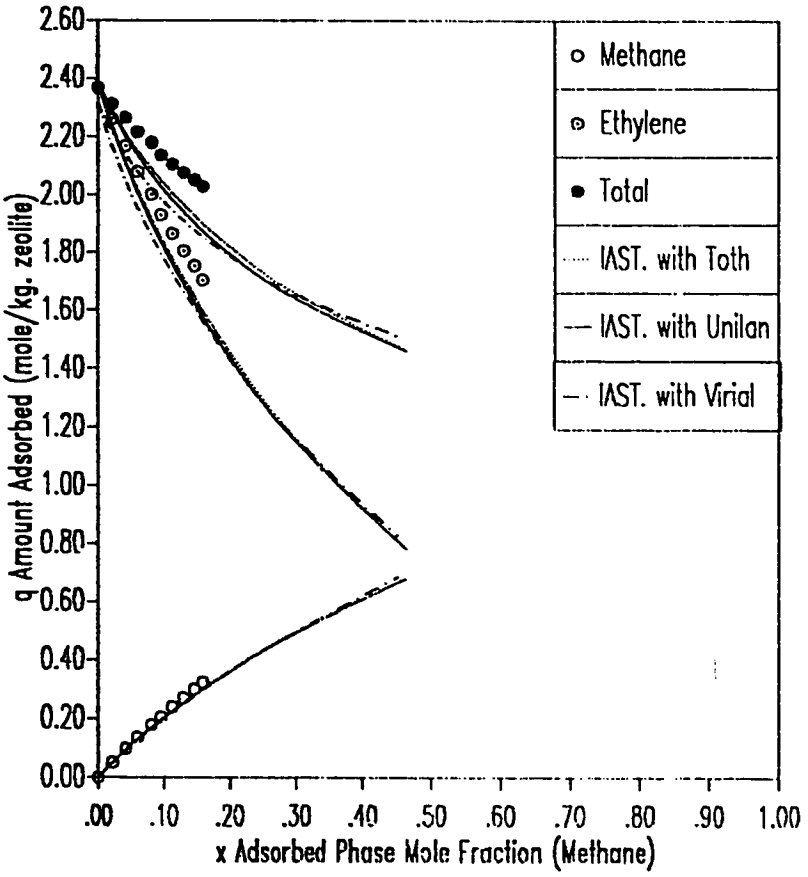

Figure 5.18 x-q Diagram for Methane-Ethylene on SR-115 Zeolite at 300 K and 200 kPa
Fit of IAST Model Using Toth, Unilan and Virial Three Constant Isotherms

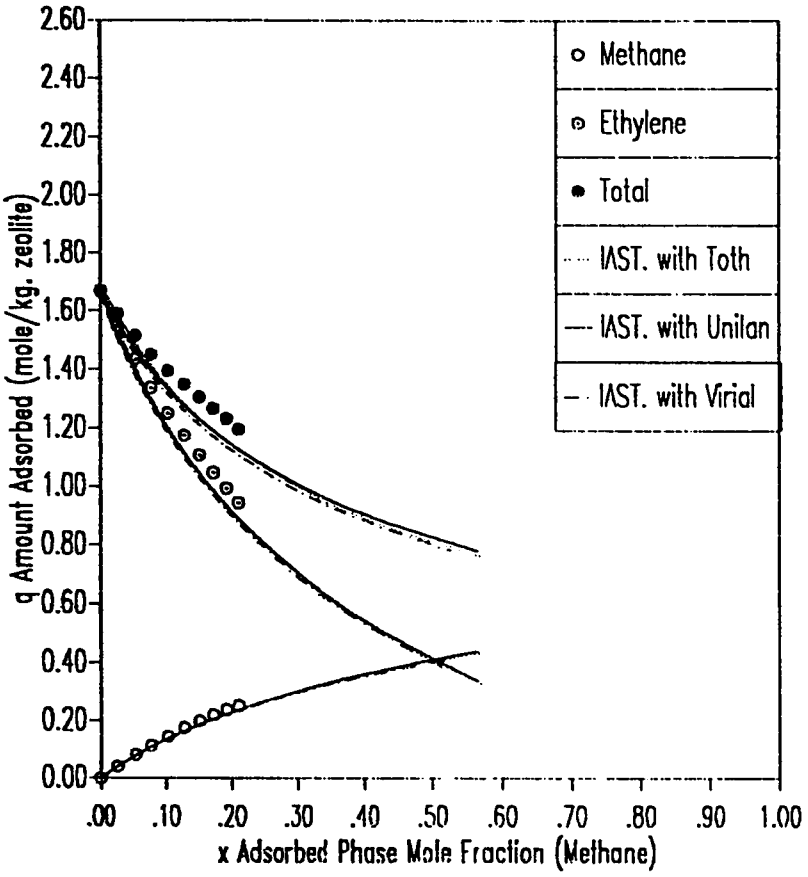

Figure 5.19 x-q Diagram for Methane-Ethylene on SR-115 Zeolite at 350 K and 200 kPa
Fit of IAST Model Using Toth, Unilan and Virial Three Constant Isotherms

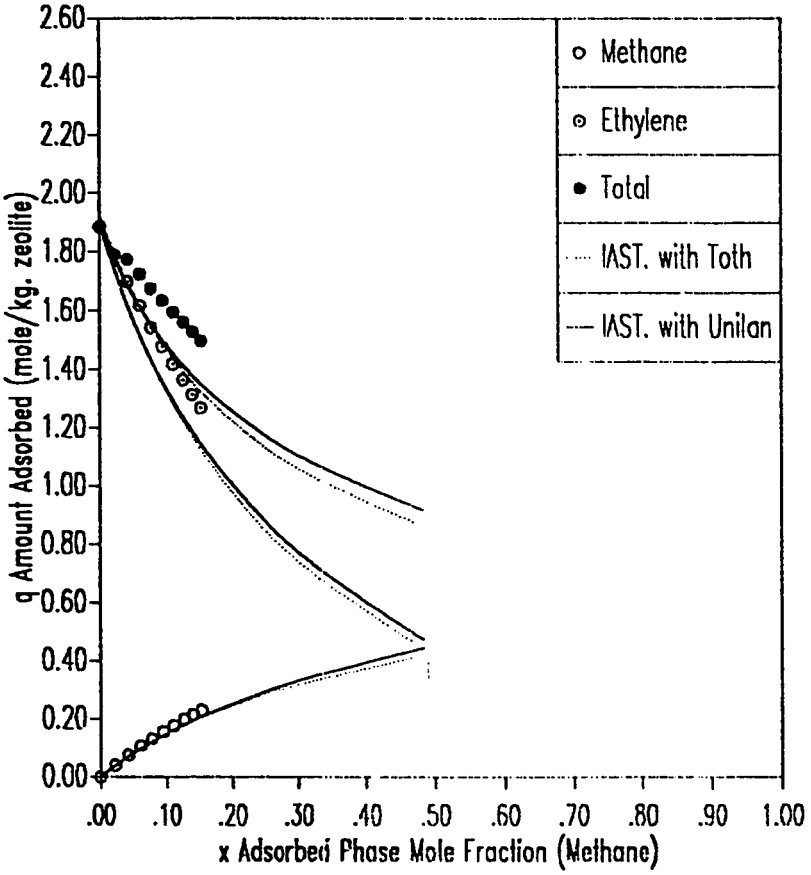

Figure 5.20 x-q Diagram for Methane-Ethylene on SR-115 Zeolite
at 325 K and 150 kPa
Fit of IAST Model Using Toth and Unilan Isotherms

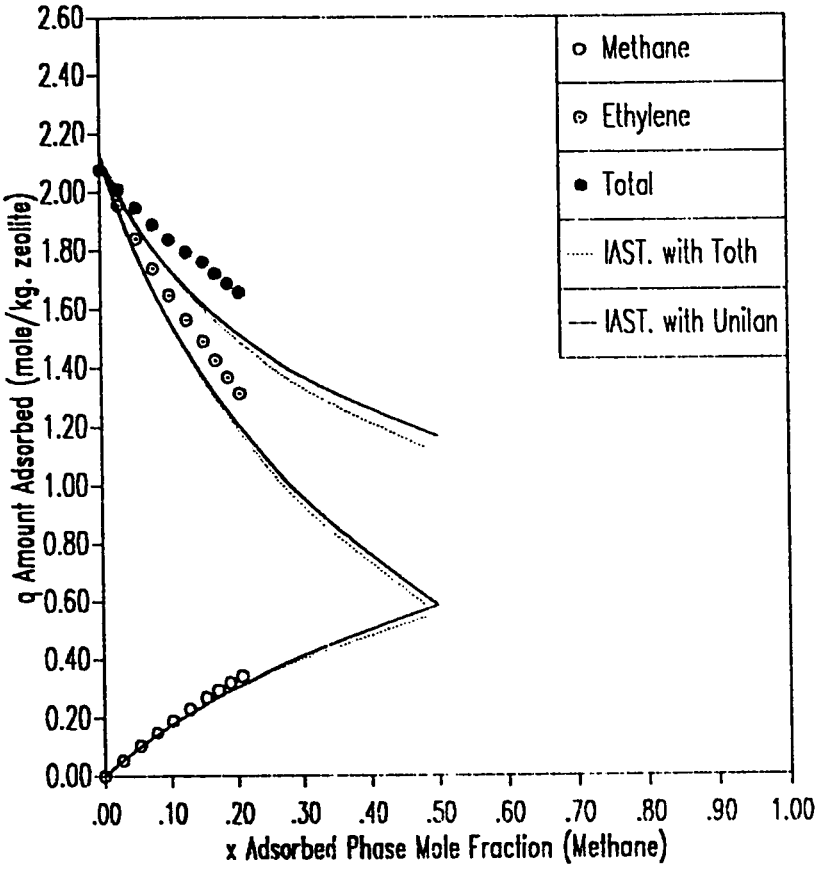

Figure 5.21 x-q Diagram for Methane-Ethylene on SR-115 Zeolite
at 325 K and 250 kPa
Fit of IAST Model Using Toth and Unilan Isotherms

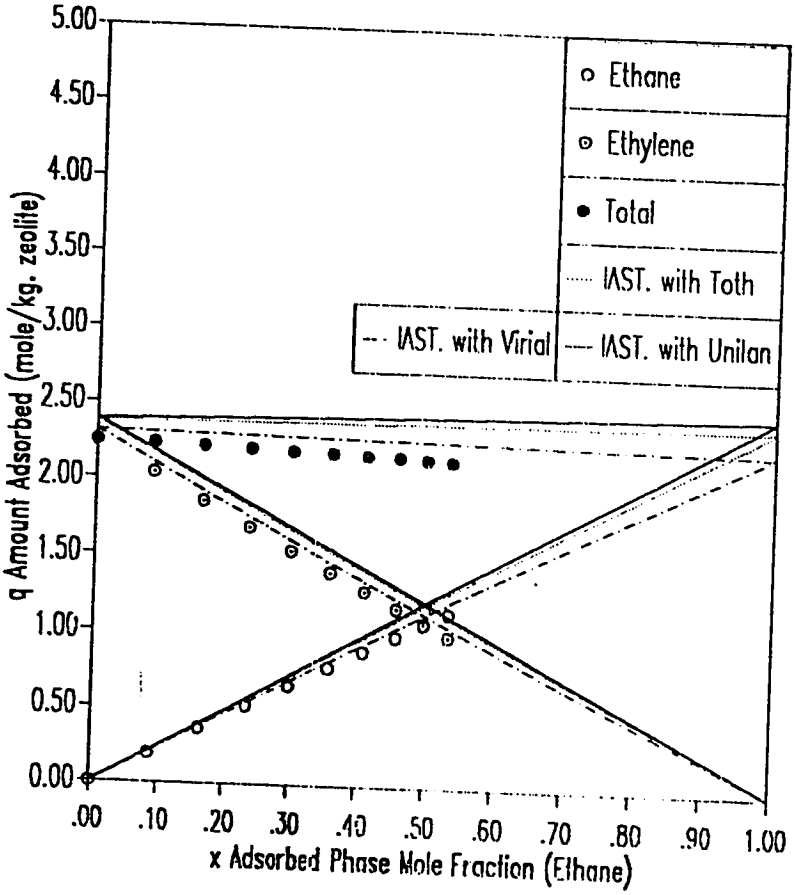

Figure 5.22 x-q Diagram for Ethane-Ethylene on SR-115 Zeolite at 300 K and 200 kPa
Fit of IAST Model Using Toth, Unilan and Virial Three Constant Isotherms

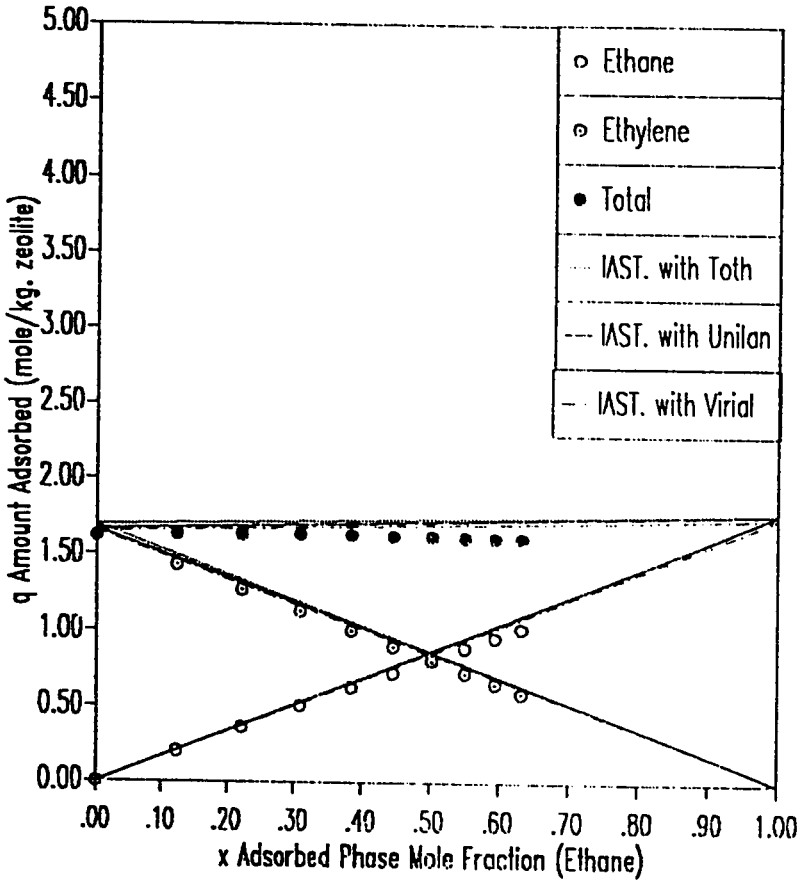

Figure 5.23 x-q Diagram for Ethane-Ethylene on SR-115 Zeolite
at 350 K and 200 kPa
Fit of IAST Model Using Toth, Unilan and Virial Three Constant
Isotherms

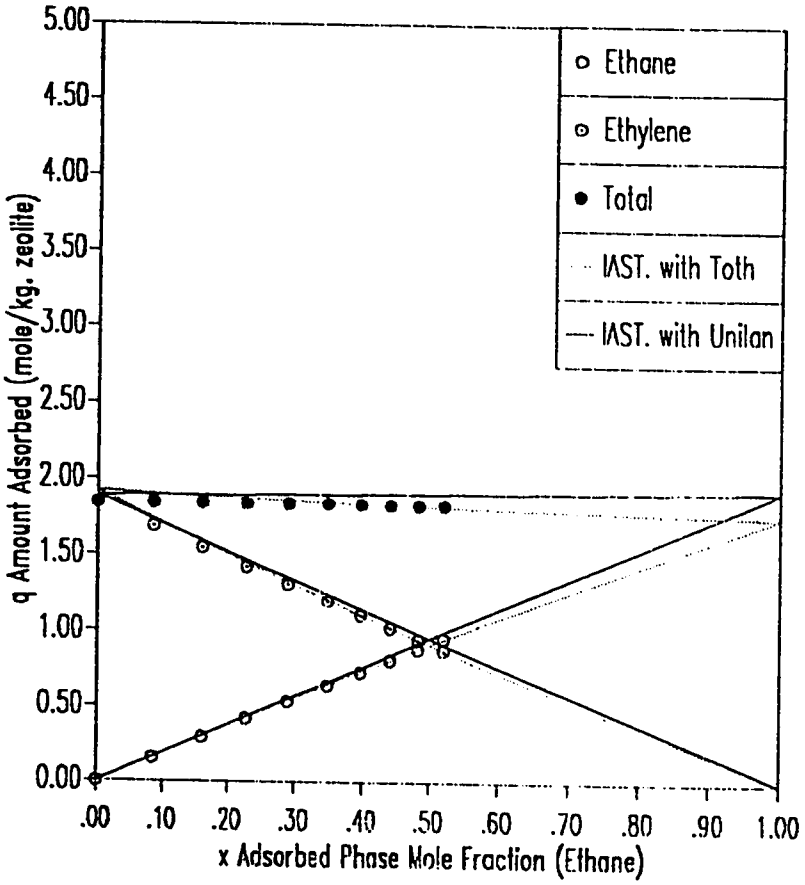

Figure 5.24 x-q Diagram for Ethane-Ethylene on SR-115 Zeolite
at 325 K and 150 kPa
Fit of IAST Model Using Toth and Unilan Isotherms

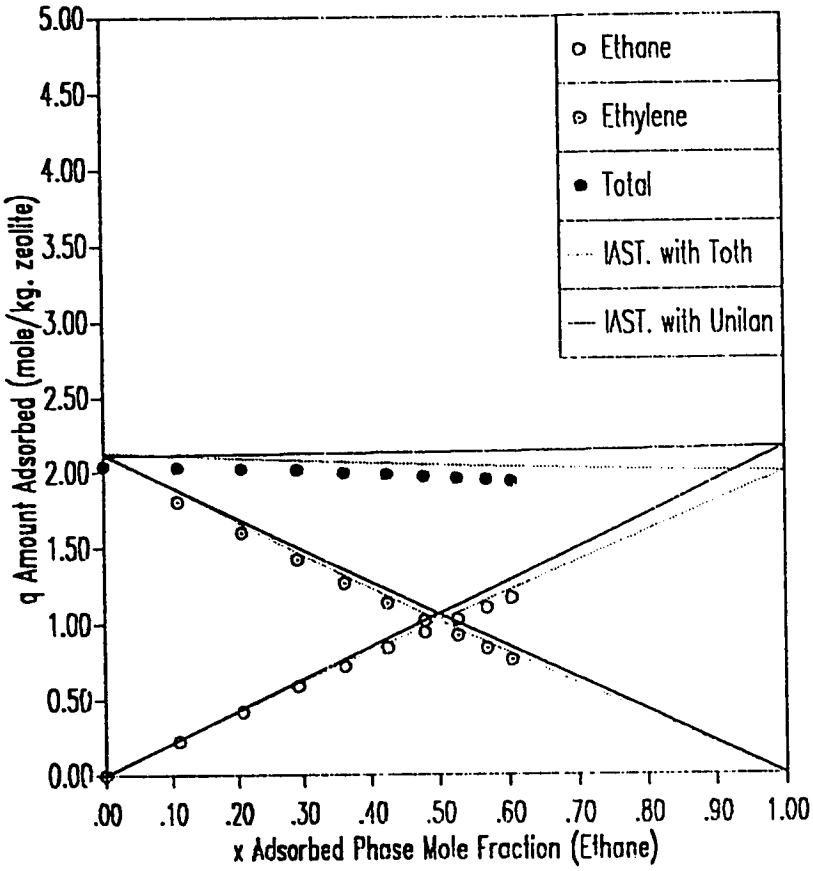

Figure 5.25 x-y Diagram for Ethane-Ethylene on SR-115 Zeolite
at 325 K and 250 kPa
Fit of IAST Model Using Toth and Unilan Isotherms

CHAPTER 6

TERNARY, BINARY AND PURE COMPONENT ADSORPTION OF METHANE, ETHANE AND ETHYLENE ON ETS-10 ZEOLITE

6.1 Introduction

To initiate the research in the area of adsorption of gases on the newly developed zeolite ETS-10, the sorption of methane, ethane and ethylene and their binary and ternary equilibrium mixtures on this type of zeolite have been determined. The ETS-10 powder was extruded using less than 5% lydox solution in the Research Institute of King Fahd University of Petroleum and Minerals.

A complete analysis of the data measured, including the fit of the ten models discussed in Chapter 2, is given in this chapter. Pure component isotherms of methane, ethane and ethylene have been measured up to 1000, 730 and 300 kPa pressure respectively. For each component, five isotherms at 280, 300, 315, 325 and 350 K are determined.

Binary equilibrium data of methane-ethane, methane-ethylene and ethane-ethylene have been measured at 280 and 325 K and pressures of 150, 250 and 500 kPa. The ternary equilibrium data has been gathered at 300 and 325 K at pressure of 200 kPa with different loadings of ethane and ethylene. The binary and ternary data have been modeled using the IAST model with the pure component isotherms of Toth, Unilan and Virial Three Constants. The multicomponent modeling is based on the constrained optimization parameters corresponding to the pure data models. An attempt to model the multicomponent data using Toth multicomponent model was unsuccessful.

6.2 Pure Component Result

The unconstrained optimization parameters for the sorption of methane, ethane and ethylene on ETS-10 zeolite are presented in Tables 6.1, 6.3 and 6.5 respectively. The fits of the ten models used to the methane adsorption data, is excellent with the exception of Freundlich model which shows poor fit as indicated by a very large sum of squares. The fit of the models to the ethylene adsorption data is comparable to the methane's. On the other hand, the fits to the ethane adsorption data is relatively the worst of the three sets. Comparing the total sum of squares error show that Radke-Prausnitz and the virial three constant models are the best. This is expected since the number of constants for each model is four.

Comparing the saturation concentration parameter obtained from the fit of each model to the methane data shows that the values obtained from Toth, Unilan, L.R.C., Langmuir-Freundlich and Mathews-Weber models are too low when compared to the theoretical value calculated from equation 2.8 (2.66 mole/kg). The values obtained from Radke-Prausnitz model are too high at 315, 325 and 350 K and low at 280 and 300 K. However, the values obtained from Volmer model are comparable to the theoretical value. Values of Henry's constant extracted from all models are comparable to the values obtained from the virial three constant model.

The values of the saturation concentration obtained from the fits of Volmer and Radke-Prausnitz models to the ethane adsorption data are too high in comparison to the theoretical value (1.75 mole/kg). However, The values obtained from the remaining models are all very close to the theoretical values.

The x-ray diffraction analysis of the extruded ETS-10 sample showed that the amount of non crystalline material is negligible. This conclusion was also

supported by the experimental values of q_s obtained for methane, ethane and ethylene which were very close to the theoretical values calculated for pure ETS-10 zeolite using equation 2.8.

Henry's constant values calculated from the Radke-Prausnitz and the Volmer models are comparable to the values obtained from the virial three constant model. The values obtained from Mathews-Weber are too low, while the values obtained from the remaining models are too high relative to virial's.

For ethylene adsorption data, the values of q_s obtained from all models except Unilan are reasonable in comparison with the theoretical value (2.00 mole/kg). The values obtained from the Unilan model are almost two times the theoretical value. The values of Henry's constant extracted from all models except the Mathews-Weber are too high when compared to the values calculated from the virial three constant model (Toth and Unilan values are at least thirty times the virial's). The values given by the Mathews-Weber model are too low.

In the constrained regression, the saturation concentration for methane, ethane and ethylene have been fixed at 2.66, 1.75 and 2.00 mole per kg of ETS-10 respectively. These values correspond to 95% of the theoretical values calculated from equation 2.8 . Other model parameters which exhibit no trend in the unconstrained regression have been optimized between the minimum and maximum values obtained from the unconstrained regression corresponding to each parameter till a minimum sum of squares error is reached. The constrained regression results are given in Tables 6.2, 6.4 and 6.6 for methane, ethane and ethylene respectively.

As a result of constraining the model parameters, the total sum of squares error obtained from each model increases. However, the values of K_H become more consistent.

The vant Hoff equation parameters for the sorption of methane, ethane and ethylene on ETS-10 zeolite are given in Table 6.7. The isosteric heat of adsorption parameters calculated for methane data using all models except the Radke-Prausnitz are consistent at approximately 21 kJ/mole. Values of K_0 determined from the Radke-Prausnitz, the Mathews-Weber and the Volmer models are too low when compared to the value obtained from the virial model. The corresponding K_0 values obtained from Toth and Unilan models are consistent with those of the virial model.

The value of heat of adsorption of Toth and Unilan models for ethane data are comparable to virial's. However, the values obtained by other models differ. Only the pre exponential factor for the Toth model approaches the value obtained for the virial three constant model.

The vant Hoff parameters obtained by all models for ethylene data deviate significantly from the values extracted for the virial three constant model. This is of course attributed to the large deviation of Henry's constant values.

Plots of the isotherms of methane, ethane and ethylene data on ETS-10 zeolite have been constructed together with the fit of Toth, Unilan and virial three constant models using the constrained parameters. The plots are shown in Figures 6.1 to 6.9.

6.3 Binary Adsorption of Methane and Ethane

Four different experiments were carried out to examine the adsorption behavior of the binary system methane-ethane on ETS-10 zeolite. The first two runs were performed at 280 K and at a pressure of 150 kPa for the first run and 500 kPa for the second. Data for the third and fourth runs were gathered at 325 K and at pressures of 150 kPa and 500 kPa. The experimental data are all symmetrical and consistent. In addition, an excellent fit has been

obtained using the IAST model with Toth, Unilan and virial three constant isotherms for the four runs. Comparison between the experimental and the theoretical values are given in Table 6.8 (x-y values) and Tables 6.12 to 6.15 (x-q values). Plots of the adsorbed phase mole fraction of methane versus the gas phase mole fraction of methane are shown in Figures 6.10 to 6.13. These plots indicate that the IAST-virial combination is the best among the models used. In addition, the three models conform with the experimental data that the separation of methane from ethane on ETS-10 is possible at any conditions and it is best at low temperature and pressure. The x-q fit of the three models to this system is given in Figures 6.22 to 6.25. Comparing the results obtained for this system on ETS-10 to those obtained by Bin Abdul Rehman on 5A, 13X and SR-115 zeolites (1) show that the separation of methane from ethane is much better on ETS-10 zeolite. The relative adsorptivity values for this system are listed in Table 6.11. These values are calculated using equation 4.4 at approximately 50% gas phase mole fraction of methane. The experimental values are comparable to the theoretical ones especially at high temperature. These relatively large values of separation factor indicates that the separation of methane from ethane is feasible on ETS-10 especially at low temperatures and pressures.

6.4 Binary Adsorption of Methane and Ethylene

This system has been examined at four different conditions, namely, 280 K-150 kPa, 280 K-250 kPa, 325 K-150 kPa and 325 K-250 kPa. Comparison between the experimental and the theoretical values are given in Table 6.9 (x-y values) and Tables 6.16 to 6.19 (x-q values). The x-y fit is given in Figures 6.14 to 6.17 while the x-q fit is given in Figures 6.26 to 6.29 for the four runs. The results obtained indicate that methane is very weakly adsorbed in the

presence of ethylene and therefore, the separation can be achieved very easily at any conditions but it is best at low temperature and pressure. This conclusion is also supported by the values of relative adsorptivity listed for this system in Table 6.11. The fit of the IAST model using the three isotherms is not as good as the fit to the data of the binary system methane-ethane.

6.5 Binary Adsorption of Ethane and Ethylene

Four experiments at the same conditions of the binary system methane-ethylene were carried out for this system. The results are shown in Tables 6.10, 6.20 to 6.23 and Figures 6.18 to 6.21 and 6.30 to 6.33. The results show that ethane adsorption on ETS-10 is weak in the presence of ethylene which indicates that ETS-10 is an appropriate adsorbent for the separation of ethane from ethylene. This conclusion is supported by the three models used to fit the experimental data for this system (IAST-Toth, IAST-Unilan and IAST-Virial).

Fits of IAST-Toth, IAST-Unilan and IAST-virial models to the data are reasonable for the four cases. However, IAST-virial fit is a little better. Comparing the x-y plots show that the pressure has negligible effect on the separation but lower temperatures give better separation.

Values of the relative adsorptivity for this system are listed in Table 6.11. Comparing these values with the values obtained for ethane-ethylene on SR-115 zeolite (Table 5.8) shows that ETS-10 zeolite adsorbs ethylene much more strongly in the presence of ethane while, the adsorption of these components on SR-115 zeolite is almost equal. Therefore, the separation is much easier on the ETS-10 adsorbent.

6.6 Adsorption of the Ternary Mixture Methane-Ethane-Ethylene

The adsorption behavior of this system on ETS-10 has been examined in four experiments at two different temperatures : 280 and 325 K and pressure of 200 kPa at different loading of ethylene and ethane. The data obtained are compared to the fit of IAST-Toth, IAST-Unilan and IAST-Virial models at the same conditions. The results are tabulated as x-y comparison in Tables 6.24 to 6.27 and x-q comparison in Tables 6.28 to 6.31. The results obtained from the three models are comparable to the data. Considering the amount adsorbed at different loading show that the concentration of ethane in the adsorbed phase is almost constant at low loading of ethane which suggests that methane molecules replace only ethylene molecules in the adsorbed phase as the partial pressure of methane increases. This conclusion is supported by the three models.

6.7 Literature Cited

1) Bin Abdul Rehman, H., Equilibrium Adsorption of Light Alkanes and Their Mixtures on 5A, 13X and SR-115, M.S. Thesis, KFUPM, Dhahran, 1988.

Table 6.1 Unconstrained Optimization Parameters for The Sorption of Methane on ETS-10 Zeolite

Toth Model

T(K)	280	300	315	325	350
ss	0.0019	0.0076	0.0059	0.0617	0.0513
q_s	1.991	2.180	1.883	1.800	2.044
b	23.71	21.70	61.36	89.14	74.25
t	0.794	0.699	0.808	0.853	0.750
K_H	0.0369	0.0267	0.0115	0.0093	0.0065

$\sum ss = 0.1284$

Unilan Model

T(K)	280	300	315	325	350
ss	0.0016	0.0129	0.0043	0.0858	0.0542
q_s	1.936	2.076	1.833	1.800	2.930
c	74.76	140.40	219.24	245.28	1366.25
s	1.384	1.786	1.311	1.280	2.794
K_H	0.0350	0.0240	0.0110	0.0095	0.0063

$\sum ss = 0.1587$

Radke-Prausnitz Model

T(K)	280	300	315	325	350
ss	0.0009	0.101	0.0031	0.0442	0.0512
q_s	2.189	2.370	2.925	3.188	3.101
b_{RP}	0.0161	0.0111	0.0038	0.0028	0.0020
c_{RP}	0.532	0.179	0.377	0.552	0.178
n_{RP}	0.346	0.436	0.184	0.090	0.261
K_H	0.0353	0.0263	0.0184	0.0088	0.0063

$\sum ss = 0.1093$

Mathews-Weber Model

T(K)	280	300	315	325	350
ss	0.0292	0.1013	0.0215	0.0203	0.0085
q_s	1.800	1.800	1.800	1.800	1.800
b_{MW}	0.0160	0.0102	0.0051	0.0043	0.0029
n_{MW}	0.981	0.968	1.023	1.045	1.082
K_H	0.0287	0.0184	0.0091	0.0077	0.0052

$\sum ss = 0.2573$

Volmer Model

T(K)	280	300	315	325	350
ss	0.0029	0.0421	0.0023	0.0740	0.0559
q_s	2.730	2.854	2.682	2.612	2.712
K_H	0.0349	0.0208	0.0107	0.0094	0.0057

$\sum ss = 0.1772$

Virial Two Constant Model

T(K)	280	300	315	325	350
ss	0.0151	0.0581	0.0037	0.0104	0.0536
A_1	0.000	0.270	0.209	0.053	0.955
A_2	0.839	0.622	0.713	0.835	0.157
K_H	0.0296	0.0192	0.0093	0.0076	0.0062

$\sum ss = 0.1409$

Virial Three Constant Model

T(K)	280	300	315	325	350
ss	0.0179	0.0186	0.0010	0.0225	0.0534
A_1	0.471	0.892	0.511	0.466	0.868
A_2	0.000	0.000	0.322	0.301	0.237
A_3	0.334	0.191	0.148	0.203	0.000
K_H	0.0291	0.0231	0.0099	0.0082	0.0061

$\sum ss = 0.1134$

Freundlich Model

T(K)	280	300	315	325	350
ss	2.0534	2.5241	2.1370	5.3088	1.0347
k_F	0.131	0.129	0.082	0.074	0.027
n_F	0.406	0.394	0.420	0.436	0.590

$\sum ss = 13.0580$

Langmuir-Freundlich Model

T(K)	280	300	315	325	350
ss	0.0151	0.0073	0.0128	0.0782	0.0486
q_s	1.9431	2.062	1.800	1.800	1.800
k_{LF}	0.0218	0.0161	0.0076	0.0059	0.0044
n_{LF}	0.884	0.834	0.913	0.927	0.911

$\sum ss = 0.1619$

Loading Ratio Correlation Model

T(K)	280	300	315	325	350
ss	0.0039	0.0079	0.0123	0.1649	0.0487
q_s	1.908	2.062	1.800	1.800	1.800
k_{LRC}	0.0139	0.0071	0.0048	0.0045	0.0026
n_{LRC}	1.094	1.199	1.091	1.064	1.097

$\sum ss = 0.2448$

Units of the Parameters are given in Table 4.1.

Table 6.2 Constrained Optimization Parameters for The Sorption of Methane on ETS-10 Zeolite

Toth Model

T(K)	280	300	315	325	350
ss	0.0803	0.0227	0.0368	0.1553	0.0699
b	10.92	13.30	20.63	22.99	29.34
K_H	0.0431	0.0307	0.0144	0.0119	0.0078

$\Sigma ss = 0.3651$

t is constrained at 0.580

Unilan Model

T(K)	280	300	315	325	350
ss	0.0898	0.0331	0.0175	0.0899	0.0569
c	207.27	291.60	625.95	748.05	1114.32
K_H	0.0341	0.0242	0.0113	0.0094	0.0063

$\Sigma ss = 0.2872$

s is constrained at 2.650

Radke-Prausnitz Model

T(K)	280	300	315	325	350
ss	0.1336	0.0650	0.0552	0.2293	0.0555
b_{RP}	0.0284	0.0286	0.0070	0.0067	0.0035
c_{RP}	0.0393	0.0295	0.0226	0.0193	0.0183
K_H	0.0756	0.0761	0.0186	0.0179	0.0093

$\Sigma ss = 0.5386$

n_{RP} is constrained at 0.640

Mathews-Weber Model

T(K)	280	300	315	325	350
ss	0.2949	0.3873	0.3886	0.3846	0.2944
b_{MW}	0.0081	0.0051	0.0025	0.0021	0.0015
K_H	0.0216	0.0134	0.0066	0.0055	0.0041

$\Sigma ss = 1.7496$

n_{MW} is constrained at 1.23

Volmer Model

T(K)	280	300	315	325	350
ss	0.0114	0.0760	0.0025	0.0901	0.0555
K_H	0.0356	0.0213	0.0106	0.0096	0.0058

$\Sigma ss = 0.2355$

123

Virial Two Constant Model

T(K)	280	300	315	325	350
ss	0.0153	0.0364	0.0016	0.0493	0.0658
A_2	0.632	0.553	0.593	0.656	0.533
K_H	0.0343	0.0209	0.0101	0.0086	0.0053

$\sum ss = 0.1684$

A_1 is constrained at 0.450

Virial Three Constant Model

T(K)	280	300	315	325	350
ss	0.0095	0.0477	0.0007	0.0275	0.0569
A_2	0.000	0.225	0.283	0.195	0.519
A_3	0.316	0.142	0.159	0.259	0.000
K_H	0.0306	0.0203	0.0100	0.0083	0.0057

$\sum ss = 0.1423$

A_1 is constrained at 0.550

Langmuir-Freundlich Model

T(K)	280	300	315	325	350
ss	0.2581	0.1184	0.1018	0.3178	0.2000
k_{LF}	0.0164	0.0123	0.0073	0.0064	0.0050

$\sum ss = 0.9961$

n_{LF} is constrained at 0.780

Loading Ratio Correlation Model

T(K)	280	300	315	325	350
ss	0.2738	0.1421	0.0961	0.2350	0.1304
k_{LRC}	0.0049	0.0035	0.0018	0.0015	0.0011

$\sum ss = 0.8774$

n_{LRC} is constrained at 1.260

Units of the parameters are given in Table 4.1.
All models requiring q_s have been constrained at 2.66 mol/kg of zeolite.
Freundlich parameters have not been constrained.

Table 6.3 Unconstrained Optimization Parameters for The Sorption of Ethane on ETS-10 Zeolite

Toth Model

T(K)	280	300	315	325	350
ss	0.0062	0.0653	0.0618	0.0604	0.3036
q_s	1.775	1.750	1.750	1.750	1.750
b	0.534	1.110	1.602	2.140	4.254
t	0.534	0.556	0.559	0.574	0.677
K_H	5.755	1.451	0.754	0.465	0.206

$\sum ss = 0.3973$

Unilan Model

T(K)	280	300	315	325	350
ss	0.0229	0.2571	0.2766	0.2780	0.1431
q_s	1.750	1.750	1.750	1.750	1.750
c	1.382	4.444	8.759	12.502	27.432
s	3.415	3.328	3.399	3.222	3.168
K_H	5.632	1.648	0.879	0.544	0.239

$\sum ss = 0.9778$

Radke-Prausnitz Model

T(K)	280	300	315	325	350
ss	0.0010	0.0049	0.0049	0.0023	0.0032
q_s	1.987	2.546	2.415	2.364	1.850
b_{RP}	1.213	0.300	0.177	0.121	0.083
c_{RP}	1.544	0.867	0.817	0.847	0.728
n_{RP}	0.234	0.107	0.132	0.124	0.278
K_H	2.410	0.765	0.428	0.286	0.153

$\sum ss = 0.0161$

Mathews-Weber Model

T(K)	280	300	315	325	350
ss	0.1229	0.2742	0.1549	0.1738	0.2793
q_s	1.750	1.750	1.750	1.750	1.750
b_{MW}	0.710	0.308	0.151	0.105	0.053
n_{MW}	1.010	1.010	1.030	1.030	1.040
K_H	1.243	0.538	0.265	0.184	0.092

$\sum ss = 1.0051$

Volmer Model

T(K)	280	300	315	325	350
ss	0.0017	0.0183	0.0141	0.0109	0.0040
q_s	2.080	1.983	2.005	1.995	2.017
K_H	2.473	0.823	0.455	0.297	0.147

$\sum ss = 0.0490$

Virial Two Constant Model

T(K)	280	300	315	325	350
ss	0.0870	0.1538	0.0922	0.0796	0.0272
A_1	0.000	0.052	0.000	0.000	0.000
A_2	2.272	2.147	2.030	1.971	1.756
K_H	4.143	0.916	0.452	0.289	0.134

$\sum ss = 0.4398$

Virial Three Constant Model

T(K)	280	300	315	325	350
ss	0.0509	0.0098	0.0099	0.0169	0.0295
A_1	0.000	0.000	0.000	0.024	0.478
A_2	1.296	0.000	0.139	0.000	0.062
A_3	0.476	1.230	1.087	1.167	0.906
K_H	2.678	0.571	0.309	0.206	0.119

$\sum ss = 0.1171$

Freundlich Model

T(K)	280	300	315	325	350
ss	0.4047	2.7875	3.1230	4.0364	4.3374
k_F	0.963	0.669	0.545	0.498	0.354
n_F	0.100	0.140	0.175	0.187	0.228

$\sum ss = 14.6890$

Langmuir-Freundlich Model

T(K)	280	300	315	325	350
ss	0.0095	0.1103	0.1962	0.1887	0.0852
q_s	1.756	1.750	1.750	1.750	1.750
k_{LF}	0.824	0.324	0.246	0.181	0.096
n_{LF}	0.611	0.676	0.626	0.647	0.693

$\sum ss = 0.5900$

Loading Ratio Correlation Model

T(K)	280	300	315	325	350
ss	0.0094	0.1294	0.2800	0.3457	0.1694
q_s	1.753	1.750	1.750	1.750	1.750
k_{LRC}	0.733	0.213	0.137	0.092	0.044
n_{LRC}	1.628	1.471	1.501	1.512	1.382

$\sum ss = 0.9339$

Units of the Parameters are given in Table 4.1.

Table 6.4 Constrained Optimization Parameters for The Sorption of Ethane on ETS-10 Zeolite

Toth Model

T(K)	280	300	315	325	350
ss	0.0060	0.0618	0.0541	0.0573	0.0236
b	0.571	1.169	1.733	2.172	3.207
K_H	4.681	1.331	0.667	0.449	0.227

$\sum ss = 0.2028$

t is constrained at 0.570

Unilan Model

T(K)	280	300	315	325	350
ss	0.0228	0.1584	0.4282	0.1881	0.1737
c	1.368	5.181	7.205	14.140	27.641
K_H	5.068	1.338	0.962	0.490	0.251

$\sum ss = 0.9712$

s is constrained at 3.25

Radke-Prausnitz Model

T(K)	280	300	315	325	350
ss	0.0213	0.0062	0.0065	0.0055	0.0057
b_{RP}	1.166	0.451	0.254	0.175	0.086
c_{RP}	2.852	1.509	1.186	1.054	0.765
K_H	2.040	0.789	0.444	0.306	0.151

$\sum ss = 0.0454$

n_{RP} is constrained at 0.31

Mathews-Weber Model

T(K)	280	300	315	325	350
ss	0.1930	0.1402	0.1577	0.2289	0.3718
b_{MW}	0.778	0.305	0.178	0.121	0.060
K_H	1.362	0.534	0.311	0.211	0.104

$\sum ss = 1.0916$

n_{MW} is constrained at 1.010

Volmer Model

T(K)	280	300	315	325	350
ss	0.4998	0.3082	0.3235	0.2557	0.1948
K_H	5.584	1.031	0.544	0.364	0.173

$\sum ss = 1.5819$

Virial Two Constant Model

T(K)	280	300	315	325	350
ss	0.0828	0.1450	0.0864	0.0848	0.0254
A_2	2.235	2.190	2.031	1.953	1.717
K_H	3.892	0.865	0.440	0.299	0.132

$\sum ss = 0.4242$

A_1 is constrained at 0.0010

Virial Three Constant Model

T(K)	280	300	315	325	350
ss	0.0266	0.0217	0.0098	0.0106	0.0279
A_2	0.000	0.000	0.000	0.000	0.099
A_3	1.040	1.095	1.040	1.032	0.881
K_H	2.218	0.691	0.379	0.256	0.120

$\sum ss = 0.0966$

A_1 is constrained at 0.480

Langmuir-Freundlich Model

T(K)	280	300	315	325	350
ss	0.0129	0.1131	0.1282	0.1435	0.1080
k_{LF}	0.793	0.330	0.218	0.168	0.102

$\sum ss = 0.5058$

n_{LF} is constrained at 0.680

Loading Ratio Correlation Model

T(K)	280	300	315	325	350
ss	0.0207	0.1173	0.1237	0.1250	0.0938
k_{LRC}	0.710	0.201	0.106	0.071	0.037

$\sum ss = 0.4808$

n_{LRC} is constrained at 1.40

Units of the parameters are given in Table 4.1.

All models requiring q_s have been constrained at 1.75 mol/kg of zeolite.

Freundlich parameters have not been constrained.

Table 6.5 Unconstrained Optimization Parameters for The Sorption of Ethylene on ETS-10 Zeolite

Toth Model

T(K)	280	300	315	325	350
ss	0.0121	0.0054	0.0104	0.0185	0.1237
q_s	2.597	2.123	2.000	2.000	2.000
b	0.146	0.245	0.349	0.468	1.017
t	0.189	0.328	0.380	0.403	0.464
K_H	687.78	154.46	31.934	13.201	19.275

$\Sigma ss = 0.1702$

Unilan Model

T(K)	280	300	315	325	350
ss	0.0334	0.0498	0.0909	0.1146	0.3534
q_s	4.058	3.961	3.946	3.917	3.883
c	272.32	337.80	508.57	535.45	714.14
s	14.93	12.78	11.75	10.58	8.55
K_H	1526.3	163.30	41.85	13.66	16.37

$\Sigma ss = 0.6421$

Mathews-Weber Model

T(K)	280	300	315	325	350
ss	0.2712	0.3394	0.4130	0.3596	0.4320
q_s	2.000	2.000	2.000	2.000	2.000
b_{MW}	2.426	1.327	0.789	0.541	0.175
n_{MW}	1.000	1.020	1.030	1.030	1.030
K_H	4.852	2.655	1.579	1.082	0.350

$\Sigma ss = 1.8152$

Volmer Model

T(K)	280	300	315	325	350
ss	0.0198	0.0220	0.0201	0.0101	0.0092
q_s	2.298	2.224	2.156	2.154	2.128
K_H	11.152	6.218	3.529	2.152	0.711

$\Sigma ss = 0.0812$

Virial Two Constant Model

T(K)	280	300	315	325	350
ss	0.0109	0.0130	0.0178	0.0271	0.0440
A_1	0.000	0.000	0.000	0.000	0.000
A_2	2.108	2.013	1.963	1.846	1.724
K_H	36.776	12.029	4.919	2.530	0.697

$\sum ss = 0.1128$

Virial Three Constant Model

T(K)	280	300	315	325	350
ss	0.0005	0.0001	0.0000	0.0001	0.0003
A_1	0.000	0.268	0.000	0.089	0.509
A_2	0.000	0.057	0.540	0.199	0.000
A_3	0.897	0.864	0.718	0.844	0.826
K_H	8.522	5.338	2.827	1.549	0.618

$\sum ss = 0.0010$

Freundlich Model

T(K)	280	300	315	325	350
ss	0.0736	0.1324	0.2658	0.3711	3.3023
k_F	1.286	1.122	0.966	0.863	0.589
n_F	0.083	0.100	0.119	0.136	0.186

$\sum ss = 4.1453$

Langmuir-Freundlich Model

T(K)	280	300	315	325	350
ss	0.0049	0.0081	0.0226	0.0409	0.4760
q_s	2.175	2.057	2.000	2.000	2.000
k_{LF}	1.375	1.107	0.827	0.634	0.313
n_{LF}	0.353	0.409	0.436	0.460	0.529

$\sum ss = 0.5526$

Loading Ratio Correlation Model

T(K)	280	300	315	325	350
ss	0.0048	0.0081	0.0217	0.0428	0.3536
q_s	2.158	2.057	2.000	2.000	2.000
k_{LRC}	2.541	1.282	0.642	0.375	0.137
n_{LRC}	2.758	2.445	2.269	2.190	1.629

$\sum ss = 0.4310$

Units of the Parameters are given in Table 4.1.

Table 6.6 Constrained Optimization Parameters for The Sorption of Ethylene on ETS-10 Zeolite

Toth Model

T(K)	280	300	315	325	350
ss	0.0217	0.0104	0.0427	0.0191	0.1783
b	0.203	0.290	0.369	0.369	0.899
K_H	88.956	38.170	21.433	10.259	2.574

$\Sigma ss = 0.2722$

t is constrained at 0.420

Unilan Model

T(K)	280	300	315	325	350
ss	0.0136	0.0244	0.0846	0.0809	1.2085
c	0.299	0.758	1.340	2.795	8.939
K_H	99.279	39.145	22.147	10.619	3.321

$\Sigma ss = 1.4121$

s is constrained at 5.00

Mathews-Weber Model

T(K)	280	300	315	325	350
ss	0.5539	0.3859	0.3919	0.3778	0.5769
b_{MW}	2.306	1.451	0.929	0.654	0.224
K_H	4.612	2.901	1.858	1.308	0.447

$\Sigma ss = 2.2864$

n_{MW} is constrained at 1.030

Volmer Model

T(K)	280	300	315	325	350
ss	0.2745	0.2061	0.1016	0.0912	0.0726
K_H	33.616	11.180	4.876	2.748	0.782

$\Sigma ss = 0.7459$

Virial Two Constant Model

T(K)	280	300	315	325	350
ss	0.0109	0.0130	0.0178	0.0271	0.0440
A_2	2.108	2.013	1.963	1.846	1.724
K_H	36.776	12.029	4.919	2.530	0.697

$\Sigma ss = 0.1128$

A_1 is constrained at 0.005

Virial Three Constant Model

T(K)	280	300	315	325	350
ss	0.0008	0.0001	0.0001	0.0001	0.0004
A_2	0.000	0.092	0.305	0.035	0.263
A_3	0.858	0.847	0.782	0.890	0.739
K_H	10.907	5.436	3.102	1.643	0.584

$\Sigma ss = 0.0014$

A_1 is constrained at 0.270

Langmuir-Freundlich Model

T(K)	280	300	315	325	350
ss	0.0195	0.0273	0.0501	0.0452	0.6406
k_{LF}	1.724	1.132	0.756	0.585	0.334

$\Sigma ss = 0.7827$

n_{LF} is constrained at 0.510

Loading Ratio Correlation Model

T(K)	280	300	315	325	350
ss	0.0324	0.0617	0.1031	0.0858	0.3898
k_{LRC}	2.732	1.216	0.572	0.345	0.117

$\Sigma ss = 0.6727$

n_{LRC} is constrained at 1.800

Units of the parameters are given in Table 4.1.
All models requiring q_s have been constrained at 2.00 mol/kg of zeolite.
Freundlich parameters have not been constrained.

Table 6.7 Vant Hoff Equation Parameters for the Sorption of Methane, Ethane and Ethylene on ETS-10 Zeolite

Methane

Model	$\sum ss$	$K_o \cdot 10^6$	$-\Delta H_o$
Toth	0.3651	4.3810	21.445
Unilan	0.2872	4.2356	21.049
Radke-Prausnitz	0.5386	0.7950	27.196
Mathews and Weber	1.7496	2.9914	20.628
Virial Two Constant	0.1684	2.0304	22.691
Virial Three Constant	0.1423	4.1354	20.784
Volmer	0.2355	3.0180	21.822

Ethane

Model	$\sum ss$	$K_o \cdot 10^6$	$-\Delta H_o$
Toth	0.2028	0.9965	35.428
Unilan	0.9712	1.5227	34.658
Radke-Prausnitz	0.0454	4.1482	30.400
Mathews and Weber	1.0916	3.3299	29.987
Virial Two Constant	0.4242	0.1677	39.025
Virial Three Constants	0.0966	0.9725	33.846
Volmer	1.5819	0.1506	39.940

Ethylene

Model	$\sum ss$	$K_o \cdot 10^6$	$-\Delta H_o$
Toth	0.2722	1.2331	42.795
Unilan	1.4121	4.7473	39.570
Mathews and Weber	2.2864	57.2460	26.747
Virial Two Constant	0.1128	0.0858	46.525
Virial Three Constants	0.0014	5.0614	34.340
Volmer	0.7459	0.2409	42.960

$\sum ss$: Total sum of square error

K_o : Preexponential factor (mol/kg/kPa)

$-\Delta H_o$: Predicted heat of adsorption (kJ/mol)

Table 6.8 Fit of IAST Model Using Toth, Unilan and Virial Isotherms for the Binary System Methane-Ethane on ETS-10 Zeolite

280 K and 150 kPa

	Experiment	IAST with Toth	IAST with Unilan	IAST with Virial
y_{CH_4}	x_{CH_4}	x_{CH_4}	x_{CH_4}	x_{CH_4}
0.000	0.000	0.0000	0.0000	0.0000
0.341	0.008	0.0167	0.0164	0.0185
0.547	0.026	0.0348	0.0339	0.0382
0.677	0.050	0.0544	0.0530	0.0601
0.756	0.079	0.0738	0.0716	0.0821
0.811	0.109	0.0943	0.0914	0.1059
0.848	0.133	0.1143	0.1106	0.1292
0.873	0.156	0.1329	0.1284	0.1506
0.892	0.177	0.1512	0.1459	0.1718
0.906	0.208	0.1683	0.1622	0.1913
1.000	—	1.0000	1.0000	1.0000

280 K and 500 kPa

	Experiment	IAST with Toth	IAST with Unilan	IAST with Virial
y_{CH_4}	x_{CH_4}	x_{CH_4}	x_{CH_4}	x_{CH_4}
0.000	0.000	0.0000	0.0000	0.0000
0.361	0.010	0.0253	0.0251	0.0325
0.581	0.044	0.0538	0.0532	0.0643
0.717	0.082	0.0858	0.0844	0.0976
0.804	0.122	0.1218	0.1195	0.1345
0.860	0.173	0.1610	0.1577	0.1752
0.895	0.214	0.1998	0.1955	0.2166
0.919	0.261	0.2394	0.2340	0.2595
0.934	0.302	0.2738	0.2675	0.2971
0.945	0.346	0.3066	0.2995	0.3332
1.000	—	1.0000	1.0000	1.0000

325 K and 150 kPa

	Experiment	IAST with Toth	IAST with Unilan	IAST with Virial
y_{CH_4}	x_{CH_4}	x_{CH_4}	x_{CH_4}	x_{CH_4}
0.000	0.000	0.0000	0.0000	0.0000
0.358	0.020	0.0289	0.0273	0.0257
0.558	0.044	0.0592	0.0554	0.0534
0.680	0.075	0.0911	0.0846	0.0831
0.755	0.105	0.1223	0.1129	0.1125
0.805	0.131	0.1529	0.1404	0.1415
0.839	0.166	0.1816	0.1661	0.1690
0.864	0.193	0.2092	0.1908	0.1957
0.882	0.218	0.2343	0.2132	0.2200
0.897	0.243	0.2597	0.2360	0.2449
1.000	—	1.0000	1.0000	

325 K and 500 kPa

	Experiment	IAST with Toth	IAST with Unilan	IAST with Virial
y_{CH_4}	x_{CH_4}	x_{CH_4}	x_{CH_4}	x_{CH_4}
0.000	0.000	0.0000	0.0000	0.0000
0.393	0.013	0.0431	0.0415	0.0363
0.616	0.054	0.0920	0.0882	0.0798
0.747	0.119	0.1468	0.1402	0.1302
0.825	0.179	0.2047	0.1950	0.1847
0.874	0.239	0.2645	0.2514	0.2419
0.904	0.296	0.3195	0.3034	0.2952
0.924	0.349	0.3703	0.3515	0.3451
0.938	0.396	0.4167	0.3957	0.3911
0.948	0.442	0.4579	0.4351	0.4322
1.000	—	1.0000	1.0000	1.0000

Table 6.9 Fit of IAST Model Using Toth, Unilan and Virial Isotherms for the Binary System Methane-Ethylene on ETS-10 Zeolite

280 K and 150 kPa

	Experiment	IAST with Toth	IAST with Unilan	IAST with Virial
y_{CH_4}	x_{CH_4}	x_{CH_4}	x_{CH_4}	x_{CH_4}
0.000	0.000	0.0000	0.0000	0.0000
0.347	0.002	0.0034	0.0032	0.0053
0.552	0.007	0.0072	0.0068	0.0103
0.684	0.018	0.0115	0.0108	0.0155
0.768	0.025	0.0163	0.0152	0.0209
0.826	0.032	0.0216	0.0202	0.0270
0.865	0.036	0.0273	0.0253	0.0336
0.891	0.043	0.0329	0.0304	0.0403
0.909	0.047	0.0383	0.0352	0.0471
0.923	0.050	0.0439	0.0401	0.0543
1.000	—	1.0000	1.0000	1.0000

280 K and 250 kPa

	Experiment	IAST with Toth	IAST with Unilan	IAST with Virial
y_{CH_4}	x_{CH_4}	x_{CH_4}	x_{CH_4}	x_{CH_4}
0.000	0.000	0.0000	0.0000	0.0000
0.352	0.001	0.0039	0.0037	—
0.569	0.008	0.0086	0.0082	0.0136
0.702	0.012	0.0140	0.0132	0.0205
0.790	0.020	0.0204	0.0192	0.0279
0.847	0.030	0.0276	0.0259	0.0359
0.884	0.040	0.0353	0.0330	0.0445
0.910	0.053	0.0437	0.0407	0.0539
0.928	0.063	0.0524	0.0485	0.0640
0.941	0.081	0.0612	0.0565	0.0747
1.000	—	1.0000	1.0000	1.0000

325 K and 150 kPa

	Experiment	IAST with Toth	IAST with Unilan	IAST with Virial
y_{CH_4}	x_{CH_4}	x_{CH_4}	x_{CH_4}	x_{CH_4}
0.000	0.000	0.0000	0.0000	0.0000
0.363	0.009	0.0051	0.0049	0.0046
0.572	0.018	0.0108	0.0102	0.0101
0.701	0.026	0.0173	0.0161	0.0167
0.784	0.035	0.0247	0.0225	0.0245
0.834	0.044	0.0319	0.0286	0.0324
0.868	0.052	0.0393	0.0348	0.0407
0.892	0.063	0.0467	0.0409	0.0493
0.909	0.073	0.0539	0.0468	0.0577
0.921	0.087	0.0606	0.0521	0.0656
1.000	—	1.0000	1.0000	1.0000

325 K and 250 kPa

	Experiment	IAST with Toth	IAST with Unilan	IAST with Virial
y_{CH_4}	x_{CH_4}	x_{CH_4}	x_{CH_4}	x_{CH_4}
0.000	0.000	0.0000	0.0000	0.0000
0.378	0.009	0.0061	0.0060	0.0056
0.598	0.025	0.0134	0.0129	0.0122
0.729	0.041	0.0219	0.0207	0.0203
0.809	0.060	0.0315	0.0293	0.0300
0.861	0.080	0.0422	0.0387	0.0416
0.893	0.099	0.0530	0.0479	0.0534
0.916	0.117	0.0647	0.0577	0.0666
0.931	0.133	0.0757	0.0668	0.0791
0.942	0.154	0.0866	0.0758	0.0918
1.000	—	1.0000	1.0000	1.0000

Table 6.10 Fit of IAST Model Using Toth, Unilan and Virial Isotherms for the Binary System Ethane-Ethylene on ETS-10 Zeolite

280 K and 150 kPa

	Experiment	IAST with Toth	IAST with Unilan	IAST with Virial
$y_{C_2H_6}$	$x_{C_2H_6}$	$x_{C_2H_6}$	$x_{C_2H_6}$	$x_{C_2H_6}$
0.000	0.000	0.0000	0.0000	0.0000
0.275	0.061	0.0364	0.0331	0.0307
0.459	0.108	0.0794	0.0729	0.0704
0.584	0.156	0.1268	0.1173	0.1163
0.672	0.197	0.1769	0.1648	0.1667
0.734	0.236	0.2265	0.2121	0.2180
0.780	0.270	0.2752	0.2589	0.2692
0.813	0.299	0.3192	0.3015	0.3158
0.839	0.327	0.3612	0.3424	0.3605
0.860	0.354	0.4011	0.3815	0.4031
1.000	—	1.0000	1.0000	1.0000

280 K and 250 kPa

	Experiment	IAST with Toth	IAST with Unilan	IAST with Virial
$y_{C_2H_6}$	$x_{C_2H_6}$	$x_{C_2H_6}$	$x_{C_2H_6}$	$x_{C_2H_6}$
0.000	0.000	0.0000	0.0000	0.0000
0.304	0.072	0.0399	0.0360	—
0.503	0.115	0.0900	0.0821	0.0756
0.630	0.190	0.1453	0.1339	0.1269
0.720	0.233	0.2072	0.1927	0.1872
0.828	0.324	0.3342	0.3155	0.3167
0.858	0.358	0.3885	0.3687	0.3733
0.880	0.391	0.4370	0.4167	0.4243
0.898	0.421	0.4838	0.4633	0.4737
1.000	—	1.0000	1.0000	1.0000

325 K and 150 kPa

	Experiment	IAST with Toth	IAST with Unilan	IAST with Virial
$y_{C_2H_6}$	$x_{C_2H_6}$	$x_{C_2H_6}$	$x_{C_2H_6}$	$x_{C_2H_6}$
0.000	0.000	0.0000	0.0000	0.0000
0.288	0.079	0.0373	0.0367	0.0424
0.475	0.138	0.0805	0.0786	0.0928
0.599	0.198	0.1271	0.1231	0.1474
0.682	0.249	0.1735	0.1672	0.2015
0.741	0.295	0.2193	0.2104	0.2540
0.785	0.340	0.2643	0.2528	0.3047
0.817	0.381	0.3055	0.2917	0.3502
0.842	0.417	0.3445	0.3285	0.3925
0.861	0.450	0.3794	0.3616	0.4297
1.000	—	1.0000	1.0000	1.0000

325 K and 250 kPa

	Experiment	IAST with Toth	IAST with Unilan	IAST with Virial
$y_{C_2H_6}$	$x_{C_2H_6}$	$x_{C_2H_6}$	$x_{C_2H_6}$	$x_{C_2H_6}$
0.000	0.000	0.0000	0.0000	0.0000
0.322	0.084	0.0426	0.0425	0.0463
0.522	0.157	0.0941	0.0932	0.1044
0.650	0.229	0.1515	0.1491	0.1700
0.735	0.299	0.2118	0.2073	0.2387
0.792	0.353	0.2705	0.2637	0.3046
0.832	0.404	0.3261	0.3171	0.3659
0.861	0.454	0.3777	0.3667	0.4215
0.883	0.496	0.4255	0.4129	0.4720
0.900	0.531	0.4694	0.4554	0.5173
1.000	—	1.0000	1.0000	1.0000

Table 6.11 Values of the Relative Adsorptivity of the Binary Systems Ethane-Methan, Ethylene-Methane and Ethylene-Ethane on ETS-10 Zeolite

Ethane-Methane

		Relative Adsorptivity			
T (K)	P (kPa)	Experiment	IAST-Toth	IAST-Unilan	IAST-Virial
280	150	45.23	33.49	34.41	30.40
280	500	30.13	24.39	24.68	20.18
325	150	27.43	20.06	21.53	22.38
325	500	21.86	17.16	18.11	19.72

Ethylene-Methane

		Relative Adsorptivity			
T (K)	P (kPa)	Experiment	IAST-Toth	IAST-Unilan	IAST-Virial
280	150	174.79	169.90	179.66	118.39
280	250	163.70	152.19	159.68	95.75
325	150	72.91	122.41	129.69	130.99
325	250	58.01	109.52	113.83	120.44

Ethylene-Ethane

		Relative Adsorptivity			
T (K)	P (kPa)	Experiment	IAST-Toth	IAST-Unilan	IAST-Virial
280	150	7.60	9.67	10.56	10.67
280	250	7.79	10.23	11.32	12.38
325	150	5.65	10.33	10.61	8.84
325	250	5.86	10.51	10.63	9.37

Table 6.12 x-q Fit of IAST Model Using Toth, Unilan and Virial Isotherms for the Binary System Methane-Ethane on ETS-10 Zeolite at 280 K and 150 kPa

	Experimental			IAST with Toth			IAST with Unilan			IAST with Virial		
x_{CH_4}	q_{CH_4}	$q_{C_2H_6}$	q_{tot}	q_{CH_4}	$q_{C_2H_6}$	q_{tot}	q_{CH_4}	$q_{C_2H_6}$	q_{tot}	q_{CH_4}	$q_{C_2H_6}$	q_{tot}
0.000	0.000	1.652	1.652	0.000	1.654	1.654	0.000	1.693	1.693	0.000	1.633	1.633
0.008	0.013	1.624	1.637	0.027	1.610	1.638	0.027	1.649	1.677	0.030	1.567	1.597
0.026	0.042	1.576	1.619	0.056	1.564	1.620	0.056	1.600	1.656	0.060	1.503	1.563
0.050	0.080	1.522	1.601	0.087	1.514	1.601	0.086	1.546	1.632	0.092	1.440	1.532
0.079	0.126	1.468	1.594	0.117	1.466	1.583	0.115	1.493	1.608	0.124	1.383	1.507
0.109	0.173	1.417	1.590	0.148	1.417	1.565	0.145	1.439	1.584	0.157	1.327	1.485
0.133	0.210	1.370	1.580	0.177	1.371	1.548	0.173	1.388	1.561	0.189	1.276	1.466
0.156	0.245	1.327	1.572	0.204	1.329	1.533	0.198	1.343	1.541	0.218	1.232	1.451
0.177	0.276	1.286	1.562	0.230	1.289	1.519	0.222	1.300	1.523	0.247	1.190	1.437
0.208	0.329	1.249	1.578	0.253	1.253	1.506	0.244	1.262	1.506	0.273	1.153	1.426
1.000	—	—	—	1.186	0.000	1.187	1.189	0.000	1.189	1.249	0.000	1.249

x: mole fraction in the adsorbed phase.
y: mole fraction in the gas phase.
q: amount adsorbed (mol/kg of zeolite)

Table 6.13 x-q Fit of IAST Model Using Toth, Unilan and Virial Isotherms for the Binary System Methane-Ethane on ETS-10 Zeolite at 280 K and 500 kPa

	Experimental			IAST with Toth			IAST with Unilan			IAST with Virial		
x_{CH_4}	q_{CH_4}	$q_{C_2H_6}$	q_{tot}	q_{CH_4}	$q_{C_2H_6}$	q_{tot}	q_{CH_4}	$q_{C_2H_6}$	q_{tot}	q_{CH_4}	$q_{C_2H_6}$	q_{tot}
0.000	0.000	1.763	1.763	0.000	1.700	1.700	0.000	1.732	1.732	0.000	1.754	1.754
0.010	0.019	1.804	1.823	0.043	1.657	1.700	0.044	1.692	1.736	0.056	1.669	1.725
0.044	0.080	1.756	1.836	0.091	1.607	1.698	0.092	1.646	1.738	0.109	1.589	1.698
0.082	0.151	1.684	1.835	0.146	1.551	1.696	0.147	1.591	1.738	0.163	1.510	1.673
0.122	0.223	1.608	1.831	0.206	1.487	1.694	0.207	1.528	1.735	0.222	1.429	1.651
0.173	0.321	1.531	1.852	0.272	1.419	1.691	0.273	1.458	1.731	0.286	1.346	1.632
0.214	0.395	1.453	1.847	0.337	1.351	1.689	0.337	1.389	1.726	0.351	1.268	1.619
0.261	0.488	1.380	1.868	0.404	1.283	1.686	0.403	1.318	1.721	0.417	1.191	1.609
0.302	0.568	1.312	1.880	0.461	1.224	1.685	0.459	1.257	1.716	0.476	1.126	1.602
0.346	0.660	1.249	1.909	0.516	1.168	1.684	0.513	1.199	1.712	0.532	1.065	1.597
1.000	—	—	—	1.6988	0.000	1.699	1.707	0.000	1.707	1.623	0.000	1.623

x: mole fraction in the adsorbed phase.

y: mole fraction in the gas phase.

q: amount adsorbed (mol/kg of zeolite)

Table 6.14 x-q Fit of IAST Model Using Toth, Unilan and Virial Isotherms for the Binary System Methane-Ethane on ETS-10 Zeolite at 325 K and 150 kPa

	Experimental			IAST with Toth			IAST with Unilan			IAST with Virial		
x_{CH_4}	q_{CH_4}	$q_{C_2H_6}$	q_{tot}	q_{CH_4}	$q_{C_2H_6}$	q_{tot}	q_{CH_4}	$q_{C_2H_6}$	q_{tot}	q_{CH_4}	$q_{C_2H_6}$	q_{tot}
0.000	0.000	1.456	1.456	0.000	1.424	1.424	0.000	1.419	1.419	0.000	1.373	1.373
0.020	0.028	1.401	1.429	0.039	1.322	1.361	0.037	1.308	1.344	0.034	1.284	1.318
0.044	0.062	1.325	1.387	0.077	1.224	1.301	0.071	1.206	1.277	0.068	1.201	1.269
0.075	0.101	1.251	1.352	0.113	1.131	1.244	0.103	1.114	1.217	0.102	1.124	1.225
0.105	0.138	1.180	1.318	0.146	1.049	1.195	0.132	1.036	1.168	0.134	1.055	1.188
0.131	0.168	1.115	1.283	0.176	0.976	1.152	0.158	0.968	1.126	0.164	0.993	1.156
0.166	0.210	1.055	1.265	0.202	0.913	1.115	0.181	0.910	1.091	0.191	0.938	1.129
0.193	0.239	1.001	1.241	0.226	0.856	1.083	0.202	0.858	1.061	0.216	0.888	1.104
0.218	0.265	0.954	1.219	0.247	0.808	1.056	0.221	0.815	1.036	0.239	0.845	1.084
0.243	0.292	0.909	1.201	0.268	0.762	1.030	0.239	0.774	1.013	0.261	0.804	1.064
1.000	—	—	—	0.6535	0.000	0.654	0.668	0.000	0.668	0.702	0.000	0.702

x: mole fraction in the adsorbed phase.
y: mole fraction in the gas phase.
q: amount adsorbed (mol/kg of zeolite)

Table 6.15 x-q Fit of IAST Model Using Toth, Unilan and Virial Isotherms for the Binary System Methane-Ethane on ETS-10 Zeolite at 325 K and 500 kPa

	Experimental			IAST with Toth			IAST with Unilan			IAST with Virial		
x_{CH_4}	q_{CH_4}	$q_{C_2H_6}$	q_{tot}	q_{CH_4}	$q_{C_2H_6}$	q_{tot}	q_{CH_4}	$q_{C_2H_6}$	q_{tot}	q_{CH_4}	$q_{C_2H_6}$	q_{tot}
0.000	0.000	1.551	1.551	0.000	1.572	1.572	0.000	1.603	1.603	0.000	1.530	1.530
0.013	0.020	1.546	1.566	0.066	1.475	1.542	0.065	1.496	1.561	0.054	1.429	1.483
0.054	0.085	1.469	1.553	0.139	1.368	1.506	0.133	1.380	1.513	0.115	1.325	1.440
0.119	0.186	1.369	1.555	0.216	1.254	1.470	0.205	1.259	1.465	0.183	1.219	1.401
0.179	0.277	1.266	1.542	0.294	1.140	1.434	0.277	1.143	1.420	0.253	1.115	1.368
0.239	0.367	1.168	1.535	0.370	1.030	1.400	0.347	1.034	1.381	0.324	1.016	1.340
0.296	0.453	1.076	1.530	0.438	0.934	1.372	0.410	0.941	1.350	0.389	0.928	1.317
0.349	0.535	0.996	1.530	0.499	0.849	1.349	0.466	0.859	1.325	0.448	0.851	1.299
0.396	0.603	0.921	1.525	0.554	0.775	1.328	0.516	0.788	1.304	0.502	0.782	1.283
0.442	0.676	0.855	1.532	0.600	0.771	1.311	0.560	0.727	1.287	0.549	0.722	1.271
1.000	—	—	—	1.151	0.000	1.151	1.155	0.000	1.155	1.150	0.000	1.150

x: mole fraction in the adsorbed phase.
y: mole fraction in the gas phase.
q: amount adsorbed (mol/kg of zeolite)

Table 6.16 x-q Fit of IAST Model Using Toth, Unilan and Virial Isotherms for the Binary System Methane-Ethylene on ETS-10 Zeolite at 280 K and 150 kPa

	Experimental			IAST with Toth			IAST with Unilan			IAST with Virial		
x_{CH_4}	q_{CH_4}	$q_{C_2H_4}$	q_{tot}	q_{CH_4}	$q_{C_2H_4}$	q_{tot}	q_{CH_4}	$q_{C_2H_4}$	q_{tot}	q_{CH_4}	$q_{C_2H_4}$	q_{tot}
0.000	0.000	1.944	1.944	0.000	1.887	1.887	0.000	1.948	1.948	0.000	1.935	1.935
0.002	0.004	1.916	1.920	0.006	1.861	1.869	0.006	1.921	1.927	0.010	1.885	1.894
0.010	0.018	1.871	1.890	0.013	1.835	1.848	0.013	1.890	1.902	0.019	1.840	1.859
0.018	0.033	1.825	1.858	0.021	1.806	1.827	0.020	1.854	1.874	0.028	1.797	1.825
0.025	0.046	1.780	1.825	0.029	1.777	1.807	0.028	1.817	1.845	0.038	1.756	1.794
0.032	0.058	1.740	1.798	0.039	1.747	1.786	0.037	1.777	1.814	0.048	1.716	1.764
0.036	0.064	1.703	1.768	0.048	1.717	1.766	0.045	1.739	1.784	0.058	1.679	1.737
0.043	0.076	1.681	1.757	0.058	1.690	1.748	0.053	1.703	1.757	0.069	1.645	1.714
0.047	0.080	1.641	1.721	0.066	1.665	1.732	0.061	1.672	1.733	0.080	1.615	1.695
0.050	0.085	1.613	1.698	0.075	1.641	1.716	0.069	1.642	1.710	0.091	1.586	1.677
1.000	—	—	—	1.186	0.000	1.187	1.189	0.000	1.189	1.249	0.000	1.249

x: mole fraction in the adsorbed phase.
y: mole fraction in the gas phase.
q: amount adsorbed (mol/kg of zeolite)

Table 6.17 x-q Fit of IAST Model Using Toth, Unilan and Virial Isotherms for the Binary System Methane-Ethylene on ETS-10 Zeolite at 280 K and 250 kPa

	Experimental			IAST with Toth			IAST with Unilan			IAST with Virial		
x_{CH_4}	q_{CH_4}	$q_{C_2H_4}$	q_{tot}	q_{CH_4}	$q_{C_2H_4}$	q_{tot}	q_{CH_4}	$q_{C_2H_4}$	q_{tot}	q_{CH_4}	$q_{C_2H_4}$	q_{tot}
0.000	0.000	2.007	2.007	0.000	1.908	1.908	0.000	1.967	1.967	0.000	1.985	1.985
0.001	0.002	1.986	1.988	0.007	1.885	1.892	0.007	1.946	1.954	—	—	—
0.006	0.012	1.933	1.945	0.016	1.859	1.875	0.016	1.920	1.935	0.026	1.883	1.919
0.012	0.023	1.882	1.905	0.026	1.832	1.858	0.025	1.889	1.914	0.038	1.836	1.874
0.020	0.038	1.830	1.868	0.038	1.801	1.839	0.036	1.852	1.889	0.051	1.790	1.841
0.030	0.055	1.782	1.837	0.050	1.770	1.820	0.048	1.813	1.861	0.065	1.745	1.810
0.040	0.073	1.737	1.810	0.064	1.738	1.802	0.061	1.774	1.835	0.079	1.704	1.783
0.053	0.094	1.697	1.791	0.078	1.706	1.784	0.073	1.734	1.807	0.095	1.663	1.758
0.063	0.111	1.660	1.771	0.093	1.675	1.768	0.086	1.696	1.782	0.111	1.625	1.736
0.081	0.114	1.627	1.771	0.107	1.645	1.752	0.099	1.659	1.759	0.128	1.588	1.717
1.000	—	—	—	1.412	0.000	1.412	1.412	0.000	1.412	1.420	0.000	1.420

x: mole fraction in the adsorbed phase.

y: mole fraction in the gas phase.

q: amount adsorbed (mol/kg of zeolite)

Table 6.18 x-q Fit of IAST Model Using Toth, Unilan and Virial Isotherms for the Binary System Methane-Ethylene on ETS-10 Zeolite at 325 K and 150 kPa

	Experimental			IAST with Toth			IAST with Unilan			IAST with Virial		
x_{CH_4}	q_{CH_4}	$q_{C_2H_4}$	q_{tot}	q_{CH_4}	$q_{C_2H_4}$	q_{tot}	q_{CH_4}	$q_{C_2H_4}$	q_{tot}	q_{CH_4}	$q_{C_2H_4}$	q_{tot}
0.000	0.000	1.715	1.715	0.000	1.736	1.736	0.000	1.735	1.735	0.000	1.705	1.705
0.009	0.015	1.662	1.677	0.009	1.681	1.690	0.008	1.660	1.668	0.008	1.646	1.654
0.018	0.029	1.604	1.633	0.018	1.626	1.643	0.016	1.588	1.605	0.016	1.591	1.607
0.026	0.041	1.548	1.589	0.028	1.569	1.597	0.025	1.520	1.545	0.026	1.536	1.562
0.035	0.054	1.494	1.547	0.038	1.513	1.551	0.033	1.456	1.489	0.037	1.483	1.521
0.044	0.066	1.447	1.514	0.048	1.463	1.511	0.041	1.403	1.444	0.048	1.438	1.486
0.052	0.077	1.404	1.481	0.058	1.416	1.474	0.049	1.355	1.404	0.059	1.395	1.455
0.063	0.092	1.365	1.456	0.067	1.374	1.441	0.056	1.313	1.369	0.070	1.356	1.427
0.073	0.104	1.330	1.434	0.076	1.335	1.411	0.063	1.277	1.339	0.081	1.322	1.402
0.087	0.124	1.298	1.422	0.084	1.302	1.386	0.068	1.246	1.315	0.091	1.291	1.382
1.000	—	—	—	0.654	0.000	0.654	0.668	0.000	0.668	0.702	0.000	0.702

x: mole fraction in the adsorbed phase.

y: mole fraction in the gas phase.

q: amount adsorbed (mol/kg of zeolite)

Table 6.19 x-q Fit of IAST Model Using Toth, Unilan and Virial Isotherms for the Binary System Methane-Ethylene on ETS-10 Zeolite at 325 K and 250 kPa

	Experimental			IAST with Toth			IAST with Unilan			IAST with Virial		
x_{CH_4}	q_{CH_4}	$q_{C_2H_4}$	q_{tot}	q_{CH_4}	$q_{C_2H_4}$	q_{tot}	q_{CH_4}	$q_{C_2H_4}$	q_{tot}	q_{CH_4}	$q_{C_2H_4}$	q_{tot}
0.000	0.000	1.760	1.760	0.000	1.783	1.783	0.000	1.804	1.804	0.000	1.762	1.762
0.009	0.016	1.715	1.731	0.011	1.732	1.743	0.010	1.733	1.744	0.010	1.702	1.711
0.025	0.043	1.651	1.694	0.023	1.677	1.700	0.022	1.660	1.6810	0.020	1.643	1.663
0.041	0.068	1.584	1.652	0.036	1.620	1.656	0.034	1.587	1.621	0.033	1.585	1.618
0.060	0.096	1.521	1.617	0.051	1.563	1.614	0.046	1.519	1.565	0.047	1.529	1.576
0.080	0.127	1.464	1.591	0.066	1.505	1.572	0.059	1.454	1.513	0.064	1.473	1.537
0.099	0.156	1.413	1.569	0.081	1.454	1.535	0.070	1.339	1.470	0.080	1.424	1.504
0.117	0.181	1.367	1.549	0.097	1.402	1.499	0.083	1.347	1.430	0.098	1.375	1.473
0.133	0.204	1.326	1.530	0.111	1.358	1.469	0.093	1.304	1.398	0.115	1.333	1.448
0.154	0.235	1.288	1.522	0.125	1.317	1.441	0.104	1.266	1.369	0.131	1.294	1.425
1.000	—	—	—	0.852	0.000	0.852	0.864	0.000	0.864	0.898	0.000	0.898

x: mole fraction in the adsorbed phase.

y: mole fraction in the gas phase.

q: amount adsorbed (mol/kg of zeolite)

Table 6.20 x-q Fit of IAST Model Using Toth, Unilan and Virial Isotherms for the Binary System Ethane-Ethylene on ETS-10 Zeolite at 280 K and 150 kPa

	Experimental			IAST with Toth			IAST with Unilan			IAST with Virial		
$x_{C_2H_6}$	$q_{C_2H_6}$	$q_{C_2H_4}$	q_{tot}	$q_{C_2H_6}$	$q_{C_2H_4}$	q_{tot}	$q_{C_2H_6}$	$q_{C_2H_4}$	q_{tot}	$q_{C_2H_6}$	$q_{C_2H_4}$	q_{tot}
0.000	0.000	1.959	1.959	0.000	1.887	1.887	0.000	1.948	1.948	0.000	1.935	1.935
0.061	0.118	1.824	1.942	0.068	1.799	1.867	0.064	1.863	1.926	0.059	1.847	1.920
0.108	0.206	1.703	1.910	0.147	1.701	1.847	0.139	1.765	1.904	0.132	1.745	1.879
0.156	0.295	1.598	1.892	0.232	1.597	1.829	0.221	1.661	1.882	0.215	1.637	1.852
0.197	0.369	1.503	1.872	0.320	1.491	1.812	0.307	1.554	1.861	0.305	1.525	1.830
0.236	0.439	1.417	1.856	0.407	1.390	1.796	0.391	1.452	1.842	0.395	1.416	1.810
0.270	0.459	1.340	1.835	0.491	1.292	1.783	0.473	1.353	1.826	0.483	1.310	1.793
0.299	0.540	1.269	1.810	0.565	1.206	1.771	0.546	1.266	1.812	0.562	1.217	1.779
0.327	0.588	1.208	1.795	0.636	1.125	1.761	0.616	1.184	1.800	0.637	1.129	1.766
0.354	0.631	1.152	1.783	0.703	1.049	1.752	0.683	1.107	1.789	0.707	1.048	1.755
1.000	—	—	—	1.654	0.000	1.654	1.693	0.000	1.693	1.633	0.000	1.633

x: mole fraction in the adsorbed phase.
y: mole fraction in the gas phase.
q: amount adsorbed (mol/kg of zeolite)

Table 6.21 x-q Fit of IAST Model Using Toth, Unilan and Virial Isotherms for the Binary System Ethane-Ethylene on ETS-10 Zeolite at 280 K and 250 kPa

	Experimental			IAST with Toth			IAST with Unilan			IAST with Virial		
$x_{C_2H_6}$	$q_{C_2H_6}$	$q_{C_2H_4}$	q_{tot}	$q_{C_2H_6}$	$q_{C_2H_4}$	q_{tot}	$q_{C_2H_6}$	$q_{C_2H_4}$	q_{tot}	$q_{C_2H_6}$	$q_{C_2H_4}$	q_{tot}
0.000	0.000	1.982	1.982	0.000	1.908	1.908	0.000	1.967	1.967	0.000	1.983	1.983
0.072	0.144	1.840	1.983	0.075	1.813	1.888	0.070	1.877	1.948	—	—	—
0.121	0.233	1.692	1.929	0.168	1.699	1.867	0.158	1.767	1.925	0.145	1.774	1.920
0.190	0.368	1.572	1.940	0.268	1.579	1.847	0.255	1.648	1.903	0.240	1.652	1.893
0.233	0.441	1.457	1.898	0.379	1.449	1.828	0.362	1.518	1.880	0.350	1.518	1.868
0.324	0.600	1.254	1.854	0.600	1.194	1.794	0.581	1.260	1.841	0.578	1.247	1.826
0.358	0.653	1.173	1.826	0.692	1.089	1.781	0.673	1.152	1.826	0.676	1.134	1.810
0.391	0.706	1.099	1.805	0.774	0.997	1.771	0.756	1.058	1.813	0.763	1.035	1.798
0.421	0.750	1.033	1.783	0.852	0.909	1.761	0.835	0.967	1.802	0.846	0.940	1.786
1.000	—	—	—	1.677	0.000	1.677	1.715	0.000	1.715	1.686	0.000	1.686

x: mole fraction in the adsorbed phase.
y: mole fraction in the gas phase.
q: amount adsorbed (mol/kg of zeolite)

Table 6.22 x-q Fit of IAST Model Using Toth, Unilan and Virial Isotherms for the Binary System Ethane-Ethylene on ETS-10 Zeolite at 325 K and 150 kPa

	Experimental			IAST with Toth			IAST with Unilan			IAST with Virial		
$x_{C_2H_6}$	$q_{C_2H_6}$	$q_{C_2H_4}$	q_{tot}	$q_{C_2H_6}$	$q_{C_2H_4}$	q_{tot}	$q_{C_2H_6}$	$q_{C_2H_4}$	q_{tot}	$q_{C_2H_6}$	$q_{C_2H_4}$	q_{tot}
0.000	0.000	1.714	1.714	0.000	1.736	1.736	0.000	1.735	1.735	0.000	1.705	1.705
0.079	0.134	1.563	1.697	0.064	1.638	1.701	0.062	1.626	1.688	0.071	1.597	1.668
0.138	0.229	1.430	1.658	0.134	1.535	1.669	0.130	1.518	1.648	0.152	1.483	1.634
0.198	0.324	1.312	1.636	0.209	1.433	1.641	0.199	1.415	1.613	0.237	1.369	1.605
0.249	0.400	1.207	1.607	0.281	1.336	1.617	0.265	1.321	1.586	0.319	1.262	1.581
0.295	0.466	1.115	1.581	0.350	1.246	1.596	0.329	1.234	1.563	0.396	1.163	1.559
0.340	0.533	1.034	1.567	0.417	1.161	1.578	0.390	1.154	1.544	0.469	1.072	1.541
0.381	0.590	0.961	1.551	0.478	1.086	1.563	0.446	1.083	1.529	0.534	0.991	1.526
0.417	0.641	0.895	1.536	0.534	1.016	1.550	0.498	1.018	1.516	0.594	0.919	1.512
0.450	0.683	0.835	1.518	0.584	0.956	1.540	0.545	0.961	1.506	0.645	0.856	1.501
1.000	—	—	—	1.424	0.000	1.424	1.419	0.000	1.419	1.373	0.000	1.373

x: mole fraction in the adsorbed phase.
y: mole fraction in the gas phase.
q: amount adsorbed (mol/kg of zeolite)

Table 6.23 x-q Fit of IAST Model Using Toth, Unilan and Virial Isotherms for the Binary System Ethane-Ethylene on ETS-10 Zeolite at 325 K and 250 kPa

	Experimental			IAST with Toth			IAST with Unilan			IAST with Virial		
$x_{C_2H_6}$	$q_{C_2H_6}$	$q_{C_2H_4}$	q_{tot}	$q_{C_2H_6}$	$q_{C_2H_4}$	q_{tot}	$q_{C_2H_6}$	$q_{C_2H_4}$	q_{tot}	$q_{C_2H_6}$	$q_{C_2H_4}$	q_{tot}
0.000	0.000	1.767	1.767	0.000	1.783	1.783	0.000	1.804	1.804	0.000	1.762	1.762
0.084	0.146	1.586	1.732	0.074	1.673	1.748	0.075	1.682	1.756	0.080	1.642	1.722
0.157	0.265	1.424	1.689	0.161	1.554	1.715	0.160	1.553	1.713	0.176	1.509	1.685
0.229	0.381	1.280	1.661	0.255	1.430	1.686	0.250	1.426	1.676	0.281	1.372	1.653
0.299	0.492	1.154	1.645	0.352	1.308	1.660	0.341	1.305	1.646	0.388	1.238	1.626
0.353	0.568	1.041	1.609	0.443	1.195	1.638	0.428	1.194	1.622	0.488	1.114	1.603
0.404	0.640	0.943	1.583	0.528	1.092	1.620	0.508	1.095	1.603	0.579	1.004	1.583
0.454	0.711	0.855	1.565	0.606	0.999	1.606	0.583	1.006	1.588	0.661	0.907	1.567
0.496	0.764	0.778	1.542	0.678	0.915	1.593	0.651	0.926	1.576	0.733	0.820	1.554
0.531	0.802	0.709	1.511	0.743	0.840	1.582	0.713	0.853	1.567	0.798	0.744	1.542
1.000	—	—	—	1.496	0.000	1.496	1.508	0.000	1.508	1.443	0.000	1.443

x: mole fraction in the adsorbed phase.
y: mole fraction in the gas phase.
q: amount adsorbed (mol/kg of zeolite)

Table 6.24 x-y Fit of IAST Model Using Toth, Unilan and Virial Isotherms for the Ternary System Methane-Ethane-Ethylene on ETS-10 Zeolite at 300 K and 200 kPa (High Ethylene Loading)

		Experimental		IAST with Toth		IAST with Unilan		IAST with Virial	
y_{CH_4}	$y_{C_2H_6}$	x_{CH_4}	$x_{C_2H_6}$	x_{CH_4}	$x_{C_2H_6}$	x_{CH_4}	$x_{C_2H_6}$	x_{CH_4}	$x_{C_2H_6}$
0.000	0.000	—	—	0.0000	0.0000	0.0000	0.0000	0.0000	0.0000
0.000	0.236	0.000	0.051	0.0000	0.0209	0.0000	0.0194	0.0000	0.0178
0.359	0.147	0.009	0.051	0.0062	0.0207	0.0062	0.0193	0.0084	0.0188
0.575	0.094	0.012	0.049	0.0133	0.0201	0.0132	0.0187	0.0168	0.0195
0.707	0.062	0.026	0.046	0.0214	0.0193	0.0210	0.0178	0.0257	0.0197
0.792	0.042	0.034	0.043	0.0305	0.0183	0.0297	0.0168	0.0357	0.0196
0.847	0.030	0.047	0.040	0.0406	0.0177	0.0391	0.0161	0.0470	0.0197
0.882	0.022	0.055	0.037	0.0506	0.0166	0.0483	0.0150	0.0586	0.0189
0.907	0.017	0.068	0.034	0.0616	0.0161	0.0582	0.0144	0.0717	0.0187
0.924	0.013	0.077	0.031	0.0718	0.0148	0.0673	0.0131	0.0841	0.0173
0.936	0.010	0.083	0.029	0.0812	0.0132	0.0756	0.0116	0.0956	0.0156
1.000	0.000	—	—	1.0000	0.0000	1.0000	0.0000	1.0000	0.0000

Table 6.25 x-y Fit of IAST Model Using Toth, Unilan and Virial Isotherms for the Ternary System Methane-Ethane-Ethylene on ETS-10 Zeolite at 300 K and 200 kPa (High Ethane Loading)

		Experimental		IAST with Toth		IAST with Unilan		IAST with Virial	
y_{CH_4}	$y_{C_2H_6}$	x_{CH_4}	$x_{C_2H_6}$	x_{CH_4}	$x_{C_2H_6}$	x_{CH_4}	$x_{C_2H_6}$	x_{CH_4}	$x_{C_2H_6}$
0.000	0.000	—	—	0.0000	0.0000	0.0000	0.0000	0.0000	0.0000
0.000	0.627	0.000	0.189	0.0000	0.1085	0.0000	0.1017	0.0000	0.1029
0.363	0.394	0.000	0.187	0.0099	0.1065	0.0098	0.0994	0.0121	0.1069
0.579	0.255	0.001	0.182	0.0210	0.1021	0.0205	0.0946	0.0246	0.1077
0.713	0.170	0.012	0.172	0.0334	0.0972	0.0324	0.0891	0.0385	0.1067
0.796	0.118	0.025	0.161	0.0467	0.0918	0.0448	0.0833	0.0537	0.1038
0.849	0.085	0.039	0.149	0.0605	0.0860	0.0573	0.0772	0.0699	0.0989
0.883	0.063	0.050	0.139	0.0729	0.0778	0.0685	0.0692	0.0849	0.0905
0.907	0.049	0.059	0.130	0.0867	0.0736	0.0808	0.0649	0.1016	0.0862
0.924	0.039	0.073	0.121	0.1000	0.0691	0.0924	0.0604	0.1177	0.0812
0.936	0.032	0.089	0.112	0.1122	0.0649	0.1030	0.0564	0.1326	0.0766
1.000	0.000	—	—	1.0000	0.0000	1.0000	0.0000	1.0000	0.0000

Table 6.26 x-y Fit of IAST Model Using Toth, Unilan and Virial Models for the Ternary System Methane-Ethane-Ethylene on ETS-10 Zeolite at 325 K and 200 kPa (High Ethylene Loading)

		Experimental		IAST with Toth		IAST with Unilan		IAST with Virial	
y_{CH_4}	$y_{C_2H_6}$	x_{CH_4}	$x_{C_2H_6}$	x_{CH_4}	$x_{C_2H_6}$	x_{CH_4}	$x_{C_2H_6}$	x_{CH_4}	$x_{C_2H_6}$
0.000	0.000	—	—	0.0000	0.0000	0.0000	0.0000	0.0000	0.0000
0.000	0.159	0.000	0.038	0.0000	0.0174	0.0000	0.0174	0.0000	0.0191
0.370	0.096	0.006	0.039	0.0063	0.0168	0.0061	0.0166	0.0057	0.0192
0.589	0.060	0.020	0.037	0.0137	0.0161	0.0130	0.0156	0.0126	0.0191
0.719	0.039	0.038	0.034	0.0220	0.0152	0.0205	0.0145	0.0209	0.0185
0.799	0.027	0.046	0.031	0.0312	0.0146	0.0286	0.0137	0.0306	0.0180
0.850	0.019	0.056	0.029	0.0409	0.0135	0.0369	0.0125	0.0412	0.0168
0.884	0.014	0.076	0.026	0.0511	0.0127	0.0455	0.0115	0.0526	0.0159
0.906	0.010	0.093	0.024	0.0603	0.0109	0.0532	0.0098	0.0631	0.0137
0.922	0.008	0.102	0.022	0.0700	0.0103	0.0611	0.0092	0.0743	0.0131
0.934	0.006	0.110	0.021	0.0793	0.0089	0.0685	0.0079	0.0852	0.0114
1.000	0.000	—	—	1.0000	0.0000	1.0000	0.0000	1.0000	0.0000

Table 6.27 x-y Fit of IAST Model Using Toth, Unilan and Virial Isotherms for the Ternary System Methane-Ethane-Ethylene on ETS-10 Zeolite at 325 K and 200 kPa (High Ethane Loading)

		Experimental		IAST with Toth		IAST with Unilan		IAST with Virial	
y_{CH_4}	$y_{C_2H_6}$	x_{CH_4}	$x_{C_2H_6}$	x_{CH_4}	$x_{C_2H_6}$	x_{CH_4}	$x_{C_2H_6}$	x_{CH_4}	$x_{C_2H_6}$
0.000	0.000	—	—	0.0000	0.0000	0.0000	0.0000	0.0000	0.0000
0.000	0.746	0.000	0.292	0.0000	0.2228	0.0000	0.2162	0.0000	0.2544
0.377	0.459	0.002	0.288	0.0131	0.2132	0.0122	0.2032	0.0122	0.2489
0.592	0.296	0.013	0.273	0.0275	0.2013	0.0251	0.1885	0.0266	0.2382
0.720	0.199	0.027	0.256	0.0428	0.1868	0.0384	0.1722	0.0425	0.2237
0.799	0.139	0.052	0.235	0.0582	0.1701	0.0516	0.1548	0.0593	0.2064
0.848	0.103	0.080	0.215	0.0737	0.1581	0.0645	0.1423	0.0766	0.1940
0.881	0.078	0.086	0.202	0.0879	0.1427	0.0760	0.1273	0.0929	0.1771
0.905	0.061	0.102	0.187	0.1036	0.1328	0.0887	0.1176	0.1112	0.1665
0.920	0.050	0.115	0.173	0.1157	0.1225	0.0983	0.1080	0.1257	0.1549
0.932	0.041	0.120	0.163	0.1271	0.1112	0.1073	0.0975	0.1395	0.1417
1.000	0.000	—	—	1.0000	0.0000	1.0000	0.0000	1.0000	0.0000

Table 6.28 x-q Fit of IAST Model Using Toth, Unilan and Virial Isotherms for the Ternary System Methane-Ethane-Ethylene on ETS-10 Zeolite at 300 K and 200 kPa (High Ethylene Loading)

		Experimental			IAST with Toth			IAST with Unilan			IAST with Virial		
x_{CH_4}	$x_{C_2H_6}$	q_{CH_4}	$q_{C_2H_6}$	$q_{C_2H_4}$	q_{CH_4}	$q_{C_2H_6}$	$q_{C_2H_4}$	q_{CH_4}	$q_{C_2H_6}$	$q_{C_2H_4}$	q_{CH_4}	$q_{C_2H_6}$	$q_{C_2H_4}$
0.000	0.000	—	—	—	0.000	0.000	1.858	0.000	0.000	1.911	0.000	0.000	1.870
0.000	0.051	0.000	0.094	1.751	0.000	0.039	1.802	0.000	0.037	1.851	0.000	0.033	1.810
0.009	0.051	0.016	0.94	1.716	0.011	0.038	1.766	0.011	0.036	1.804	0.015	0.034	1.753
0.012	0.049	0.022	0.087	1.664	0.024	0.036	1.728	0.024	0.034	1.752	0.030	0.034	1.699
0.026	0.046	0.045	0.081	1.619	0.038	0.034	1.689	0.037	0.032	1.699	0.044	0.034	1.648
0.034	0.043	0.059	0.074	1.579	0.053	0.032	1.648	0.051	0.029	1.645	0.060	0.033	1.599
0.047	0.040	0.079	0.067	1.540	0.069	0.030	1.605	0.066	0.027	1.592	0.078	0.033	1.550
0.055	0.037	0.091	0.061	1.503	0.085	0.028	1.567	0.080	0.025	1.545	0.096	0.031	1.508
0.068	0.034	0.112	0.055	1.471	0.102	0.027	1.527	0.094	0.023	1.498	0.116	0.030	1.465
0.077	0.031	0.124	0.050	1.441	0.117	0.024	1.493	0.107	0.021	1.460	0.134	0.028	1.430
0.083	0.029	0.132	0.046	1.414	0.131	0.021	1.465	0.118	0.018	1.429	0.151	0.025	1.400
1.000	0.000	—	—	—	1.163	0.000	0.000	1.166	0.000	0.000	1.196	0.000	0.000

Table 6.29 x-q Fit of IAST Model Using Toth, Unilan and Virial Isotherms for the Ternary System Methane-Ethane-Ethylene on ETS-10 Zeolite at 300 K and 200 kPa (High Ethane Loading)

		Experimental			IAST with Toth			IAST with Unilan			IAST with Virial		
x_{CH_4}	$x_{C_2H_6}$	q_{CH_4}	$q_{C_2H_6}$	$q_{C_2H_4}$	q_{CH_4}	$q_{C_2H_6}$	$q_{C_2H_4}$	q_{CH_4}	$q_{C_2H_6}$	$q_{C_2H_4}$	q_{CH_4}	$q_{C_2H_6}$	$q_{C_2H_4}$
0.000	0.000	—	—	—	0.000	0.000	1.858	0.000	0.000	1.911	0.000	0.000	1.870
0.000	0.189	0.000	0.334	1.435	0.000	0.194	1.593	0.000	0.185	1.632	0.000	0.182	1.558
0.000	0.187	0.001	0.326	1.413	0.017	0.187	1.554	0.017	0.176	1.580	0.021	0.185	1.523
0.001	0.182	0.002	0.308	1.386	0.036	0.177	1.517	0.036	0.164	1.530	0.042	0.182	1.467
0.012	0.172	0.021	0.286	1.360	0.057	0.165	1.478	0.055	0.150	1.480	0.064	0.177	1.415
0.025	0.161	0.042	0.263	1.334	0.078	0.153	1.439	0.074	0.137	1.433	0.087	0.168	1.367
0.039	0.149	0.064	0.241	1.309	0.099	0.141	1.403	0.092	0.124	1.390	0.112	0.158	1.326
0.050	0.139	0.080	0.221	1.286	0.118	0.126	1.377	0.108	0.109	1.359	0.134	0.142	1.299
0.059	0.130	0.092	0.203	1.266	0.139	0.118	1.342	0.125	0.100	1.321	0.158	0.134	1.262
0.073	0.121	0.113	0.187	1.247	0.158	0.109	1.311	0.141	0.092	1.289	0.181	0.125	1.230
0.089	0.112	0.137	0.173	1.230	0.175	0.101	1.284	0.155	0.085	1.261	0.202	0.117	1.203
1.000	0.000	—	—	—	1.163	0.000	0.000	1.166	0.000	0.000	1.196	0.000	0.000

Table 6.30 x-q Fit of IAST Model Using Toth, Unilan and Virial Isotherms for the Ternary System Methane-Ethane-Ethylene on SR-115 Zeolite at 325 K and 200 kPa (High Ethylene Loading)

		Experimental			IAST with Toth			IAST with Unilan			IAST with Virial		
x_{CH_4}	$x_{C_2H_6}$	q_{CH_4}	$q_{C_2H_6}$	$q_{C_2H_4}$	q_{CH_4}	$q_{C_2H_6}$	$q_{C_2H_4}$	q_{CH_4}	$q_{C_2H_6}$	$q_{C_2H_4}$	q_{CH_4}	$q_{C_2H_6}$	$q_{C_2H_4}$
0.000	0.000	—	—	—	0.000	0.000	1.763	0.000	0.000	1.775	0.000	0.000	1.737
0.000	0.038	0.000	0.067	1.673	0.000	0.030	1.717	0.000	0.030	1.722	0.000	0.033	1.686
0.006	0.039	0.010	0.066	1.625	0.011	0.029	1.664	0.010	0.028	1.651	0.009	0.032	1.627
0.020	0.037	0.033	0.061	1.572	0.023	0.027	1.608	0.021	0.025	1.578	0.020	0.031	1.569
0.038	0.034	0.062	0.056	1.516	0.036	0.025	1.552	0.032	0.023	1.510	0.033	0.029	1.513
0.046	0.031	0.072	0.050	1.465	0.049	0.023	1.496	0.043	0.021	1.446	0.047	0.028	1.460
0.056	0.029	0.087	0.045	1.418	0.062	0.021	1.444	0.054	0.018	1.390	0.062	0.025	1.411
0.076	0.026	0.117	0.041	1.376	0.076	0.019	1.394	0.065	0.016	1.339	0.077	0.023	1.365
0.093	0.024	0.140	0.037	1.337	0.088	0.016	1.354	0.074	0.014	1.300	0.091	0.020	1.329
0.102	0.022	0.152	0.033	1.302	0.100	0.015	1.313	0.083	0.012	1.261	0.105	0.019	1.291
0.110	0.021	0.161	0.031	1.270	0.111	0.013	1.278	0.091	0.011	1.228	0.119	0.016	1.258
1.000	0.000	—	—	—	0.763	0.000	0.000	0.776	0.000	0.000	0.813	0.000	0.000

Table 6.31 x-q Fit of IAST Model Using Toth, Unilan and Virial Isotherms for the Ternary System Methane-Ethane-Ethylene on ETS-10 Zeolite at 325 K and 200 kPa (High Ethane Loading)

		Experimental			IAST with Toth			IAST with Unilan			IAST with Virial		
x_{CH_4}	$x_{C_2H_6}$	q_{CH_4}	$q_{C_2H_6}$	$q_{C_2H_4}$	q_{CH_4}	$q_{C_2H_6}$	$q_{C_2H_4}$	q_{CH_4}	$q_{C_2H_6}$	$q_{C_2H_4}$	q_{CH_4}	$q_{C_2H_6}$	$q_{C_2H_4}$
0.000	0.000	—	—	—	0.000	0.000	1.763	0.000	0.000	1.775	0.000	0.000	1.737
0.000	0.292	0.000	0.486	1.182	0.000	0.363	1.267	0.000	0.347	1.260	0.000	0.406	1.188
0.002	0.288	0.003	0.470	1.162	0.021	0.337	1.222	0.019	0.313	1.209	0.019	0.384	1.139
0.013	0.273	0.020	0.435	1.138	0.042	0.308	1.179	0.037	0.279	1.163	0.040	0.356	1.098
0.027	0.256	0.042	0.397	1.114	0.063	0.277	1.141	0.055	0.245	1.123	0.062	0.325	1.065
0.052	0.235	0.079	0.360	1.091	0.084	0.245	1.110	0.071	0.213	1.092	0.084	0.292	1.039
0.080	0.215	0.121	0.327	1.070	0.103	0.221	1.074	0.086	0.190	1.058	0.106	0.268	1.008
0.086	0.202	0.127	0.297	1.050	0.120	0.195	1.051	0.099	0.166	1.037	0.126	0.240	0.990
0.102	0.187	0.148	0.271	1.032	0.138	0.177	1.017	0.113	0.149	1.007	0.148	0.221	0.960
0.115	0.173	0.164	0.247	1.015	0.151	0.160	0.996	0.123	0.135	0.989	0.165	0.203	0.943
0.120	0.163	0.167	0.227	1.000	0.164	0.143	0.980	0.132	0.120	0.975	0.181	0.183	0.930
1.000	0.000	—	—	—	0.763	0.000	0.000	0.776	0.000	0.000	0.813	0.000	0.000

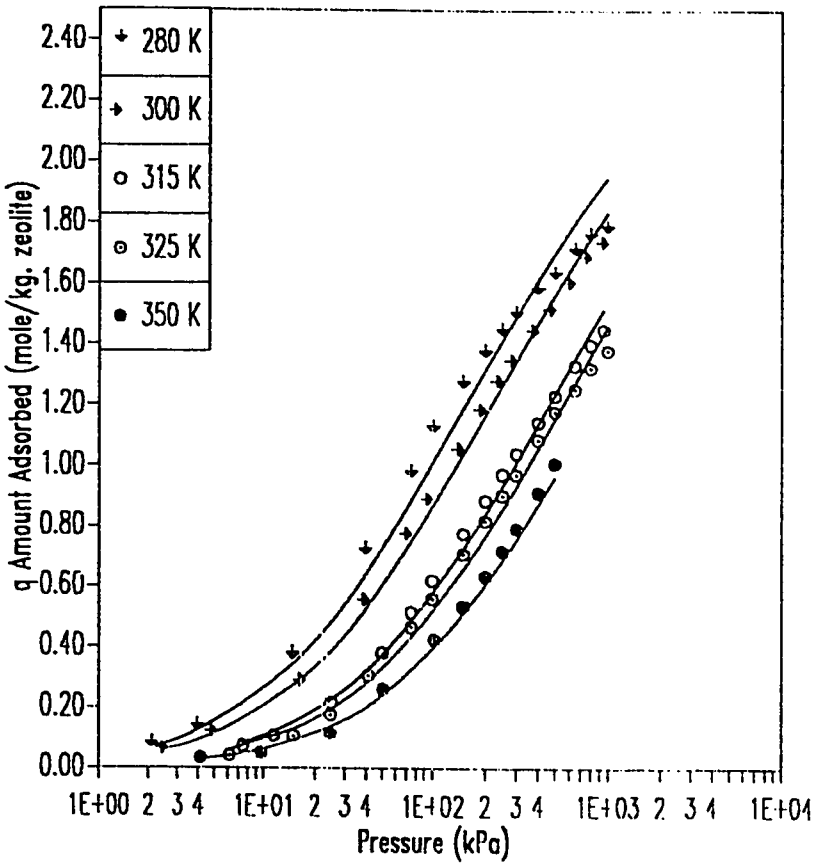

Figure 6.1 Isotherms of Methane on ETS-10 Zeolite:
Fit of Toth Model (—)

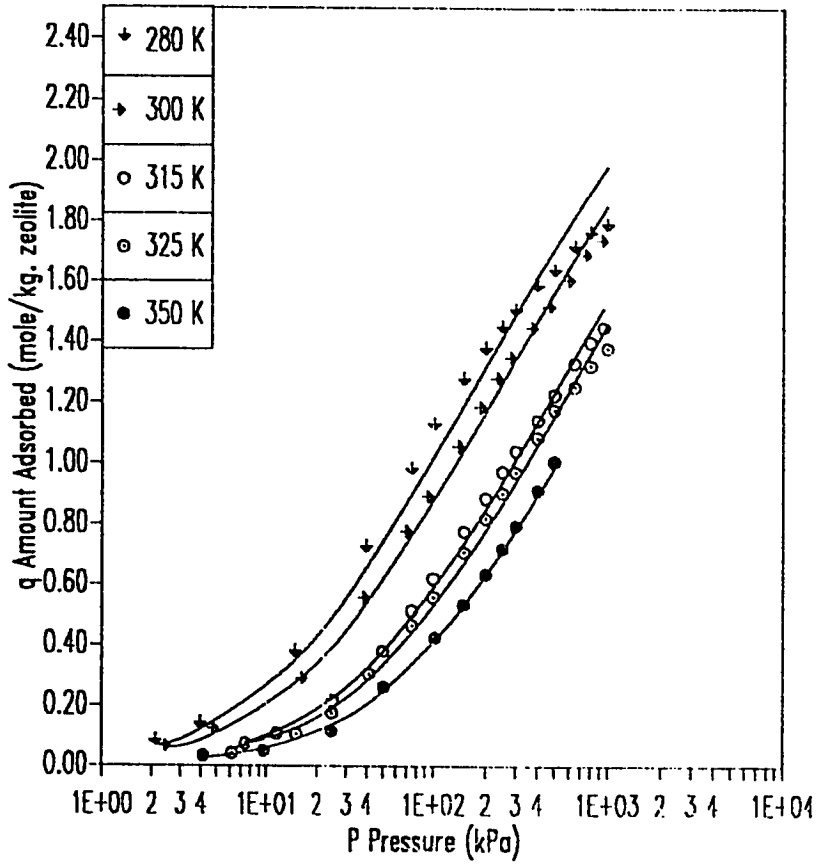

Figure 6.2 Isotherms of Methane on ETS-10 Zeolite:
Fit of Unilan Model (—)

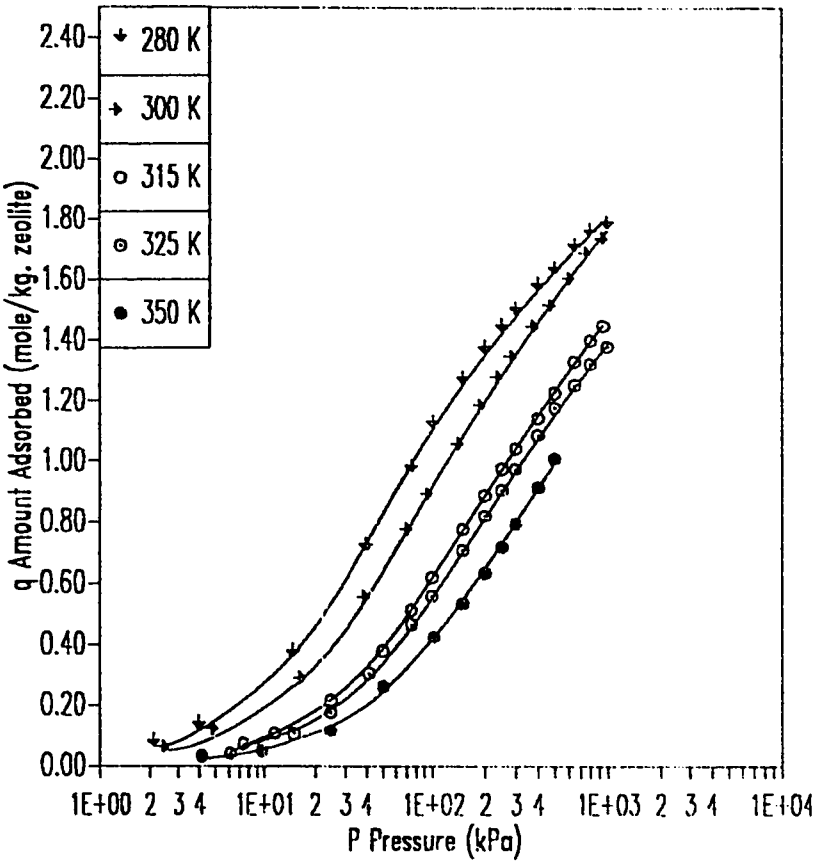

Figure 6.3 Isotherms of Methane on ETS-10 Zeolite:
Fit of Virial Three Constant Model (—)

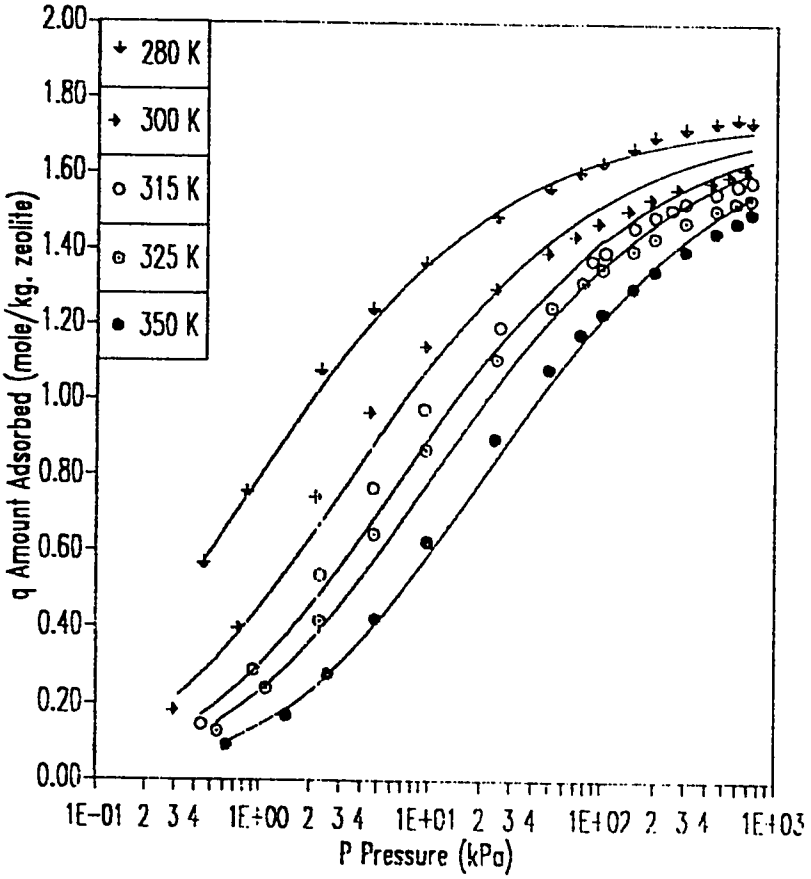

Figure 6.4 Isotherms of Ethane on ETS-10 Zeolite:
Fit of Toth Model (—)

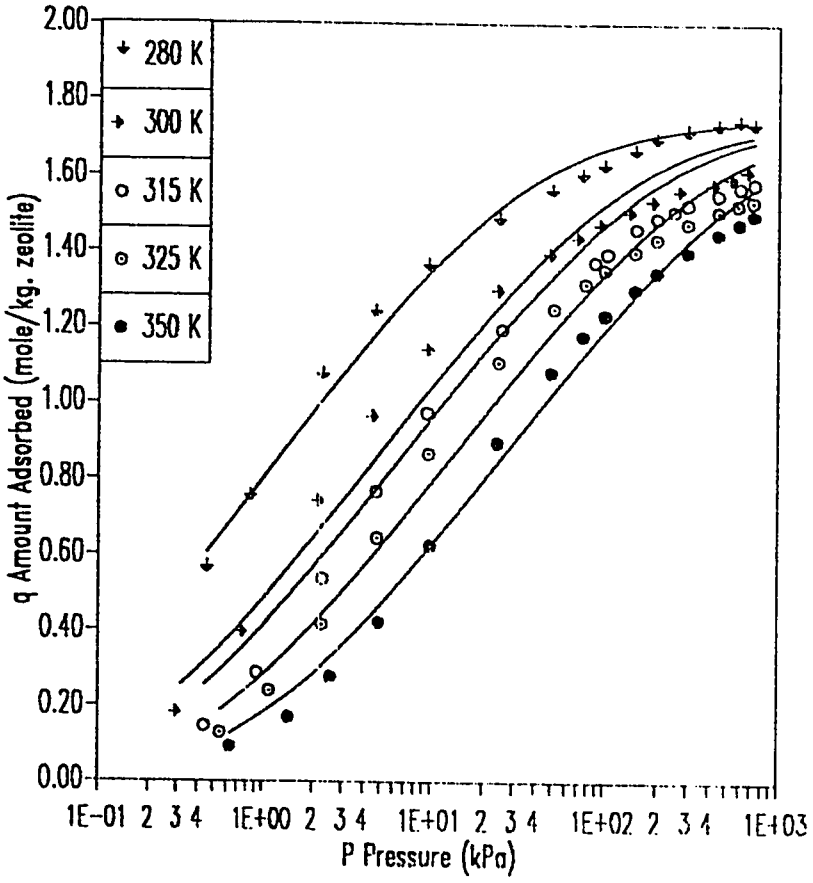

Figure 6.5 Isotherms of Ethane on ETS-10 Zeolite:
Fit of Unilan Model (—)

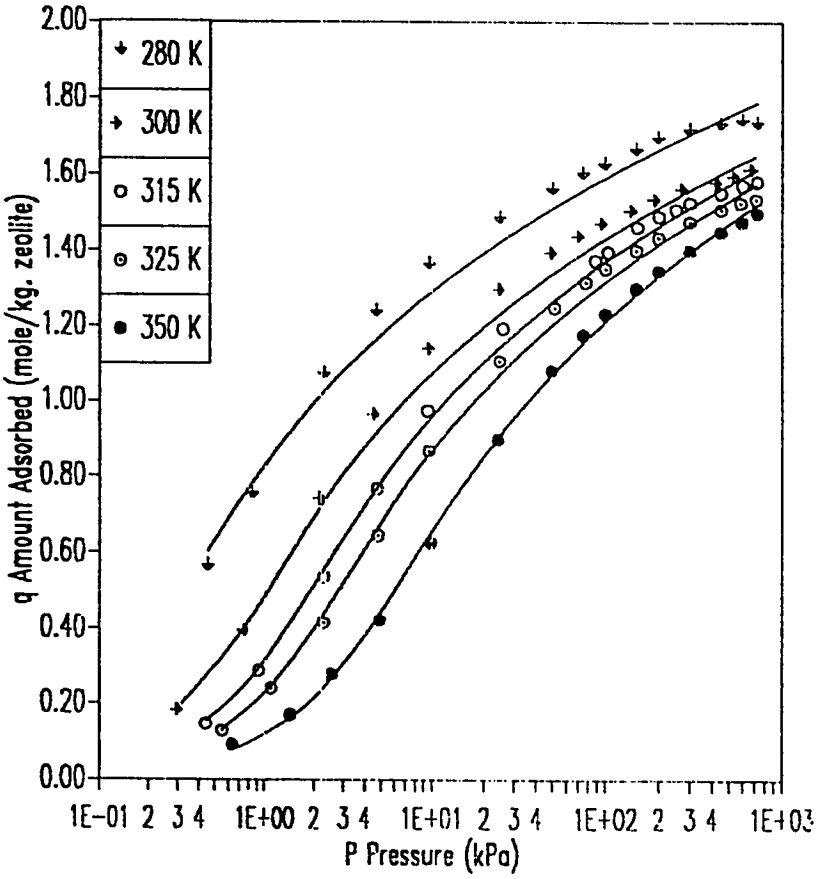

Figure 6.6 Isotherms of Ethane on ETS-10 Zeolite:
Fit of Virial Three Constant Model (—)

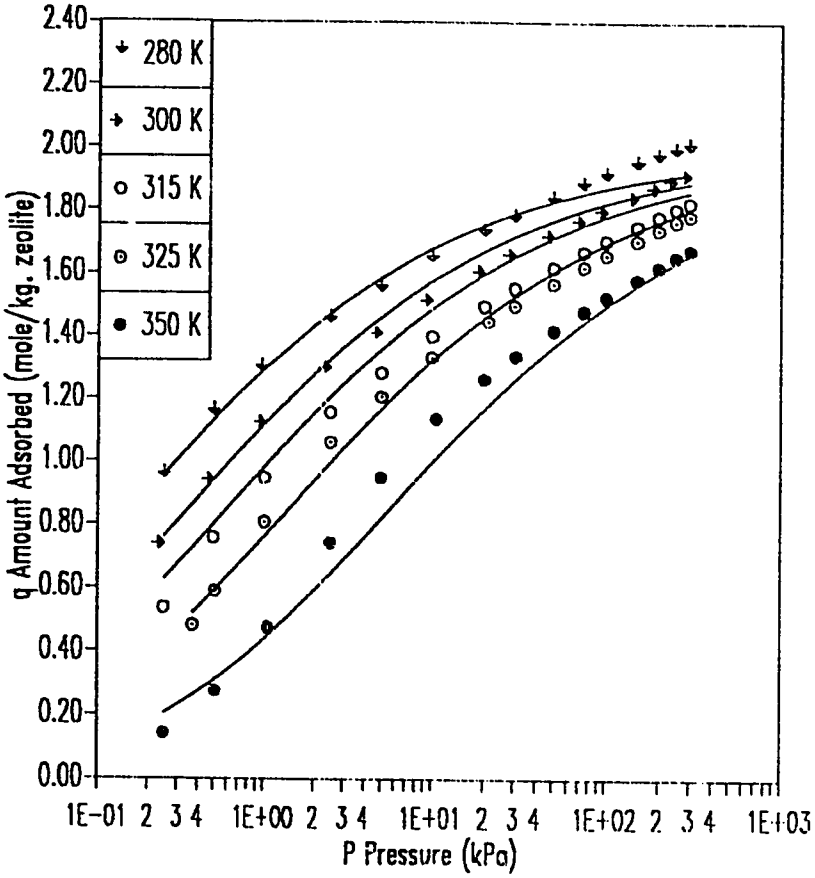

Figure 6.7 Isotherms of Ethylene on ETS-10 Zeolite:
Fit of Toth Model (—)

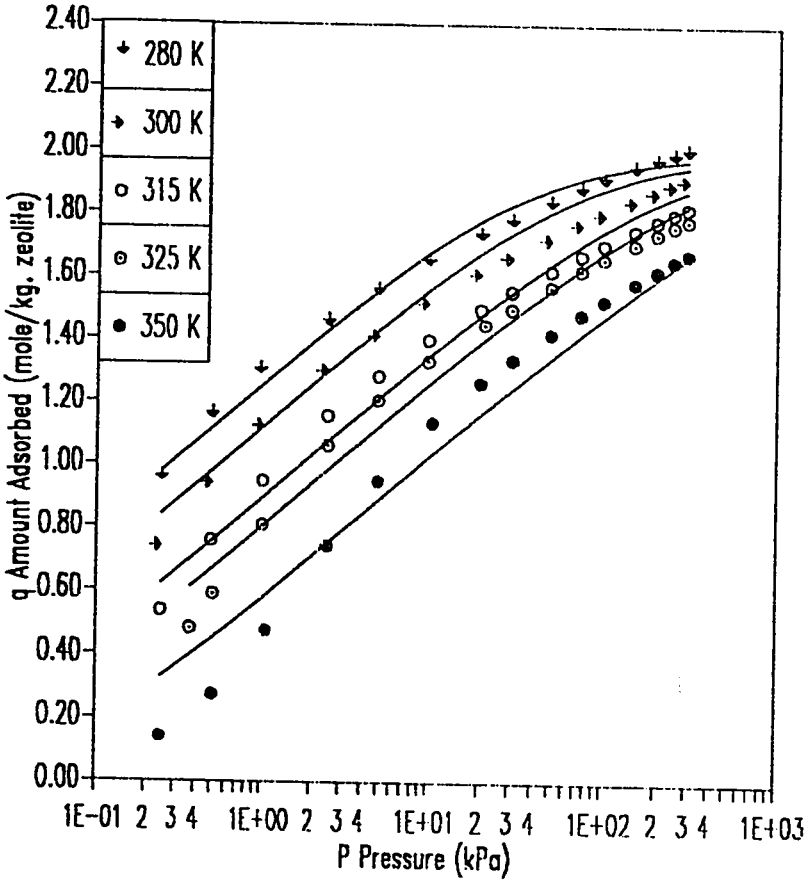

Figure 6.8 Isotherms of Ethylene on ETS-10 Zeolite:
Fit of Unilan Model (—)

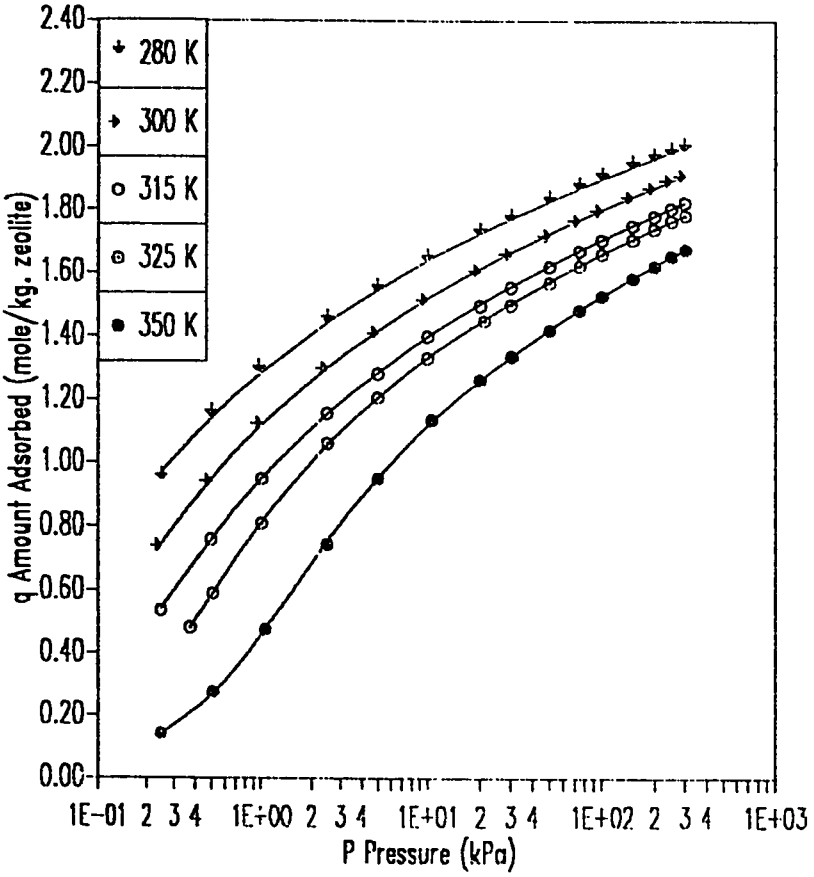

Figure 6.9 Isotherms of Ethylene on ETS-10 Zeolite:
Fit of Virial Three Constant Model (—)

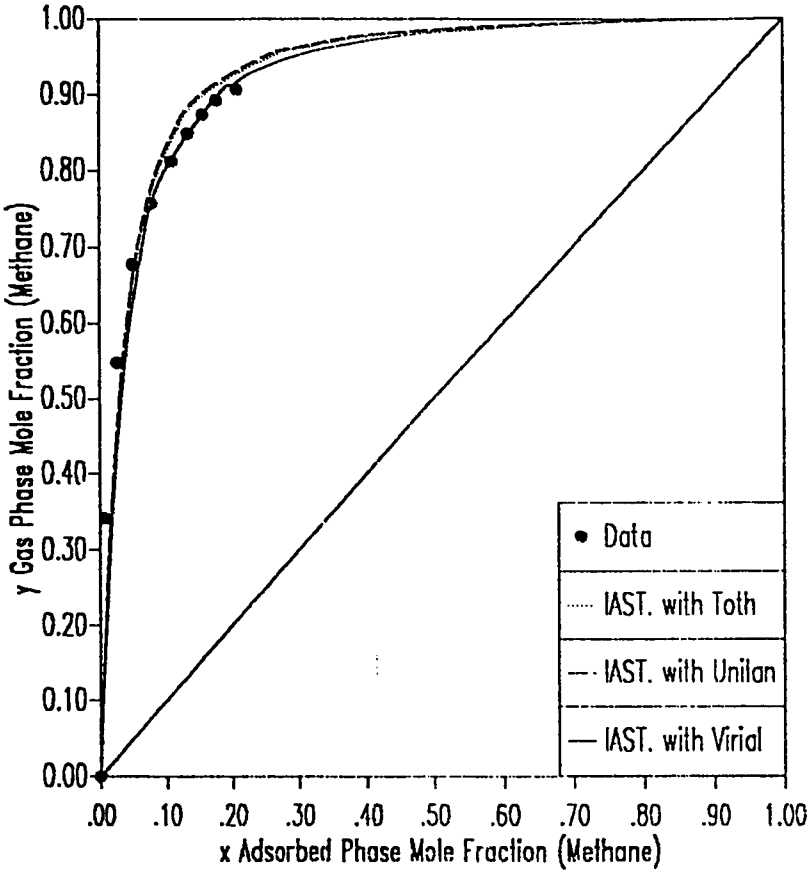

Figure 6.10 x-y Diagram for Methane-Ethane on ETS-10 Zeolite at 280 K and 150 kPa
Fit of IAST Model Using Toth, Unilan and Virial Three Constant Isotherms

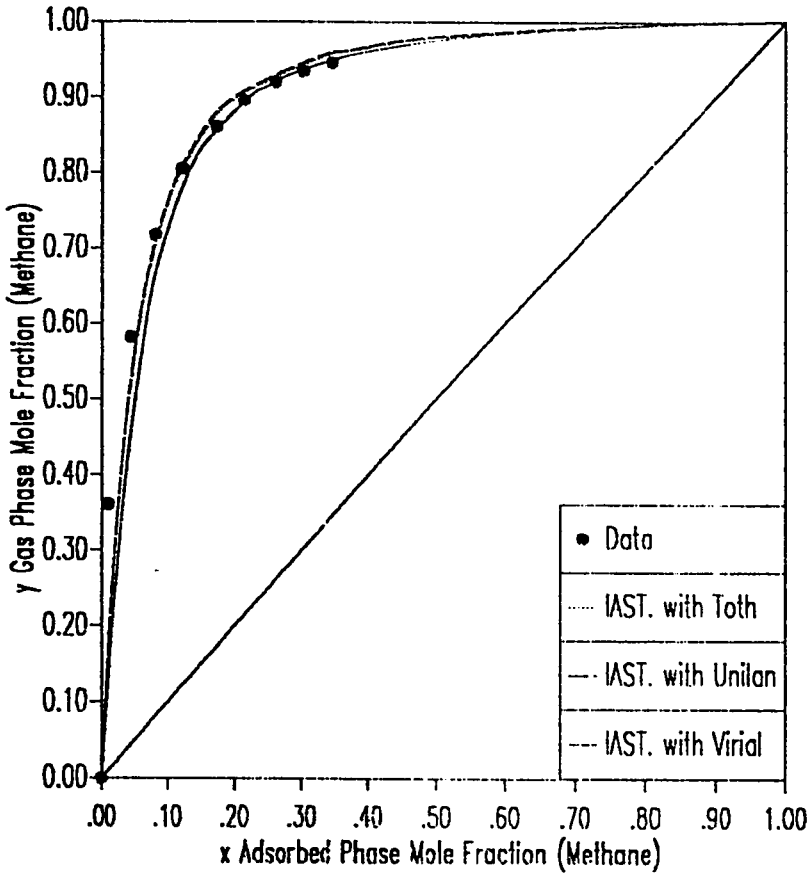

Figure 6.11 x-y Diagram for Methane-Ethane on ETS-10 Zeolite
at 280 K and 500 kPa
Fit of IAST Model Using Toth, Unilan and Virial Three Constant
Isotherms

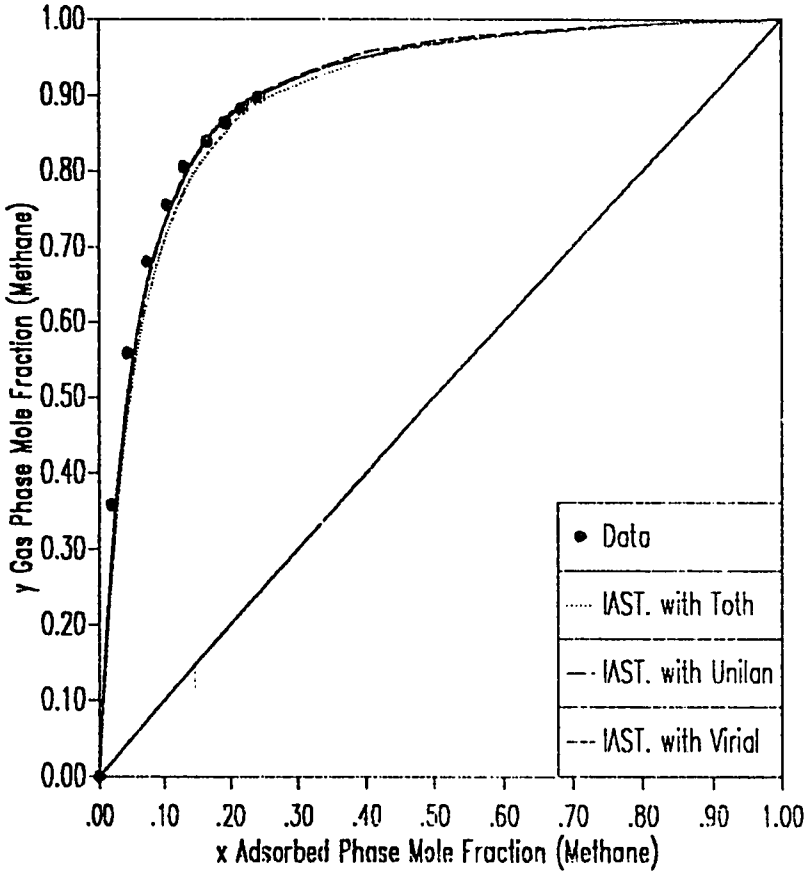

Figure 6.12 x-y Diagram for Methane-Ethane on ETS-10 Zeolite
at 325 K and 150 kPa
Fit of IAST Model Using Toth, Unilan and Virial Three Constant
Isotherms

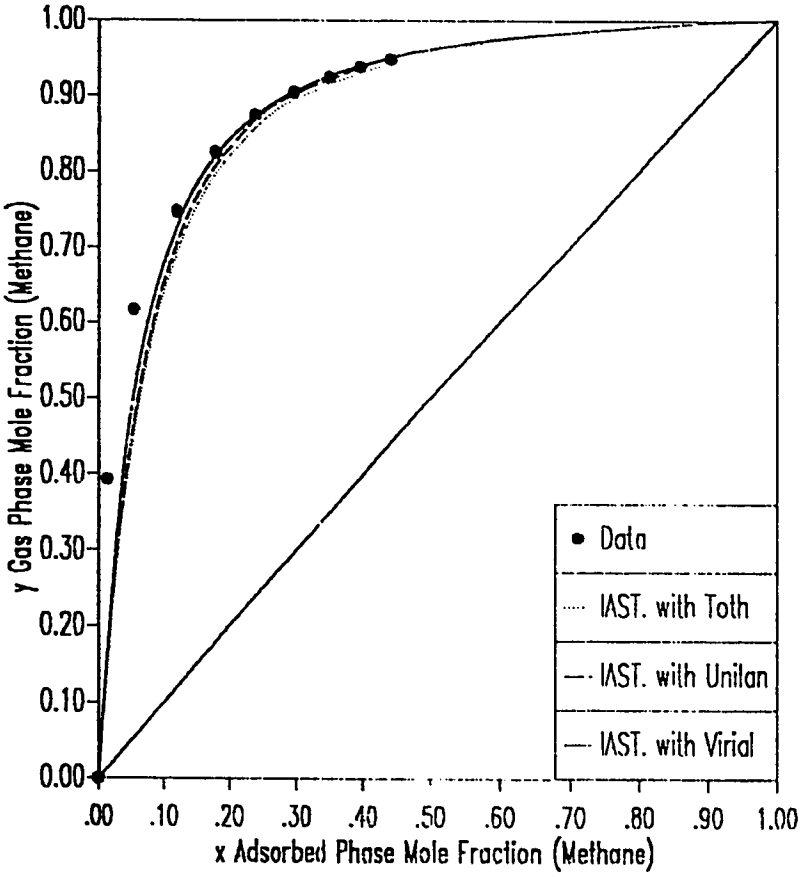

Figure 6.13 x-y Diagram for Methane-Ethane on ETS-10 Zeolite
at 325 K and 500 kPa
Fit of IAST Model Using Toth, Unilan and Virial Three Constant
Isotherms

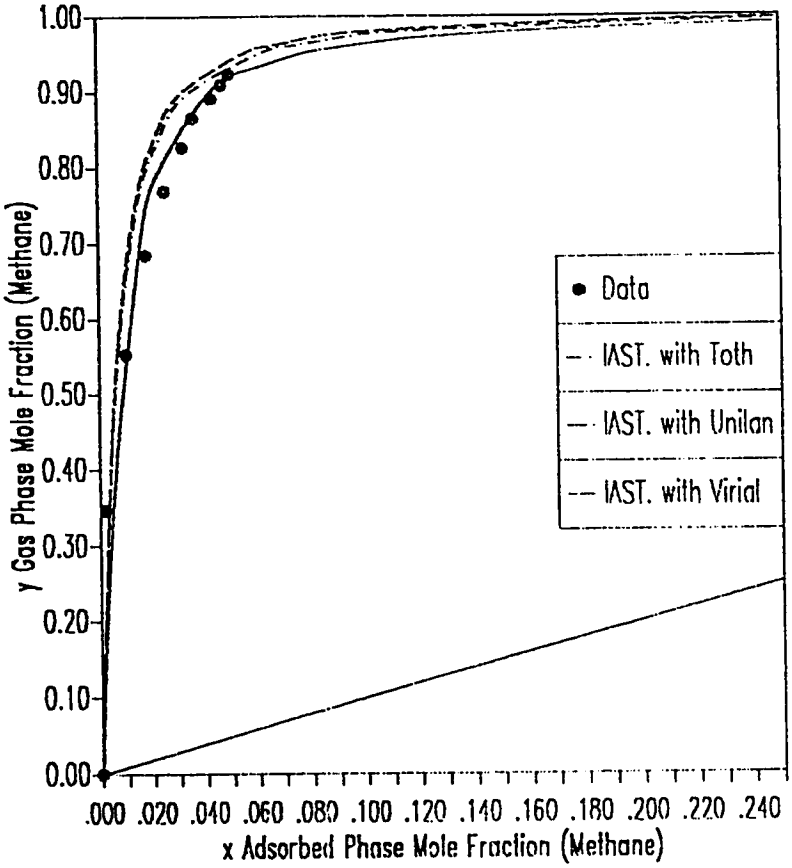

Figure 6.14 x-y Diagram for Methane-Ethylene on ETS-10 Zeolite at 280 K and 150 kPa
Fit of IAST Model Using Toth, Unilan and Virial Three Constant Isotherms

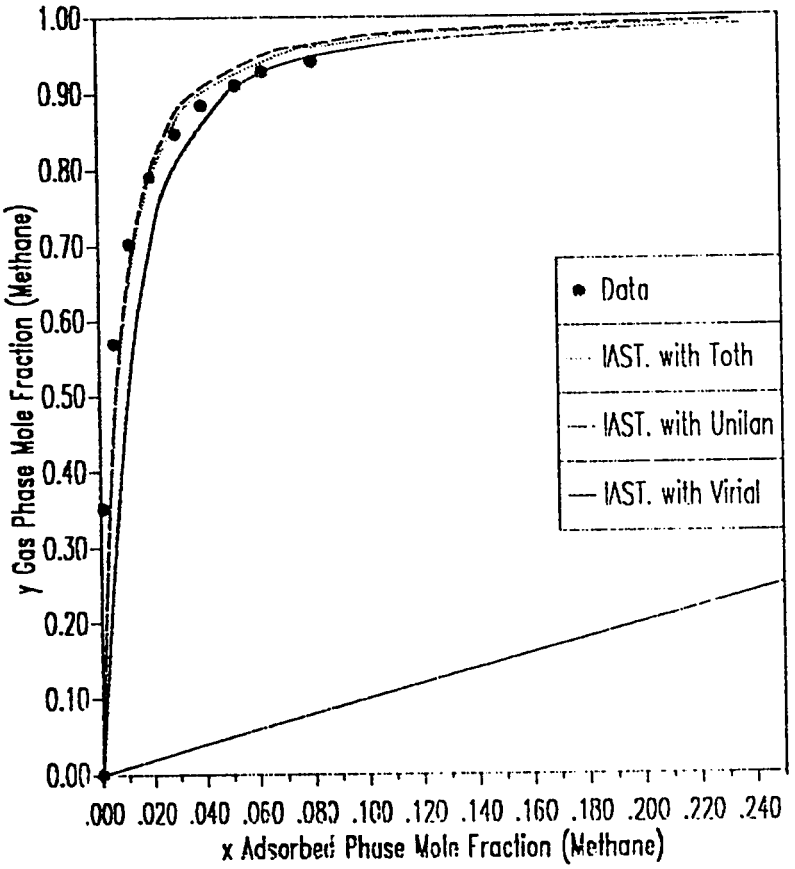

Figure 6.15 x-y Diagram for Methane-Ethylene on ETS-10 Zeolite at 280 K and 250 kPa
Fit of IAST Model Using Toth, Unilan and Virial Three Constant Isotherms

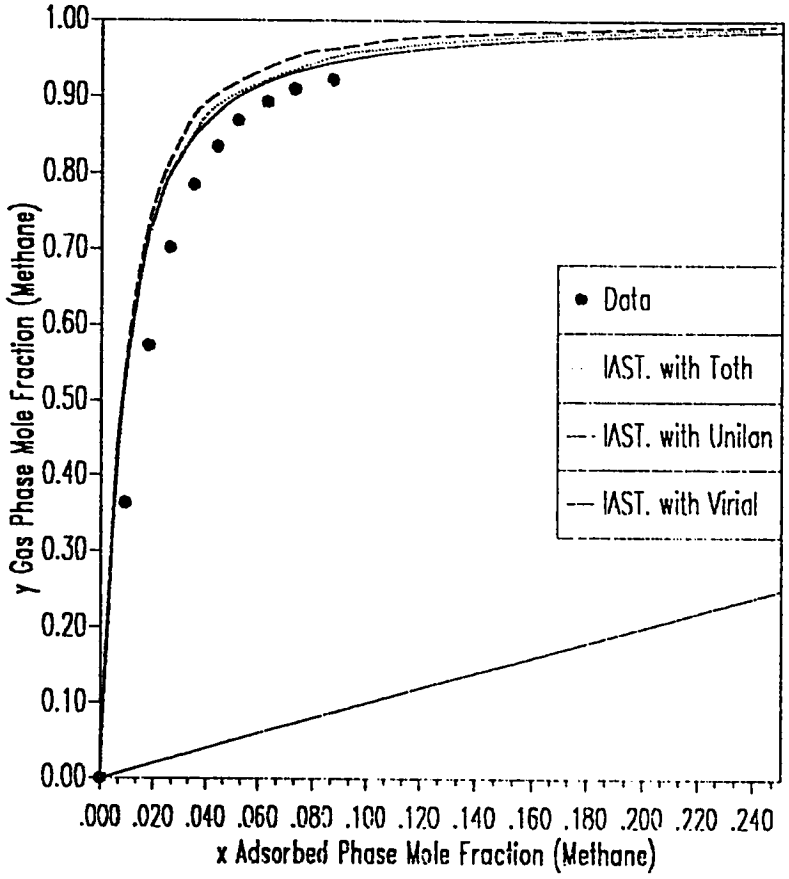

Figure 6.16 x-y Diagram for Methane-Ethylene on ETS-10 Zeolite
at 325 K and 150 kPa
Fit of IAST Model Using Toth, Unilan and Virial Three Constant
Isotherms

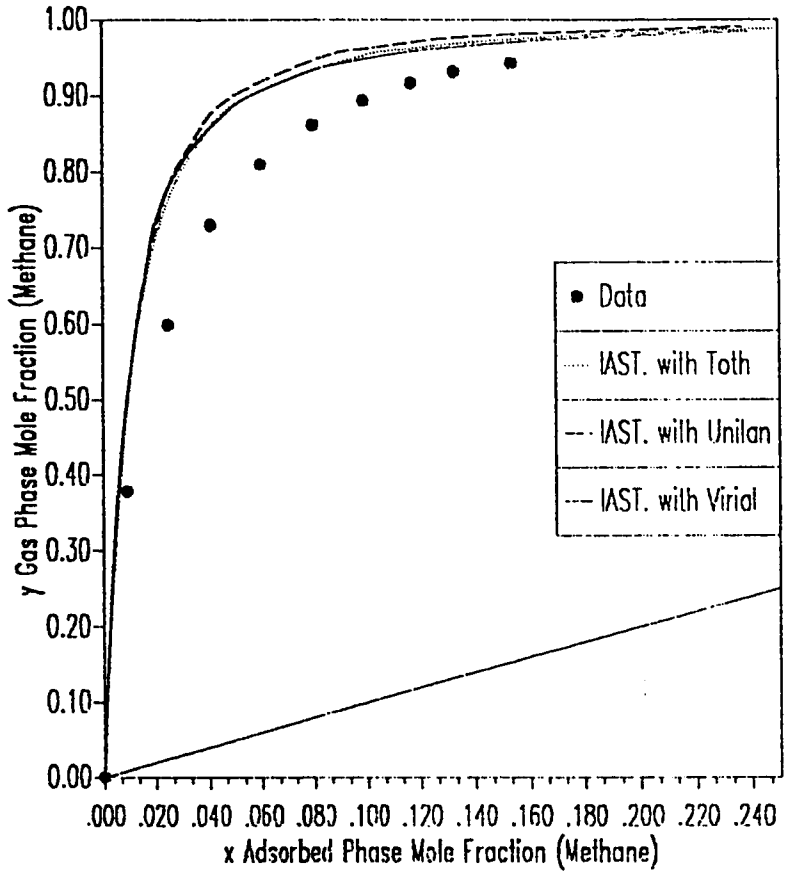

Figure 6.17 x-y Diagram for Methane-Ethylene on ETS-10 Zeolite
at 325 K and 250 kPa
Fit of IAST Model Using Toth, Unilan and Virial Three Constant
Isotherms

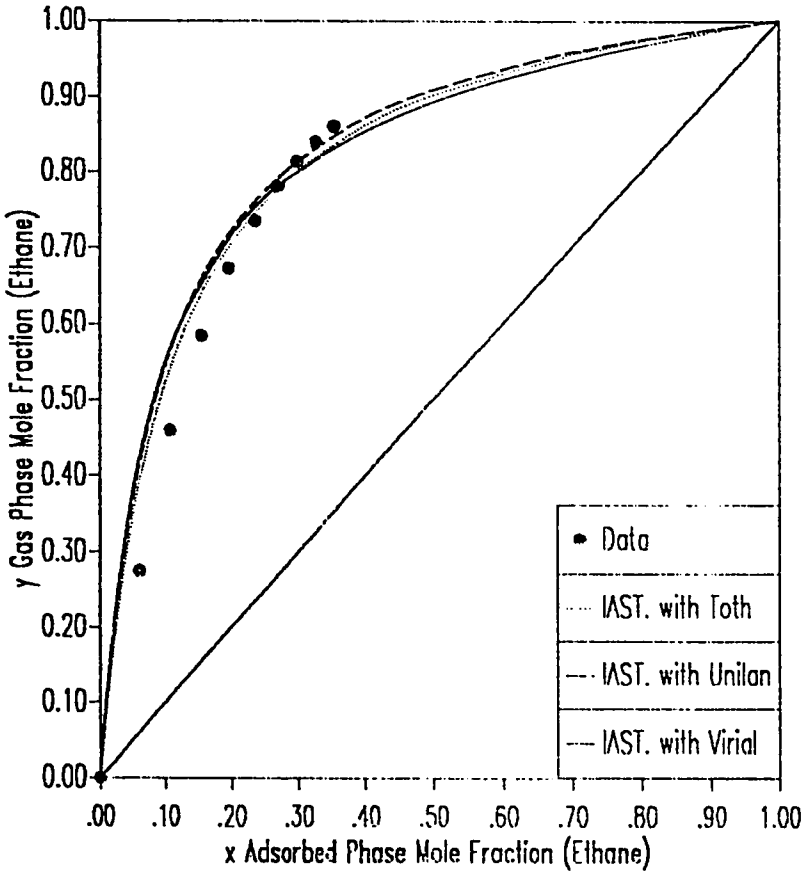

Figure 6.18 x-y Diagram for Ethane-Ethylene on ETS-10 Zeolite
at 280 K and 150 kPa
Fit of IAST Model Using Toth, Unilan and Virial Three Constant
Isotherms

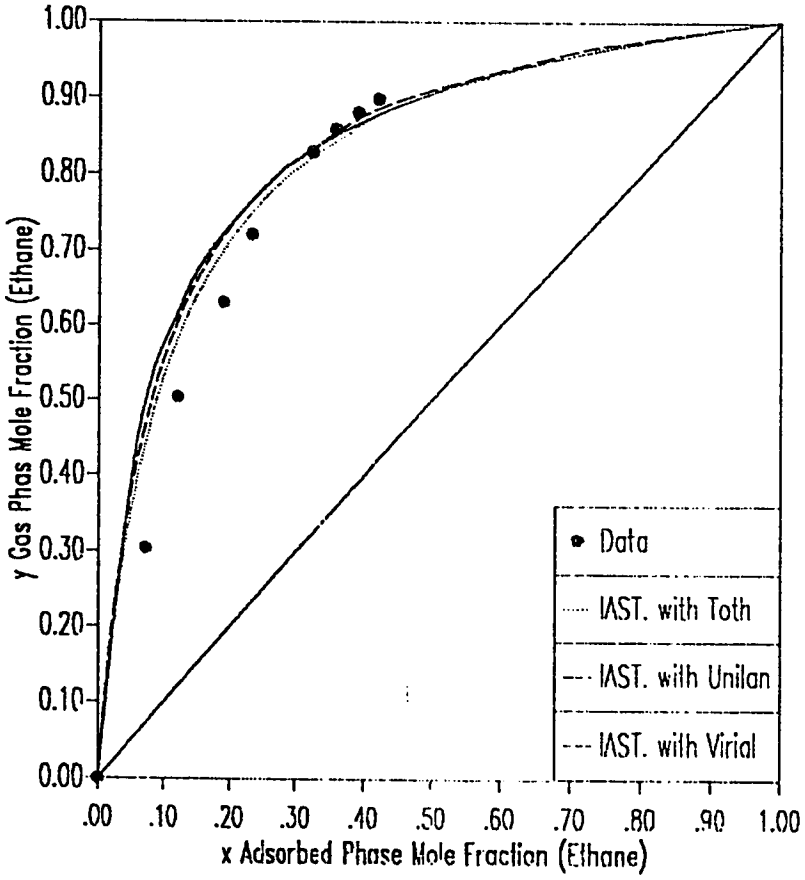

Figure 6.19 x-y Diagram for Ethane-Ethylene on ETS-10 Zeolite
at 280 K and 250 kPa
Fit of IAST Model Using Toth, Unilan and Virial Three Constant
Isotherms

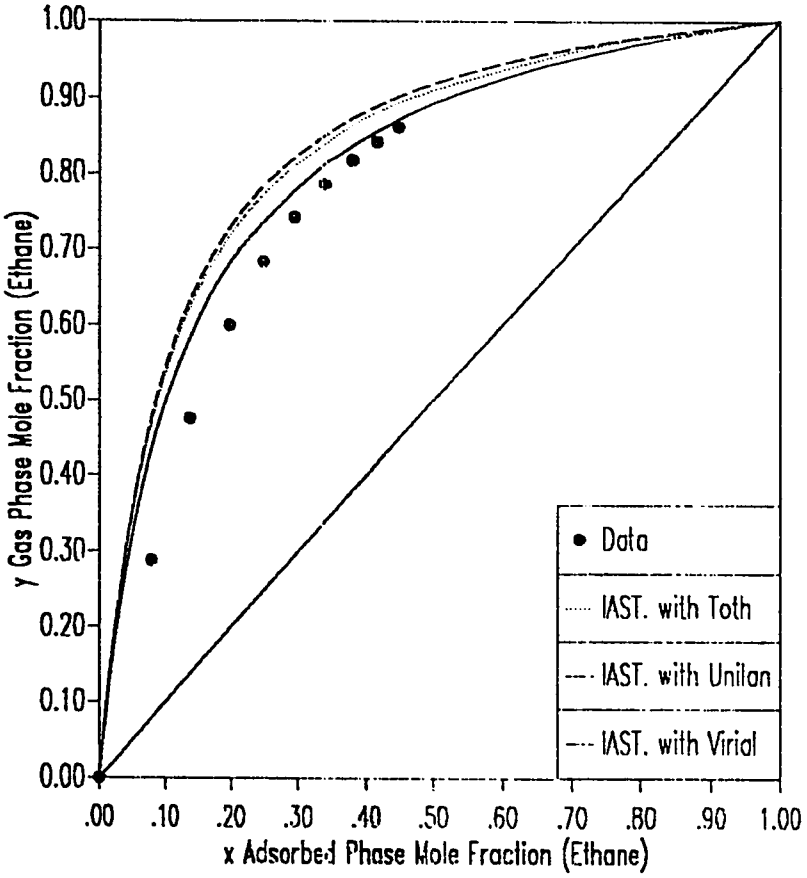

Figure 6.20 x-y Diagram for Ethane-Ethylene on ETS-10 Zeolite
at 325 K and 150 kPa
Fit of IAST Model Using Toth, Unilan and Virial Three Constant
Isotherms

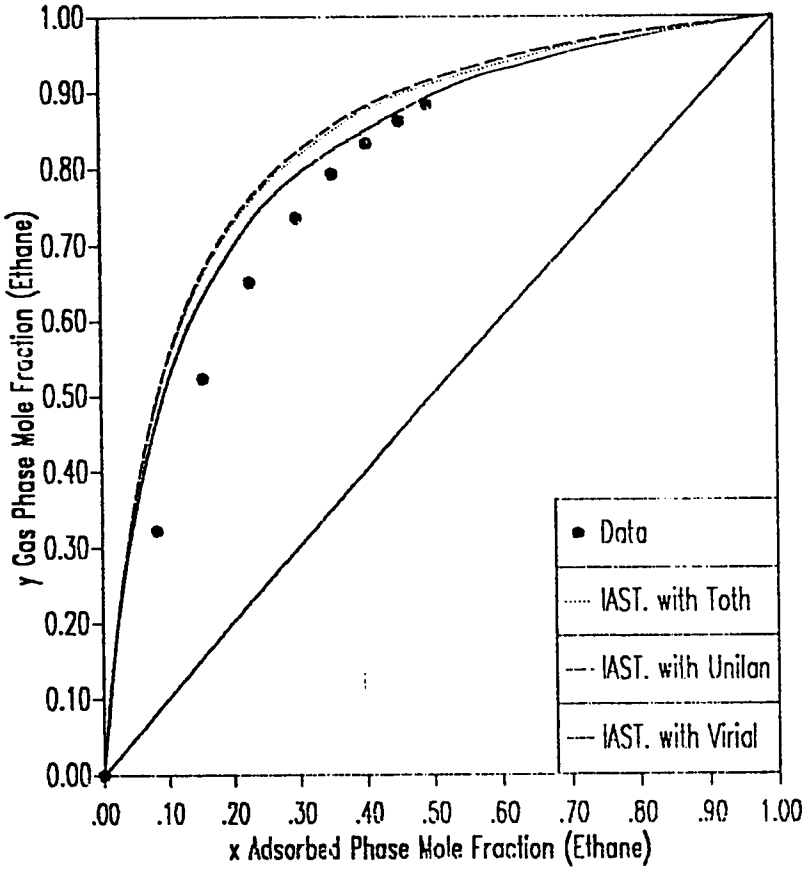

Figure 6.21 x-y Diagram for Ethane-Ethylene on ETS-10 Zeolite
at 325 K and 250 kPa
Fit of IAST Model Using Toth, Unilan and Virial Three Constant
Isotherms

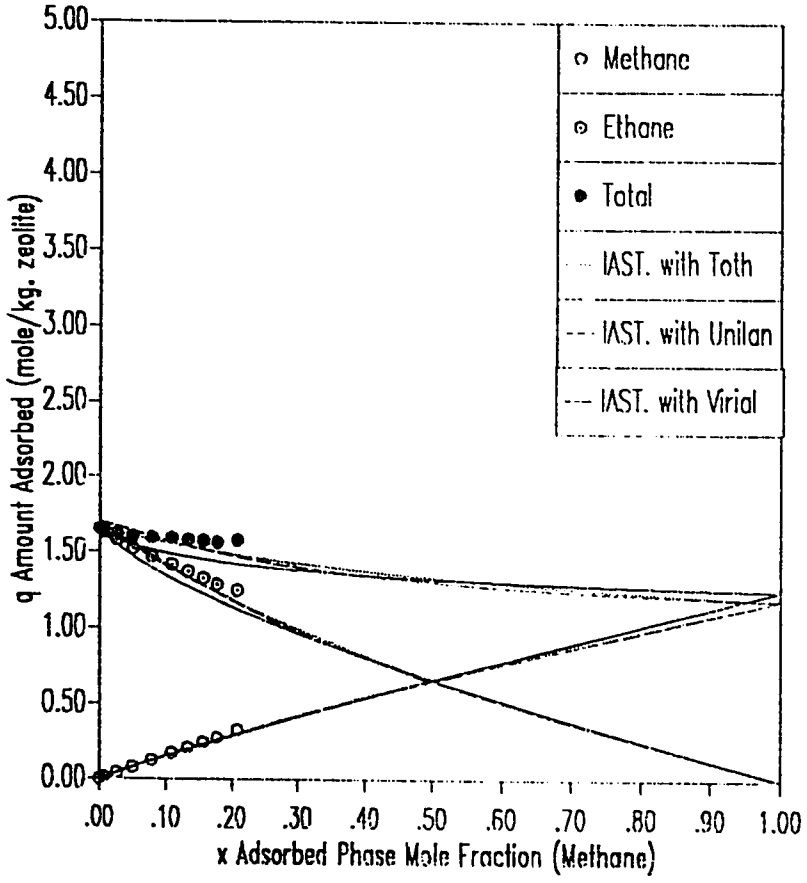

Figure 6.22 x-q Diagram for Methane-Ethane on ETS-10 Zeolite
at 280 K and 150 kPa
Fit of IAST Model Using Toth, Unilan and Virial Three Constant
Isotherms

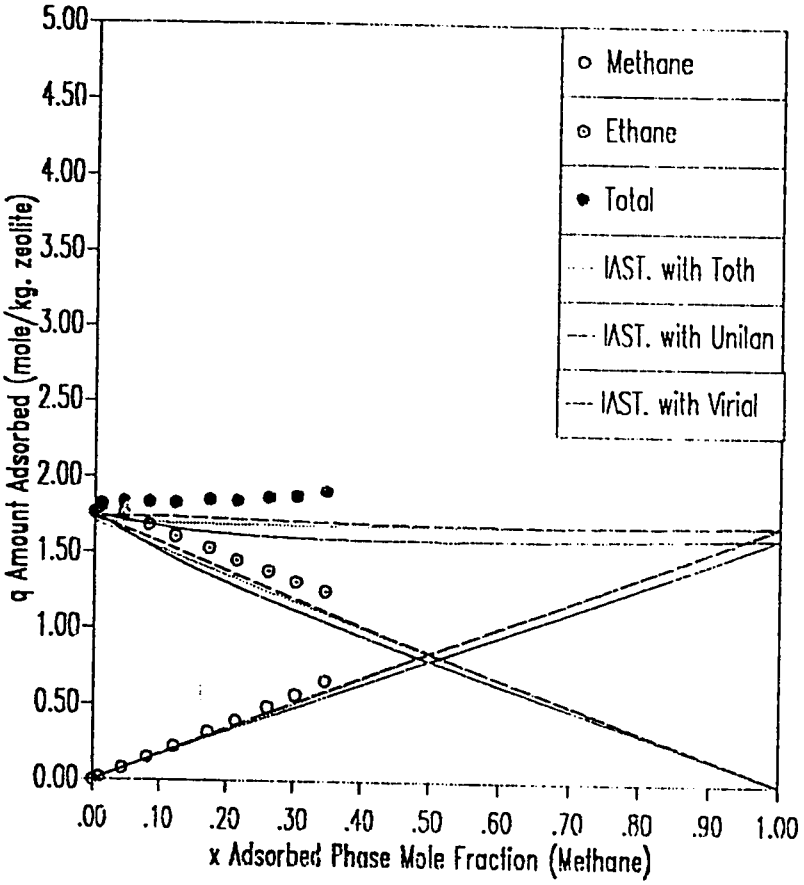

Figure 6.23 x-q Diagram for Methane-Ethane on ETS-10 Zeolite at 280 K and 500 kPa
Fit of IAST Model Using Toth, Unilan and Virial Three Constant Isotherms

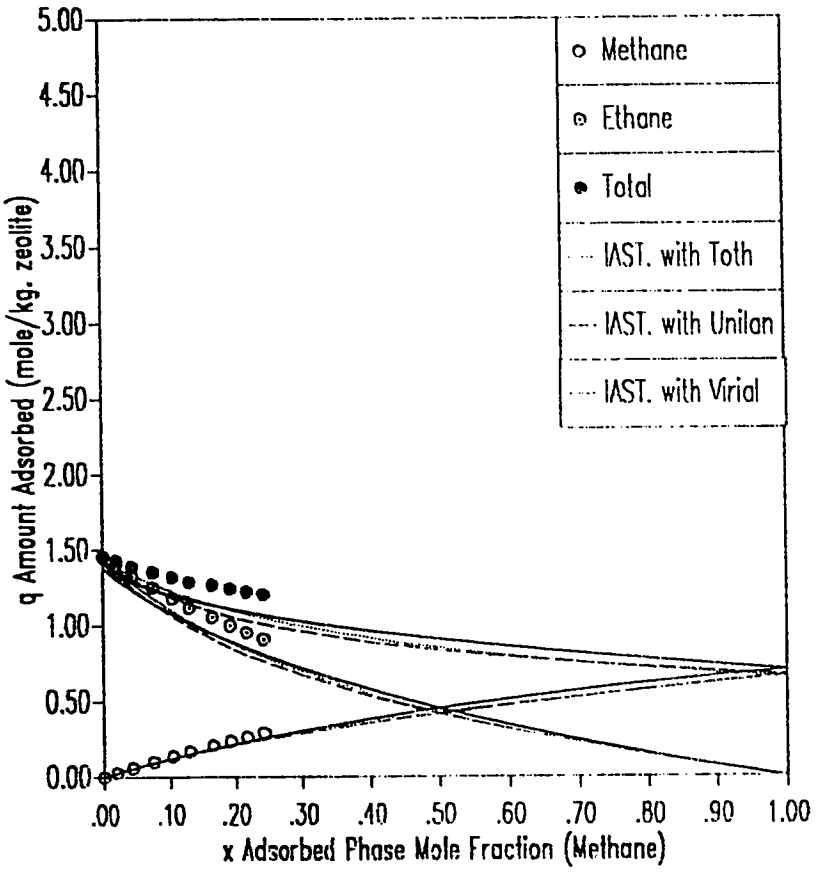

Figure 6.24 x-q Diagram for Methane-Ethane on ETS-10 Zeolite
at 325 K and 150 kPa
Fit of IAST Model Using Toth, Unilan and Virial Three Constant
Isotherms

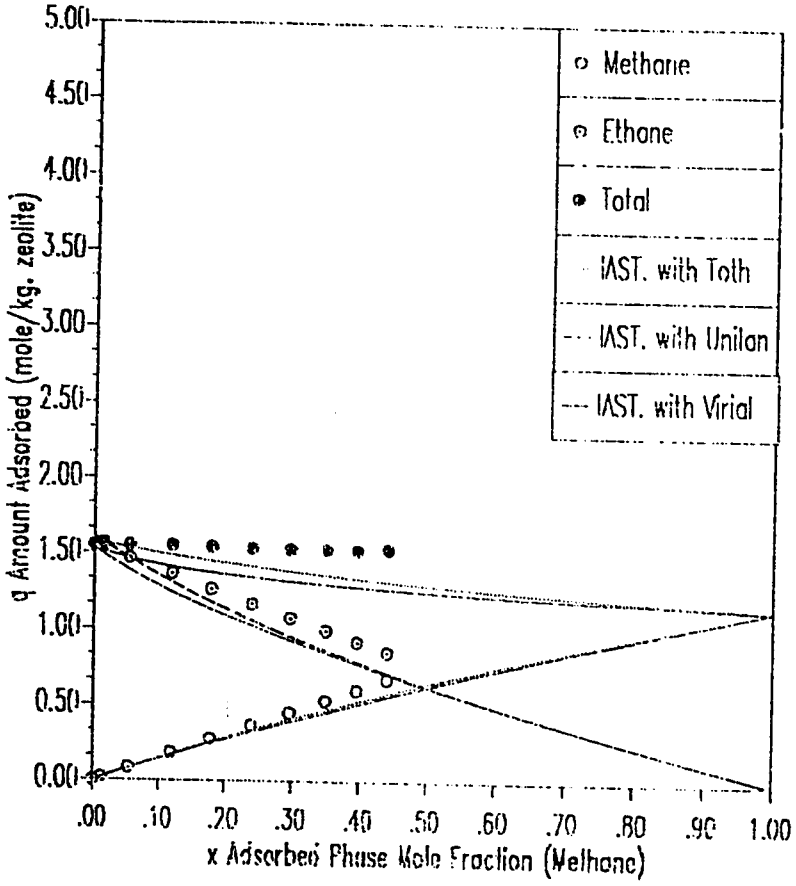

Figure 6.25 x-q Diagram for Methane-Ethane on ETS-10 Zeolite
at 325 K and 500 kPa
Fit of IAST Model Using Toth, Unilan and Virial Three Constant
Isotherms

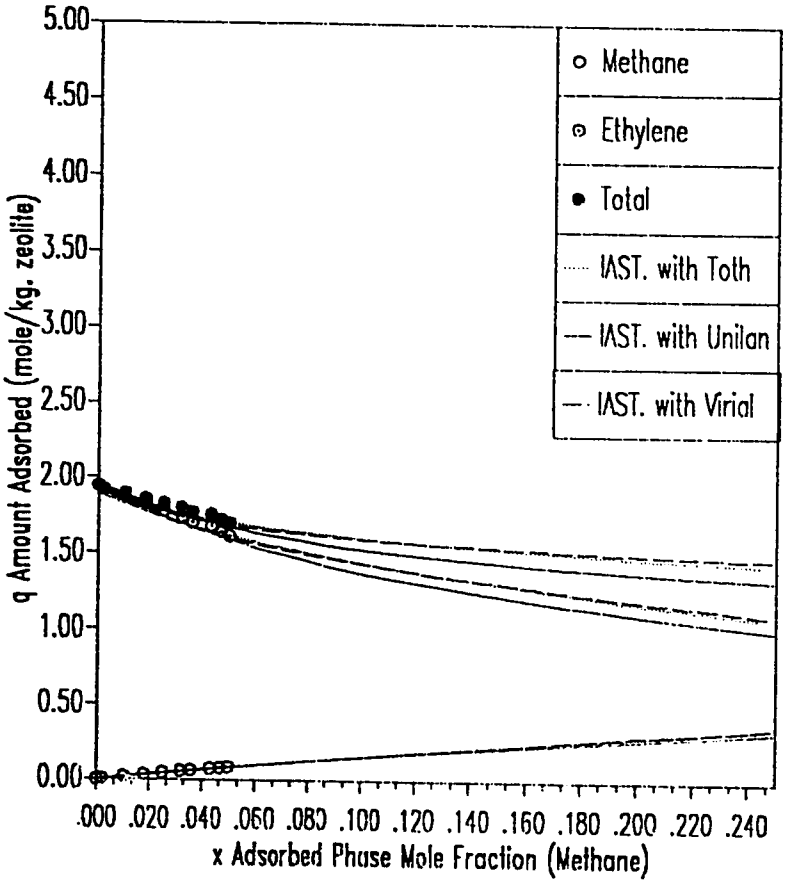

Figure 6.26 x-q Diagram for Methane-Ethylene on ETS-10 Zeolite at 280 K and 150 kPa
Fit of IAST Model Using Toth, Unilan and Virial Three Constant Isotherms

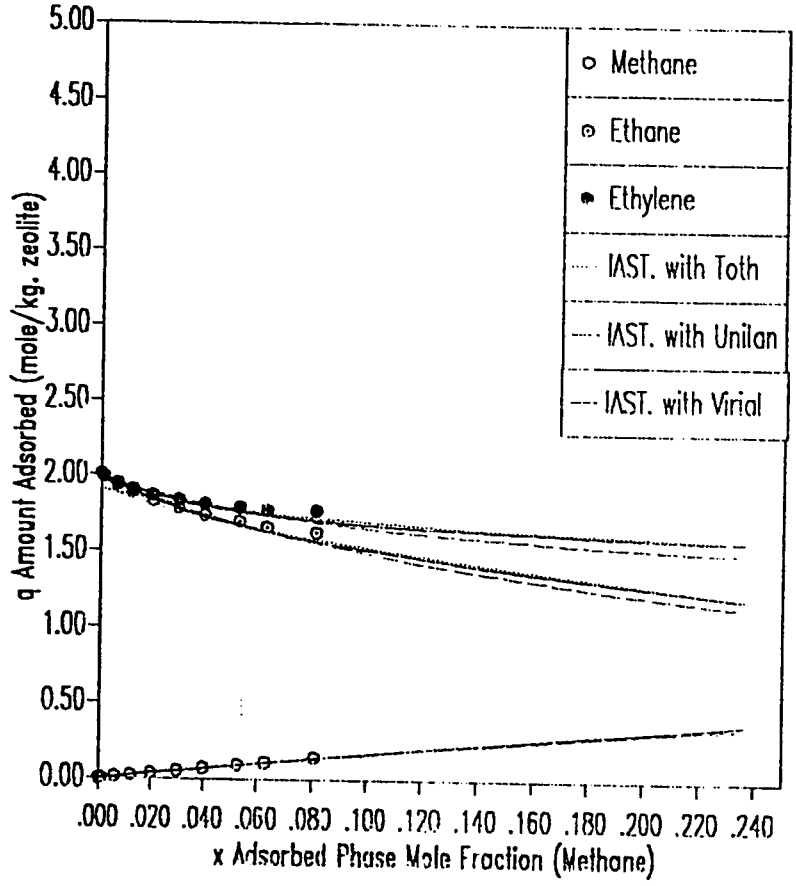

Figure 6.27 x-q Diagram for Methane-Ethylene on ETS-10 Zeolite at 280 K and 250 kPa
Fit of IAST Model Using Toth, Unilan and Virial Three Constant Isotherms

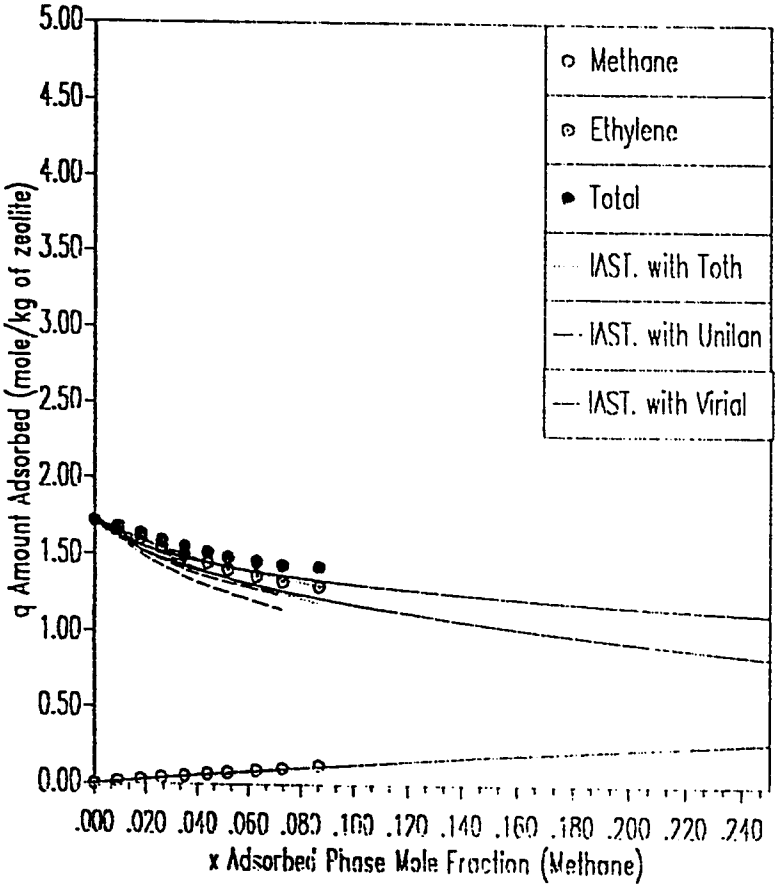

Figure 6.28 x-q Diagram for Methane-Ethylene on ETS-10 Zeolite at 325 K and 150 kPa
Fit of IAST Model Using Toth, Unilan and Virial Three Constant Isotherms

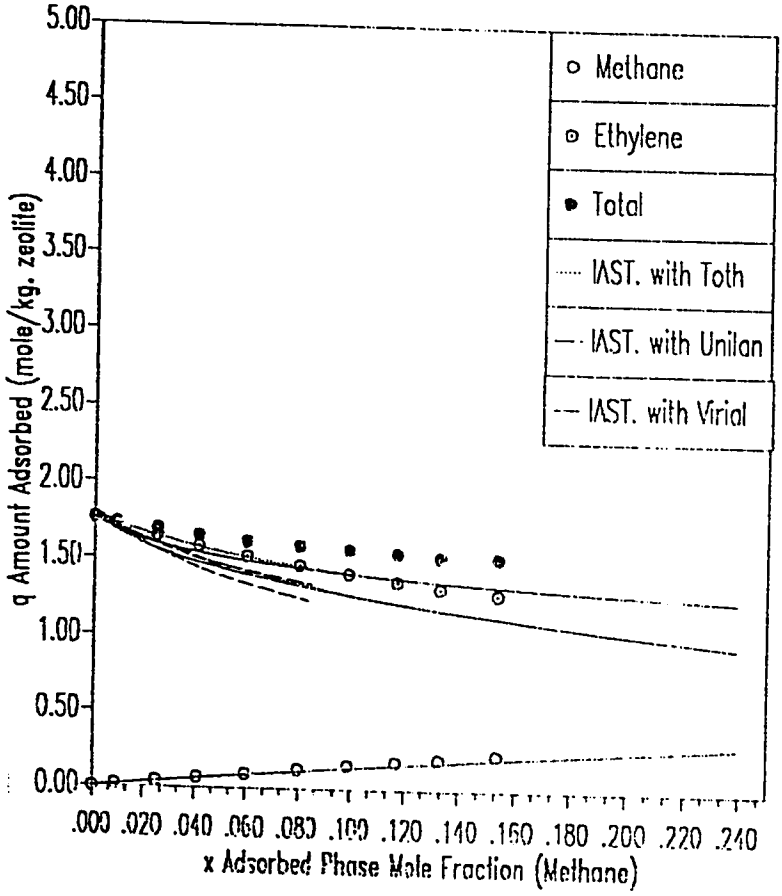

Figure 6.29 x-q Diagram for Methane-Ethylene on ETS-10 Zeolite at 325 K and 250 kPa
Fit of IAST Model Using Toth, Unilan and Virial Three Constant Isotherms

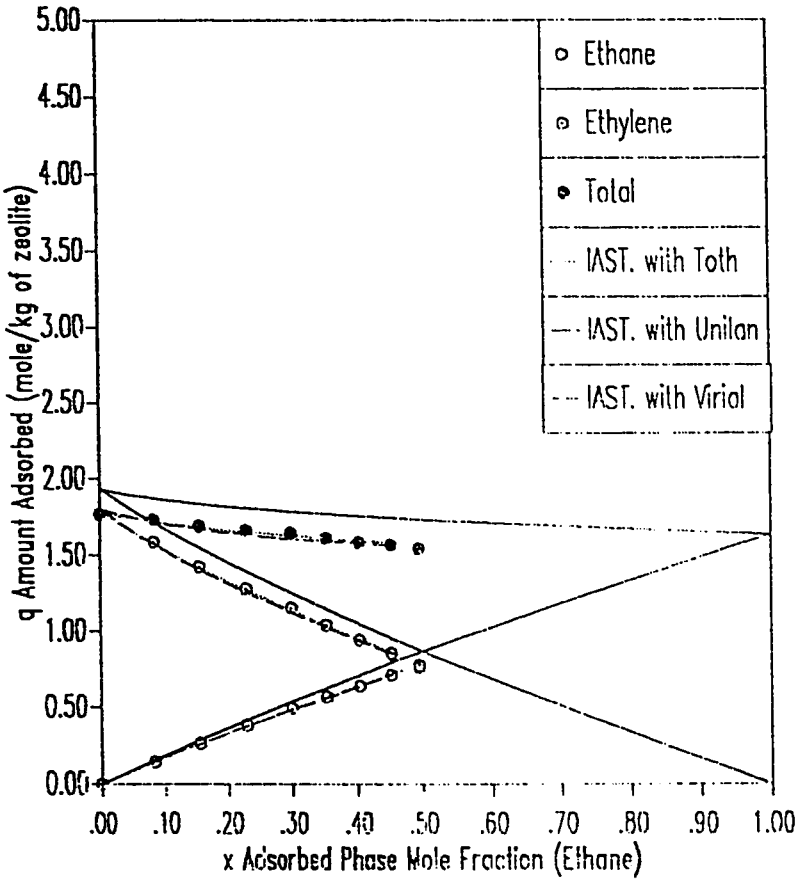

Figure 6.30 x-q Diagram for Ethane-Ethylene on ETS-10 Zeolite at 280 K and 150 kPa
Fit of IAST Model Using Toth, Unilan and Virial Three Constant Isotherms

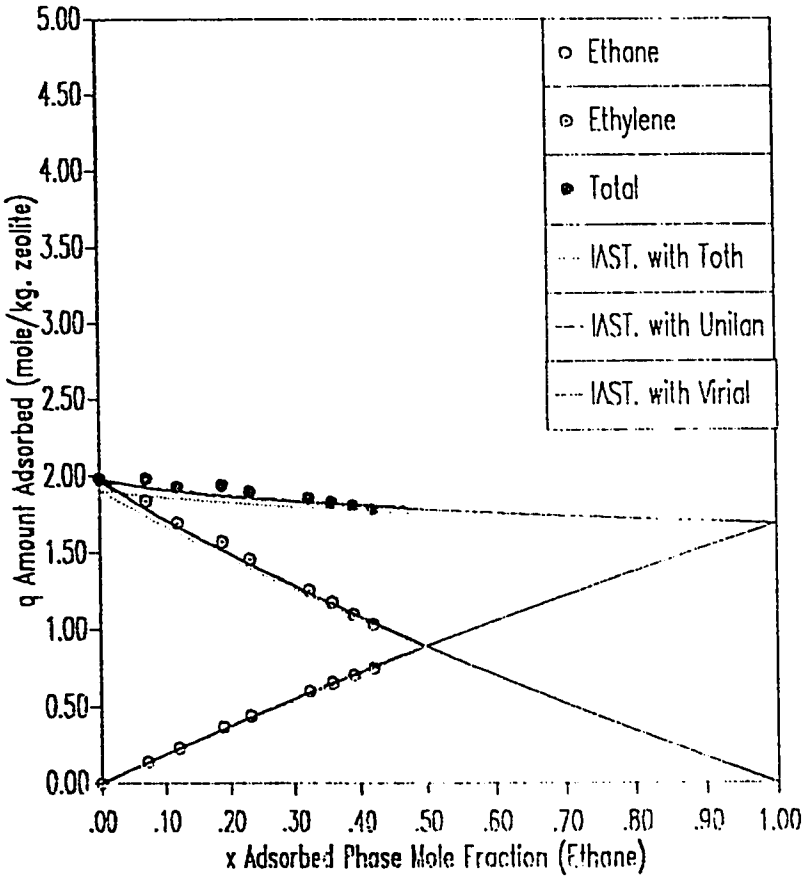

Figure 6.31 x-q Diagram for Ethane-Ethylene on ETS-10 Zeolite at 280 K and 250 kPa
Fit of IAST Model Using Toth, Unilan and Virial Three Constant Isotherms

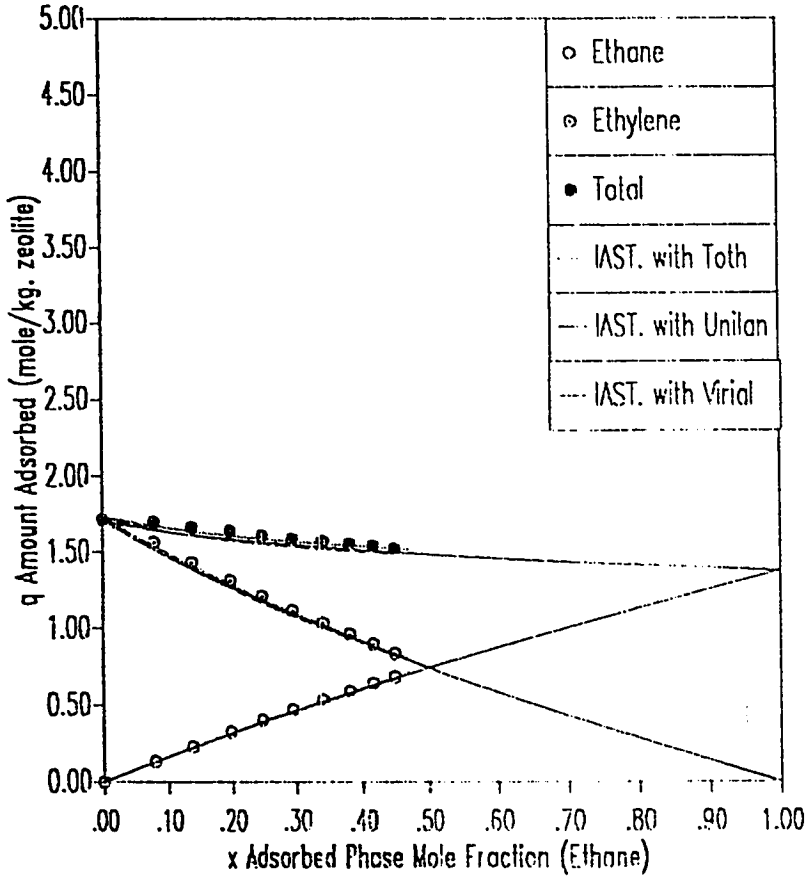

Figure 6.32 x-q Diagram for Ethane-Ethylene on ETS-10 Zeolite at 325 K and 150 kPa
Fit of IAST Model Using Toth, Unilan and Virial Three Constant Isotherms

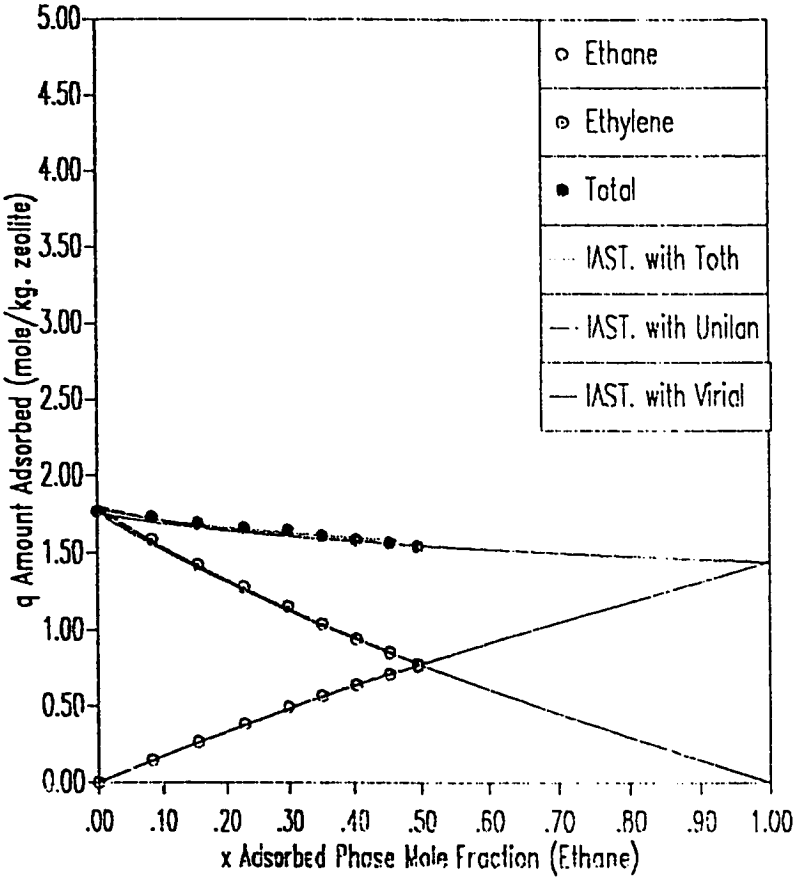

Figure 6.33 x-q Diagram for Ethane-Ethylene on ETS-10 Zeolite at 325 K and 250 kPa
Fit of IAST Model Using Toth, Unilan and Virial Three Constant Isotherms

CHAPTER 7

CONCLUSIONS AND RECOMMENDATIONS

7.1 Conclusions

Pure equilibrium data for nitrogen, carbon dioxide, methane, ethane and ethylene and binary and ternary mixtures of these components on Linde SR-115 zeolite have been experimentally determined. Excluding nitrogen and carbon dioxide, similar measurements have been made for these gases on ETS-10 zeolites. The pure data have been modeled using ten different equilibrium isotherm models namely, Toth, Unilan, Radke-Prausnitz, Mathews-Weber, Volmer, Virial with two and three constants, Freundlich, Langmuir-Freundlich, and the Loading Ratio Correlation. Both constrained and unconstrained optimization have been successfully applied using these models. In the unconstrained optimization, the model parameters were left to relax to their optimum values. However, in the constrained regression , the saturation concentration parameter has been fixed at 95% the theoretical value calculated from the Dubinin equation. In addition, the parameters which were observed in the unconstrained regression to exhibit no dependence on temperature, have been optimized till a minimum sum of squares error were achieved. Constraining the model parameters has generally a negative effect on the total sum of squares error. On the other hand, the values of Henry's constant become adjusted such that better straight lines are obtained upon plotting semilogarithmly the values of Henry's constant versus the reciprocal of temperature. Hence, more accurate Vant' Hoff parameters are obtained.

The fit of all models except Freundlich to the pure data of nitrogen on SR-115 zeolite were excellent. It was also observed that the fit of the loading ratio correlation to the nitrogen data is the best in the

unconstrained regression, while the fit of virial three constant model was the best in the constrained regression.

All the models used fail to represent satisfactorily the equilibrium data of pure carbon dioxide on SR-115 zeolite. That suggested developing a new model which takes into consideration the adsorption of carbon dioxide on the zeolite binder.

The fits of the ten models to the equilibrium adsorption data of pure methane, ethane, and ethylene on SR-115 zeolite were respectively, good, satisfactory and excellent. For ethylene data, the best fit was obtained by the Radke-Prausnitz model. For methane and ethane data, the best fits were respectively obtained by the virial three constant and the virial two constant models.

With the exception of the Freundlich model, the fits of the other nine models to the pure adsorption equilibrium data of methane, ethane, and ethylene on ETS-10 zeolite were excellent. The Radke-Prausnitz model was the most appropriate to the methane and ethane data. However, virial three constant model was best to the ethylene data.

The ideal adsorbed solution theory model (IAST) was used to fit all the multicomponent data obtained on both SR-115 and ETS-10 zeolites. The constrained optimized parameters of Toth, Unilan and virial three constant isotherms were used in the IAST equations. Similar results have been obtained from the three isotherms. The fit of IAST to the multicomponent systems ethane-ethylene, methane-ethylene, methane-ethane-ethylene on both SR-115 and ETS-10 zeolites and methane-ethane on ETS-10 zeolite was satisfactory and encouraging. However, the fit of this model to the binary system nitrogen-carbon dioxide on SR-115 zeolite was very poor. This was attributed to the inaccurate Henry's constant values extracted from the fits of the pure models to the data of carbon dioxide due to the presence of binder.

The values of relative adsorptivity calculated from the binary data and the IAST fit of the data are comparable in most cases. The data and the IAST fit agree that the separation of methane from ethane is possible on both SR-115 and ETS-10 zeolites. However, the separation on the latter zeolite is better especially at low temperatures and high pressures. The separation of methane from ethane on ETS-10 zeolite is also possible and is better than the separation on SR-115, 13X and 5A adsorbents (1). The separation of ethane from ethylene is not feasible on SR-115 at any conditions. On the other hand, it is observed that this separation is possible on ETS-10 zeolite especially at low temperatures. Also, the separation of methane from the ternary mixture methane-ethane-ethylene is quite feasible on both types of zeolite. The effect of pressure on the separation of ethane-ethylene on ETS-10 is insignificant.

Values of the relative adsorptivity calculated from the experimental data reveals that the separation of nitrogen from carbon dioxide on SR-115 zeolite is technically feasible at pressures below 350 kPa and temperatures below 280 K.

7.2 Recommendations

It is recommended to generate separate equilibrium data for carbon dioxide on the pure form of SR-115 and on the binder of this adsorbent and compare the results with those obtained in this work. A new model that takes into consideration the amount adsorbed of carbon dioxide on the zeolite binder can be developed. The new Henry's constant values can then be used together with other parameters to fit the binary data of nitrogen-carbon dioxide.

Pure isotherms of Radke-Prausnitz, Mathews-Weber, Langmuir-Freundlich, L.R.C. and Volmer can be used in conjunction with the IAST model to fit the multicomponent data generated in this work.

The non ideal adsorbed solution theory (NAS) may also be used to fit the multicomponent data generated. Values of activity coefficient can then be determined.

Pure data for nitrogen, carbon dioxide and binary data of these components on ETS-10 zeolites are required. The adsorption behavior of these systems on ETS-10 can be compared with the data obtained on SR-115 zeolite. Adsorption data for other hydrocarbons are also required on this adsorbent.

Plots of the relative adsorptivity values versus gas phase mole fraction are required for both the data and the IAST fit of the data to test the consistency and validity of the IAST model.

7.3 Literature Cited

1) Bin Abdul Rehman, H., Equilibrium Adsorption of Light Alkanes and Their Mixtures on 5A, 13X and SR-115, M.S. Thesis, KFUPM, Dhahran 1988.

APPENDICES

A : SET-UP DATA

B : PURE COMPONENT DATA

C : COMPUTER PROGRAMS

APPENDIX A

SET-UP DATA

1) Dry Weight of Adsorbents Placed in Volumetric Cell E.

Weight of SR-115 Zeolite : 154.0 g (this includes 20% binder)

Weight of ETS-10 Zeolite : 43.5 g (this includes no binder)

2) Volume of Cells

a) SR-115 zeolite as the adsorbent

Volume of cell B : 982.47 cc

Volume of cell D : 378.87 cc

Volume of cell E : 570.81 cc

b) ETS-10 zeolite as the adsorbent

Volume of cell B : 982.47 cc

Volume of cell D : 382.61 cc

Volume of cell E : 630.66 cc

3) G.C. Calibration of Gases

Carrier Gas	: Helium
Separation Column	: Alumina
Flow Rate of Carrier Gas	: 117.0 ml/min
Operating Temperature	: 45 °C
Current	: 110 mA

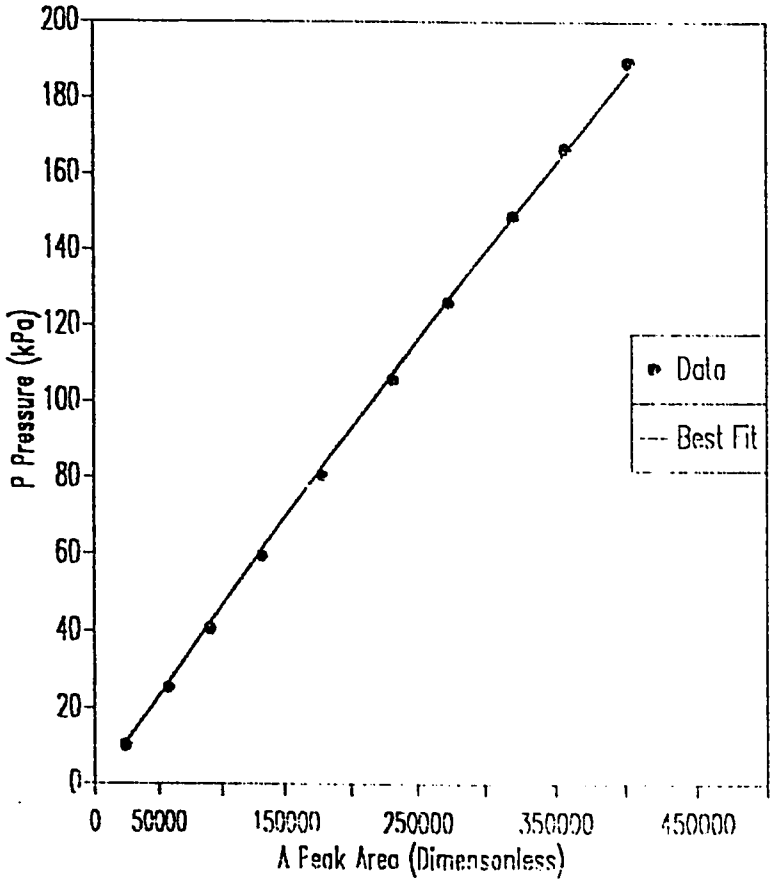

Figure A.1 G.C. Calibration of Methane

(Slope = $4.6299*10^{-4}$ kPa)

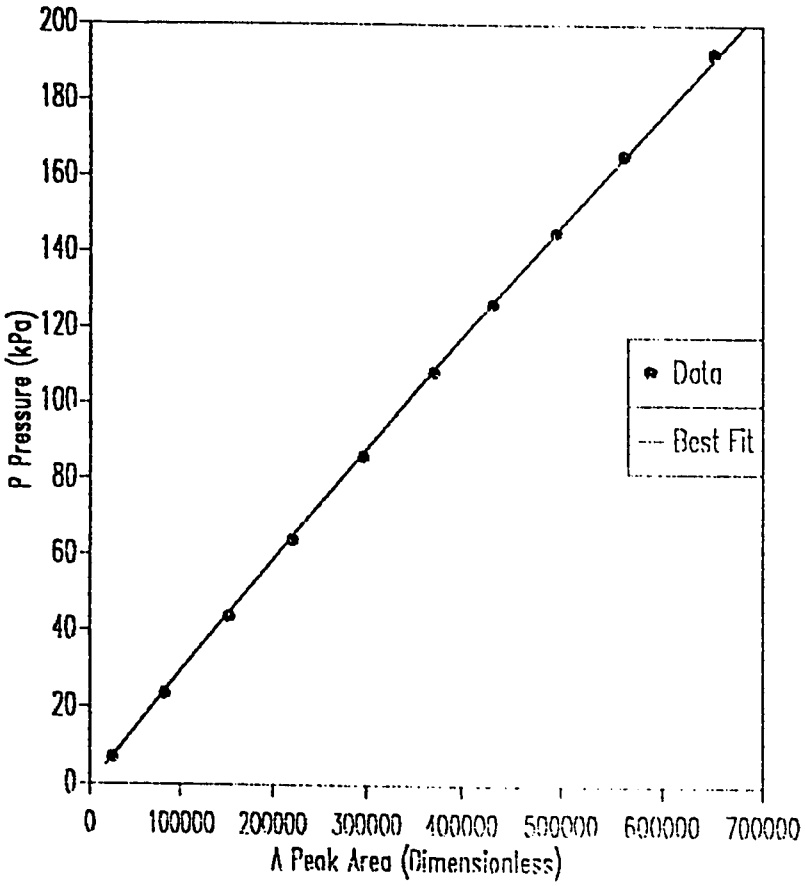

Figure A.2 G.C. Calibration of Ethane

(Slope = $2.9296*10^{-4}$ kPa)

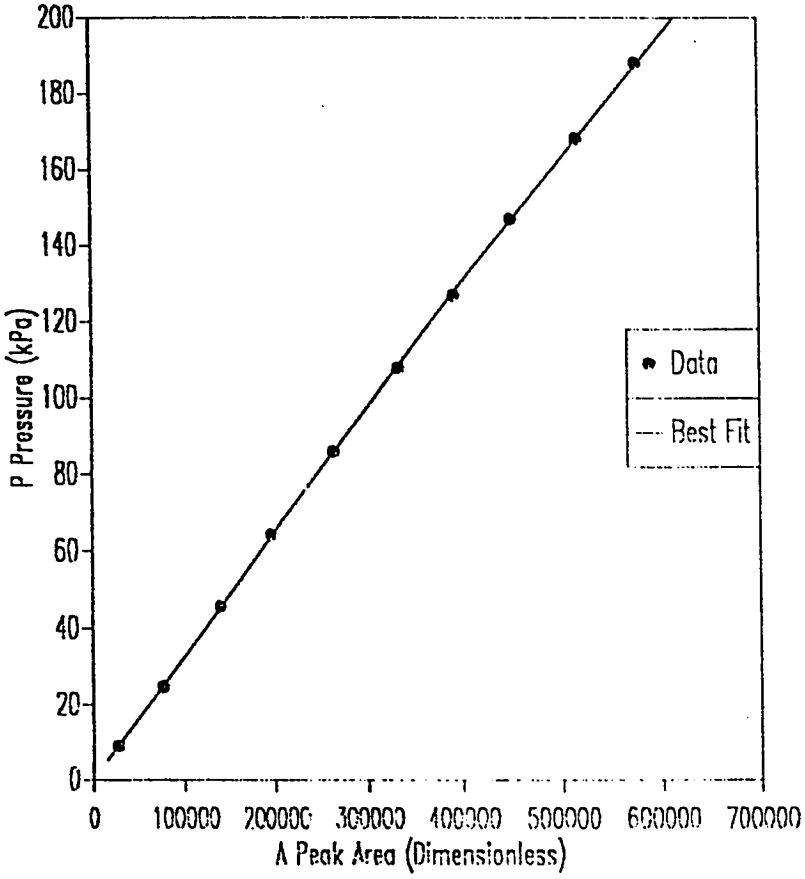

Figure A.3 G.C. Calibration of Ethylene

(Slope = $3.2464*10^{-4}$ kPa)

APPENDIX B

PURE COMPONENT DATA

Table B.1 Equilibrium Adsorption Data of Nitrogen on SR-115 Zeolite

280 K		298.2 K		300 K	
P	q	P	q	P	q
17.83	0.101	11.72	0.040	12.48	0.035
22.06	0.123	19.24	0.059	36.06	0.099
31.69	0.165	32.75	0.096	54.14	0.143
39.93	0.196	42.82	0.123	78.24	0.201
51.35	0.241	52.87	0.151	108.62	0.269
59.93	0.271	66.53	0.187	148.90	0.349
72.75	0.330	78.26	0.218	247.65	0.526
86.63	0.376	82.39	0.228	349.80	0.684
101.61	0.423	102.73	0.275	506.56	0.872
149.79	0.560	149.64	0.373	921.26	1.196
199.73	0.683	236.50	0.534	1105.27	1.328
249.73	0.790	299.73	0.640		
299.73	0.886	399.73	0.786		
399.73	1.046	499.65	0.900		
501.99	1.178	599.65	1.006		
599.72	1.291	699.72	1.105		
699.72	1.385	799.65	1.184		
785.52	1.459	899.70	1.255		
899.73	1.548	974.15	1.303		

P : Pressure (kPa)

q : Amount Adsorbed (mole/kg. zeolite)

Table B.2 Equilibrium Adsorption Data of Carbon Dioxide on SR-115 Zeolite

280 K		300 K		315 K		325 K		350 K	
P	q	P	q	P	q	P	q	P	q
0.11	0.131	0.76	0.211	0.54	0.178	0.50	0.119	0.52	0.084
0.36	0.255	2.36	0.410	1.09	0.239	1.01	0.186	1.41	0.131
0.87	0.461	4.87	0.604	2.36	0.343	2.36	0.284	2.76	0.190
4.87	0.956	14.87	1.018	4.87	0.518	4.87	0.414	5.18	0.266
9.86	1.259	146.72	2.374	9.86	0.690	10.00	0.585	10.01	0.376
25.00	1.791	250.00	2.670	25.00	1.019	26.68	0.908	24.94	0.599
51.41	2.253	300.97	2.763	49.99	1.345	48.93	1.174	50.00	0.839
75.00	2.493	393.94	2.891	75.21	1.581	75.00	1.393	75.00	1.013
102.73	2.668	499.99	2.993	99.97	1.751	100.00	1.558	100.00	1.156
150.00	2.859	599.86	3.070	149.69	1.990	150.00	1.809	164.69	1.448
246.35	3.076	750.00.	3.149	200.00	2.160	247.60	2.109	250.65	1.693
350.76	3.225	890.31	3.198	350.00	2.448	399.95	2.383	400.56	1.980
499.99	3.341			500.01	2.625	549.99	2.541	559.55	2.179
650.00.	3.421			700.00	2.770	700.00	2.650	750.00	2.309
786.21	3.471			1084.5	2.939	870.50	2.748	876.19	2.416
979.55	3.529								

P : Pressure (kPa)

q : Amount Adsorbed (mole/kg. zeolite)

Note: the pellet of Linde SR-115 zeolite contains 20% binder. To change to mole/kg. pellet, multiply the result for q by 0.80.

Table B.3 Equilibrium Adsorption Data of Methane on ETS-10 Zeolite

280 K		300 K		315 K		325 K		350 K	
P	q	P	q	P	q	P	q	P	q
2.10	0.068	2.59	0.065	7.47	0.074	6.19	0.042	4.137	0.033
3.97	0.125	5.13	0.124	11.53	0.108	15.00	0.107	9.625	0.050
14.78	0.363	17.43	0.291	25.00	0.217	24.73	0.176	24.63	0.115
39.74	0.709	41.37	0.556	49.99	0.380	41.37	0.306	50.54	0.261
74.82	0.966	74.62	0.776	74.96	0.513	75.00	0.465	102.50	0.423
101.06	1.112	99.81	0.892	100.00	0.619	99.73	0.558	149.41	0.533
149.66	1.260	149.81	1.057	150.00	0.775	149.95	0.707	199.66	0.632
199.83	1.361	199.89	1.185	200.00	0.885	200.00	0.818	249.66	0.717
249.82	1.432	250.03	1.280	249.96	0.973	250.00	0.903	299.62	0.792
299.78	1.489	299.59	1.348	299.94	1.041	297.89	0.972	400.45	0.911
399.63	1.569	399.66	1.446	399.92	1.142	398.81	1.085	498.06	1.007
499.80	1.620	499.54	1.516	499.32	1.229	499.99	1.177		
649.82	1.699	647.29	1.604	649.96	1.329	650.00.	1.251		
799.79	1.746	799.63	1.689	799.83	1.398	798.30	1.321		
996.93	1.772	999.64	1.737	947.66	1.447	999.99	1.379		

P : Pressure (kPa)

q : Amount Adsorbed (mole/kg. zeolite)

Table B.4 Equilibrium Adsorption Data of Ethane on ETS-10 Zeolite

280 K		300 K		315 K		325 K		350 K	
P	q	P	q	P	q	P	q	P	q
0.46	0.553	0.32	0.183	0.44	0.147	0.55	0.129	0.63	0.092
0.84	0.742	0.80	0.396	0.92	0.288	1.10	0.241	1.45	0.170
2.30	1.061	2.32	0.742	2.30	0.536	2.29	0.416	2.56	0.278
4.67	1.226	4.83	0.965	4.74	0.767	4.80	0.645	4.92	0.422
9.63	1.350	10.22	1.140	9.43	0.974	9.65	0.867	9.87	0.625
24.63	1.472	25.98	1.296	25.65	1.193	24.53	1.107	24.12	0.896
49.60	1.548	52.07	1.393	87.88	1.372	51.21	1.248	49.42	1.081
74.57	1.589	74.97	1.436	103.56	1.395	77.64	1.315	75.08	1.176
99.20	1.615	101.52	1.471	151.97	1.461	100.26	1.351	100.39	1.231
149.64	1.653	149.59	1.505	200.13	1.489	149.63	1.400	149.52	1.298
199.63	1.684	201.64	1.534	251.20	1.508	199.63	1.433	199.84	1.344
299.62	1.705	287.77	1.562	299.65	1.525	299.91	1.475	299.22	1.398
449.43	1.721	449.44	1.580	448.68	1.551	450.63	1.507	449.59	1.447
599.14	1.730	570.98	1.595	599.36	1.571	583.19	1.525	592.54	1.473
721.81	1.723	706.35	1.614	723.66	1.581	711.53	1.534	718.97	1.497

P : Pressure (kPa)

q : Amount Adsorbed (mole/kg. zeolite)

Table B.5 Equilibrium Adsorption Data of Ethylene on ETS-10 Zeolite

280 K		300 K		315 K		325 K		350 K	
P	q	P	q	P	q	P	q	P	q
0.25	0.946	0.25	0.740	0.25	0.536	0.37	0.481	0.25	0.140
0.50	1.146	0.50	0.942	0.50	0.7586	0.51	0.589	0.51	0.273
0.97	1.288	1.00	1.124	1.00	0.947	1.00	0.808	1.06	0.474
2.50	1.445	2.50	1.299	2.50	1.155	2.51	1.060	2.50	0.742
4.98	1.543	5.00	1.411	5.00	1.281	5.01	1.205	4.99	0.947
10.00	1.637	10.00	1.515	10.01	1.398	10.00	1.330	10.58	1.133
19.99	1.720	19.97	1.607	19.99	1.495	21.10	1.447	19.99	1.260
30.00	1.766	30.00	1.659	30.00	1.553	30.01	1.497	30.42	1.335
49.99	1.824	50.00	1.718	49.99	1.619	49.99	1.568	50.00	1.417
74.20	1.868	74.56	1.766	74.45	1.688	74.67	1.621	74.34	1.480
100.00	1.900	100.00	1.798	99.95	1.703	100.00	1.658	100.00	1.524
150.00	1.937	150.00	1.841	150.00	1.749	150.00	1.704	150.00	1.581
199.56	1.961	199.63	1.870	199.52	1.779	199.33	1.738	199.48	1.619
249.87	1.979	249.70	1.894	249.19	1.804	249.96	1.764	249.99	1.651
298.10	1.993	298.52	1.910	298.03	1.823	298.14	1.782	300.91	1.673

P : Pressure (kPa)

q : Amount Adsorbed (mole/kg. zeolite)

APPENDIX C

COMPUTER PROGRAMS

Program # 1

This program is constructed to calculate the amount adsorbed for pure components as a function of pressure. It converts the temperature and pressure readings to moles using SOAVE-REDLICH-KWONG equation of state.

Program Input:

SORBAT	: Sorbate name
SORBNT	: Sorbent name
EXPER	: Experiment type.
REF	: Reference
FILEN	: File name
J	: Sorbate number
NDATE	: Date of the experiment (day).
MONTH	: Date of the experiment(month)
NYEAR	: Date of the experiment(year)
TE	: Experiment temperature (°C)
ZEOL	: Zeolite type
VOLB	: Volume of cell B (cc)
VOLD	: Volume of cell D (cc)
VOLE	: Volume of cell E (cc)
PRESSB	: Pressure of cell B (psia)
TB	: Temperature of cell B (°C)
PRESSD	: Pressure of cell D (psia)

```
      COMMON/PARA/NC,ICOD,NOMBRE(12)
      DIMENSION Y(12),DENMOL(12),FV(12)
      DIMENSION MOLDEB(50),MOLDED(50),PRESSE(50)
      DIMENSION MOLDEE(50),PRESSB(50)
      DIMENSION PBCRB(50),MOLADD(50),FUGAD(50)
      DIMENSION MOLTOT(50),MOLADS(50)
      DIMENSION TB(50),PRESSD(50),PDCOR(50)
      REAL MOLADD,MOLTOT,MOLADS,MOLDEB,MOLDED,MOLDEE,NC,TE,T
      CHARACTER*60,SORBAT,SORBNT,EXPER,REF,FILEN
      DATA J/5/
C     FORMAT SECTION
1     FORMAT(I2)
2     FORMAT(3I5)
3     FORMAT(5F10.5)
4     FORMAT(/ 3X,'J=',I2,' ANALYSIS BY USING SOAVE
     &REDLICH KWONG EOS'/)
6     FORMAT( 3X,'DATE',I3,2X,'MONTH',I3,2X,'YEAR',I5// 3X,
     &'WEIGHT OF ZEOLITE = ',F7.2,2X,'GRAMS'/)
7     FORMAT(3F10.5)
10    FORMAT( 3X,'ISOTHERM TEMPERATURE =',F7.2,
     &' DEGREES KELVIN',/)
15    FORMAT( 3X,'VOLB=',F8.3,'C.C',3X,'VOLD=',F8.3,'C.C',3X,
     &'VOLE=',F8.3,'C.C'//)
16    FORMAT(11X,'PRESSB    PRESSD  FUGACITY MOLADSORB
     &MOLESADD MOLESTOT MOLEDB')
```

```
20    FORMAT(12X,'PSIA       PSIA       PSIA   MMOL/GM ZEOL
     &MMOLE   MMOLE  M  MOL/C.C.'/)
25    FORMAT(10X,7(F8.3,1X))
C     READ IN DATA SECTION
      READ(5,*)SORBAT
      READ(5,*)SORBNT
      READ(5,*)EXPER
      READ(5,*)REF
      READ(5,*)FILEN
      WRITE(8,*)SORBAT
      WRITE(8,*)SORBNT
      WRITE(8,*)EXPER
      WRITE(8,*)REF
      WRITE(8,*)FILEN
      WRITE(6,*)SORBAT
      WRITE(6,*)SORBNT
      WRITE(6,*)EXPER
      WRITE(6,*)REF
      WRITE(6,*)FILEN
      READ(5,1)J
      READ(5,2)NDATE,MONTH,NYEAR
      READ(5,3)TE,ZEOL,VOLB,VOLD,VOLE
      I=1
100   READ(5,7)PRESSB(I),TB(I),PRESSD(I)
      TB(I)=TB(I)+273.14
```

```
      IF(PRESSB(I).LT.0.0) GO TO 120
      I=I+1
      GO TO 100
120   N=I-1
      WRITE(8,*)N
C     ECHO DATA INPUT SECTION
      WRITE(8,4)J
      WRITE(8,6)NDATE,MONTH,NYEAR,ZEOL
      WRITE(8,10)TE
      WRITE(8,15)VOLB,VOLD,VOLE
      WRITE(6,4)J
      WRITE(6,6)NDATE,MONTH,NYEAR,ZEOL
      WRITE(6,10)TE
      WRITE(6,15)VOLB,VOLD,VOLE
      DO 200 I=1,N
200   WRITE(6,25)PRESSB(I),TB(I),PRESSD(I)
C     CALCULATION SECTION
C     CALCULATE MOLAR DENSITIES
C     FIRST FIX MOLE FRACTIONS
      DO 299 M=1,6
      Y(M)=0.0
299   CONTINUE
      WRITE(8,*)Y(1),Y(2),Y(3),Y(4),Y(5),Y(6)
      Y(J)=1.0
      WRITE(8,*)Y(1),Y(2),Y(3),Y(4),Y(5),Y(6)
```

```
      DO 300 I=1,N
      T=TB(I)
      P=PRESSB(I)
      WRITE(8,*)T,P
      CALL COMP(T,P,Y,DENMOL)
      MOLDEB(I)=DENMOL(J)
      PRESSE(I)=PRESSD(I)
      P=PRESSE(I)
      CALL COMP(T,P,Y,DENMOL)
      MOLDED(I)=DENMOL(J)
      WRITE(8,*)MOLDEB(I),MOLDED(I)
300   CONTINUE
C     CALCULATE MILLMOLES ADDED
      MOLADD(1)=MOLDEB(1)*VOLB
      DO 320 K=2,N
      IF(PRESSB(K)-PRESSB(K-1))310,310,315
310   MOLADD(K)=0.0
      GO TO 320
315   MOLADD(K)=(MOLDEB(K)-MOLDEB(K-1))*VOLB
320   CONTINUE
C     CALCULATE TOTAL MOLES IN SYSTEM
      MOLTOT(1)=MOLADD(1)
      DO 340 I=2,N
      MOLTOT(I)=MOLTOT(I-1)+MOLADD(I)
340   CONTINUE
```

```
C     CALCULATE MOLES ADSORBED
      MOLADS(1)=0.0
      FUGAD(1)=0.0
      DO 360 JJ=2,N
      T=TE
      P=PRESSD(JJ)
      CALL COMP(T,P,Y,DENMOL)
      CALL FUGA(T,P,Y,FV)
      FUGAD(JJ)=FV(5)
      MOLDEE(JJ)=DENMOL(J)
      MOLADS(JJ)=(MOLTOT(JJ)-MOLDEB(JJ)*VOLB-MOLDED(JJ)*VOLD
     &-MOLDEE(JJ)*VOLE)/ZEOL
360   CONTINUE
C     PRINT RESULTS
      WRITE(6,16)
      WRITE(6,20)
      DO 400 I=1,N
      WRITE(6,25)PRESSB(I),PRESSD(I),FUGAD(I),MOLADS(I),
     &MOLADD(I),MOLTOT(I),MOLDEB(I)
400   CONTINUE
C     FREE SECTIONS
1000  STOP
      END

C     CALCULATION OF MOLAR DENSITY
      SUBROUTINE COMP(T,P,Y,DENMOL)
```

```
      CHARACTER NOMBRE*10
      DIMENSION Y(12),DENMOL(12)
      COMMON/CAST/AC(12),B(12),A(12),DEL(12,12)
      COMMON/CRIT/TC(12),PC(12),W(12),TB(12)
      COMMON/PARA/NC,ICOD,NOMBRE(12)
      R=82.054*14.696
      DO 140 I=1,NC
      DO 140 J=1,NC
      DEL(I,J)=0.
140   CONTINUE
      IF (NC.EQ.1) GO TO 7
      GO TO 9
7     Y(1)=1.
9     IM=1.0
      CALL COST(ZV,T,P,Y,AA,BB,2)
      DO 315 I=1,NC
      DENMOL(I)=Y(I)*P/R/T/ZV*1000
315   CONTINUE
      RETURN
      END

C     BLOCK DATA
      COMMON/CRIT/TC(12),PC(12),W(12),TB(12)
      COMMON/PARA/NC,ICOD,NOMBRE(12)
      CHARACTER NOMBRE*10
      DATA NC/ 6/
```

```
      DATA TC(1),PC(1),W(1),TB(1),NOMBRE(1) /190.6,667.2,
     *0.008,111.7, 'METHANE'/
      DATA TC(2),PC(2),W(2),TB(2),NOMBRE(2) /305.4,708.35,
     *0.098,184.5,'ETHANE'/
      DATA TC(3),PC(3),W(3),TB(3),NOMBRE(3) /365.0,669.37,
     *0.148,225.3, 'PROPENE'/
      DATA TC(4),PC(4),W(4),TB(4),NOMBRE(4) /425.2,551.1,
     *0.193,272.7, 'BUTANE'/
      DATA TC(5),PC(5),W(5),TB(5),NOMBRE(5) /304.2,1071.34,
     *0.420,194.7, 'CARBON DIO'/
      DATA TC(6),PC(6),W(6),TB(6),NOMBRE(6) /126.2, 492.32,
     *0.040,77.3, ' NITROGEN '/
      END

      SUBROUTINE COST(ZL,T,P,Y,AA,BB,IK)
      DIMENSION TR(12),PR(12),Y(12),AM(12)
      COMMON/CAST/AC(12),B(12),A(12),DEL(12,12)
      COMMON/ CRIT/TC(12),PC(12),W(12),TB(12)
      COMMON/PARA/NC,ICOD,NOMBRE(12)
      DO 20 I=1,NC
      TR(I)=T/TC(I)
      PR(I)=P/PC(I)
20    CONTINUE
      DO 30 I=1,NC
      AM(I)=0.480+1.574*W(I)-0.176*W(I)**2
      AC(I)=( 1. + AM(I)*(1.-SQRT(TR(I))) )**2.
```

```
      A(I)=0.42747*AC(I)*PR(I)/(TR(I)**2.)
      B(I)=0.08664*PR(I)/TR(I)
30    CONTINUE
      BB=0.
      AA=0.
      IF(NC.EQ.1) GO TO 1
      DO 40 I=1,NC
      BB=BB+Y(I)*B(I)
      DO 50 J=1,NC
      AA=AA+Y(I)*Y(J)*(1.-DEL(I,J))*SQRT(A(I)*A(J))
50    CONTINUE
40    CONTINUE
      CALL ZETAAB(AA,BB,ZRL,ZRG,IER)
8     IF(IK.EQ.1) GO TO 5
      IF(IER.NE.1) GO TO 6
      IF(ZRL.GT.0.4) GO TO 6
      WRITE(6,*)'ERROR ,SOLO EXISTE FASE LIQUIDA'
      ZL=0.333
      RETURN
6     ZL=ZRG
      RETURN
5     IF(IER.NE.1) GO TO 7
      IF(ZRL.LT.0.4) GO TO 7
      ZL=0.333
      RETURN
```

```
7     ZL=ZRL
      RETURN
1     AA=A(1)
      BB=B(1)
      CALL ZETAAB(AA,BB,ZRL,ZRG,IER)
      GO TO 8
      END

      SUBROUTINE ZETAAB(A,B,ZRL,ZRG,IER)
      DIMENSION VEC(3)
      ICON=0
      IER=0
      C=1.
      Q=(A-B-B**2)
      R=A*B
      Z=0.001
98    FX=Z**3-C*Z**2+Q*Z-R
      FX1=3*Z**2-2*C*Z+Q
      FX2=6*Z-2*C
      CONV=ABS(FX*FX2/(FX1**2))
      IF(CONV.LT.1) GO TO 99
      Z=Z+0.09
      ICON=ICON+1
      IF(ICON.EQ.500) GO TO 1009
      GO TO 98
1009  WRITE(6,1001)
```

```
1001 FORMAT(1X,15HNO CONVERGENCIA)
     RETURN
99   Z0=Z
     XTOL=0.010
     FTOL=0.001
     NLIM=500
     I=0
     CALL NEWTON(Z0,XTOL,FTOL,NLIM,I,Q,R,C)
     RAIZ=(-C+Z0)**2-4*(Q+Z0*(-C+Z0))
     IF(ABS(RAIZ).LE.0.0001) GO TO 100
     IF(RAIZ.LT.0) GO TO 109
     VEC(1)=Z0
     I=0
     Z01=(-(-C+Z0)+RAIZ**0.5)/2.
     CALL NEWTON(Z01,XTOL,FTOL,NLIM,I,Q,R,C)
     VEC(2)=Z01
     I=0
     Z02=(-(-C+Z0)-RAIZ**0.5)/2.
     CALL NEWTON(Z02,XTOL,FTOL,NLIM,I,Q,R,C)
     VEC(3)=Z02
30   DO 10 I=1,3
     AMAY=VEC(I)
     KK1=I
     DO 20 K=I,3
     IF(AMAY.LT.VEC(K)) GO TO 20
```

```
      AMAY=VEC(K)
      KK1=K
20    CONTINUE
      AUX=VEC(I)
      VEC(I)=VEC(KK1)
      VEC(KK1)=AUX
10    CONTINUE
      IF(VEC(1).GT.0) GO TO 101
      IF(VEC(2).GT.0) GO TO 102
      IF(VEC(3).GT.0) GO TO 103
      Z=1.
      GO TO 98
101   ZRL=VEC(1)
      ZR=VEC(2)
      ZRG=VEC(3)
      GO TO 1000
102   ZRL=VEC(2)
      ZR=VEC(1)
      ZRG=VEC(3)
      GO TO 1000
103   ZRL=VEC(3)
      ZR=ZRL
      ZRG=ZRL
      IER=1
      GO TO 1000
```

```
100  Z03=-(-C+Z0)/2.
     I=0
     CALL NEWTON(Z03,XTOL,FTOL,NLIM,I,Q,R,C)
     VEC(1)=Z0
     VEC(2)=Z03
     VEC(3)=0.
     GO TO 30
109  VEC(1)=Z0
     VEC(2)=0.
     VEC(3)=0.
     GO TO 30
1000 RETURN
     END

     SUBROUTINE NEWTON(Z0,XTOL,FTOL,NLIM,I,Q,R,C)
     LOGICAL PRINT
     PRINT=.TRUE.
     IF(I.NE.0) PRINT=.FALSE.
     FZ=FCN(Z0,Q,R,C)
     DO 20 J=1,NLIM
     DELZ=FZ/FDER(Z0,Q,R,C)
     Z0=Z0-DELZ
     FZ=FCN(Z0,Q,R,C)
     IF(.NOT.PRINT) GO TO 5
5    IF(ABS(DELZ).LE.XTOL) GO TO 60
     IF(ABS(FZ).LE.FTOL) GO TO 70
```

```
20    CONTINUE
      I=-1
      RETURN
60    I=1
70    I=2
      RETURN
      END

      FUNCTION FCN(Z0,Q,R,C)
      FCN=Z0**3-C*Z0**2+Q*Z0-R
      RETURN
      END

      FUNCTION FDER(Z0,Q,R,C)
      FDER=3*(Z0**2)-2*C*Z0+Q
      RETURN
      END

      SUBROUTINE FUGA(T,P,Y,FV)
      CHARACTER NOMBRE*10
      COMMON/CAST/AC(12),B(12),A(12),DEL(12,12)
      COMMON/CRIT/TC(12),PC(12),W(12),TB(12)
      COMMON/PARA/NC,ICOD,NOMBRE(12)
      DIMENSION Y(12),CFV(12),FV(12)
      CALL FUGACI(T,P,Y,CFV,ZV,2)
      DO 315 I=1,NC
      FV(I)=CFV(I)*Y(I)*P
```

```
315  CONTINUE
     RETURN
     END

     SUBROUTINE FUGACI(T,P,Y,CFV,ZL,IK)
     COMMON/CAST/AC(12),B(12),A(12),DEL(12,12)
     COMMON/CRIT/TC(12),PC(12),W(12),TB(12)
     COMMON/PARA/NC,ICOD,NOMBRE(12)
     DIMENSION C(12),Y(12),CFV(12)
     CALL COST(ZL,T,P,Y,AA,BB,IK)
     DO 10 I=1,NC
     AP1=0.
     DO 20 J=1,NC
     AP1=AP1 + Y(J)*SQRT(A(J)*A(I))*(1-DEL(I,J))
20   CONTINUE
     AP=2.*AP1/AA - B(I)/BB
     CF=(ZL-1.)*B(I)/BB - ALOG(ZL-BB) - (AA/BB)*AP*ALOG
    &((ZL+BB)/ZL)
     CFV(I)=EXP(CF)
10   CONTINUE
     RETURN
     END
```

Program # 2

This program is constructed to calculate the amount adsorbed for multicomponent systems. The temperature and pressure readings are converted to moles using SOAVE-REDLICH-KWONG equation of state. The program calculates also the adsorbed phase mole fractions of the given components as a function of the gas phase mole fractions.

Program Input:

I, J, K and L	: Integers corresponding to the components numbers
NFIRST	: The day of the start of the experiment
NLAST	: The day of the end of the experiment
MONTH	: The month of the experiment
NYEAR	: The year of the experiment
TE	: Experiment temperature (K)
ZEOL	: Zeolite name
VOLB	: Volume of cell B (cc)
VOLD	: Volume of cell D(cc)
VOLE	: Volume of cell E (cc)
M1, M2, M3 and M4	: Integers corresponding to the component numbers
PRESSB	: Pressure of cell B (psia)
TB	: Temperature of cell B (K)
PRESSD	: Pressure of cell D (psia)
Y(MI)	: Gas phase mole fraction of component MI

```
      COMMON/PARA/NC,ICOD,NOMBRE(12)
      DIMENSION Y(12),DENMOL(12),FV(12)
      DIMENSION MOLDEB(80,4),MOLDED(80,4),MOLDEE
      DIMENSION PRESSB(80),PRESSD(80),TB(80)
      DIMENSION PRESSE(80),PBCRB(80),PDCOR(80)
      DIMENSION PPRESS(80,4),FUGAC(80,4)
      DIMENSION MOLADD(80,4),MOLREM(80,4)
      DIMENSION MOLTOT(80,4),MOLADS(80,4)
      DIMENSION FUGAD(80,4),YDE(80,4),YB(80,4),XADS(80,4)
      REAL  MOLADD,MOLREM,MOLTOT,MOLADS,MOLDEB,MOLDED,MOLDEE
C     FORMAT SECTION
5     FORMAT(/////35X,'ANALYSIS BY USING SOAVE REDLICH
     &KWONG EQUATION'/)
10    FORMAT(35X,'COMPONENTS USED ARE ',I2,',',I2,',',I2,
     &' AND ',I2,
     &'  WHERE'/35X,'      1 STANDS FOR METHANE '/
     &       35X,'      2 STANDS FOR ETHANE '/
     &       35X,'      3 STANDS FOR ETHYLENE'/
     &       35X,'      4 STANDS FOR PROPANE '/)
15    FORMAT(35X,'DATE',I3,'TH TO',I3,'TH OF THE '
     &,I3,'TH MONTH IN ',I5/)
20    FORMAT(35X,'TYPE OF ZEOLITE USED IS LINDE SR115
     &SILICALITE PELLETS'/)
22    FORMAT(35X,'WEIGHT OF ZEOLITE = ',F6.2,'  GRAMS'/)
```

```
25   FORMAT(35X,'EQUILIBRIUM TEMPERATURE =',F7.2,
     &' DEGREES KELVIN'/)
30   FORMAT(35X,'VOLB=',F8.3,'C.C',3X,'VOLD=',F8.3,'C.C'
     &,3X,'VOLE=',F8.3,'C.C'/)
33       FORMAT(20X,'M      PRESSB      TEMPB      PRESSD      PRESSE
YB(1)YB(2)YB(3)YB(4)  YD
     &YB(3)YB(4)  YD(1)  YDE(2)  YDE(3)  YDE(4)')
35   FORMAT(3X,'PRESSB      PRESSD      PRESSE      FUGACB
     &      FUGACD')
38   FORMAT(20X,'    PSIA  KELVIN PSIA    PSIA      %      %
     &%     %     %     %       %        %        % '/)
40   FORMAT(3X,' PSIA         PSIA        PSIA        PSIA
     &         PSIA')
45   FORMAT(/3X,'M         MOLADDED(MMOLES)
     &                  MOLREMOVED(MMOLES)
     &                       TOTALMOLES(MMOLES)')
50   FORMAT(3X,' METHANE  ETHANE  ETHYLENE  PROPANE
     &   METHANE  ETHANE  ETHYLENE  PROPANE  METHANE
     &  ETHANE  ETHYLENE  PROPANE'/)
52   FORMAT(1X,I3,4(F7.2,2X),2X,4(F7.2,2X),2X,4(F7.2,2X))
53   FORMAT(1X,I3,4(F7.2,2X),2X,4(F7.3,1X),2X,4(F7.3,1X))
55   FORMAT(/3X,'M   MOLADSORBED(MOLES/KG. ZEOL)
     &          ADSORBED PHASE FRACTION
     &                  GAS PHASE FRACTION')
60   FORMAT(4I5)
```

123

```
65   FORMAT(5F10.5)
80   FORMAT(8F10.5)
85   FORMAT(18X,I3,4(1X,F6.2),4(1X,F4.1),4(1X,F7.4))
90   FORMAT(/3X,'M        PARTIAL PRESSURES
     &            FUGACITY COEFFICIENT SPECIES I')
91   FORMAT(2X,F6.2,3X,13(F5.3,4X))
92   FORMAT(3X,' METHANE  ETHANE  ETHYLENE PROPANE
     &    METHANE ETHANE   ETHYLENE  PROPANE   METHANE
     &    ETHANE ETHYLENE  PROPANE'/)
94   FORMAT(1X,I3,4(F7.2,2X),2X,4(F7.2,2X),2X,4(F7.2,2X))
95   FORMAT(//9X,'                    TABLE
     &        '//2X,' TABULATION OF DATA FOR  METHANE-
     &ETHYLENE BINARY ON LINDE SR-115 '/20X, 'SILICALITE
     &PELLETS AT 300K AND 350KPA.          '/)
96   FORMAT(' PRESSURE      MOLES ADSORBED    ADS. PHASE
     &  FRACTION GAS PHASE FRACTION
     &    '/'   PSIA  METHANE ETHYLENE   TOTAL  METHANE
     & ETHYLENE  TOTAL  METHANE ETHYLENE  METHANE  ETHYLENE')
C    READ AND PRINT HEADINGS
     READ(5,60)I,J,K,L
     READ(5,60)NFIRST,NLAST,MONTH,NYEAR
     READ(5,65)TE,ZEOL,VOLB,VOLD,VOLE
     READ(5,60)M1,M2,M3,M4
     WRITE(6,10)I,J,K,L
     WRITE(6,15)NFIRST,NLAST,MONTH,NYEAR
```

```
      WRITE(6,20)
      WRITE(6,22)ZEOL
      WRITE(6,25)TE
      WRITE(6,30)VOLB,VOLD,VOLE
      WRITE(6,33)
      WRITE(6,38)
C     INPUT DATA AND ECHO
      M=0
100   M=M+1
      READ(5,80)PRESSB(M),TB(M),PRESSD(M),QQ,Y(M1),
     &Y(M2),Y(M3),Y(M4)
      DO 110 I=1,4
      YDE(M,I)=Y(I)/100.
110   CONTINUE
      IF(PRESSB(M).EQ.-1.0)GO TO 120
      IF(PRESSD(M).NE.0.0)PRESSE(M)=PRESSD(M)
      IF(PRESSD(M).EQ.0.0)PRESSE(M)=PRESSD(M-1)
      GO TO 100
120   CONTINUE
      N=M-1
      PRESSE(1)=PRESSD(1)
      DO 130 M=1,N
      READ(5,80)PRESSB(M),TB(M),PRESSD(M),QQ,Y(M1),Y(M2),Y(M3),Y(M4)
      DO 125 I=1,4
      YB(M,I)=Y(I)/100.
```

123

```
125  CONTINUE
     WRITE(6,85)M,PRESSB(M),TB(M),PRESSD(M),PRESSE(M),
    &YB(M,1),YB(M,2),YB(M,3),YB(M,4),YDE(M,1),
    &YDE(M,2),YDE(M,3),YDE(M,4)
130  CONTINUE
C    CALCULATE MOLAR DENSITIES
     DO 250 I1=1,N
     T=TB(I1)
     P=PRESSB(I1)
     DO 202 I=1,4
     Y(I)=YB(I1,I)
202  CONTINUE
     CALL COMP(T,P,Y,DENMOL)
     DO 204 I2=1,4
     MOLDEB(I1,I2)=DENMOL(I2)
204  CONTINUE
     P=PRESSD(I1)
     DO 206 I=1,4
     Y(I)=YDE(I1,I)
206  CONTINUE
     CALL COMP(T,P,Y,DENMOL)
     DO 207 I=1,4
     MOLDED(I1,I)=DENMOL(I)
207  CONTINUE
     T=TE
```

```
      P=PRESSE(I1)
      CALL COMP(T,P,Y,DENMOL)
      IF(I1.EQ.1)GO TO 236
      CALL FUGA(T,P,Y,FV)
236   DO 240 I2=1,4
      MOLDEE(I1,I2)=DENMOL(I2)
      IF(I1.EQ.1)GO TO 238
      FUGAD(I1,I2)=FV(I2)
      IF(YDE(I1,I2).EQ.0.0)GO TO 238
      FUGAC(I1,I2)=FV(I2)/P/YDE(I1,I2)
      GO TO 240
238   FUGAC(I1,I2)=1.0
240   CONTINUE
250   CONTINUE
C     CALCULATE MILLIMOLES ADDED OR REMOVED
C     MOLADD REFERS TO CHAMBER B ONLY
C     MOLREM REFERS TO CHAMBER D ONLY
C     FIRST SET DEFAULT VALUES
      WRITE(6,45)
      WRITE(6,50)
      DO 300 K=1,N
      DO 300 L=1,4
      MOLADD(K,L)=0.0
      MOLREM(K,L)=0.0
300   CONTINUE
```

```
      DO 305 L=1,4
      MOLADD(1,L)=MOLDEB(1,L)*VOLB
  305 CONTINUE
      K1=i
      DO 340 K1=2,N
      IF(PRESSB(K1).EQ.0.0)GO TO 330
      IF(PRESSB(K1)-PRESSB(K1-1))336,336,330
  330 CONTINUE
      DO 335 L1=1,4
      MOLADD(K1,L1)=(MOLDEB(K1,L1)-MOLDEB(K1-1,L1))*VOLB
  335 CONTINUE
  336 CONTINUE
  340 CONTINUE
      K2=1
      DO 380 K2=2,N
      IF(PRESSD(K2).EQ.0.0)GO TO 360
      GO TO 375
  360 CONTINUE
      DO 370 L2=1,4
      MOLREM(K2,L2)=(MOLDED(K2,L2)-MOLDED(K2-1,L2))*VOLD
  370 CONTINUE
  375 CONTINUE
  380 CONTINUE
C     CALCULATE TOTAL MOLES IN SYSTEM
      JJ=1
```

```
      DO 400 L=1,4
      MOLTOT(1,L)=MOLADD(1,L)+MOLREM(1,L)
400   CONTINUE
      DO 420 L=2,N
      DO 415 J=1,4
      MOLTOT(L,J)=MOLTOT(L-1,J)+MOLADD(L,J)+MOLREM(L,J)
415   CONTINUE
420   CONTINUE
      DO 430 L=1,N
      WRITE(6,52)L,(MOLADD(L,J),J=1,4),(MOLREM(L,J),J=1,4)
     &,(MOLTOT(L,J),J=1,4)
430   CONTINUE
C     CALCULATE MOLES ADSORBED
C     FIRST SET DEFAULT VALUES
      DO 500 K=1,N
      DO 500 L=1,4
      MOLADS(K,L)=0.0
500   CONTINUE
      DO 550 K=1,N
      DO 550 L=1,4
      MOLADS(K,L)=(MOLTOT(K,L)-MOLDEB(K,L)*VOLB-
     &MOLDEB(K,L)*VOLB-MOLDED(K,L)*VOLD-MOLDEE(K,L)*VOLE)/ZEOL
550   CONTINUE
C     OUTPUT RESULTS
C     SET DEFAULT VALUES
```

123

```
      DO 600 J=1,N
      DO 600 L=1,4
      XADS(J,L)=0.0
600   CONTINUE
      WRITE(6,55)
      WRITE(6,50)
      DO 615 K=1,N
      ADSORP=0.0
      DO 605 L=1,4
      ADSORP=ADSORP+MOLADS(K,L)
605   CONTINUE
      IF(ADSORP.EQ.0.0)GO TO 610
      DO 608 L=1,4
      XADS(K,L)=MOLADS(K,L)/ADSORP
608   CONTINUE
610   CONTINUE
615   CONTINUE
      DO 620 K=1,N
      WRITE(6,53)K,(MOLADS(K,L),L=1,4),(XADS(K,L),L=1,4)
     &,(YDE(K,L),L=1,4)
620   CONTINUE
      WRITE(6,90)
      WRITE(6,92)
      DO 630 L=1,4
      FUGAD(1,L)=0.0
```

```
630   CONTINUE
      DO 650 J=1,N
      DO 640 I=1,4
      PPRESS(J,I)=YDE(J,I)*PRESSE(J)
640   CONTINUE
      WRITE(6,94)J,(PPRESS(J,I),I=1,4),(FUGAD(J,I),I=1,4),
     &,(FUGAD(J,I),I=1,4),(FUGAC(J,I),I=1,4)
650   CONTINUE
C     PREPARE TABLES
      WRITE(6,95)
      WRITE(6,96)
      DO 700 M=1,N
      TOTAL=MOLADS(M,1)+MOLADS(M,3)
      WRITE(6,91)PRESSE(M),MOLADS(M,1),MOLADS(M,3),TOTAL
     &,XADS(M,1),XADS(M,3),YDE(M,1),YDE(M,3)
700   CONTINUE
      STOP
      END

C     CALCULATION OF MOLAR DENSITY
      SUBROUTINE COMP(T,P,Y,DENMOL)
      CHARACTER NOMBRE*10
      DIMENSION Y(12),DENMOL(12)
      COMMON/CAST/AC(12),B(12),A(12),DEL(12,12)
      COMMON/CRIT/TC(12),PC(12),W(12),TB(12)
      COMMON/PARA/NC,ICOD,NOMBRE(12)
```

```
      R=82.054*14.696
      DO 140 I=1,NC
      DO 140 J=1,NC
      DEL(I,J)=0.
140   CONTINUE
      IF (NC.EQ.1) GO TO 7
      GO TO 9
7     Y(1)=1.
9     IM=1.0
      CALL COST(ZV,T,P,Y,AA,BB,2)
      DO 315 I=1,NC
      DENMOL(I)=Y(I)*P/R/T/ZV*1000
315   CONTINUE
      RETURN
      END
      BLOCK DATA
      COMMON/CRIT/TC(12),PC(12),W(12),TB(12)
      COMMON/PARA/NC,ICOD,NOMBRE(12)
      CHARACTER NOMBRE*10
      DATA NC /6/
      DATA TC(1),PC(1),W(1),TB(1),NOMBRE(1) /190.6,667.2,
     &0.008,111.7, 'METHANE'/
      DATA TC(5),PC(5),W(5),TB(5),NOMBRE(5) /126.2,492.3,
     &0.040,77.3, 'NITROGEN'/
      DATA TC(3),PC(3),W(3),TB(3),NOMBRE(3) /305.4,708.35,
```

```
     &0.098,184.5, 'ETHANE'/
      DATA TC(2),PC(2),W(2),TB(2),NOMBRE(2) /304.2,1071.34,
     &0.420,194.7 'CAR DIOXID'/
      DATA TC(6),PC(6),W(6),TB(6),NOMBRE(6) /425.2,551.1,
     &0.193,272.7, 'BUTANE'/
      DATA TC(4),PC(4),W(4),TB(4),NOMBRE(4) /283.1,742.15,
     &0.073,169.5, 'ETHYLENE'/
      END

      SUBROUTINE COST(ZL,T,P,Y,AA,BB,IK)
      DIMENSION TR(12),PR(12),Y(12),AM(12)
      COMMON/CAST/AC(12),B(12),A(12),DEL(12,12)
      COMMON/ CRIT/TC(12),PC(12),W(12),TB(12)
      COMMON/PARA/NC,ICOD,NOMBRE(12)
      DO 20 I=1,NC
      TR(I)=T/TC(I)
      PR(I)=P/PC(I)
20    CONTINUE
      DO 30 I=1,NC
      AM(I)=0.480+1.574*W(I)-0.176*W(I)**2
      AC(I)=( 1. + AM(I)*(1.-SQRT(TR(I))) )**2.
      A(I)=0.42747*AC(I)*PR(I)/(TR(I)**2.)
      B(I)=0.08664*PR(I)/TR(I)
30    CONTINUE
      BB=0.
      AA=0.
```

```
      IF(NC.EQ.1) GO TO 1
      DO 40 I=1,NC
      BB=BB+Y(I)*B(I)
      DO 50 J=1,NC
      AA=AA+Y(I)*Y(J)*(1.-DEL(I,J))*SQRT(A(I)*A(J))
50    CONTINUE
40    CONTINUE
      CALL ZETAAB(AA,BB,ZRL,ZRG,IER)
8     IF(IK.EQ.1) GO TO 5
      IF(IER.NE.1) GO TO 6
      IF(ZRL.GT.0.4) GO TO 6
      WRITE(6,*)'ERROR ,SOLO EXISTE FASE LIQUIDA'
      ZL=0.333
      RETURN
6     ZL=ZRG
      RETURN
5     IF(IER.NE.1) GO TO 7
      IF(ZRL.LT.0.4) GO TO 7
      ZL=0.333
      RETURN
7     ZL=ZRL
      RETURN
1     AA=A(1)
      BB=B(1)
      CALL ZETAAB(AA,BB,ZRL,ZRG,IER)
```

```
      GO TO 8
      END

      SUBROUTINE ZETAAB(A,B,ZRL,ZRG,IER)
      DIMENSION VEC(3)
      ICON=0
      IER=0
      C=1.
      Q=(A-B-B**2)
      R=A*B
      Z=0.001
98    FX=Z**3-C*Z**2+Q*Z-R
      FX1=3*Z**2-2*C*Z+Q
      FX2=6*Z-2*C
      CONV=ABS(FX*FX2/(FX1**2))
      IF(CONV.LT.1) GO TO 99
      Z=Z+0.09
      ICON=ICON+1
      IF(ICON.EQ.500) GO TO 1009
      GO TO 98
1009  WRITE(6,1001)
1001  FORMAT(1X,15HNO CONVERGENCIA)
      RETURN
99    Z0=Z
      XTOL=0.01
      FTOL=0.001
```

```
      NLIM=500
      I=0
      CALL NEWTON(Z0,XTOL,FTOL,NLIM,I,Q,R,C)
      RAIZ=(-C+Z0)**2-4*(Q+Z0*(-C+Z0))
      IF(ABS(RAIZ).LE.0.0001) GO TO 100
      IF(RAIZ.LT.0) GO TO 109
      VEC(1)=Z0
      I=0
      Z01=(-(-C+Z0)+RAIZ**0.5)/2.
      CALL NEWTON(Z01,XTOL,FTOL,NLIM,I,Q,R,C)
      VEC(2)=Z01
      I=0
      Z02=(-(-C+Z0)-RAIZ**0.5)/2.
      CALL NEWTON(Z02,XTOL,FTOL,NLIM,I,Q,R,C)
      VEC(3)=Z02
30    DO 10 I=1,3
      AMAY=VEC(I)
      KK1=I
      DO 20 K=I,3
      IF(AMAY.LT.VEC(K)) GO TO 20
      AMAY=VEC(K)
      KK1=K
20    CONTINUE
      AUX=VEC(I)
      VEC(I)=VEC(KK1)
```

```
      VEC(KK1)=AUX
10    CONTINUE
      IF(VEC(1).GT.0) GO TO 101
      IF(VEC(2).GT.0) GO TO 102
      IF(VEC(3).GT.0) GO TO 103
      Z=1.
      GO TO 98
101   ZRL=VEC(1)
      ZR=VEC(2)
      ZRG=VEC(3)
      GO TO 1000
102   ZRL=VEC(2)
      ZR=VEC(1)
      ZRG=VEC(3)
      GO TO 1000
103   ZRL=VEC(3)
      ZR=ZRL
      ZRG=ZRL
      IER=1
      GO TO 1000
100   Z03=-(-C+Z0)/2.
      I=0
      CALL NEWTON(Z03,XTOL,FTOL,NLIM,I,Q,R,C)
      VEC(1)=Z0
      VEC(2)=Z03
```

```
      VEC(3)=0.
      GO TO 30
  109 VEC(1)=Z0
      VEC(2)=0.
      VEC(3)=0.
      GO TO 30
 1000 RETURN
      END

      SUBROUTINE NEWTON(Z0,XTOL,FTOL,NLIM,I,Q,R,C)
      LOGICAL PRINT
      PRINT=.TRUE.
      IF(I.NE.0) PRINT=.FALSE.
      FZ=FCN(Z0,Q,R,C)
      DO 20 J=1,NLIM
      DELZ=FZ/FDER(Z0,Q,R,C)
      Z0=Z0-DELZ
      FZ=FCN(Z0,Q,R,C)
      IF(.NOT.PRINT) GO TO 5
    5 IF(ABS(DELZ).LE.XTOL) GO TO 60
      IF(ABS(FZ).LE.FTOL) GO TO 70
   20 CONTINUE
      I=-1
      RETURN
   60 I=1
   70 I=2
```

```
      RETURN
      END

      FUNCTION FCN(Z0,Q,R,C)
      FCN=Z0**3-C*Z0**2+Q*Z0-R
      RETURN
      END
C
      FUNCTION FDER(Z0,Q,R,C)
      FDER=3*(Z0**2)-2*C*Z0+Q
      RETURN
      END

      SUBROUTINE FUGA(T,P,Y,FV)
      CHARACTER NOMBRE*10
      COMMON/CAST/AC(12),B(12),A(12),DEL(12,12)
      COMMON/CRIT/TC(12),PC(12),W(12),TB(12)
      COMMON/PARA/NC,ICOD,NOMBRE(12)
      DIMENSION Y(12),CFV(12),FV(12)
      CALL FUGACI(T,P,Y,CFV,ZV,2)
      DO 315 I=1,NC
      FV(I)=CFV(I)*Y(I)*P
315   CONTINUE
      RETURN
      END

      SUBROUTINE FUGACI(T,P,Y,CFV,ZL,IK)
```

```
      COMMON/CAST/AC(12),B(12),A(12),DEL(12,12)
      COMMON/CRIT/TC(12),PC(12),W(12),TB(12)
      COMMON/PARA/NC,ICOD,NOMBRE(12)
      DIMENSION C(12),Y(12),CFV(12)
      CALL COST(ZL,T,P,Y,AA,BB,IK)
      DO 10 I=1,NC
      AP1=0.
      DO 20 J=1,NC
      AP1=AP1 + Y(J)*SQRT(A(J)*A(I))*(1-DEL(I,J))
20    CONTINUE
      AP=2.*AP1/AA - B(I)/BB
      CF=(ZL-1.)*B(I)/BB - ALOG(ZL-BB) - (AA/BB)*AP*
     &ALOG((ZL+BB)/ZL)
      CFV(I)=EXP(CF)
10    CONTINUE
      RETURN
      END
```

Program # 3

This program is constructed to calculate the x-y and the x-q fits of IAST model for binary systems using Toth parameters for the pure components. The program can be modified to calculate the x-y and x-q fits of multicomponent systems.

Program Input:

M1 : Saturation concentrations for components 1 (mole/kg. zeoloite)

M2 : Saturation concentrations for components 2 (mole/kg. zeoloite)

B1 : Unilan equilibrium parameters for components 1 $(kPa)^{-T1}$

B2 : Unilan equilibrium parameters for components 2 $(kPa)^{-T2}$

T1 : Unilan heterogeneity parameters for components 1 (unitless)

T2 : Unilan hetrogeneoity parameters for components 2 (unitless)

H1 : Henry's constants for components 1 (mole/kg. zeolite/ kPa)

H2 : Henry's constants for components 2 (mole/kg. zeolite/ kPa)

P : Required pressure (kPa)

Y1 : Gas phase mole fraction of component 1

```
EXTERNAL FN,FPSI
REAL FN,FPSI,M1,M2,B1,B2,T1,T2,H1,H2,P
REAL S1,S2,DELTA,EPS,N1,N2,NT
REAL Y1(100),Y2(100),X1(100),X2(100)
REAL SUM(100),Q1(100),Q2(100),QT(100)
REAL PSI(100),P1(100),P2(100)
READ (5,*) NP,M1,B1,T1,H1,M2,B2,T2,H2,P
WRITE(6,10)
WRITE(6,*)
WRITE(6,20)
WRITE(6,30)
WRITE(6,60)
WRITE(6,40)
WRITE(6,*)
DO 11 J=1,NP
READ (5,*) Y1(J)
Y2(J)=1.0-Y1(J)
P1(J)=Y1(J)*P
P2(J)=Y2(J)*P
PSI(J)=(FPSI(P,M1,B1,T1)*Y1(J))+Y2(J)*FPSI(P,M2,B2,T2)
DO 1 I =1,10
CALL PINV(FN,FPSI,H1,M1,B1,T1,PSI(J),PP1)
CALL PINV(FN,FPSI,H2,M2,B2,T2,PSI(J),PP2)
N1=FN(PP1,M1,B1,T1)
N2=FN(PP2,M2,B2,T2)
```

```
      S1=(Y1(J)/PP1)+(Y2(J)/PP2)
      S2=(Y1(J)/(PP1*N1))+(Y2(J)/(PP2*N2))
      DELTA=(P*S1-1.0)/(P*S2)
      EPS=ABS(DELTA)/PSI(J)
      IF(EPS.LE.1.0E-7)THEN
      GO TO 2
      ENDIF
      PSI(J)=PSI(J)+DELTA
1     CONTINUE
2     X1(J)=P1(J)/PP1
      X2(J)=P2(J)/PP2
      QT(J)=1.0/((X1(J)/N1)+(X2(J)/N2))
      Q1(J)=QT(J)*X1(J)
      Q2(J)=QT(J)*X2(J)
      SUM(J)=X1(J)+X2(J)
      WRITE(6,50) Y1(J),Y2(J),X1(J),X2(J)
      WRITE(6,50) Q1(J),Q2(J),QT(J),SUM(X)
11    CONTINUE
10    FORMAT(14X,'FIT OF IAST IN CONJUNCTION WITH TOTH MODEL')
20    FORMAT(2X,'SYSTEM : METHANE/ETHANE ON ETS-10')
30    FORMAT(2X,'TEMPERATURE = 280 K     PRESSURE = 150 KPA')
40    FORMAT(2X,'YC2H6',3X,'YC2H4',3X,'XC2H6',3X,'
     +XC2H4',3X,'QCH4',2X,'QC2H6',3X,'QTOT',3X,'SUM')
50    FORMAT(2X,5(F6.4,2X),3(F6.3,1X))
60    FORMAT(62('-'))
```

123

```
70  FORMAT(2(F6.4,2X))
    STOP
    END


    SUBROUTINE PINV(FN,FPSI,A,B,C,D,E,F)
    REAL G,DELTA,EPS,N
    F=(B/A)*(EXP(E/B)-1.0)
    DO 10 I=1,10
    N=FN(F,B,C,D)
    G=FPSI(F,B,C,D)-E
    DELTA=G*F/N
    EPS=ABS(DELTA)/F
    IF(EPS.LE.1.0E-7)THEN
    F=F-DELTA
    GO TO 2
    ENDIF
    F=F-DELTA
10  CONTINUE
2   RETURN
    END


    FUNCTION FN(A,B,C,D)
    FN=(A*B)/((C+A**D)**(1.0/D))
    RETURN
```

```
      END

      FUNCTION FPSI(A,B,C,D)
      REAL TH,SUM(1000),SUMCON
      TH=(A)/((C+A**D)**(1.0/D))
      SUM(1)=0.0
      DO 1 J =1,1000
      SUM(J+1)=SUM(J)+(TH**(REAL(J)*D+1.0))/(REAL(J)*D*(REAL(J)*D+1.0))
      IF(ABS(SUM(J+1)-SUM(J)).LE.1.0E-7)THEN
      SUMCON=SUM(J+1)
      GO TO 2
      ENDIF
1     CONTINUE
2     FPSI=B*(TH-(TH/D)*ALOG(1.0-TH**D)-SUMCON)
      RETURN
      END
```

Program # 4

This program is constructed to calculate the x-y and the x-q fits of IAST. model for binary systems using Unilan parameters of the pure components. The program can be modified to calculate the x-y and x-q fits of multicomponent systems.

Program Input:

M1 : Saturation concentrations for components 1 (mole/kg. zeoloite)

M2 : Saturation concentrations for components 2 (mole/kg. zeoloite)

C1 : Unilan equilibrium parameters for components 1 $(kPa)^{-1}$

C2 : Unilan equilibrium parameters for components 2 $(kPa)^{-1}$

S1 : Unilan hetrogeneoity parameters for components 1 (unitless)

S2 : Unilan hetrogeneoity parameters for components 2 (unitless)

H1 : Henry's constants for components 1 (mole/kg. zeolite/ kPa)

H2 : Henry's constants for components 2 (mole/kg. zeolite/ kPa)

P : Required pressure (kPa)

Y1 : Gas phase mole fraction of component 1

```
EXTERNAL F,Q
REAL M1,M2,C1,C2,S1,S2,H1,H2,P
REAL SUM1,SUM2,DELTA,EPS,N1,N2,NT
REAL Y1(100),Y2(100),X1(100),X2(100)
REAL SUM(100),Q1(100),Q2(100),QT(100)
REAL PSI(100),P1(100),P2(100),PSI1(100),PSI2(100)
READ (5,*) M1,C1,S1,H1,M2,C2,S2,H2,P
WRITE(6,10)
WRITE(6,*)
WRITE(6,20)
WRITE(6,30)
WRITE(6,60)
WRITE(6,40)
WRITE(6,*)
DO 100 J=1,21
Y1(J)=0.05*REAL(J-1)
Y2(J)=1.0-Y1(J)
P1(J)=Y1(J)*P
P2(J)=Y2(J)*P
CALL GAUS(F,P,M1,C1,S1,PSI1(J))
CALL GAUS(F,P,M2,C2,S2,PSI2(J))
PSI(J)=PSI1(J)*Y1(J)+Y2(J)*PSI2(J)
DO 1 I =1,10
CALL PINV(F,Q,H1,M1,C1,S1,PSI(J),PP1)
CALL PINV(F,Q,H2,M2,C2,S2,PSI(J),PP2)
```

```
      N1=Q(PP1,M1,C1,S1)
      N2=Q(PP2,M2,C2,S2)
      SUM1=(Y1(J)/PP1)+(Y2(J)/PP2)
      SUM2=(Y1(J)/(PP1*N1))+(Y2(J)/(PP2*N2))
      DELTA=(P*SUM1-1.0)/(P*SUM2)
      EPS=ABS(DELTA)/PSI(J)
      IF(EPS.LE.1.0E-7)THEN
      GO TO 2
      ENDIF
      PSI(J)=PSI(J)+DELTA
1     CONTINUE
2     X1(J)=P1(J)/PP1
      X2(J)=P2(J)/PP2
      QT(J)=1.0/((X1(J)/N1)+(X2(J)/N2))
      Q1(J)=QT(J)*X1(J)
      Q2(J)=QT(J)*X2(J)
      SUM(J)=X1(J)+X2(J)
      WRITE(6,50)Y1(J),Y2(J),X1(J),X2(J),Q1(J),Q2(J),QT(J),SUM(J)
100   CONTINUE
10    FORMAT(14X,'FIT OF IAST IN CONJUNCTION WITH UNILAN MODEL')
20    FORMAT(2X,'SYSTEM : ETHANE-ETHYLENE/ETS-10')
30    FORMAT(2X,'TEMPERATURE = 280 K     PRESSURE = 150 KPA')
40    FORMAT(2X,'YC2H6',3X,'YC2H4',3X,'XC2H6',3X,'XC2H4',3X
     +,'QC2H6',3X,'QC2H4',3X,'QTOT',2X,'SUM')
50    FORMAT(2X,4(F6.4,2X),3(F6.3,1X),F6.4)
```

```
60  FORMAT(62('-'))
70  FORMAT(2(F6.4,2X))
    STOP
    END

    SUBROUTINE GAUS(F,GP,GM,GC,GS,R)
    REAL C,M,W(15),Z(15),A,B
    A=-GS
    B=GS
    M=(B-A)/2.0
    C=(B+A)/2.0
    Z(1)=0.00
    Z(2)=0.2011940940
    Z(3)=-Z(2)
    Z(4)=0.3941513471
    Z(5)=-Z(4)
    Z(6)=0.5709721726
    Z(7)=-Z(6)
    Z(8)=0.7244177314
    Z(9)=-Z(8)
    Z(10)=0.8482065834
    Z(11)=-Z(10)
    Z(12)=0.9372733924
    Z(13)=-Z(12)
    Z(14)=0.9879925180
    Z(15)=-Z(14)
```

```
      W(1)=0.2025782419
      W(2)=0.1984314853
      W(3)=W(2)
      W(4)=0.1861610001
      W(5)=W(4)
      W(6)=0.1662692058
      W(7)=W(6)
      W(8)=0.1395706779
      W(9)=W(8)
      W(10)=0.1071592205
      W(11)=W(10)
      W(12)=0.0703660475
      W(13)=W(12)
      W(14)=0.0307532420
      W(15)=W(14)

      SUM=0.0
      DO 10 I=1,15
      SUM=SUM+W(I)*F((M*Z(I)+C),GP,GC)
   10 CONTINUE
      R=M*SUM*GM/(2.0*GS)
      RETURN
      END
```

```
      SUBROUTINE PINV(F,Q,PH,PM,PC,PS,PPSI,PP)
      REAL G,DELTA,EPS,N,G1
      PP=(PM/PH)*(EXP(PPSI/PM)-1.0)
      DO 10 I=1,100
      N=Q(PP,PM,PC,PS)
      CALL GAUS(F,PP,PM,PC,PS,G1)
      G=G1-PPSI
      DELTA=G*PP/N
      PP=PP-DELTA
      EPS=ABS(DELTA)/PP
      IF(EPS.LE.1.0E-7)THEN
      PP=PP-DELTA
      GO TO 2
      ENDIF
10    CONTINUE
2     RETURN
      END

      FUNCTION F(FX,FP,FC)
      F=ALOG(1.0+(FP/FC)*EXP(FX))
      RETURN
      END
```

```
FUNCTION Q(QP,QM,QC,QS)
REAL Q1,Q2,Q3
Q1=QC+QP*EXP(QS)
Q2=QC+QP*EXP(-1.0*QS)
Q3=Q1/Q2
Q=(QM/(2.0*QS))*ALOG(Q3)
RETURN
END
```

Program # 5

This program is constructed to calculate the x-y and the x-q fits of IAST. model to binary systems using Virial Three Constant parameters of the pure components . The program can be modified to calculate the x-y and x-q fits for multicomponent systems.

Program Input:

M1 : Saturation concentrations for components 1 (mole/kg. zeoloite)

M2 : Saturation concentrations for components 2 (mole/kg. zeoloite)

B1 : Henry's constants for components 1 (mole/kg. zeolite/ kPa)

C1 : Henry's constants for components 2 (mole/kg. zeolite/ kPa)

B2 : Virial first constant for component 1 (kg. zeolite/mole)

C2 : Virial first constant for component 2 (kg. zeolite/mole)

B3 : Virial second constant for component 1 (kg. zeolite/mole)^2

C3 : Virial second constant for component 2 (kg. zeolite/mole)^2

B4 : Virial third constant for component 1 (kg. zeolite/mole)^3

C4 : Virial third constant for component 2 (kg. zeolite/mole)^3

P : Required pressure (kPa)

Y : Gas phase mole fraction of component 1

```
EXTERNAL F,Q
REAL B1,B2,B3,B4,C1,C2,C3,C4,P0,P
REAL S1,S2,DELTA,EPS,N1,N2,NT,H1,H2,M1,M2
REAL Y1(100),Y2(100),X1(100),X2(100)
REAL SUM(100),Q1(100),Q2(100),QT(100)
REAL PSI(100),P1(100),P2(100),PSI1(100),PSI2(100)
REAL PSI(100),P1(100),P2(100),PSI1(100),PSI2(100)
READ(5,*)M1,B1,B2,B3,B4,M2,C1,C2,C3,C4,P
H1= B1
H2= C1
P0= 0.00
WRITE(6,10)
WRITE(6,*)
WRITE(6,20)
WRITE(6,30)
WRITE(6,60)
WRITE(6,40)
WRITE(6,*)
DO 100 J=1,11
READ(5,*) Y1(J)
Y2(J)=1.0-Y1(J)
P1(J)=Y1(J)*P
P2(J)=Y2(J)*P
CALL GAUS(F,P0,P,B1,B2,B3,B4,PSI1(J))
CALL GAUS(F,P0,P,C1,C2,C3,C4,PSI2(J))
```

```
      PSI(J)=Y1(J)*PSI1(J)+Y2(J)*PSI2(J)
      DO 1 I =1,20
      CALL PINV(F,Q,P0,H1,M1,B1,B2,B3,B4,PSI(J),PP1)
      CALL PINV(F,Q,P0,H2,M2,C1,C2,C3,C4,PSI(J),PP2)
      N1=Q(PP1,B1,B2,B3,B4)
      N2=Q(PP2,C1,C2,C3,C4)
      S1=(Y1(J)/PP1)+(Y2(J)/PP2)
      S2=(Y1(J)/(PP1*N1))+(Y2(J)/(PP2*N2))
      DELTA=(P*S1-1.0)/(P*S2)
      EPS=ABS(DELTA)/PSI(J)
      IF(EPS.LE.1.0E-7)THEN
      GO TO 2
      ENDIF
      PSI(J)=PSI(J)+DELTA
1     CONTINUE
2     X1(J)=P1(J)/PP1
      X2(J)=P2(J)/PP2
      QT(J)=1.0/((X1(J)/N1)+(X2(J)/N2))
      Q1(J)=QT(J)*X1(J)
      Q2(J)=QT(J)*X2(J)
      SUM(J)=X1(J)+X2(J)
      WRITE(6,50)Y1(J),Y2(J),X1(J),X2(J),Q1(J),Q2(J),QT(J),SUM(J)
100   CONTINUE
10    FORMAT(14X,'FIT OF IAST IN CONJUNCTION WITH VIRIAL MODEL')
20    FORMAT(2X,'SYSTEM : ETHANE-ETHYLENE/ETS-10')
```

```
30  FORMAT(2X,'TEMPERATURE = 280 K      PRESSURE = 150 KPA')
40  FORMAT(2X,'YC2H6',3X,'YC2H4',3X,'XC2H6',3X,'XC2H4',3X,
   +'QC2H6',3X,'QC2H4',3X,'QTOT',2X,'SUM')
50  FORMAT(2X,4(F6.4,2X),3(F6.3,1X),F6.4)
60  FORMAT(62('-'))
70  FORMAT(2(F6.4,2X))
    STOP
    END

    SUBROUTINE GAUS(F,A,B,GB1,GB2,GB3,GB4,R)
    REAL C,M,W(15),Z(15)
    M=(B-A)/2.0
    C=(B+A)/2.0
    Z(1)=0.00
    Z(2)=0.2011940940
    Z(3)=-Z(2)
    Z(4)=0.3941513471
    Z(5)=-Z(4)
    Z(6)=0.5709721726
    Z(7)=-Z(6)
    Z(8)=0.7244177314
    Z(9)=-Z(8)
    Z(10)=0.8482065834
    Z(11)=-Z(10)
    Z(12)=0.9372733924
    Z(13)=-Z(12)
```

```
      Z(14)=0.9879925180
      Z(15)=-Z(14)
      W(1)=0.2025782419
      W(2)=0.1984314853
      W(3)=W(2)
      W(4)=0.1861610001
      W(5)=W(4)
      W(6)=0.1662692058
      W(7)=W(6)
      W(8)=0.1395706779
      W(9)=W(8)
      W(10)=0.1071592205
      W(11)=W(10)
      W(12)=0.0703660475
      W(13)=W(12)
      W(14)=0.0307532420
      W(15)=W(14)
      SUM=0.0
      DO 10 I=1,15
      SUM=SUM+W(I)*F((M*Z(I)+C),GB1,GB2,GB3,GB4)
   10 CONTINUE
      R=M*SUM
      RETURN
      END

      SUBROUTINE PINV(F,Q,PA,PH,PM,PB1,PB2,PB3,PB4,PPS1,PP)
```

```
      REAL N,G,G1,EPS,DELTA
      PP=(PM/PH)*((EXP(PPSI/PM))-1.0)
      DO 1 I=1,10
      N=Q(PP,PB1,PB2,PB3,PB4)
      CALL GAUS(F,PA,PP,PB1,PB2,PB3,PB4,G1)
      G=G1-PPSI
      DELTA=G*PP/N
      PP=PP-DELTA
      EPS=ABS(DELTA)/PP
      IF(EPS.LE.1.0E-5)THEN
      GO TO 2
      ENDIF
1     CONTINUE
2     PP=PP-DELTA
      RETURN
      END

      FUNCTION F(FP,A1,A2,A3,A4)
      REAL X,QOLD
      EQ(X)=FP-(X/A1)*EXP(A2*X+A3*X*X+A4*X*X*X)
      DEQ(X)=(-1.0/A1)*(1+X*(A2+2.0*A3*X+3.0*A4*X*X))*EXP(A2*X+A3*X*X
     &+A4*X*X*X)
      QOLD=2.00
      DO 1 I=1,10
      QNEW=QOLD-EQ(QOLD)/DEQ(QOLD)
      EPS=ABS(QNEW-QOLD)
```

123

```
      IF(EPS.LE.1.0E-7)THEN
      GO TO 2
      ENDIF
      QOLD=QNEW
    1 CONTINUE
    2 F=QNEW/FP
      RETURN
      END

      FUNCTION Q(FP,A1,A2,A3,A4)
      REAL X,QOLD
      EQ(X)=FP-(X/A1)*EXP(A2*X+A3*X*X+A4*X*X*X)
      DEQ(X)=(-1.0/A1)*(1+X*(A2+2.0*A3*X+3.0*A4*X*X))*EXP(A2*X+A3*X*X
     &+A4*X*X*X)
      QOLD=2.00
      DO 1 I=1,100
      QNEW=QOLD-EQ(QOLD)/DEQ(QOLD)
      EPS=ABS(QNEW-QOLD)
      IF(EPS.LE.1.0E-7)THEN
      GO TO 2
      ENDIF
      QOLD=QNEW
    1 CONTINUE
    2 Q=QNEW
      RETURN
      END
```

123

VITA

Name	Nadhir Abbas Hussain.
Family Name	Al-Baghli.
Religion	Muslim.
Nationality	Saudi.
Personal Data	Born in 1968. Married since 1991.
Education	Bachelors Degree in Chemical Engineering from King Fahd University of Petroleum & Minerals in 1991.
Publication	N. Al-Baghli, M.M. Hassan, and K.F. Loughlin, "Ternary, Binary and Pure Component Sorption of Hydrocarbons on ETS-10 Zeolite", a poster paper # 183P presented at the AIChE meeting in St. Louis, USA November 1993.